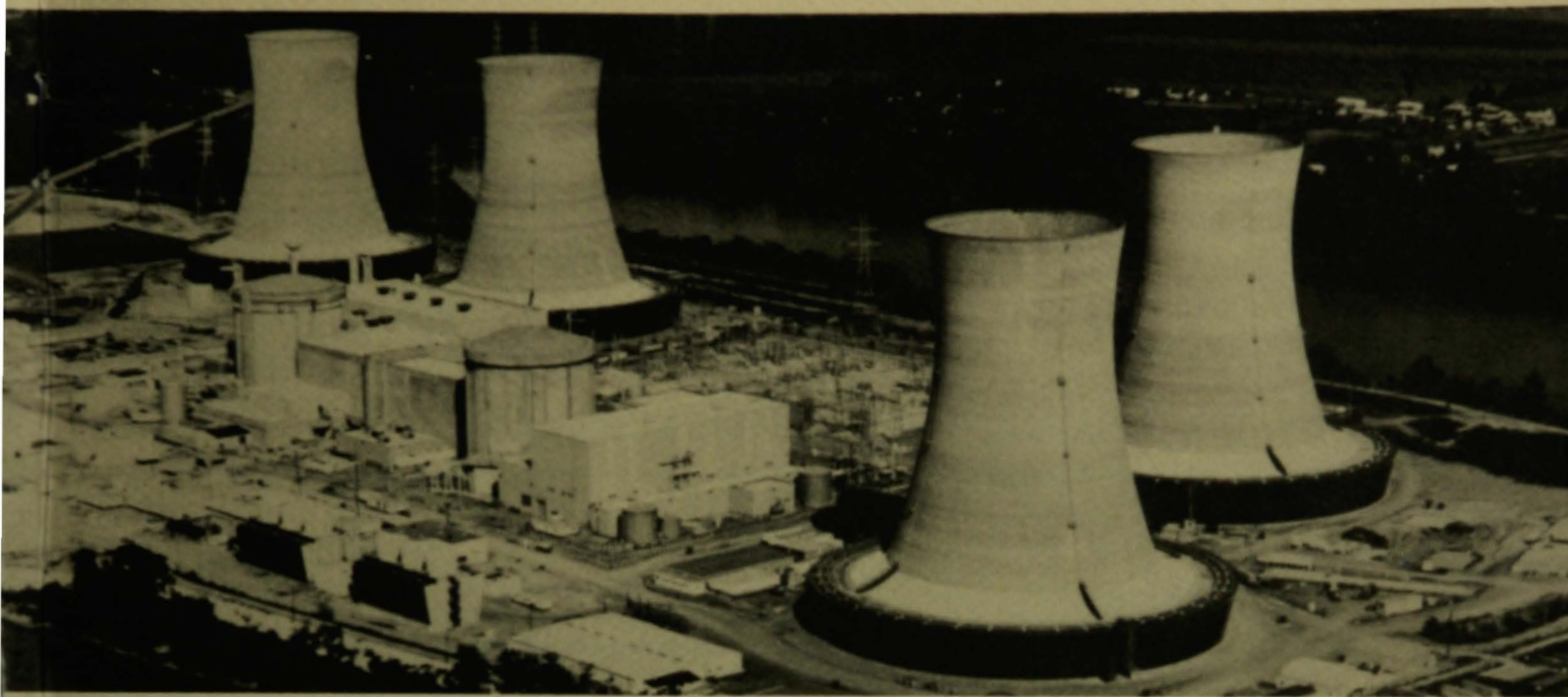


✓
07013

C1



This is an informal report intended for use as a preliminary or working document

GEND

General Public Utilities • Electric Power Research Institute • U.S. Nuclear Regulatory Commission • U.S. Department of Energy

EXAMINATION OF THE TMI-2 CORE
DISTINCT COMPONENTS

LOAN COPY

THIS REPORT MAY BE RECALLED
AFTER TWO WEEKS. PLEASE
RETURN PROMPTLY TO:

INEL TECHNICAL LIBRARY

S.M. Jensen
D.W. Akers
R.W. Garner
G.S. Roybal

FEB 10 1994
5-16-94
D. Clayton 6-3-03

Prepared for the
U.S. Department of Energy
Three Mile Island Operations Office
Under Contract No. DE-AC07-76ID01570

DISCLAIMER

This book was prepared as an account of work sponsored by an agency of the United States Government. Neither the United States Government nor any agency thereof, nor any of their employees, makes any warranty, express or implied, or assumes any legal liability or responsibility for the accuracy, completeness, or usefulness of any information, apparatus, product or process disclosed, or represents that its use would not infringe privately owned rights. References herein to any specific commercial product, process, or service by trade name, trademark, manufacturer, or otherwise, does not necessarily constitute or imply its endorsement, recommendation, or favoring by the United States Government or any agency thereof. The views and opinions of authors expressed herein do not necessarily state or reflect those of the United States Government or any agency thereof.

EXAMINATION OF THE TMI-2 CORE DISTINCT COMPONENTS

**S. M. Jensen
D. W. Akers
R. W. Garner
G. S. Roybal**

September 1987

**EG&G Idaho, Inc.
Idaho Falls, Idaho 83415**

**Prepared for the
U.S. Department of Energy
Three Mile Island Operations Office
Under DOE Contract No. DE-AC07-76ID01570**

ABSTRACT

This report discusses the acquisition and examination of partial fuel assembly upper ends from the TMI-2 core. Examinations included photovisual and radiographic characterization and metallurgical and radiochemical analyses. Results of these examinations indicate the following:

- Fuel assembly upper ends experienced steep temperature gradients and temperatures exceeding 1750 K.
- Radiographic examinations indicate silver-indium-cadmium relocated upwards into the control rod plenum region.
- Elemental examinations indicate low deposition (<7.0 kg) of core materials on upper core region surfaces.
- Radiochemical examinations indicate low deposition (<0.1% of core inventory) of any fission product on upper core region (i.e., fuel assembly) surfaces.

CONTENTS

ABSTRACT	11
1. INTRODUCTION	1
1.1 Background	1
1.2 TMI-2 Core History	5
1.2.1 Preaccident Conditions and Configuration	5
1.2.2 TMI-2 Accident Sequence	9
1.2.3 Postaccident Reactor Vessel Internals Disassembly Activities	15
1.2.3.1 Quick-Look Video Surveys	15
1.2.3.2 APSR Assembly--Insertion	15
1.2.3.3 Ultrasonic Scanner Survey	16
1.2.3.4 Reactor Vessel Head Removal.....	16
1.2.3.5 Plenum Assembly Removal	21
1.2.3.6 Early Fuel Removal	21
2. DISTINCT COMPONENT ACQUISITION	24
2.1 Loading of Canisters at TMI-2	24
2.2 Unloading of Canisters at the INEL	24
3. SAMPLE EXAMINATION AND ANALYSIS METHODS	28
3.1 Nondestructive Examinations	28
3.1.1 Video Tapes (CCTV)	28
3.1.2 Hot Cell Photography	30
3.1.3 Neutron Radiography	30
3.1.4 Gamma Spectroscopy	31
3.2 Destructive Examinations	31
3.2.1 Metallography	32
3.2.2 Radionuclide and Elemental Analyses	33
3.2.2.1 Sample Handling and Analysis Methods	34
3.2.2.2 Gamma Spectroscopy	34
3.2.2.3 Fissile/Fertile Analyses	35
3.2.2.4 Sr-90 Analysis	35
3.2.2.5 I-129 Analysis	35
3.2.2.6 Elemental Analyses	36
4. VISUAL EXAMINATION DATA AND TEMPERATURE ESTIMATION	37

FUEL AND CONTROL ROD SAMPLE CHARACTERIZATION AND SELECTION	42
FUEL AND CONTROL ROD SAMPLE EXAMINATIONS	51
6.1 Control Rod Metallurgical Examinations	51
6.1.1 Examination of the Debris in Control Rod 3-1C	54
6.1.2 Characterization of the Melted Control Rod Material Behavior	58
6.1.3 Characterization of the Zircaloy Guide Tube Behavior	58
6.2 Fuel Rod Metallurgical Examinations	63
6.2.1 Characterization of the Fuel Morphology	67
6.2.2 Characterization of the Zircaloy Cladding Behavior	74
6.3 Radionuclide and Elemental Analyses	79
6.3.1 Gamma Spectroscopy of Intact Rods	81
6.3.2 Radiochemical and Chemical Analysis Results	90
6.3.2.1 Chemical Analysis Results	91
6.3.2.2 Radiochemical Analysis Results	106
6.3.2.3 Fuel Pellet Analyses	111
SUMMARY AND CONCLUSIONS	122
REFERENCES	126
APPENDIX A--RESULTS OF NEUTRON RADIOGRAPHY EXAMINATIONS	A-1
APPENDIX B--GAMMA SCAN RESULTS	B-1
APPENDIX C--DISTINCT COMPONENT ACQUISITION	C-1
APPENDIX D--VISUAL EXAMINATION DATA AND TEMPERATURE ESTIMATION	D-1

FIGURES

TMI-2 core loading diagram	6
Side, top, and cross-sectional views of TMI-2 fuel assembly (from Reference 4)	7
Orifice rod assembly (from Reference 4)	8
Burnable poison rod assembly (from Reference 4)	10

5.	Control rod assembly (from Reference 4)	11
6.	Axial-power-shaping-rod (APSR) assembly (from Reference 4)	12
7.	TMI-2 core void topographical plot elevations -2 through -14	17
8.	TMI-2 core void topographical plot elevations -16 through -40	18
9.	TMI-2 core void topographical plot elevations -42 through -78	19
10.	TMI-2 core void topographical plot cross sections	20
11.	Damage map of the TMI-2 fuel assembly upper grid plate	22
12.	TMI-2 core loading diagram showing locations of components removed from canisters D-141 and D-153	27
13.	Bottom view of component D-141-3 after removal of most fuel rods	38
14.	Bottom view of component D-153-9	39
15.	Fuel and control rod locations in component D-141-3. Partial fuel assembly in core location C7	43
16.	Fuel rod locations in component D-141-11. Partial fuel assembly in core location H1	43
17.	Approximate lengths of fuel and control rods remaining in component D-141-3 (cm)	45
18.	Lengths of fuel rods remaining in component D-141-11 (cm)	45
19.	Sorting rack with some of the fuel rods from D-141-3	46
20.	Typical broken fuel rod endtips	48
21.	Melted stainless steel cladding on control rod endtips	49
22.	Damaged endtips on control rods	50
23.	Sectioning diagrams for fuel rods and control rod/guide tubes	52
24.	Neutron radiographs of control rods 3-1C and 3-14C/G	53
25.	Bottom endtip of control rod 3-14C/G	55
26.	Metallographic samples from control rod 3-1C	56
27.	Metallographic samples from control rod 3-14C/G	57
28.	Debris near the broken endtip of control rod 3-1C	59

29.	Dendritic structures in previously melted Ag-Cd-In control material	60
30.	Previously melted Ag-Cd-In control material in plenum spring region of sample M-15	61
31.	Previously melted control material in rod 3-14C/G	62
32.	Zircaloy hydrides in the guide tube of control rod 3-14C/G	64
33.	Neutron radiographs of fuel rods 3-30 and 3-42	65
34.	Metallographic samples from fuel rod 3-30	68
35.	Metallographic samples from fuel rod 3-42	69
36.	Fuel morphology in sample M-1 near broken end of fuel rod 3-30	70
37.	Fuel morphology in sample M-3 from fuel rod 3-30	71
38.	Fuel morphology in sample M-5 from fuel rod 3-42	72
39.	Fuel morphology in sample M-7 from fuel rod 3-42	73
40.	Isolated region of enlarged grain size in sample M-7	75
41.	Variations in zircaloy oxidation on fuel rod 3-42	76
42.	Gross gamma scan of segment 3-30 fuel rod	83
43.	Gross gamma scan of segment 3-42 fuel rod	83
44.	Gross gamma scan of segment 3-1C control rod	84
45.	Gross gamma scan of segment 3-1G guide tube	84
46.	Gross gamma scan of segment 3-14C/G control rod/guide tube	85

TABLES

1.	TMI-2 reactor core composition	13
2.	Fuel canister D-141 contents	25
3.	Fuel canister D-153 contents	26
4.	TMI-2 distinct core component examination program	29
5.	Oxide layer measurements on zircaloy guide tube 3-14C/G	66

6.	Zircaloy cladding measurements from fuel rod 3-30	77
7.	Zircaloy cladding measurements from fuel rod 3-42	78
8.	Selected components for radiochemical analysis	80
9.	Radioisotopic surface activities	82
10.	Fuel rod segment surface deposit elemental analysis results	92
11.	Control rod and control rod/guide tube surface deposit elemental analysis results	93
12.	Guide tube surface deposit elemental analysis results	95
13.	Average and range of elemental surface concentrations for core constituents	97
14.	Zirconium/tin ratio	100
15.	Elemental ratios for Ag, In, and Cd	103
16.	Fuel pellet radionuclide concentrations	107
17.	Fuel rod segment surface deposit radiochemical analysis results	108
18.	Control rod and control rod/guide tube surface deposit radiochemical analysis results	109
19.	Guide tube surface deposit radiochemical analysis results	110
20.	Calculated radionuclide retention for the intact pellets	112
21.	Average radionuclide retention normalized to Ce-144	114
22.	Average radionuclide concentration on exterior surfaces	116
23.	Radionuclide content of upper core surfaces	120

1. The first part of the document is a list of names and addresses of the members of the committee. The names are listed in alphabetical order, and the addresses are given in full. The list includes the names of the members of the committee, the names of the members of the sub-committee, and the names of the members of the advisory committee. The addresses are given in full, including the street, city, and state.

2. The second part of the document is a list of the names and addresses of the members of the committee. The names are listed in alphabetical order, and the addresses are given in full. The list includes the names of the members of the committee, the names of the members of the sub-committee, and the names of the members of the advisory committee. The addresses are given in full, including the street, city, and state.

3. The third part of the document is a list of the names and addresses of the members of the committee. The names are listed in alphabetical order, and the addresses are given in full. The list includes the names of the members of the committee, the names of the members of the sub-committee, and the names of the members of the advisory committee. The addresses are given in full, including the street, city, and state.

4. The fourth part of the document is a list of the names and addresses of the members of the committee. The names are listed in alphabetical order, and the addresses are given in full. The list includes the names of the members of the committee, the names of the members of the sub-committee, and the names of the members of the advisory committee. The addresses are given in full, including the street, city, and state.

5. The fifth part of the document is a list of the names and addresses of the members of the committee. The names are listed in alphabetical order, and the addresses are given in full. The list includes the names of the members of the committee, the names of the members of the sub-committee, and the names of the members of the advisory committee. The addresses are given in full, including the street, city, and state.

EXAMINATION OF THE TMI-2 CORE DISTINCT COMPONENTS

1. INTRODUCTION

The purpose of this report is to provide descriptions of fuel assembly components (distinct components) that have been removed from the TMI-2 core and shipped to the Idaho National Engineering Laboratory (INEL) for examination and storage and to present the examination results of fuel and control rod samples obtained from these components. The objectives of the examinations are: (a) to characterize the conditions of representative samples from the core, (b) to aid in providing a better understanding of the temperature conditions that existed in the core during the accident, (c) to provide additional information related to the transport, deposition, and interaction of fuel and control rod materials with other core materials during a severe core damage accident, and (d) to obtain information on the retention and surface deposition of fission products on intact fuel assemblies.

The examination of TMI-2 core distinct components is part of the TMI-2 reactor sample acquisition and examination program, which is summarized in the EG&G Idaho, Inc. report entitled, TMI-2 Accident Evaluation Program Sample Acquisition and Examination Plan.¹

1.1 Background

Although the March 28, 1979, accident at TMI-2 involved severe damage to the core of the reactor, it had no observable effects on the health and safety of the public in the area.¹ That such a severe core-disruption accident would have no consequent health or safety effects has resulted in the questioning of earlier light water reactor (LWR) safety studies and estimates. In an effort to resolve these questions, several major research programs have been initiated by a variety of organizations concerned with nuclear power plant safety. The U.S. Nuclear Regulatory Commission (NRC) has embarked on a thorough review of reactor safety issues, particularly the causes and effects of core-damage accidents. As part of this effort,

the U.S. Department of Energy (DOE) established the TMI-2 Program to develop technology for recovery from a serious reactor accident and to conduct relevant research and development that will enhance nuclear power plant safety.

Immediately after the TMI-2 accident, four organizations with interests in both plant recovery and accident data acquisition formally agreed to cooperate in these areas. These organizations, commonly referred to as the GEND Group--GPU Nuclear Corporation, Electric Power Research Institute, Nuclear Regulatory Commission, and Department of Energy--are actively involved in reactor recovery and accident research. At present, DOE is providing a portion of the funds for reactor recovery (in those areas where accident recovery knowledge will be of generic benefit to the U.S. LWR industry) as well as the majority of funds for severe accident technical data acquisition (such as the examination of the damaged core).

The INEL involvement with TMI-2 has been continuous since the accident, providing technical support and consultation. In 1979, the INEL received an assignment from DOE to collect, analyze, distribute, and preserve significant technical information available from TMI-2. This assignment was expanded (in 1981 and 1984) to include: (a) conducting research and development activities intended to effectively exploit the generic research and development challenges at TMI-2, and (b) developing an understanding of the accident sequence of events in the area of core damage and behavior of fission products and materials.

The TMI-2 Accident Evaluation Program report² defines the program required to implement the DOE assignments and contains the guidelines and requirements for TMI-2 sample acquisition and examinations.

The TMI-2 core examination plan describes four categories of examination. The first category includes in situ examinations at TMI-2 and is intended to provide on-site documentation of the postaccident condition of the core. This is done primarily by closed circuit television camera

(CCTV) inspections of the core and lower vessel, as well as ultrasonic mapping of the core cavity. Examples of CCTV examination results are provided in Reference 3.

The second category includes characterization of surface deposits on reactor coolant system (RCS) artifacts from locations other than the core region. It includes examination of the following reactor coolant system components and structures: control rod leadscrews, leadscrew support tubes, plenum cover debris, resistance thermal detector (RTDs) thermowells, steam generator manway cover backing plates, and makeup and letdown system filters.

The third category includes characterization of the condition of the core by examination of samples taken from the reactor core and lower vessel. Samples include core debris grab samples from the rubble bed, fuel rod segments, core stratification samples, distinct fuel assembly and control rod cluster components (e.g., cladding, control rods, spiders, spacer grids, end fittings, holddown springs), incore instrumentation, and debris from the lower vessel.

The fourth category includes examination of miscellaneous components and items not specifically included in categories one, two, and three. Examinations in this category include those of reactor building basement sediment and the reactor coolant drain tank contents.

The already-completed portion of the Sample Acquisition and Evaluation (SA&E) Plan includes in situ measurements and sample acquisition and examinations involving private organizations and state and federal agencies. It has provided the postaccident core and fission product end-state data that indicate the following:

- Large regions of the core exceeded cladding melting (~2200 K). Also, significant fuel liquefaction by melted zircaloy and some fuel melting occurred with temperatures up to at least 3100 K.

- The May 1987 estimate of damage and configuration of the core is as follows:

Core Region	Core Material (%)
Still standing rod bundle geometry	42
Loose debris (unmelted and previously molten core material mixture) below the cavity in the upper core region (the cavity was 26% of the original core volume)	23
Previously molten core material:	35:
Retained in core boundary	19
Escaped from core boundary	16

- Fission-product retention in core materials is significant. The retention of fission products outside the core was primarily in reactor cooling system (RCS) water, water in the basement, and in basement concrete.

Significant consequences resulting from these findings include:

(a) increased technical interest in the TMI-2 accident because it represents a full-scale severe-core-damage (SCD) event and provides evidence of a large difference between actual and predicted SCD event offsite radiation release, (b) a reconsideration of the plans and equipment for defueling the TMI-2 reactor, and (c) an expansion in the TMI-2 accident examination plan to determine the consequences of high temperature interactions between core components and to determine the release from the fuel of the lower volatility fission products.

A major task of the TMI-2 Accident Evaluation Program is to examine fuel samples taken from the core and lower vessel (category three described previously). Fuel removal was initiated on November 12, 1985. During FY-1986, fuel removal was limited to the core cavity walls and floor and consisted of upper end fittings from fuel, control rod and burnable poison rod (BPR) assemblies, partial fuel assemblies, and unsegregated loose debris. This represents a cumulative total weight of 51,000 lbs of the 300,000 lbs of material present in the reactor core. These distinct core

components and materials were removed from the reactor vessel in specially designed fuel canisters. A total of 49 fuel canisters had been loaded and transferred to the TMI Fuel Handling Building by October 1, 1986, and 21 of these were shipped to the INEL for unloading and/or interim storage in FY-1986.

1.2 TMI-2 Core History

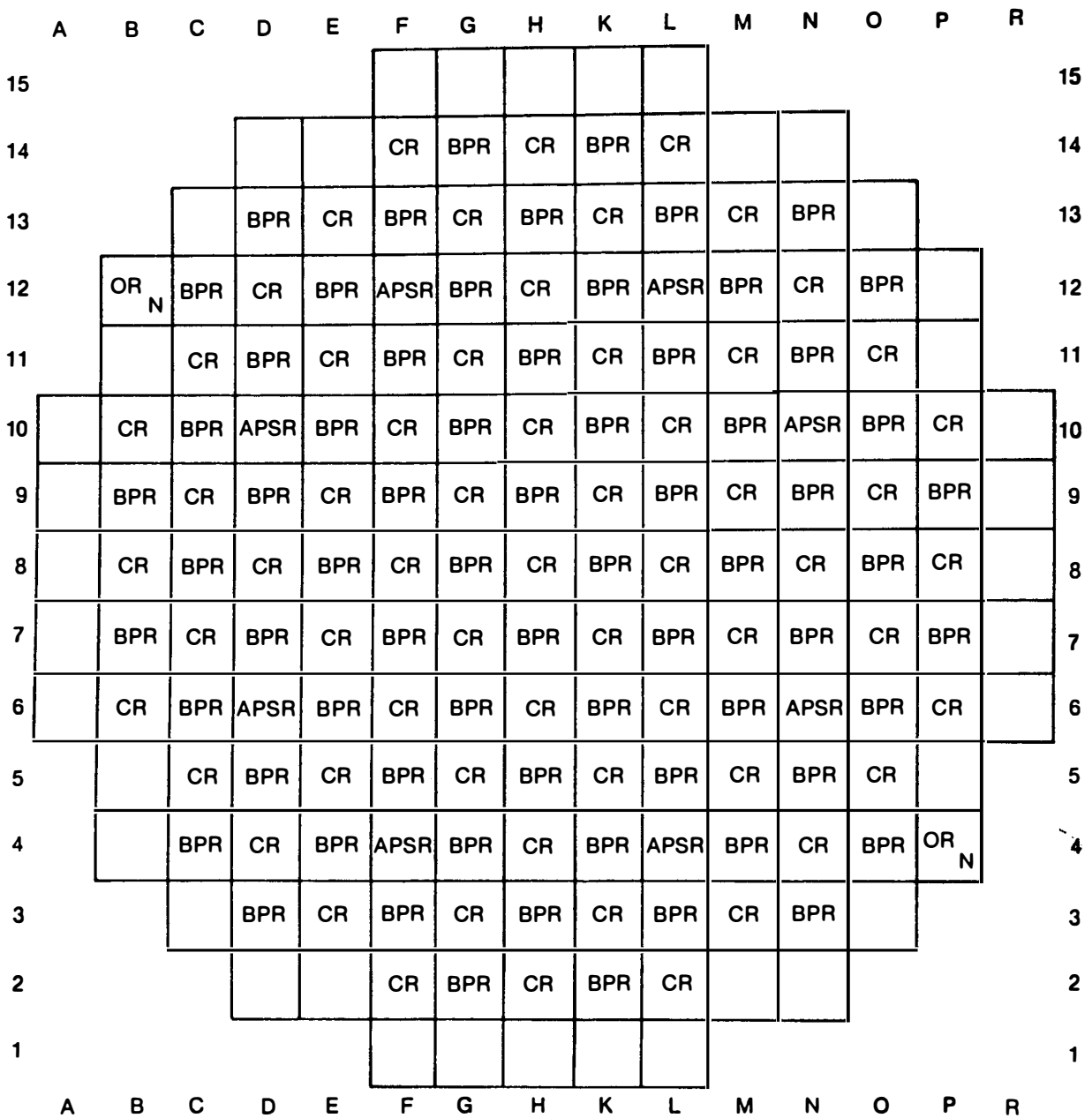
The periods of interest in the history of the TMI-2 core distinct components examinations are: (a) the core loading and operation before the accident, (b) the accident sequence that damaged the core components, and (c) the postaccident reactor vessel internals disassembly activities that caused further relocation and separation of core components. Each of these periods is briefly described.

1.2.1 Preaccident Conditions and Configuration

At accident initiation, the TMI-2 core was in the initial fuel cycle at 97% of full power with 3258 MWD/MTU average core burnup. The core loading consisted of 177 fuel assemblies and 139 rod assemblies arranged in the core positions as shown in Figure 1.

Each of the fuel assemblies (see Figure 2) is a 15 x 15 array of 208 fuel rods, 16 zircaloy guide tubes and 1 center-position zircaloy instrument tube connected to and supported by 8 Inconel spacer grids and 304L stainless steel upper and lower end fittings. An Inconel, coil-type holddown spring is located in the upper end fitting.

All interior and 2 of 40 peripheral core positions also have rod assemblies consisting of 16 rods connected together at the top by arms extending from a central hub. The rods fit into the fuel assembly guide tubes. Two peripheral fuel assemblies (core positions B12 and P4, next to the core former wall) contain a stationary orifice rod assembly (see Figure 3) with 12-in.-long stainless steel rods extending into the guide tubes to restrict coolant flow, of which one in each assembly is assumed to

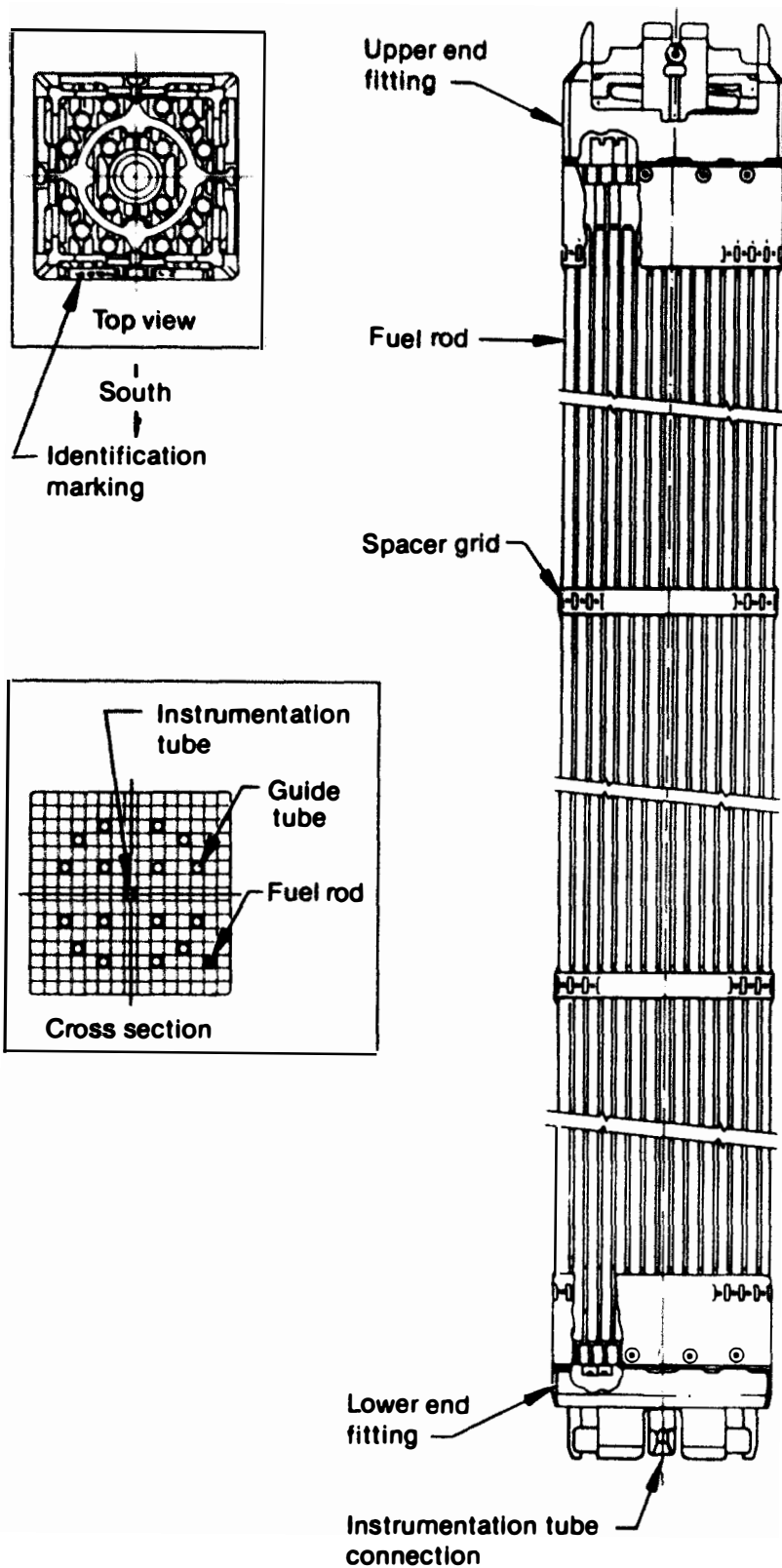


OR Orifice Rod Assembly
 CR Control Rod Assembly
 BPR Burnable Poison Rod Assembly

APSR Axial-Power-Shaping Rod Assembly
 N Primary Neutron Source

6 4690

Figure 1. TMI-2 core loading diagram.



7-0527

Figure 2. Side, top, and cross-sectional views of TMI-2 fuel assembly (from Reference 4).

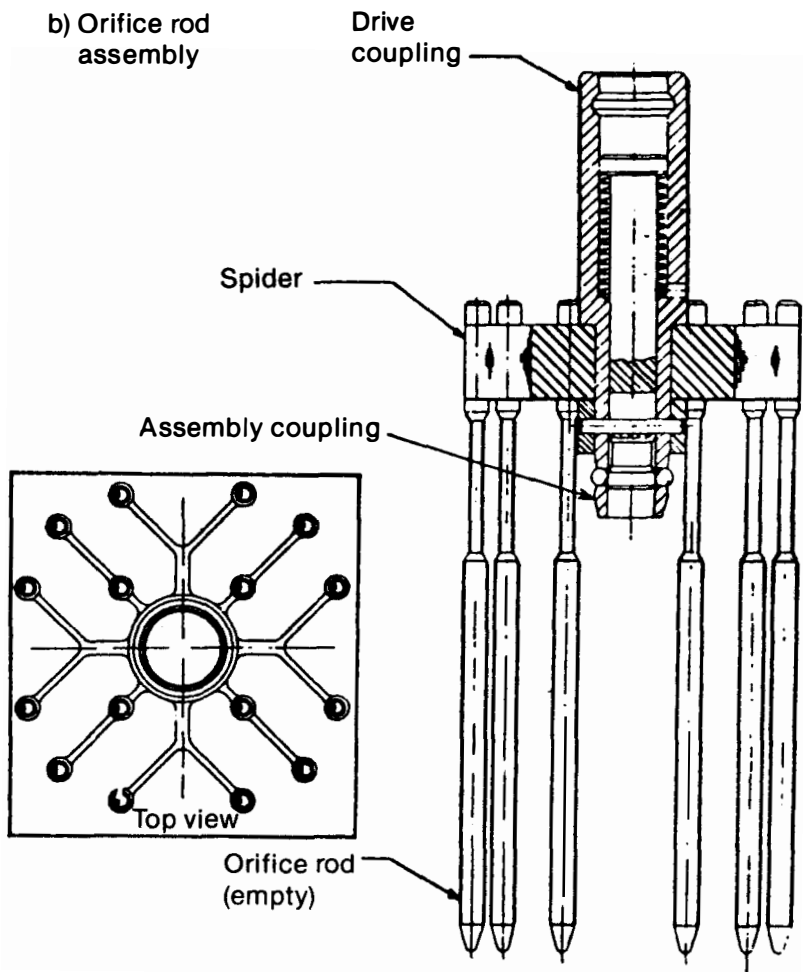


Figure 3. Orifice rod assembly (from Reference 4).

be modified to include a neutron source rod. Interior fuel assemblies contain one of three types of rod assemblies as follows:

- Burnable Poison Rod (BPR) Assembly (see Figure 4)--The stationary burnable poison rod assemblies are located in 72 core positions as shown in Figure 1. Each BPR rod contains a 126-in.-long stack of ceramic pellets [Al_2O_3 (0.95), B_4C (0.01), and impurities (0.04)] clad in zircaloy, except for core position N13, which is assumed to contain 8 rods with borated graphite instead of $\text{Al}_2\text{O}_3\text{-B}_4\text{C}$ (per assumed design specifications).
- Control Rod (CR) Assembly (Figure 5)--The CR assemblies are located in the 61 core positions shown in Figure 1. The rods contain 134-in. lengths of Ag-In-Cd clad in Type 304L stainless steel. The CR assemblies were fully inserted during the accident sequence.
- Axial Power Shaping Rod (APSR) Assembly (Figure 6)--The APSR assemblies are located in the eight symmetrical core positions shown on Figure 1. Each rod contains a 36-in.-length of Ag-In-Cd material clad in stainless steel. The APSR assemblies remained withdrawn at 37 in. during the accident sequence. The original elemental composition and total weights of principal components for the core and a control rod fuel assembly are presented in Table 1.

1.2.2 TMI-2 Accident Sequence

Reference 2 includes the current theory of the TMI-2 core damage progression. A summary of this theory is as follows:

"The accident was initiated by cessation of secondary feedwater flow. The steam generator boiled dry, and the resultant reduction of primary-to-secondary heat exchange caused the primary coolant to heat up, surge into the pressurizer, and increase the primary system pressure. The pilot-operated relief valve (PORV) opened to relieve pressure but failed to close when the pressure decreased. The first 100 min of the accident can be

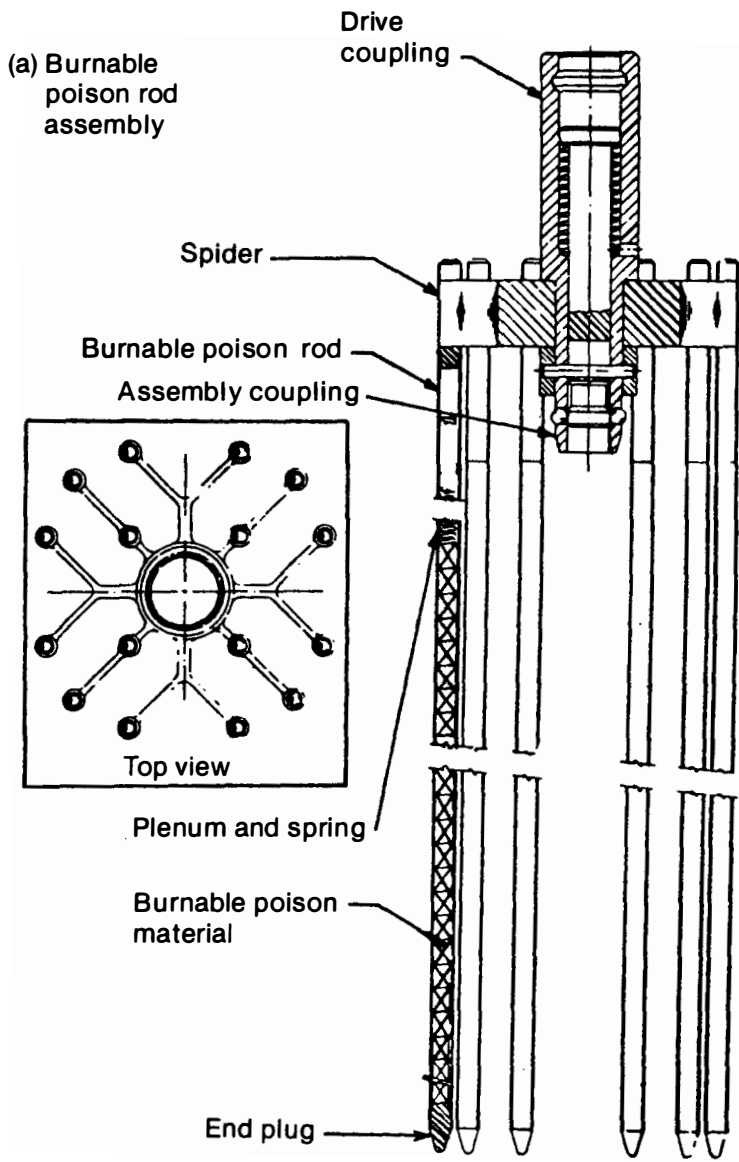


Figure 4. Burnable poison rod assembly (from Reference 4).

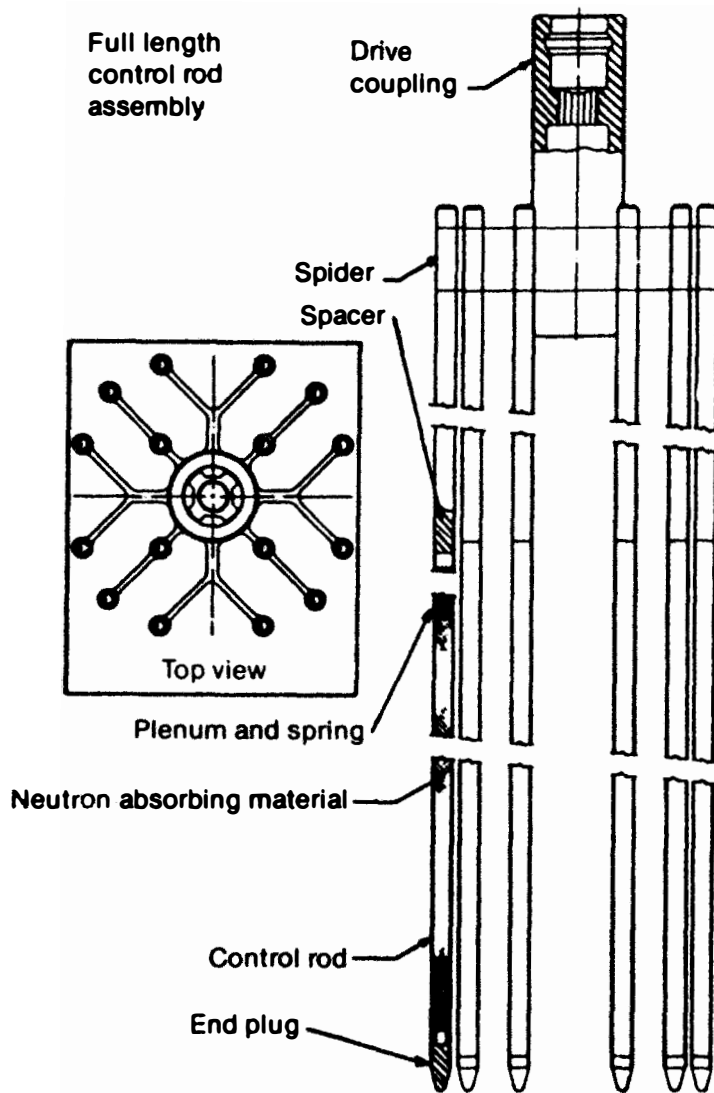


Figure 5. Control rod assembly (from Reference 4).

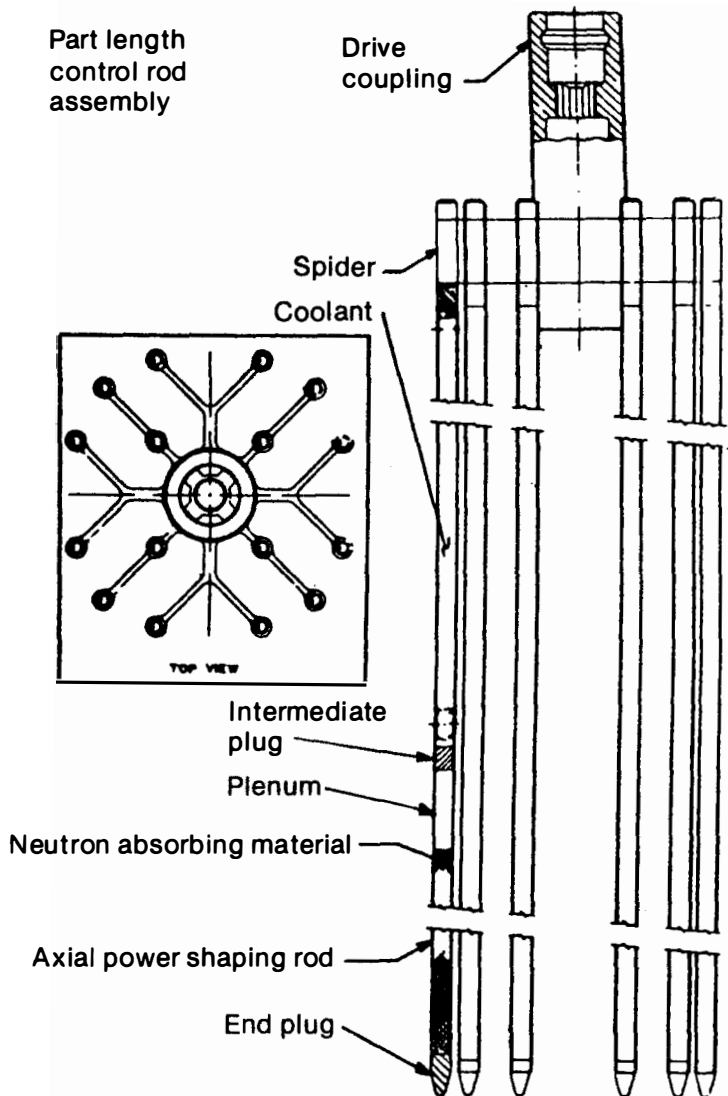


Figure 6. Axial-power-shaping-rod (APSR) assembly (from Reference 4).

TABLE 1. TMI-2 REACTOR CORE COMPOSITION

Material (Weight)	Element	Weight Percent	Material (Weight)	Element	Weight Percent	
UO ₂ (94,029 kg) (531.9 kg) ^b	U-235 ^a	2.265	Inconel-718 (1,211 kg) (6.8 kg) ^b	Ni ^a	51.900	
	U-238 ^a	85.882		Cr ^a	19.000	
	O	11.853		Fe ^a	18.000	
Zircaloy-4 (23,177 kg) (125 kg) ^b	Zr ^a	97.907	Ag-In-Cd (2,749 kg) (43.6 kg) ^b	Nb ^a	5.553	
	Sn ^a	1.60		Mo ^a	3.000	
	Fe ^a	0.225		Ti	0.800	
	Cr ^a	0.125		Al ^a	0.600	
	O	0.095		Co	0.470	
Type 304 Stainless Steel (676 kg) and Unidentified Stainless Steel (3,960 kg) (16.8 kg) ^b	Fe ^a	68.635		B ₄ C-Al ₂ O ₃ (626 kg) (0 kg) ^b	Si ^a	0.200
	Cr ^a	19.000			Mn ^a	0.200
	Ni ^a	9.000			N	0.130
	Mn ^a	2.000		Gd ₂ O ₃ -UO ₂ (131.5 kg) (0 kg) ^b	Cu	0.100
	Si ^a	1.000			Ag ^a	80.0
	N	0.130			In ^a	15.0
C	0.080	Cd ^a			5.0	
Co ^a	0.080	Gd ^a		Al ^a	34.33 ^c	
			O	30.53 ^c		
			B ^a	27.50 ^c		
			C	7.64 ^c		
			Gd ^a	10.27 ^c		
			U ^a	77.72 ^c		
			O	12.01 ^c		

- a. Elements for which ICP analysis was performed.
- b. Weight of material in a control rod fuel assembly.
- c. Data are suspect.

characterized as a small break loss-of-coolant accident (LOCA) with resultant loss of primary coolant and decreasing pressure. It differed from the scenario expected during such a LOCA in that the pressurizer liquid level remained high. This was interpreted by the reactor operator as indicating that the reactor coolant system (RCS) was full of water when in fact, the RCS was continually voiding. Up to 100 min, the core was covered with sufficient water to be cooled.

The reactor coolant pumps were turned off at 100 min, and core heatup was initiated as the water level stratified and decreased below the core top. By 150 min, a zircaloy-steam exothermic reaction was initiated, dramatically increasing the core heatup rate. As a result, zircaloy melting temperatures were exceeded, resulting in relocation of the molten zircaloy and some liquefied fuel to the lower core regions, solidifying near the coolant interface. This continued until 174 min, when a large region of consolidated, degraded core material existed in the lower, central regions of the core. Coolant flow through this consolidated core region indicates that the lower 0.5 m of the core remained cool.

A reactor coolant pump was turned on briefly at 174 min, and coolant was pumped into the reactor vessel. The resultant thermal-mechanical forces generated from the rapid steam formation are believed to have shattered the oxidized fuel rod remnants in the upper regions of the core, forming a rubble bed on top of the consolidated core materials. The consolidated core materials continued to heat up during the next 50 min (174 to 224 min), even though coolant delivery to the reactor vessel from the pump transient and emergency core cooling injection is estimated to have covered the core by approximately 210 min. By 224 min, much of the consolidated region had reached temperatures sufficient to melt the U-Zr-O ternary mixture.

On-line TMI-2 data recorded during the accident indicate that the crust surrounding the consolidated core failed and some of the molten core material relocated to the lower plenum between 224 and 226 min. Based on the end-state core and core support assembly (CSA) configuration and supporting analysis of the degraded core heatup, it is believed that the crust failure occurred near the top of the molten core region in the southeast quadrant of the reactor vessel. Limited damage to the CSA occurred as the core material flowed to the lower plenum. Estimates of the maximum pressure vessel wall temperatures indicate that the melting point of stainless steel was not exceeded, even at the inside surface of the pressure vessel liner. The instrument assemblies, however, may have melted in the lower plenum above the vessel penetration weld. If this occurred, freezing of the molten material is predicted to have plugged any holes in the instrument assembly tubes."

Since the accident, the core components have remained at ambient temperature and pressure and are submerged in water with the following target specifications:

- pH: 7.5 to 7.7
- boron: >4350 ppm

1.2.3 Postaccident Reactor Vessel Internals Disassembly Activities

A series of disassembly activities, including precursor examinations, was accomplished between the accident-sequence termination and December 22, 1985. These activities affected or determined the condition of the core cavity walls and floor. No activities or examinations were attempted until personnel access inside the reactor building was reestablished in 1981. A summary of significant examination and disassembly events that have occurred is as follows:

1.2.3.1 Quick-Look Video Surveys. In 1982, control rod leadscrews from core positions H8, E9, and 88 were removed for possible CCTV access to the core area. The CR spider was still in place at 88, but was missing at core positions H8 and E9. The CCTV survey discovered a large void (core cavity) in the upper core region.

1.2.3.2 APSR Assembly--Insertion.⁵ In the first quarter of CY 1983, an attempt was made to insert all eight APSR assemblies which, if successful, would relocate the APSRs 37 in. downward (see Figure 1 for APSR core locations). Insertion into the core cavity depths were as follows:

<u>Core Position</u>	<u>Insertion Depth (in.)</u>
D6	0
D10	4
F4	30
F12	35
L4	8
L12	31
N6	0
N10	37

1.2.3.3 Ultrasonic Scanner Survey.⁶ On August 31, 1983, an ultrasonic scanner survey was made to determine the shape and dimensions of the core cavity. Figures 7 through 10 are the topographical maps of the core cavity. The core topographical features included the following:

- The cavity extended from the upper grid-plate bottom downward to approximately 7.5 ft above the core bottom and radially to the core former wall in some places.
- The core cavity volume was equivalent to approximately 26% of the original core region.
- Fuel assembly remnants appeared to encircle the core cavity completely toward the upper grid plate; the maximum fuel assembly damage appeared to be on the core east side, and the least fuel assembly damage on the core west side.
- The APSRs that had been inserted projected from the cavity ceiling and interfered with ultrasonic-scanner measurement of topography in the cavity upper regions.

1.2.3.4 Reactor Vessel Head Removal.⁷ In July 1984, the reactor vessel head removal, which included prerequisite uncoupling of the leadscrews from the CR assemblies and raising the leadscrew into the control rod drive mechanism (CRDM), was accomplished. The leadscrew uncoupling indicated the following:

- Thirty CR spiders were supported by the fuel assembly upper end fitting.
- Twenty-three CR spiders appeared to be unsupported by the fuel assembly upper end fitting, or were missing.
- Four CR spiders became supported by the fuel assembly upper end fitting when lowered a small distance (less than 2 in.).

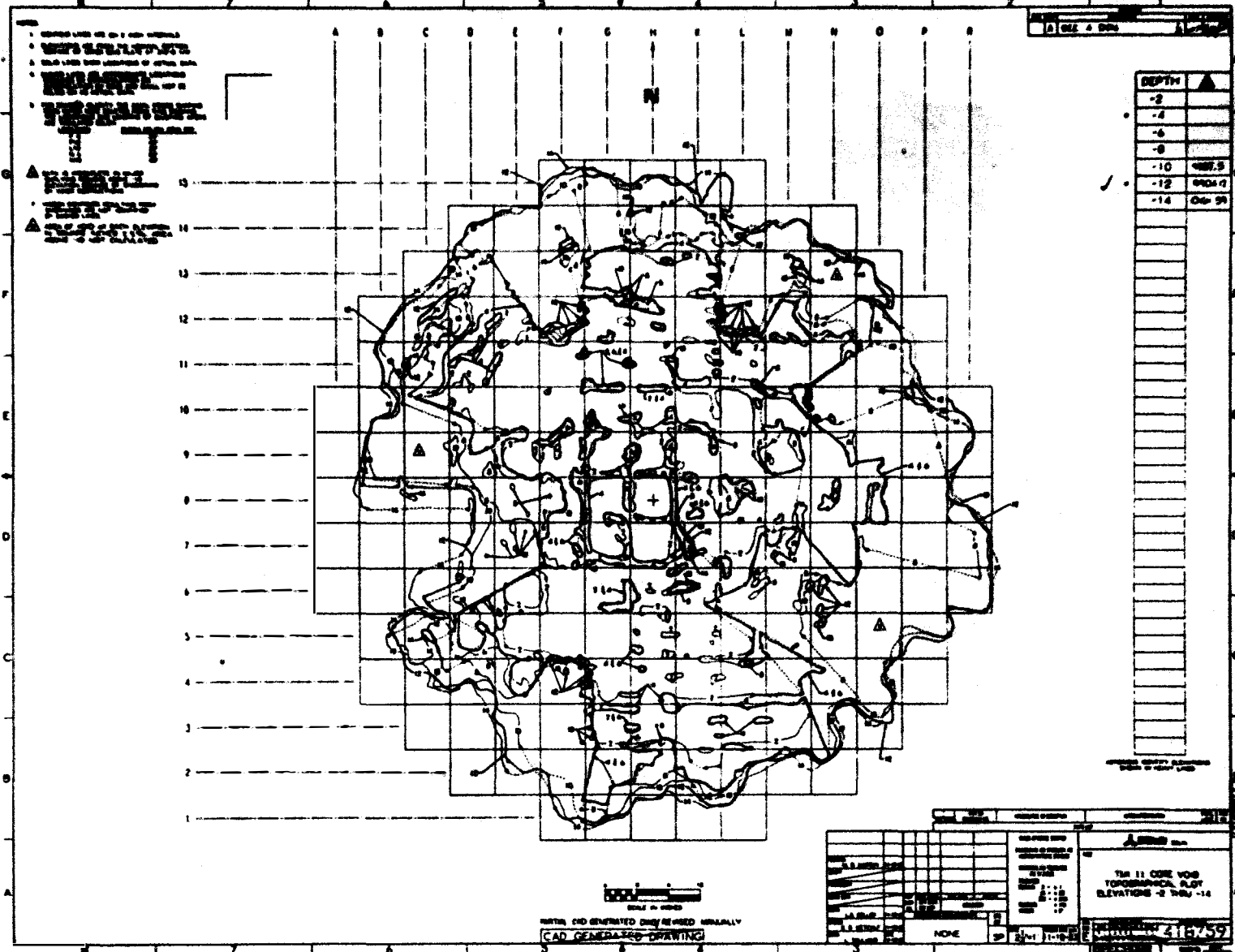


Figure 7. TMI-2 core void topographical plot elevations -2 through -14.

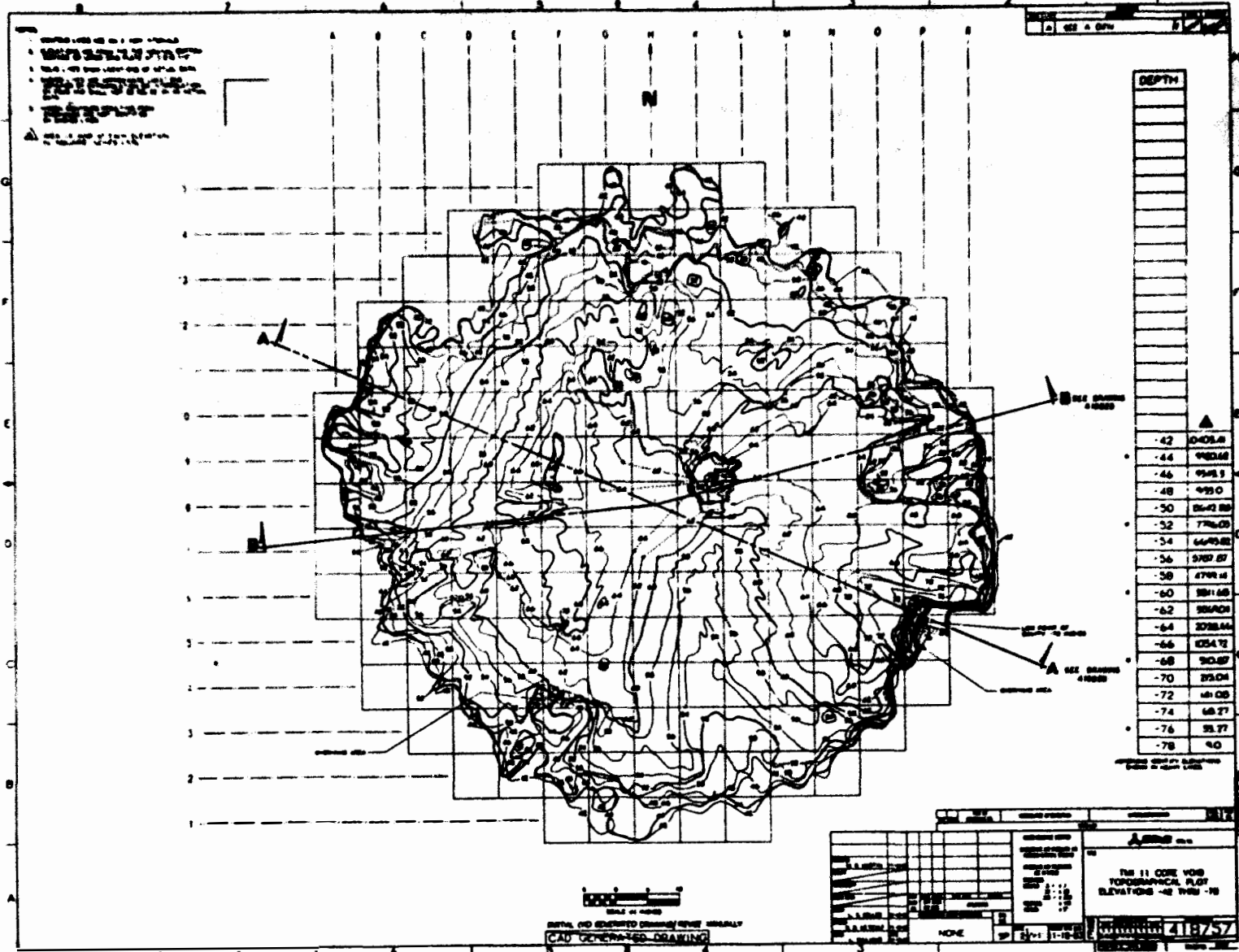


Figure 9. TMI-2 core void topographical plot elevations -42 through -78.

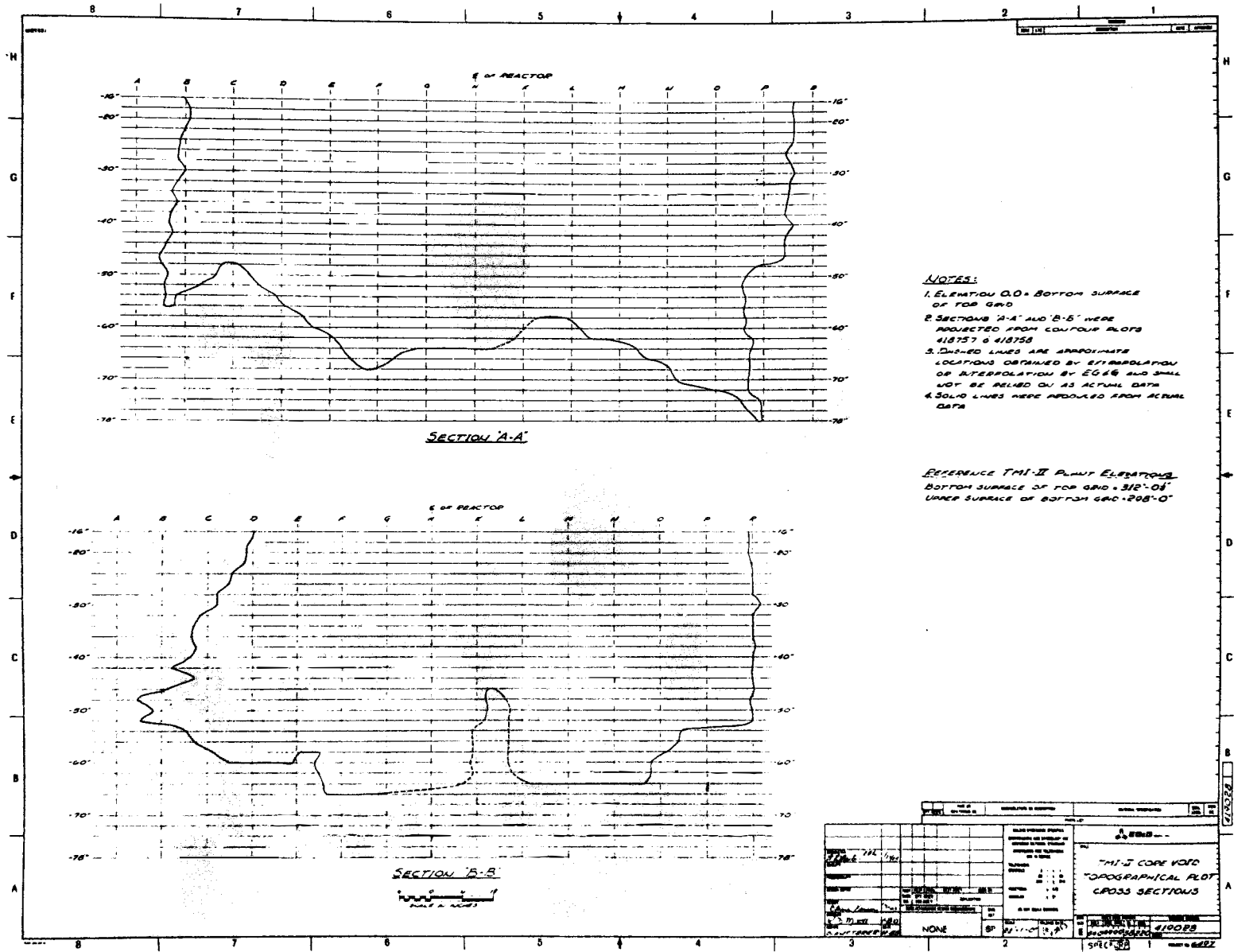


Figure 10. TMI-2 core void topographical plot cross sections.

1.2.3.5 Plenum Assembly Removal.^{8,9} In May 1985, the plenum assembly removal, which included prerequisite removal of fuel assembly upper end fittings⁸ and water jet flushing of loose debris from horizontal (upward facing) surfaces,⁹ was accomplished. The dislodging of fuel assembly upper end fittings indicated the following:

- Four upper end fittings (core positions D5, F3, F13, and K14) could not be dislodged.
- Ten upper end fittings (core positions E4, G14, K6, L2, L13, O3, O8, O11, P8, and R6) could only be partially dislodged.
- All other end fittings were missing, dislodged, or attached to their respective fuel bundles.

Damage to the plenum assembly bottom surface that was in contact with the fuel assembly upper end fittings is shown in Figure 11. The damage map was determined from video surveys.

The water jet flushing removed loose debris "ranging in size from very fine particles to nearly fuel pellet size"⁹ from the plenum assembly, upward-facing, horizontal surfaces. Post-flushing CCTV inspection indicated "some of the debris actually adhered to the plenum and could not be removed."⁹

1.2.3.6 Early Fuel Removal. Early fuel removal commenced on November 12, 1985. By January 27, 1986, eighteen fuel canisters, including D-141 and D-153, had been loaded with approximately 110 upper end fittings from fuel, CR and BPR assemblies, five partial-fuel assemblies, and miscellaneous loose debris. The early fuel removal included some successful and unsuccessful attempts to topple standing peripheral fuel assemblies onto the core cavity floor to provide clearance for the fuel canisters, occasional unaided toppling of unstable standing peripheral fuel assemblies onto the core cavity floor, and shear-tool sectioning of some partial fuel assemblies lying on the floor of the core cavity.

R P O N M L K H G F E D C B A

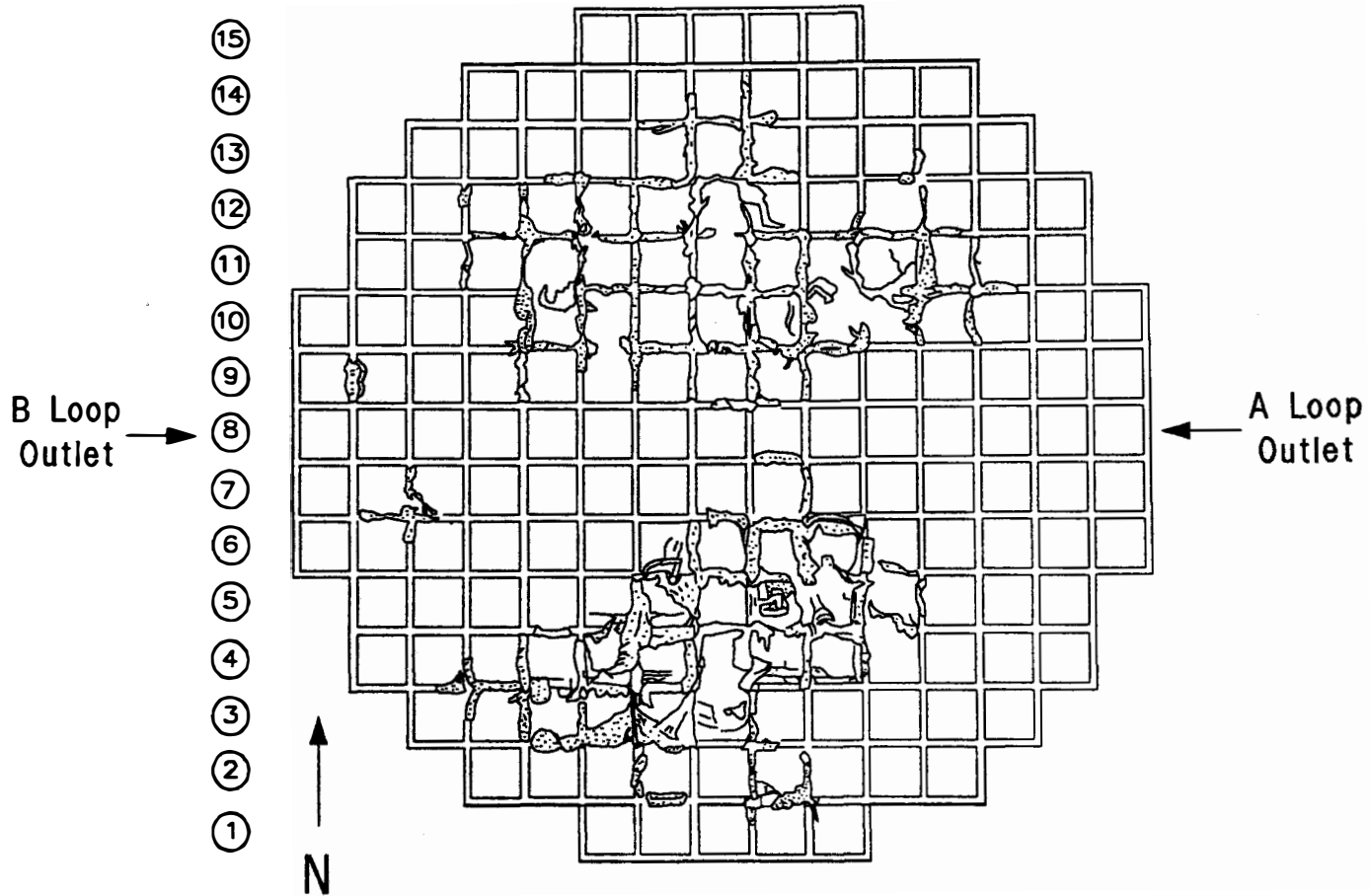


Figure 11. Damage map of the TMI-2 fuel assembly upper grid plate.

Acquisition of the distinct components that were loaded into canisters D-141 and D-153 is described briefly in Section 2. Sample examination and analysis methods are described in Section 3. Section 4 presents a brief description of the visual examination of the components that were removed from fuel canisters D-141 and D-153. Specific fuel and control rod sample characterization and selections are described in Section 5, and the metallurgical, radionuclide, and elemental analysis results from these samples are presented in Section 6. A summary and conclusions are provided in Section 7. Neutron radiography and gamma scan results are provided in Appendices A and B, respectively. Appendix C contains a more extensive discussion of the acquisition of distinct components, and Appendix D provides additional details on the visual examination of the components removed from canisters D-141 and D-153.

2. DISTINCT COMPONENT ACQUISITION

This section provides a brief description of the distinct components that were removed from the TMI-2 core and examined at the INEL.

2.1 Loading of Canisters at TMI-2

Removal of distinct components from the damaged TMI-2 core was initiated in November 1985. The procedure involved reaching into the core cavity with a long-handled grappling tool, picking up loose debris, usually in the form of upper end fittings from which all the fuel and/or control rods had fallen out (or were otherwise removed), and putting the debris into specially designed "fuel canisters" that had been placed in the reactor vessel. During FY-1986 a total of 49 fuel canisters had been loaded and transferred to the TMI Fuel Handling Building, and 21 of these had been shipped to the INEL for unloading and/or interim storage.

2.2 Unloading of Canisters at the INEL

Fuel canisters D-141 and D-153 were unloaded in the INEL Test Area North (TAN) hot cell in August 1986. The components removed from the two canisters are listed in Tables 2 and 3. Figure 12 shows the TMI-2 core loading diagram with the specific locations from which the identified components from both canisters D-141 and D-153 were removed.

All components removed from the canisters were visually examined to identify areas of melting and other temperature-related phenomena. In addition to the visual examinations, specific fuel rods and control rods inside guide tubes were selected from the partial fuel assemblies from core positions C7 and H1 for full-length gamma scanning and neutron radiography. Selected fuel and control rod samples were then obtained for metallographic and radiochemical examinations.

TABLE 2. FUEL CANISTER D-141 CONTENTS

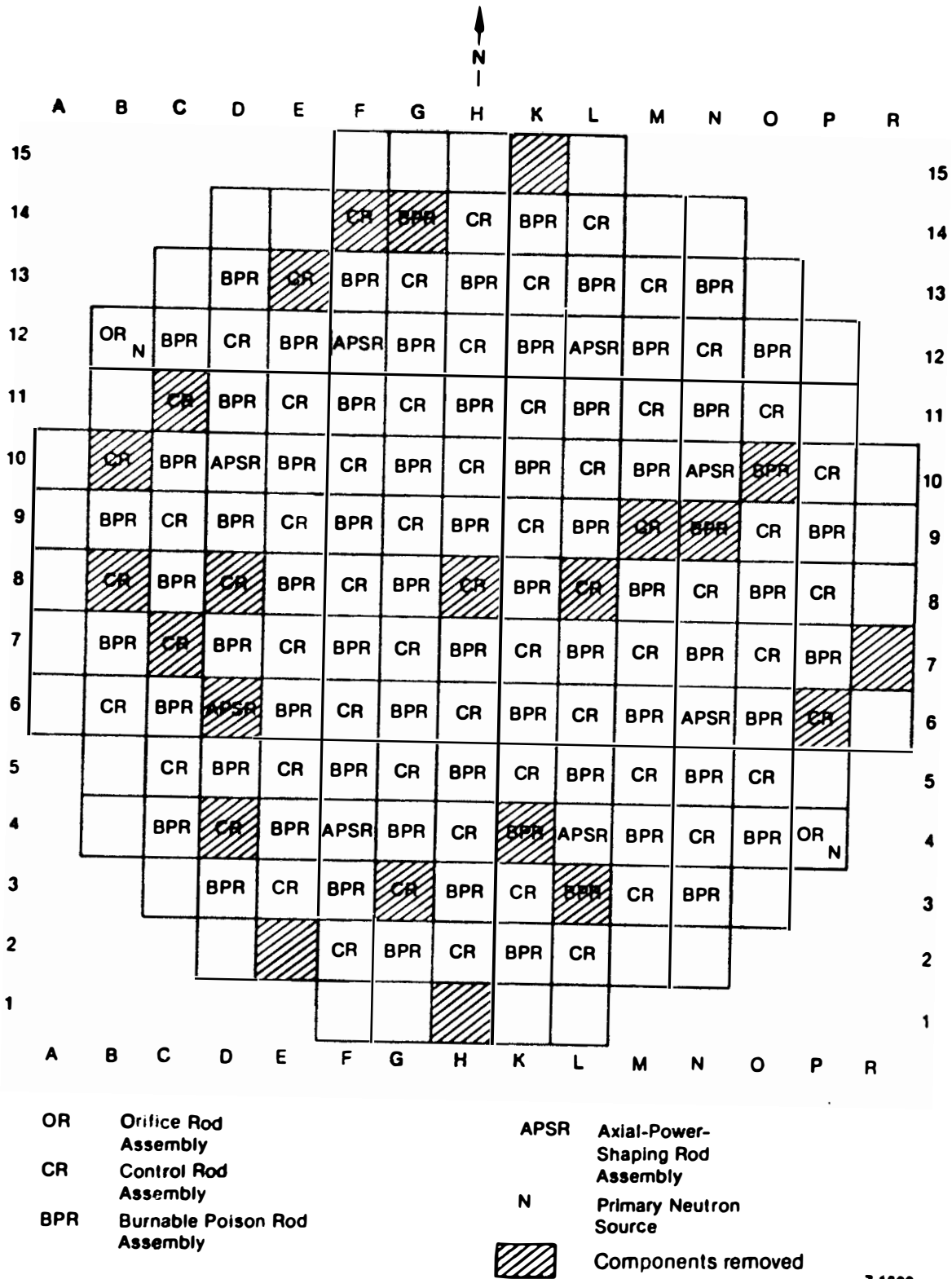
Canister Item Number	Core Position	Description	Identification Marking
1	E13	Fuel assembly partial upper end fitting and control rod spider.	C-157
2 ^a	C11	Partially melted control rod spider.	C-156
3 ^a	C7	Fuel assembly upper section with 119 fuel rod and 16 control rod/guide tube upper segments.	NJ 00Q8
4 ^a	N9	Fuel assembly partial upper end fitting (burnable poison rod assembly site).	NJ 00RZ
5 ^a	N9	Burnable poison rod assembly partial upper end fitting.	8-181
6 ^a	L3	Burnable poison rod assembly retainer.	L-051
7 ^a	K15	Peripheral fuel assembly partial upper end fitting.	NJ 00UV
8 ^a	M9	Fuel assembly partial upper end fitting Control rod assembly partial upper end fitting.	NJ 00RI C-167
9	LB	Fuel assembly partial upper end fitting Control rod assembly partial upper end fitting.	NJ 00RO C-142
10 ^a	H8	Fuel assembly partial upper end fitting Control rod assembly partial upper end fitting.	NJ 00RR C-123
11 ^a	H1	Peripheral fuel assembly upper section with 7 fuel rod and some guide tube upper segments (core instrument string is missing).	NJ 00UU

a. Stored in drums for possible future examinations.

TABLE 3. FUEL CANISTER D-153 CONTENTS

Canister Item Number	Core Position	Description	Identification Marking
1 ^a	K4	Burnable poison rod assembly retainer	L045
2	G14	Burnable poison rod assembly retainer	L037
3 ^a	D8	Fuel assembly partial upper end fitting Control rod assembly upper end fitting	Missing C-144
4 ^a	G3	Fuel assembly partial upper end fitting Control rod assembly upper end fitting	Missing C-178
5	E2	Peripheral fuel assembly upper end (without fuel rods)	NJ 00UZ
6 ^a	010	Burnable poison rod assembly partial upper end fitting	NJ 00SU
7	R7	Peripheral fuel assembly upper end fitting corner	NJ 00TL
8 ^a	P6	Fuel assembly partial upper end fitting Control rod assembly upper end fitting	NJ 00UP
9 ^a	B8	Fuel assembly partial upper end fitting Control rod assembly upper end fitting	NJ 00UB C-124
10	D4	Fuel assembly partial upper end fitting Control rod assembly upper end fitting	NJ 00PV C-155
11	F14	Control rod fuel assembly upper end fitting corner	NJ 00UQ
12	06	APSR fuel assembly partial upper end fitting	NJ 00UA
13 ^a	B10	Fuel assembly partial upper end fitting Control rod assembly upper end fitting	NJ 00UA C-132

a. Stored in drums for possible future examinations.



7-1633

Figure 12. TMI-2 core loading diagram showing locations of components removed from canisters 0-14T and D-153.

3. SAMPLE EXAMINATION AND ANALYSIS METHODS

Table 4 summarizes the specific examinations that were performed on the TMI-2 distinct core components and categorizes the examinations as nondestructive and destructive. As was described in Section 2, all components removed from the TMI-2 core were viewed in situ, via closed circuit television (CCTV). These observations helped to identify the locations in the core from which the components were removed and to evaluate the physical condition and appearance of each component prior to removal from the reactor vessel.

Following receipt of the shipping canisters at the INEL TAN hot cells, all components removed from the canisters were again visually examined and were photographed. Gross and spectral gamma scans and neutron radiographic examinations of the fuel and control rods also provided important information used in the selection of specific samples for additional analyses. This section briefly describes the techniques used to perform the various examinations and the information obtained from each.

3.1 Nondestructive Examinations

As shown in Table 4, nondestructive examinations of the TMI-2 distinct core components included CCTV video tapes, photographs that were taken in the INEL TAN hot cell, neutron radiographs that were taken of specific fuel and control rods, and gamma scans of some of the same fuel and control rods on which neutron radiography was performed.

3.1.1 Video Tapes (CCTV)

The in situ video tapes were taken with an underwater camera with a light source that provided a viewing range of 2-3 feet in clear water, but maybe only a few inches in turbid water. The turbidity of the water in the TMI-2 vessel changed from time to time during the unloading process.

TABLE 4. TMI-2 DISTINCT CORE COMPONENT EXAMINATION PROGRAM

<u>Component</u>	<u>Nondestructive Exams</u>				<u>Destructive Exams</u>		
	<u>In Situ CCTV</u>	<u>Hot Cell Photograph</u>	<u>Neutron Radiograph</u>	<u>Gamma Scans</u>	<u>Metallography</u>	<u>Chemical Composition</u>	<u>Radiochemical</u>
Fuel assembly upper end fittings	X	X					
Control and burnable poison rod assembly upper end fittings	X	X					
Fuel rod upper ends	X	X	X	X	X	x ^a	x ^a
Control rod upper ends	X	X	X	X	X	x ^a	x ^a

a. Examinations in progress.

The video tapes provided a means for observing and recording the initial conditions of the core following the accident and for identifying the original location of the distinct components as they were removed from the core and loaded into the shipping canisters.

3.1.2 Hot Cell Photography

A variety of photographs (35 mm, Polaroid, black and white, color, etc.) were taken of all the distinct components as they were removed from the canisters and as they were visually examined in the hot cell. Photographs were usually taken of all six orientations (the four sides, top, and bottom). The results of these examinations are discussed in Section 4. Visual observations and photographs provided the basis for identifying prior molten, or otherwise damaged areas, for estimating fuel and other component temperatures that occurred during the accident, and for selection of fuel and control rod sections from which samples were subsequently taken for additional analyses.

3.1.3 Neutron Radiography

Neutron radiography was performed on 22 fuel rods, 7 control rods, and 7 guide tubes from the C7 and H1 fuel assemblies. The measurements were performed at the Coupled Fast Reactivity Measurement Facility (CFRMF) at the INEL. Individual rods were packaged in aluminum cylinders that were transported to the reactor facility in lead shielded transport tubes. Individual tubes were placed vertically over the entrance to the radiography port on the reactor and the top end cap removed. A cable was then connected to the handling ring attached to the top of the aluminum cylinder, and the cylinder was lifted off the bottom surface of the transport tube. The bottom end cap on the transport tube was then removed and the aluminum cylinder lowered into the reactor.

The neutron radiography facility at the CFRMF uses an epithermal neutron flux at a lower level of 100 kW. Experiments were performed to determine the necessary irradiation period to obtain radiographs with the

best resolution. It was determined that a one hour irradiation was appropriate using the dysprosium radiography foils normally used at the CFRMF.

3.1.4 Gamma Spectroscopy

Gamma spectroscopy measurements were performed using a gamma spectroscopy system developed at the INEL. The system is composed of an IBM PC-based data acquisition and control system, a high rate ORTEC intrinsic germanium detector, a 14 cm thick tungsten collimator system, and a scanning bed that can be used with samples up to 14 ft in length.

To perform this analysis, each rod or guide/tube was placed in a sealed aluminum tube which was placed on the spectrometer scanning bed. This allowed the rods to be translated past the collimated detector at a controlled rate of speed.

The gross gamma scan of each rod was performed to characterize the distribution of gross radioactivity and to identify locations of special interest. This was followed by isotopic measurements at approximately 3 cm intervals and at locations of interest determined from the gross scan information. From the twenty-nine rod sections that were gamma-scanned, five were chosen to provide samples for destructive analysis.

3.2 Destructive Examinations

Fuel rods 3-30 and 3-42, control rod 3-1C, control rod guide tube 3-1G, and the control rod/guide tube combination 3-14C/G from the D-141-3 partial fuel assembly were selected for destructive examinations. These particular rods were chosen to provide data on interior and exterior rod positions in the fuel assembly from core position C7, and on fuel rods located both adjacent to and away from control rod positions.

Three types of destructive examinations were performed: metallography, radiochemistry, and chemical composition (elemental analysis). The specific information obtained from each type of examination is discussed below.

3.2.1 Metallography .

The initial metallographic examinations of the distinct components from the TMI-2 core used only optical metallography, and the visual examinations provided data on the extent of fuel and zircaloy oxidation, fuel grain size and porosity, material behavior, and interactions between the different core materials. In addition, the observance of prior molten control rod materials and phase changes in the zircaloy cladding were useful in estimating peak temperatures.

The optical metallography technique involves viewing highly polished particles using a light microscope at magnifications up to about 500X. In addition, the samples are often treated with etchants to highlight grain boundaries and secondary phases. A brass holder is used to mount the sample in a lead/bismuth alloy. The alloy is melted (melting point 123.9°C) in a metal beaker and then poured into a preheated brass mount. The sample is then placed in the mount with the surface to be examined facing up. If the sample should float, it is held down so the examination surface is even with the surface of the lead/bismuth alloy.

The following grinding and polishing sequence was used for the TMI-2 core debris particles:

1. Coarse grind with water-lubricated silicon carbide 120 grit paper with a whirlamat.
2. Medium grind with 240 and 400 grit paper. Wash between grit sizes.
3. Final grind with 600 grit paper.
4. Initial polish with a mineral oil-type fluid lubricated by 6 μm diamond grit on a hard paper with a whirlamat.
5. Final polish with 3 μm diamond grit on a short nap nylon.

In general, a swab-etching technique was used, with the etching time varying, depending on whether a heavy or light etch was appropriate. The following fuel etchant was used for ceramic materials because all the debris samples were ceramic and contained urania: 85% H_2O_2 and 15% H_2SO_4 .

A zircaloy etch is used for the zircaloy cladding materials, but this etch is also useful for etching the Ag-In-Cd control rod materials. This etchant consists of the following ingredients:

- Lactic Acid 55%
- Nitric Acid 19%
- Water 19%
- Hydrofluoric Acid 7%

3.2.2 Radionuclide and Elemental Analyses

The objectives of performing radionuclide and elemental analyses on the TMI-2 distinct components are to characterize the distribution of fission products and core structural materials on surfaces in the upper core region, and to evaluate the retention of fission products in intact fuel material. To characterize the distribution of radionuclides and/or structural components on surfaces in the upper core region, two methods were used: (a) the intact fuel rods, control rods, and guide tubes were analyzed using gamma spectroscopy to evaluate the distribution of the deposited fission products, and (b) thirteen samples were obtained from the intact rods for quantitative radiochemical and elemental analyses.

To evaluate fission product retention in the intact fuel material, gamma spectroscopy measurements were made on the fuel rods to determine the variation in fission product generation in the fueled portions of the rods. Also, samples of the rods were obtained for a quantitative measurement of fission product retention in the intact fuel.

3.2.2.1 Sample Handling and Analysis Methods. The initial analysis performed on the intact fuel rods, control rods, or guide tube sections was gamma spectroscopy, which was described above under nondestructive analysis techniques.

For the fuel material analyses, the fuel pellets were removed from the cladding and dissolved using 5 M nitric acid in a closed system, which allowed the volatile I-129 to be retained and analyzed. Radioactive tracers were included for I-129 and Sr-90 to evaluate losses of these fission products on the surfaces of the dissolution apparatus.

For the cladding, control rod, and guide tube samples, the ends of the intact tubes or rods were sealed so that the radionuclide deposition on the inner and outer surfaces of the tubes could be analyzed separately. The exterior and interior surface leaches were done separately using 6 M hydrochloric acid. Tracers were included in the leach samples for I-129 and Sr-90. Two samples were not complete tubes, and therefore both surfaces (inside and outside) were leached at the same time. Based on the visual appearance of the samples and a series of repeated leaches performed on similar samples, only single leaches were performed on the remainder of the samples.

Aliquots of the leach and dissolution solutions were obtained for the following analyses: (a) quantitative gamma spectroscopy, (b) fissile material (U-235), (c) Sr-90, (d) I-129, and (e) elemental composition.

3.2.2.2 Gamma Spectroscopy. The initial radiochemical analysis performed on the sample aliquots was gamma spectroscopy. An aliquot of the leach solution was diluted to 60 ml and analyzed at calibrated distances from the germanium detector ranging up to 195 cm, depending upon the activity of the sample. The spectra obtained from the samples were then analyzed with a computerized gamma spectroscopy system using a VAX computer (analysis program GAP). This program identifies the radionuclides associated with the gamma-ray energy peaks and determines their emission rates corrected for detector efficiency, random pulse summing, and decay

during analysis. The equipment used was fabricated by EG&G Idaho, Inc. and calibrated using standard materials from the National Bureau of Standards.

The uncertainty associated with gamma spectroscopy analysis is less than 15%. However, with sampling and calibration uncertainties, the total uncertainty increases to approximately 20%, with the exception of those radionuclides whose concentrations were determined using low energy gamma rays (e.g., Eu-155). For this latter category, the total uncertainty is approximately 30%.

3.2.2.3 Fissile/Fertile Analyses. The fissile material content of all leach solutions was measured by neutron activation/delayed neutron analysis at the Coupled Fast Reactivity Measurement Facility (CFRMF) at the INEL. The total fissile content of the samples was measured by remotely exposing individual 1- by 5-cm cylinders containing liquid sample material to a thermal neutron flux, causing the U-235 and Pu-239 within the sample to fission and emit delayed neutrons. It was assumed that the quantity of Pu-239 was insignificant (<2 wt% of the U-235 based on theoretical predictions). This technique has an uncertainty of $\pm 10\%$ when insignificant amounts of neutron absorbers are present in the sample. To determine if significant quantities of the neutron absorbers (boron, silver, indium, or cadmium) were present, elemental analyses were also performed on the samples by inductively coupled plasma spectroscopy (ICP).

3.2.2.4 Sr-90 Analysis. The Sr-90 content of all aliquots was measured using liquid scintillation analysis. In this process, an aliquot of the leach or dissolution solution that contains the strontium carrier and tracer are subjected to a series of precipitations which separate Sr-90 from the other materials present in the sample. The separated Sr-90 then undergoes beta analysis in a liquid scintillation counter (Packard Tricarb 3385). The total uncertainty associated with this analysis is $\pm 10-20\%$.

3.2.2.5 I-129 Analysis. The I-129 analysis on all aliquots was performed using neutron activation analysis. The I-129 was volatilized during the dissolution of the sample material and, along with the I-131 tracer, was trapped in a dilute sodium hydroxide solution. The I-131

tracer was used to determine the amount of I-129 lost on surfaces during the dissolution. The I-129 was separated from the solution using an organic separations technique. The sample was then activated with standards in the Advanced Test Reactor (ATR) and analyzed using gamma spectroscopy for the neutron activation product I-130, from which the I-129 content could be calculated. The uncertainty associated with this analysis is approximately $\pm 10-15\%$.

3.2.2.6 Elemental Analyses. The elemental analyses performed on the aliquots of the leach solutions were performed to determine the quantities of core structural components deposited on surfaces within the core region. Elements for which analyses were performed are Ag, Al, B, Cd, Co, Cr, Fe, Gd, In, Mn, Mo, Ni, Nb, Si, Sn, U, and Zr. This analysis is performed using inductively coupled plasma (ICP) spectroscopy. The technique has an uncertainty of less than 10%.

4. VISUAL EXAMINATION DATA AND TEMPERATURE ESTIMATION

This section presents representative results from visual examinations of the distinct components from the upper regions of the TMI-2 core. Visual examinations provided information on the peak temperature distribution in these regions during the accident as well as the physical condition of the core following the accident. These temperature estimates were based upon the observance of the melted/unmelted boundary on various components. In addition, the possibility exists of a Fe-Zr eutectic interaction between the zircaloy guide tubes and the 304 SS tie plate and control rod cladding, and similarly a Ni-Zr eutectic interaction between the zircaloy guide tubes and the Inconel spacer grids at a minimum temperature of approximately 1220 K. At this temperature, the steel-zircaloy interaction is believed to proceed very slowly; however, at temperatures above 1470 K the reaction approaches equilibrium in a matter of minutes.¹⁰

In the following discussions of information obtained from the individual components, all orientations are referenced looking down on the top of the assembly, and it is assumed that all assemblies had been loaded into the TMI-2 core with the end fitting identification markings facing the south side of the core. Consequently, in views looking at the bottom side of a component, east and west appear switched from their normal compass positions.

Two of the components, D-141-3 and D-153-9, were upper end boxes from fuel assemblies that were originally in core positions C7 and B8, respectively. Both these components contained remnants of fuel rods and control rods, from which additional samples were obtained for detailed metallurgical and radiochemical analyses. Photographs of components D-141-3 and D-153-9 are shown in Figures 13 and 14, respectively.

Component D-141-3 was intact from the upper spacer grid to the top of the control rod spider and had fuel and control rods extending well below the upper spacer grid. Most of the fuel rods were later removed from the assembly and had lengths ranging from approximately 47 cm (19 in.) in the

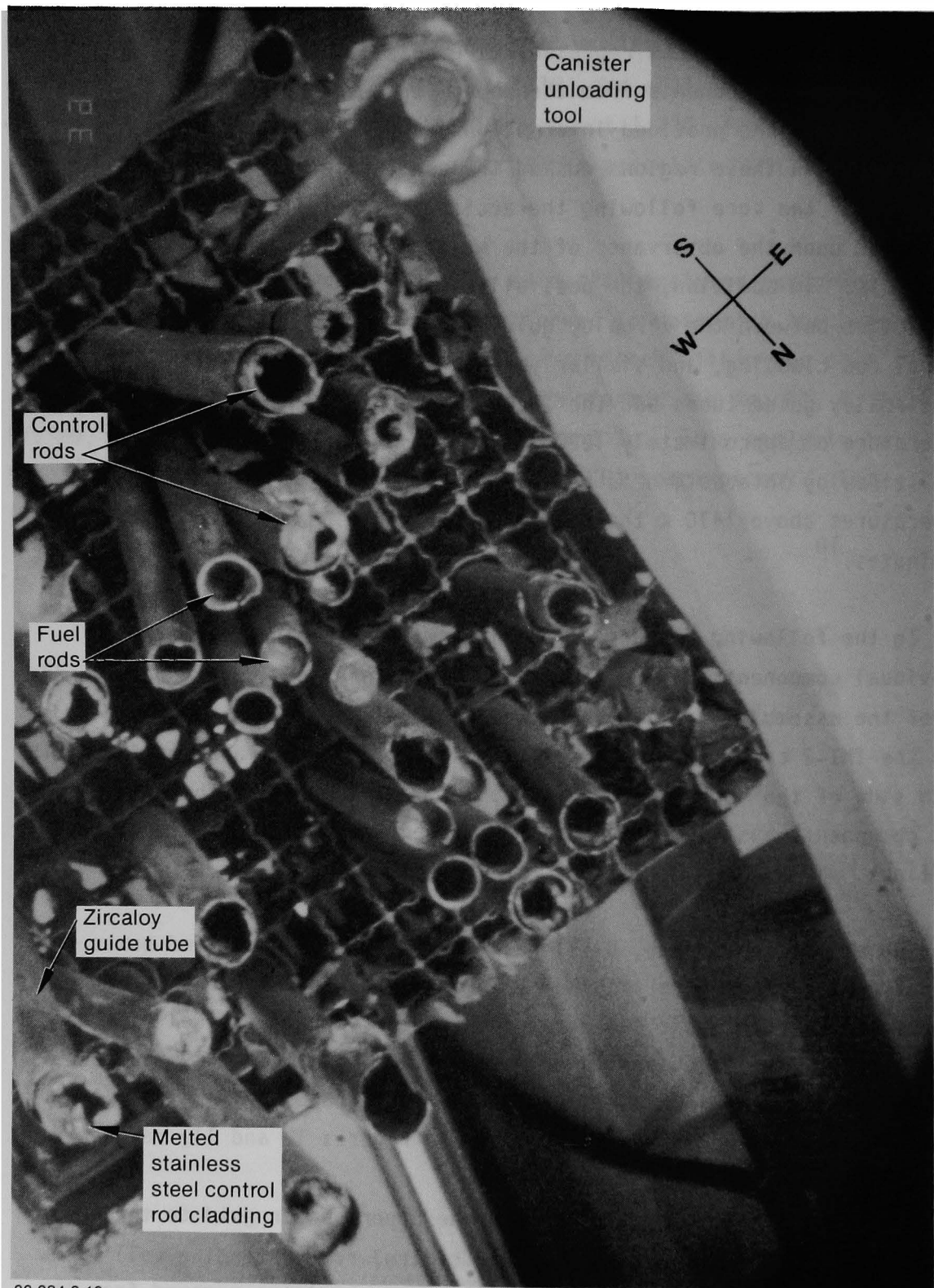
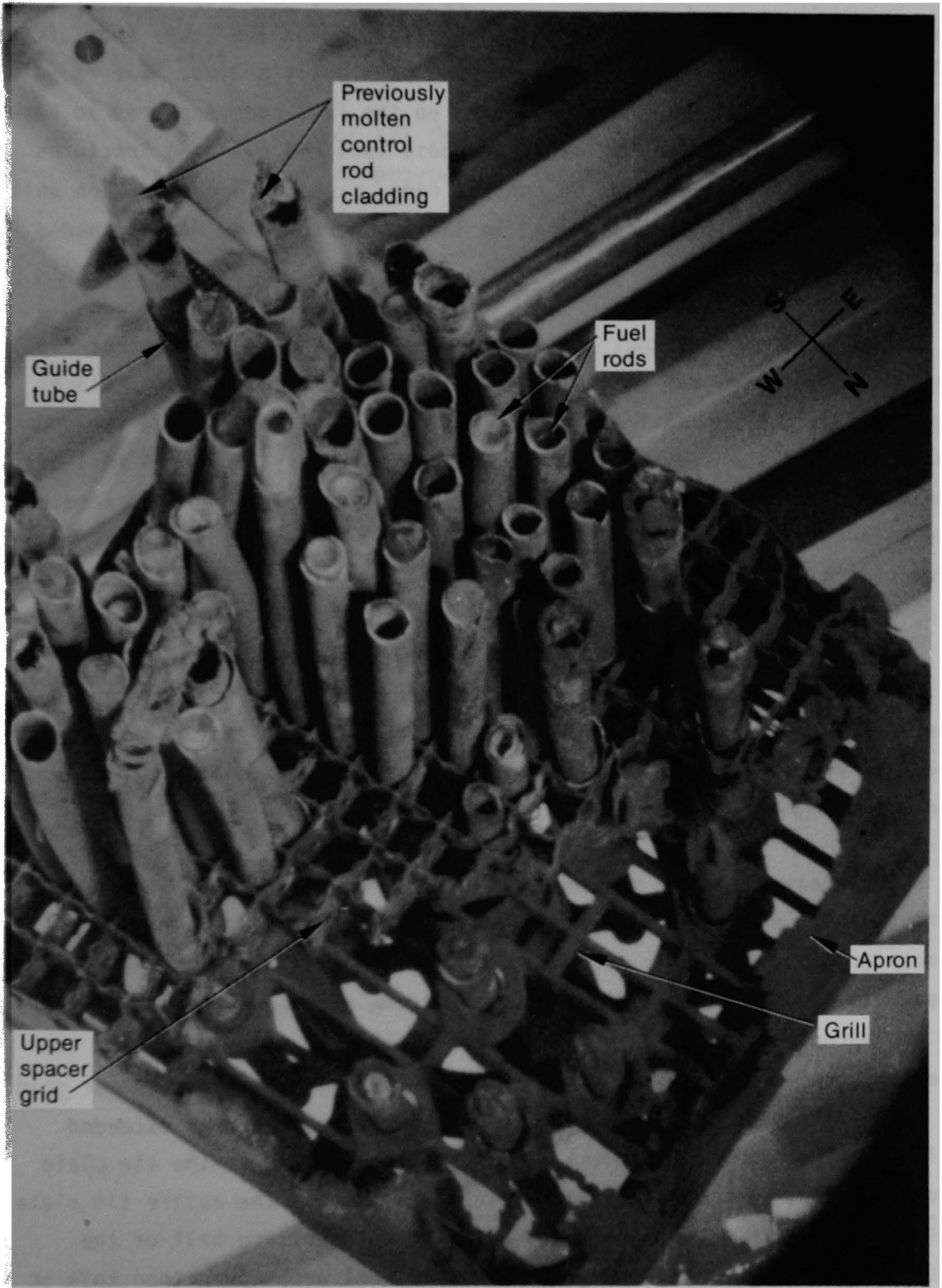


Figure 13. Bottom view of component D-141-3 after removal of most fuel rods.



86-384-9-2

Figure 14. Bottom view of component D-153-9.

southwest corner to about 20 cm (8 in.) in the northeast corner. The control rods were cut from the assembly just below the upper spacer grid, and the removed sections ranged from approximately 15 to 38 cm (6 to 15 in.) in length. The stainless steel cladding on the lower ends of some of the control rods appeared to have been previously melted; however, all the lower ends of the zircaloy cladding on the fuel rods appeared to have been broken off in a brittle manner. These fuel rod cladding fractures, along with some bent endtips on control rods, probably occurred when this component fell to the debris floor in the reactor or when it was loaded into the canister.

The presence of intact stainless steel cladding on the control rods, which in some cases was melted near the endtips, indicates temperatures were near 1673 K, approximately 20 to 25 cm (8 to 10 in.) below the upper spacer grid in the southeast corner and approximately 35 cm (14 in.) below the upper spacer grid on the west side of the assembly. The presence of the intact spacer grid indicates temperatures were less than 1533 K at this elevation.

Some of the fuel and control rod/guide tubes removed from this assembly were examined by neutron radiography and gamma scanning and were then sectioned to obtain samples for metallography and radiochemical analyses of surface deposits. The results of those examinations are presented in Section 5.

The greatest damage to component D-153-9 occurred in the northwest corner of the assembly, particularly along the north side. The upper spacer grid and tie plate were intact except in this region, with the damage to the tie plate limited to the extreme northwest corner. Portions of the apron were also melted on the north and west sides. Most of the fuel and control rods were intact 20 to 25 cm below the upper spacer grid on the southeastern half of the assembly. Peak temperatures exceeded 1673 K in the extreme northwest corner of the assembly at the tie plate elevation, but were generally lower than this across the entire tie plate. Temperatures were higher than 1533 K on the northwestern half of the assembly at the upper spacer grid elevation, but were lower than this on

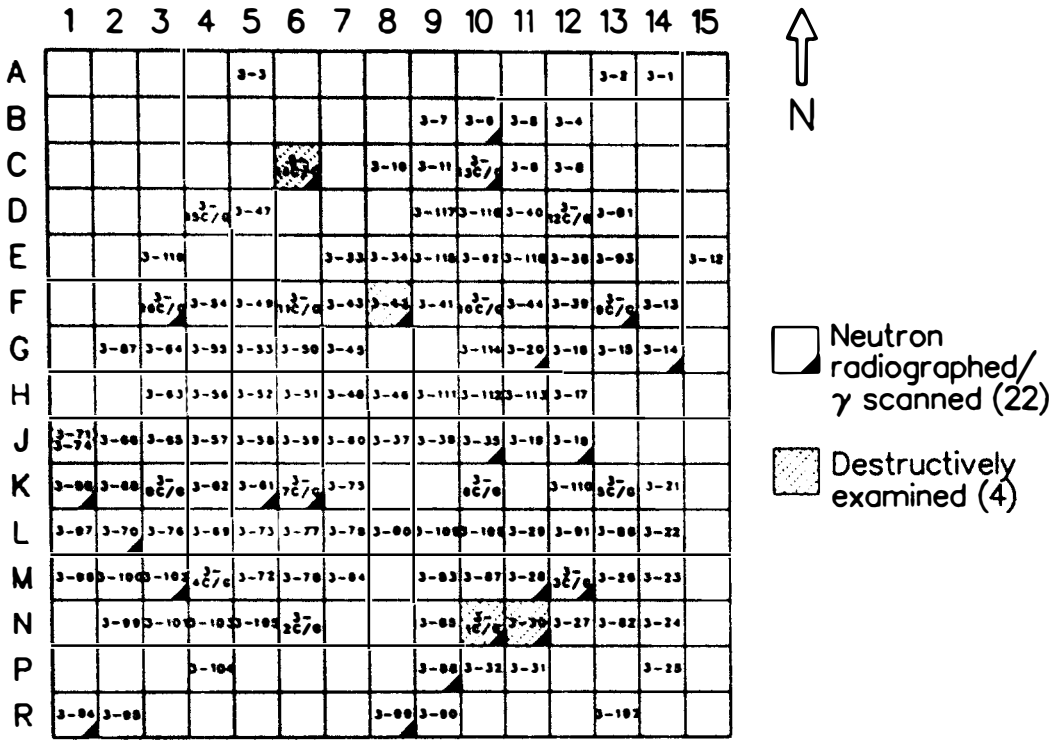
the southeastern side. In the extreme southeastern corner, approximately 25 cm below the upper spacer grid, the peak temperatures were near 1673 K. These peak temperatures were evidenced by partially melted control rod cladding (Figure 14).

Detailed descriptions of all the components removed from canisters D-141 and D-153 are provided in Appendix D.

5. FUEL AND CONTROL ROD SAMPLE CHARACTERIZATION AND SELECTION

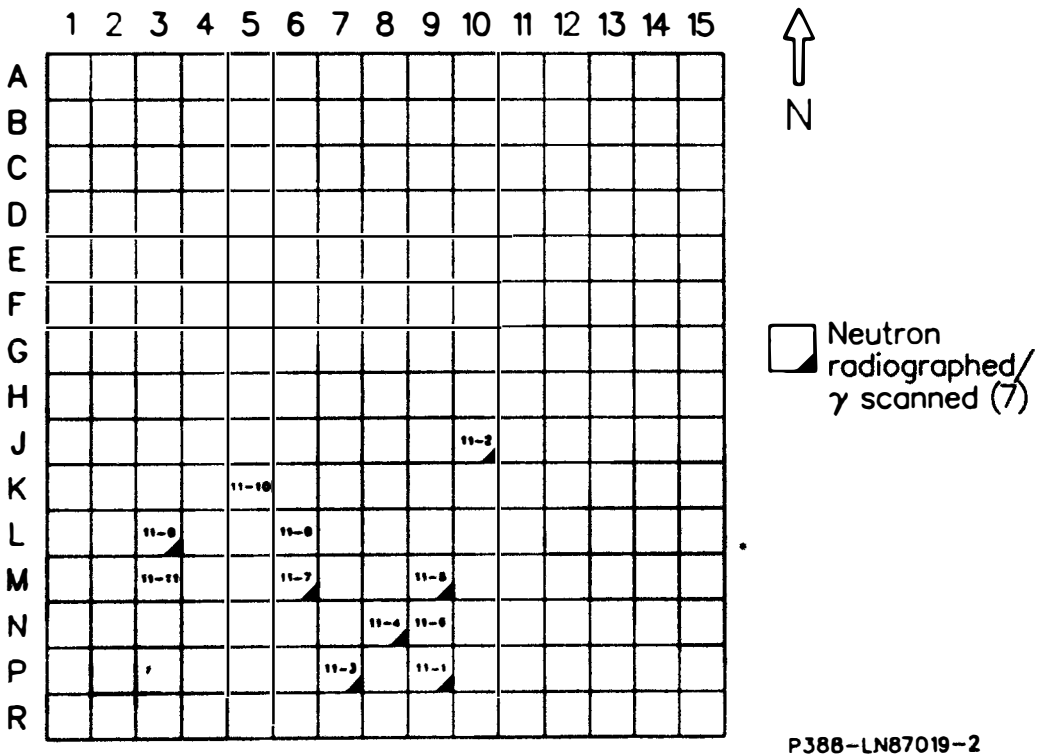
Fuel and control rods were removed from two partial fuel assemblies for detailed examinations. One hundred and nineteen fuel rods and all 16 control rod/guide tubes were removed from component D-141-3, which had been located in core position C7. Eleven fuel rods were removed from component D-141-11, which was a peripheral fuel assembly located in core position H1. As the fuel rods were removed from the assemblies, they were numbered consecutively as 3-1, 3-2, 3-3 through 3-119 or 11-1, 11-2, 11-3 through 11-11 for components numbered D-141-3 and D-141-11, respectively. Also, the control rod and guide tube segments that were cut from D-143-3 were numbered 3-1C through 3-16C or 3-1G through 3-16G. Letter C indicates a control rod, a letter G indicates guide tube, and letters C/G indicate a control rod/guide tube combination. The locations of all the rods that were removed from their respective assemblies are shown in Figures 15 and 16. For convenience, those rods are identified that were subsequently selected for neutron radiography, gamma scanning, and, in some cases, destructive examinations.

The D-141-3 partial fuel assembly component was loaded into the canister with the fuel and control rods pointing upward. When attempts were made to remove the entire component, the fuel rods became stuck on the lip of the canister, and consequently it was decided to pull most of the fuel rods out of the assembly before removing the rest of the component. The orientations of all the fuel rods in the assembly were later determined by noting the orientation of the assembly with respect to markings on the shipping canister during withdrawal. One hundred and six fuel rods were pulled from component D-141-3 before the rest of the component could be removed from the canister. Following visual examinations and photography of the component (see Section 3), the 16 control rod/guide tubes were cut off approximately 2 to 7 cm below the upper spacer grid because the spider could not be removed from the end fitting. During this operation an additional ten fuel rods that were stuck in the upper spacer grid were also cut off, and three other fuel rods were able to be pulled out once some of the other rods were removed.



P388-LN87019-1

Figure 15. Fuel and control rod locations in component D-141-3. Partial fuel assembly in core location C7.



P388-LN87019-2

Figure 16. Fuel rod locations in component D-141-11. Partial fuel assembly in core location H1.

All eleven fuel rods removed from component D-141-11 were simply pulled out of the fuel assembly upper spacer grid. No cutting was required to remove them. The few remaining empty guide tube remnants were cut off and discarded.

The lengths of all the fuel and control rods were measured to assist in selecting rods for further examination, except for the last thirteen fuel rods from D-141-3, which were either cut or discarded. It should be restated that the measured control rod lengths are measured only to where they were cut, approximately 2 to 7 cm below the upper spacer grid. The approximate lengths include both the control rod and associated guide tube. The fuel rod and approximate control rod lengths for the respective partial fuel assemblies are shown on Figures 17 and 18. The longest fuel rods in component D-141-3 were in the southwest corner, which was oriented toward the core periphery.

Based upon visual examinations of the rods, their lengths, and their positions in the assembly, some of the rods were placed in a sorting rack as possible samples for further examination. A photograph of this rack with some of the fuel rods from D-141-3 is shown in Figure 19. The rods placed in this sorting rack were also weighed to estimate the amount of fuel or control material present in each rod. Since the material inside the rods was not always visible at the rod endtip, this weight was used to further assist in the final selection of rods to be neutron-radiographed and gamma-scanned. Fifteen fuel rods and seven control rod/guide tubes were selected from D-141-3 for neutron radiography and gamma scanning. Similarly, seven fuel rods from D-141-11 were also selected. The positions of all rods selected for neutron radiography and/or gamma scanning are shown in Figures 15 and 16.

Neutron radiographs of the selected fuel rods and control rod/guide tubes are presented in Appendix A. All of these rods were very similar in appearance, and the detailed results from subsequent destructive examinations are presented in Section 6. In general, melted Ag-Cd-In control rod material relocated upward into the plenum spring region on all the control rods examined. No significant cracking or breakup of the fuel

	1	2	3	4	5	6	7	8	9	10	11	12	13	14	15
A					21								20	20	
B									27	27	20	20			
C						23		27	20	17	20	20			
D				30	30						24	16	21		
E							20	20		27		27	10		10
F			33	33	20	10	20	20	20	17	25	25	10	20	
G		30	33	30	32	31	27				22	24	25	22	
H			32	32	34	30	20	20				24			
J	44	33	35	32	33	31	20	27	26	27	20	10			
K	37	30	20	30	30	20	30			23			17	17	
L	42	30	42	42	41	40	43	41			31	27	21	16	
M	41	44	44	34	40	40	41		43	42	45	23	25	10	
N		40	43	47	47	30			40	36	41	32	30	10	
P				40					40	40	42			23	
R	47	42						44	42						



P388-LN87019-3

Figure 17. Approximate lengths of fuel and control rods remaining in component D-141-3 (cm).

	1	2	3	4	5	6	7	8	9	10	11	12	13	14	15
A															
B															
C															
D															
E															
F															
G															
H															
J										47					
K					31										
L			01			40									
M			01			00			01						
N								01	N/A						
P							00		00						
R															



P388-LN87019-4

Figure 18. Lengths of fuel rods remaining in component D-141-11 (cm).



86-384-1-22

Figure 19. Sorting rack with some of the fuel rods from D-141-3.

was apparent in the fuel rod sections examined. The darkened regions in the upper sections of the fuel rods are due to highly borated water entrapped inside the rods, which flowed to this area because these rods were neutron-radiographed with the fuel rod inverted. Where possible, control rods and their associated guide tubes were separated prior to these examinations in order to determine if differences in deposited material could be observed. However, no significant differences were observed.

The endtips of all the fuel rods examined appeared to have been snapped off in a brittle manner, possibly due to handling damage or as a result of falling to the debris bed in the reactor. Some typical examples are shown in Figure 20. Similarly, the zircaloy guide tubes surrounding the control rods also appeared to have been broken off. However, in many cases the stainless steel control rod cladding appeared to have been previously melted, as typified in Figure 21. Some of these control rod/guide tubes were bent on the endtips (see Figure 22).

86T-26



a) Fuel rod 3-35

Manipulator

86T-36



b) Fuel rod 3-98

Figure 20. Typical broken fuel rod endtips.



86T-66

a) Control rod/guide tube 3-3C/G



86T-68

b) Control rod/guide tube 3-4C/G

Figure 21. Melted stainless steel cladding on control rod endpoints.



86T-73

a) Control rod/guide tube 3-6 C/G



86T-75

b) Control rod/guide tube 3-7 C/G

Figure 22. Damaged endtips on control rods.

6. FUEL AND CONTROL ROD SAMPLE EXAMINATIONS

Two fuel rods (3-30 and 3-42), one control rod (3-1C), one guide tube (3-1G), and one control rod/guide tube combination (3-14C/G) from the D-141-3 partial fuel assembly located in core position C7 (component D-141-3) were selected for destructive examinations. These particular rods were selected to provide data on interior and exterior rod positions in this fuel assembly and on fuel rods located both adjacent to and away from control rod positions. The locations of these rods in the C7 assembly position are shown in Figure 15. Sectioning diagrams showing the locations and identifications of all the metallurgical (M designations) and radiochemical samples (SE designations) are shown in Figure 23. Samples V-4A and V-12 were cut to provide visual examinations of the rod internals, but did not show anything unusual. Note that for control rod 3-1 the control rod and guide tube were separated prior to sample acquisition. The sample locations were chosen to characterize axial differences in fuel and control rod behavior. The metallurgical examination results are presented in Sections 6.1 and 6.2, and the results from the radiochemical analyses are presented in Section 6.3.

6.1 Control Rod Metallurgical Examinations

The neutron radiographs of control rods 3-1C and 3-14C/G are shown in Figure 24. Also shown in this figure are the locations of the examined faces of metallographic samples M-10A, M-10B, M-13, and M-15. Longitudinal samples extend over an axial length, whereas the transverse samples are only at one location. The letter designations accompanying the rod identifications indicate that 3-1C was separated from its guide tube 3-1G after it was cut from the bundle, whereas 3-14C/G indicates that the guide tube remained attached to the control rod. The guide tube on 3-1C was removed so that it could be neutron-radiographed and gamma-scanned separately and was sectioned to provide radiochemical samples for fission product deposition. The guide tube on 3-14C/G remained attached to the control rod because the control rod was bent outwards through a crack in the guide tube near the bottom end and they could not easily be separated. This is believed to have occurred either when the assembly fell to the

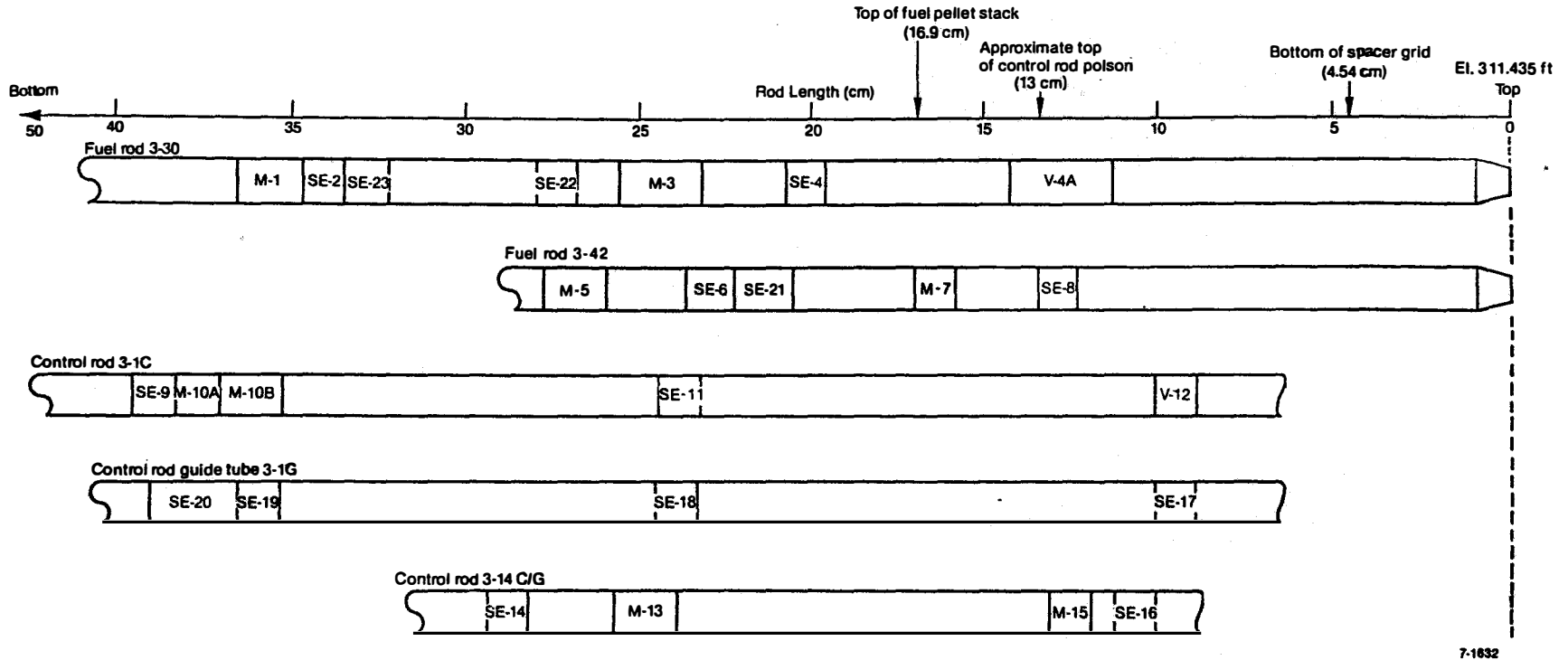
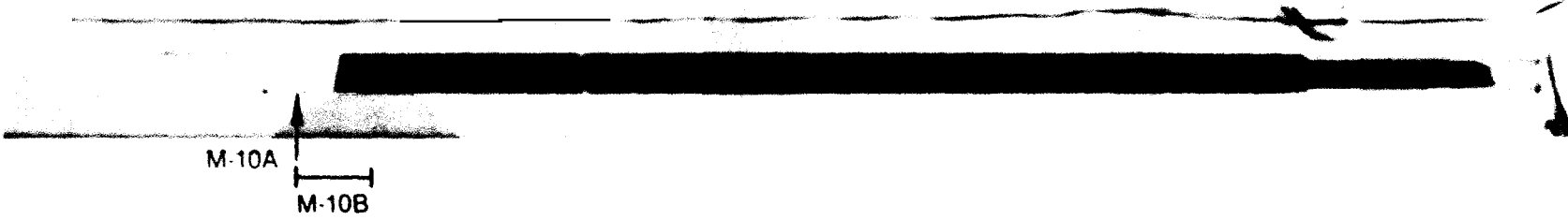


Figure 23. Sectioning diagrams for fuel rods and control rod/guide tubes.

TMI-2 control rod 3-1C



TMI-2 control rod 3-14C/G



7-0329

Figure 24. Neutron radiographs of control rods 3-1C and 3-14C/G (top of the rods is to the right of this figure).

upper core debris bed or as a result of handling damage in inserting and removing the assembly from the shipping canister. A photomosaic of the 3-14C/G endtip is shown in Figure 25.

In order to remove the control rod/guide tubes from the assembly, they had to be cut just below the upper spacer grid. As shown in the neutron radiographs, this sectioning location was in the plenum spring region of both control rods. As shown in Figure 26, transverse metallographic sample M-10A and an adjacent longitudinal metallographic sample M-10B were selected from control rod 3-1C to provide information on the debris material on the cladding inner surface (which appears in the neutron radiographs in this region) as well as on the condition of the control rod material at the endtip. M-10A was located 32.4 cm (12.75 in.) below the cut end of the control rod, and M-10B was located from 30.5 to 32.4 cm (12 to 12.75 in.) below the cut end of the control rod. Longitudinal sample M-13 from control rod 3-14C/G was selected to examine the deformed control rod material at the endtip, and transverse metallographic sample M-15 was chosen to examine the control rod material that had relocated into the plenum spring region. Sample M-13 was located from 15.9 to 17.8 cm (6.25 to 7.0 in.) below the cut end of the control rod, and M-15 was located 3.2 cm (1.25 in.) below the cut end of the control rod. The cut ends were approximately 2.5 cm (1 in.) below the upper spacer grid for control rod/guide tube 3-1C/G and 5 cm (2 in.) for 3-14C/G. Photographs of these samples are presented in Figure 27.

The information obtained from these examinations can be categorized into three topic areas: (a) examinations of the debris in the lower end of control rod 3-1C, (b) characterization of the melted control rod material behavior, and (c) characterization of the zircaloy behavior in the guide tube from 3-14C/G. Each of these topics is discussed in the following sections.

6.1.1 Examination of the Debris in Control Rod 3-1C

This debris was a mixture of metallic and ceramic materials, with occasional bits of what appeared to be control rod material sometimes

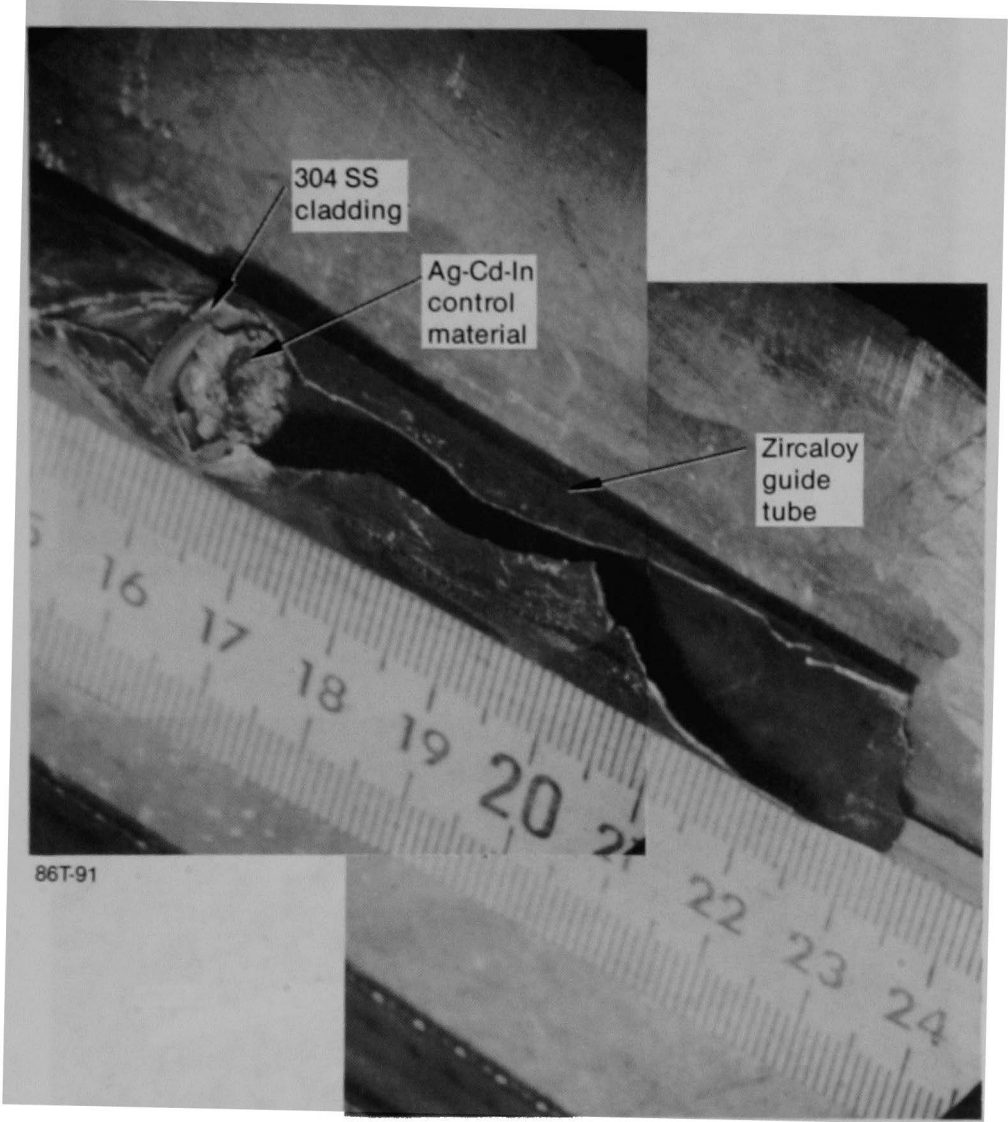
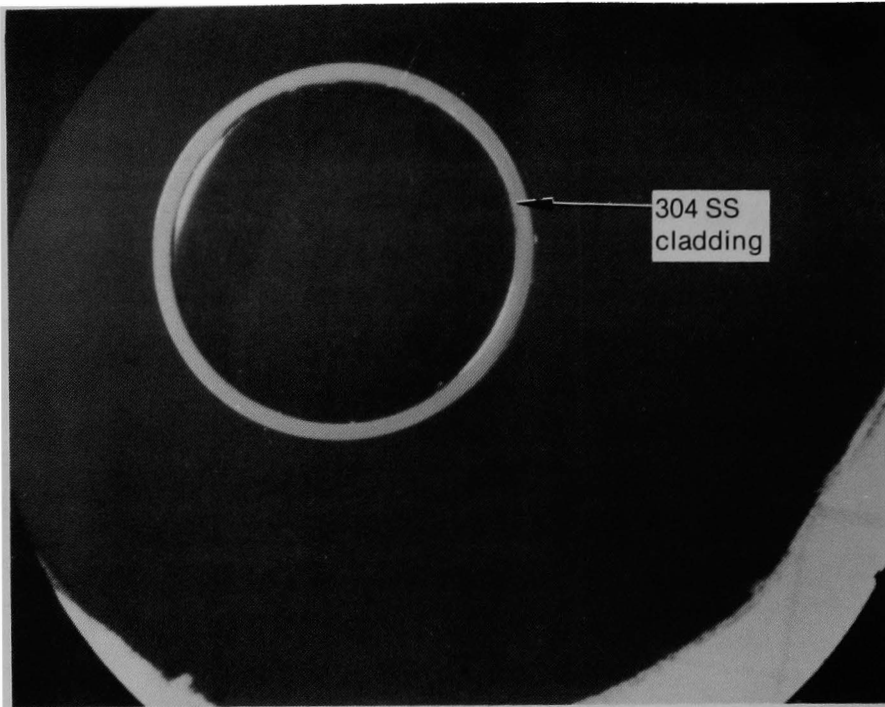
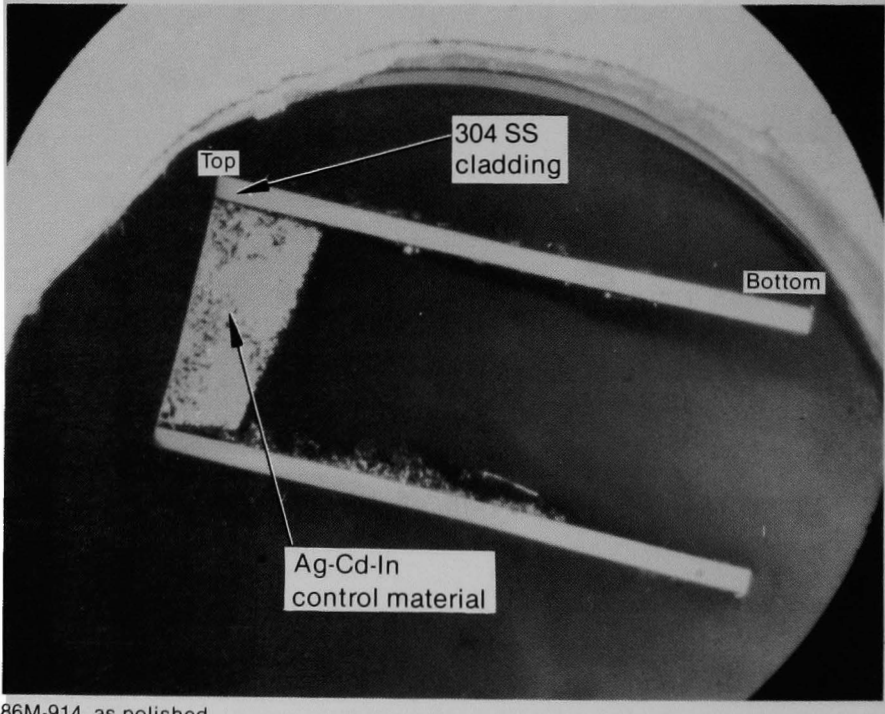


Figure 25. Bottom endtip of control rod 3-14C/G.



86M-915, as polished

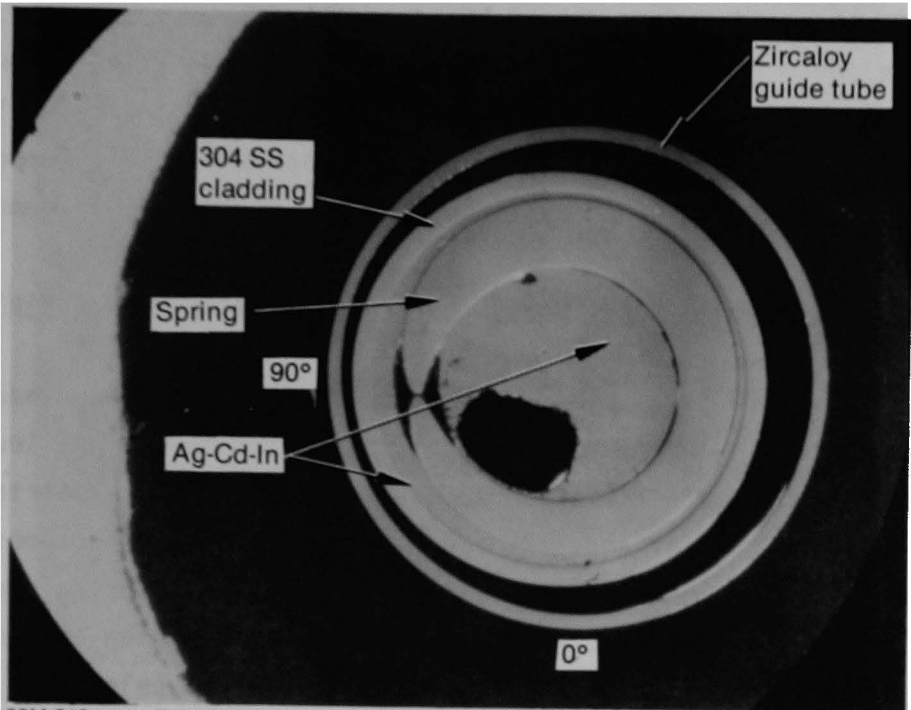
a) Sample M-10A



86M-914, as polished

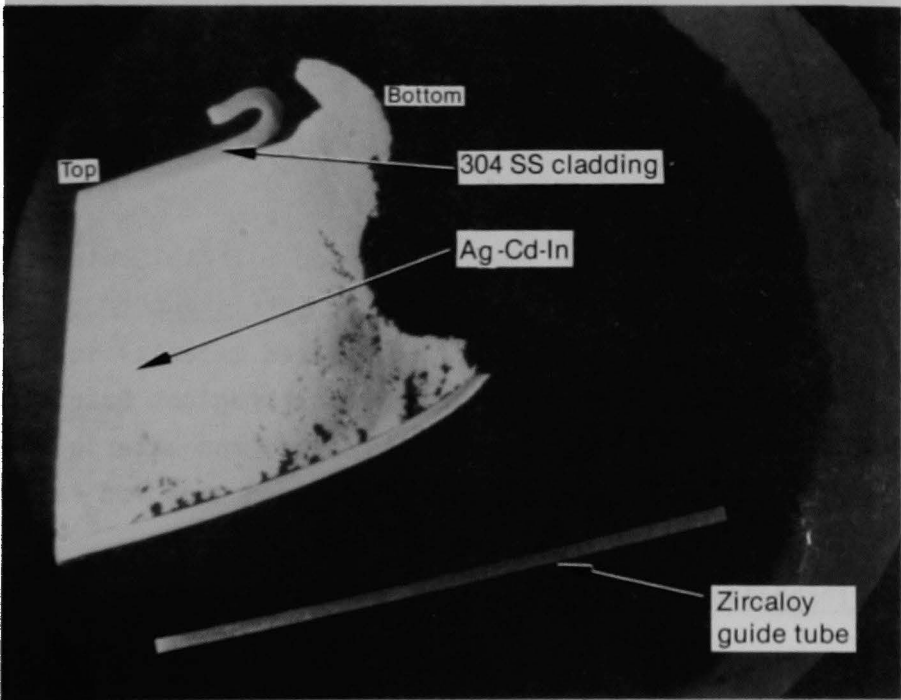
b) Sample M-10B

Figure 26. Metallographic samples from control rod 3-1C.



86M-912, as polished

a) Sample M-15



86M-975, as polished

b) Sample M-13

Figure 27. Metallographic samples from control rod 3-14C/G.

included with the ceramic material, as shown in Figure 28. The metallic material was not affected by zircaloy and stainless steel etchants. As shown in the photograph of sample M-10B in Figure 26, this debris was preferentially deposited on a cladding inner and outer surface, which suggests that it may have settled out of the water while this component was lying horizontal on the upper debris bed after plenum assembly removal.

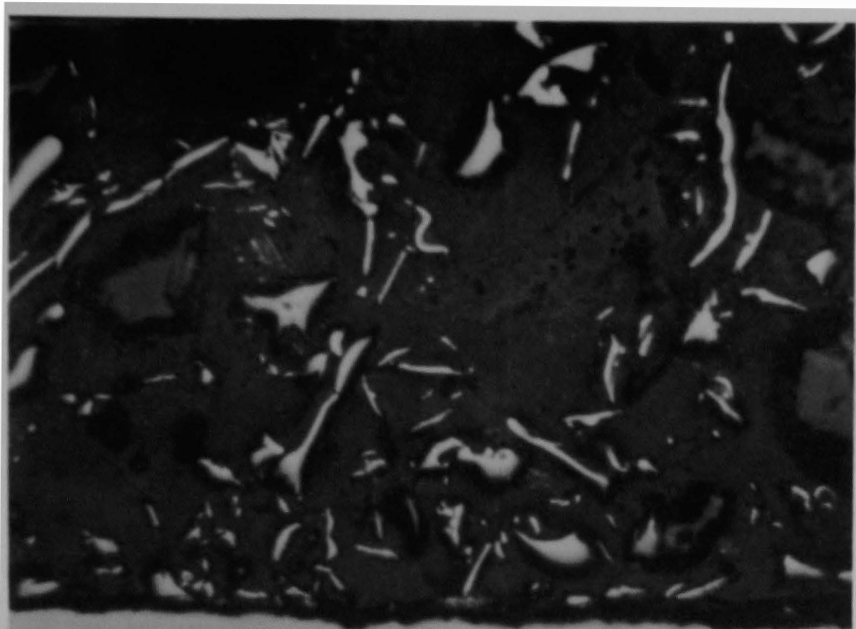
6.1.2 Characterization of the Melted Control Rod Material Behavior

All of the Ag-Cd-In control rod material that was examined had a dendritic structure. This indicates that this material was previously melted. Representative photomicrographs of the control rod material at the endtips of the two control rods are shown in Figure 29. A photomosaic of the previously melted control rod material in the plenum spring region of 3-14C/G is shown in Figure 30. The dendrites in this region are much finer than those located near the endtip, approximately 13 cm below this location (see Figure 31). This indicates that the control rod material in the plenum cooled somewhat faster than the lower control rod material and exemplifies the changes in material behavior that occurred over relatively short distances. The presence of previously melted Ag-Cd-In control material adjacent to unmelted 304 stainless steel cladding indicates that peak temperatures in the plenum spring region were between 1073 K and 1673 K. There was no interaction between the melted control rod material and either the cladding or the spring.

It is postulated that after the control rod material melted, the pressures in the core during the accident were sufficient to collapse the heated control rod cladding and squeeze the melted material into the plenum spring region. It then solidified in these upper regions before the control rod cladding failed. However, the control rod material lower down may have remained melted and may have been released upon rod failure.

6.1.3 Characterization of the Zircaloy Guide Tube Behavior

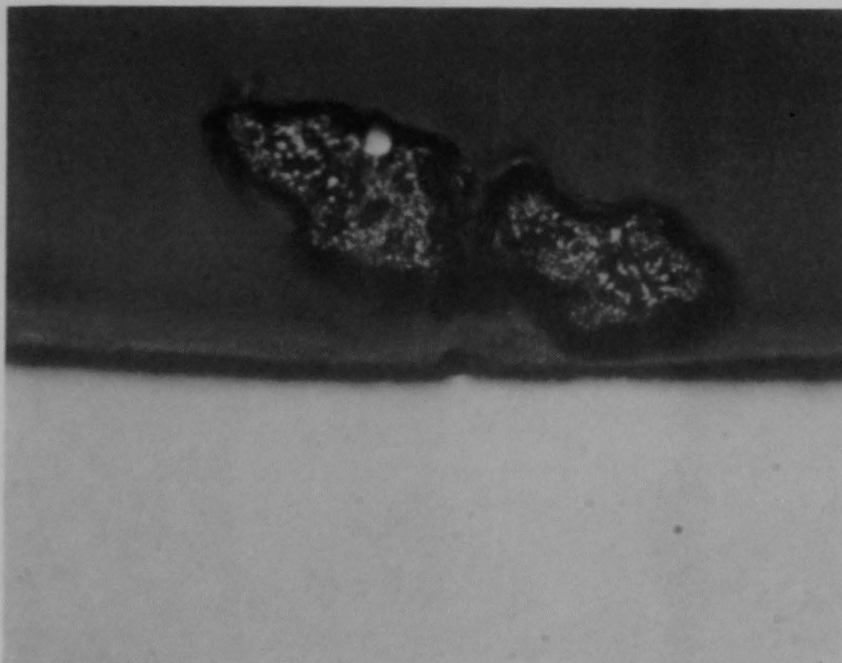
Hydriding of the zircaloy guide tube was observed on both metallographic samples obtained from control rod 3-14C/G. The amount of



86M-967, as polished

a) Metallic debris
(Sample M-10B)

50 μm

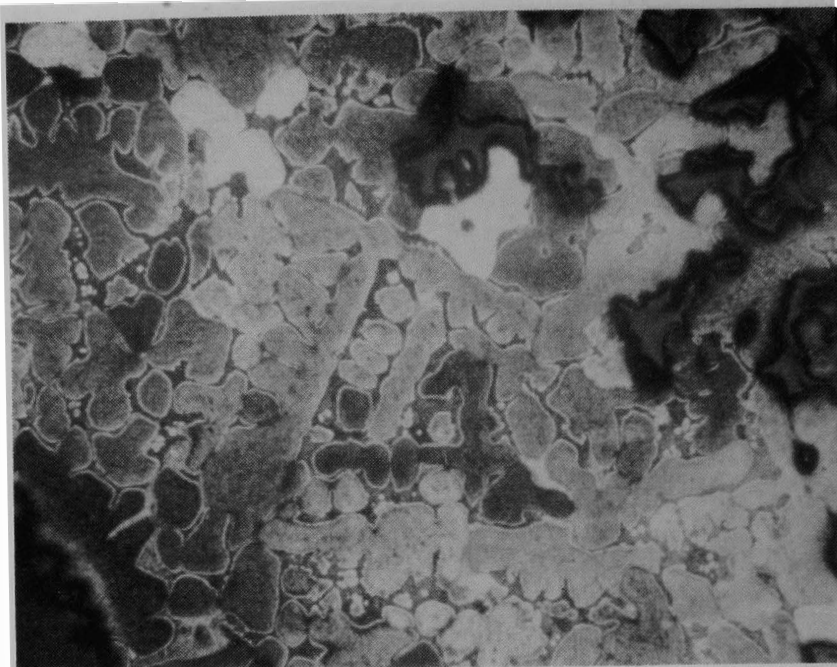


86M-971, as polished

b) Ceramic debris with metallic inclusion
(Sample M-10A)

50 μm

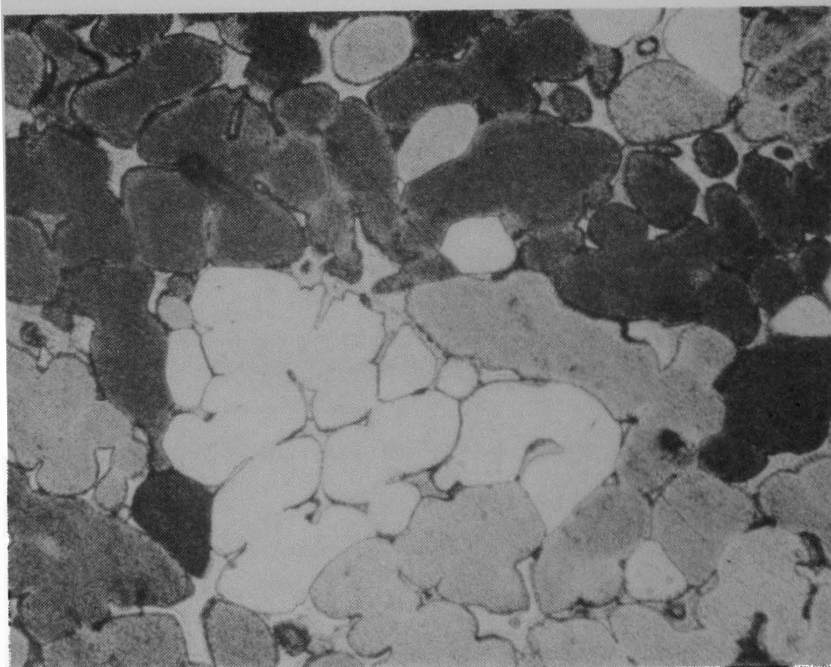
Figure 28. Debris near the broken endtip of control rod 3-1C.



86M-1056, etched

200 μm

a) Control material in Rod 3-1C
(Sample M-10B)

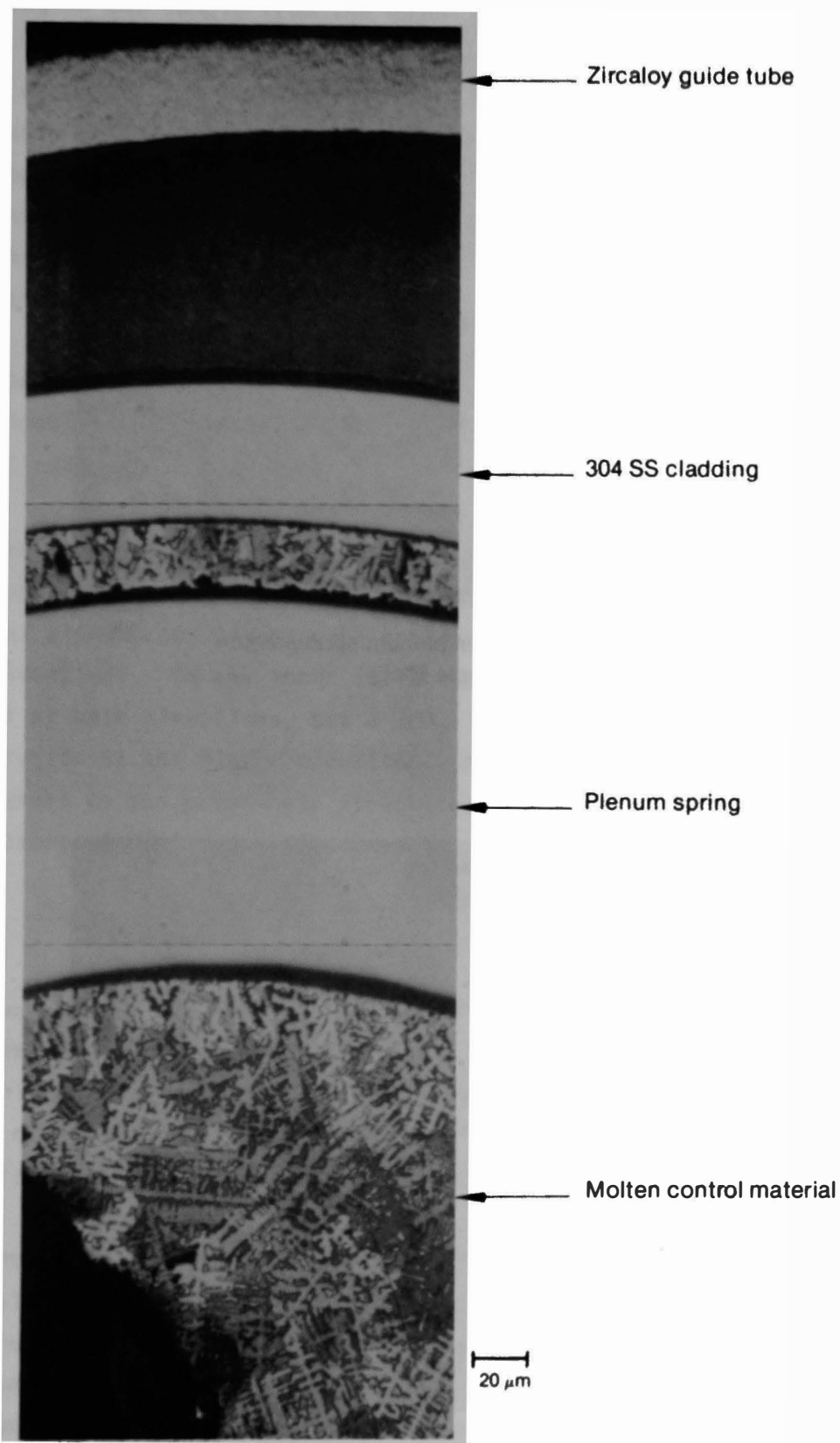


86M-1021, etched

100 μm

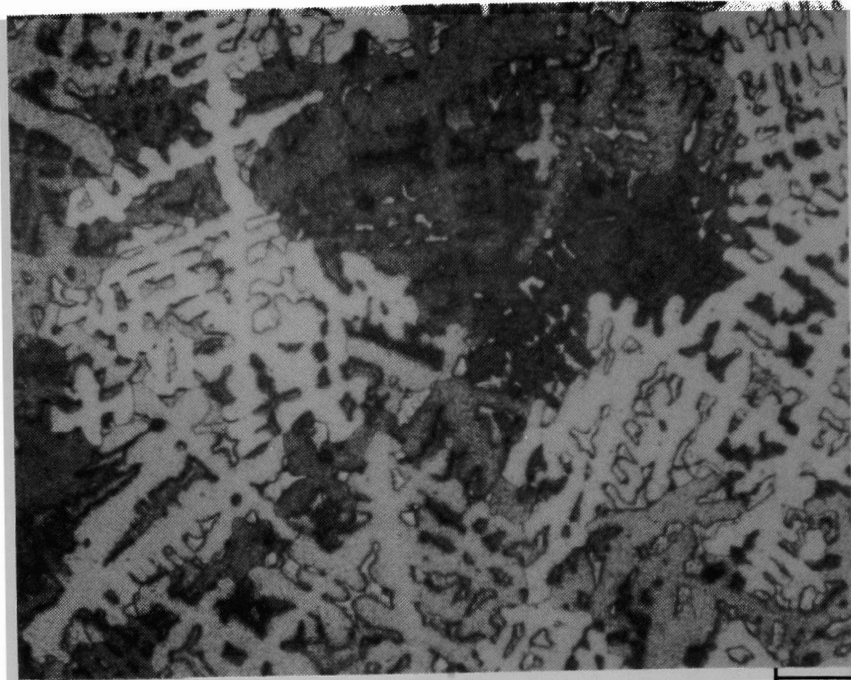
b) Control material in Rod 3-14C/G
(Sample M-13)

Figure 29. Dendritic structures in previously melted Ag-Cd-In control material.



SEM-938, 939, 940, etched

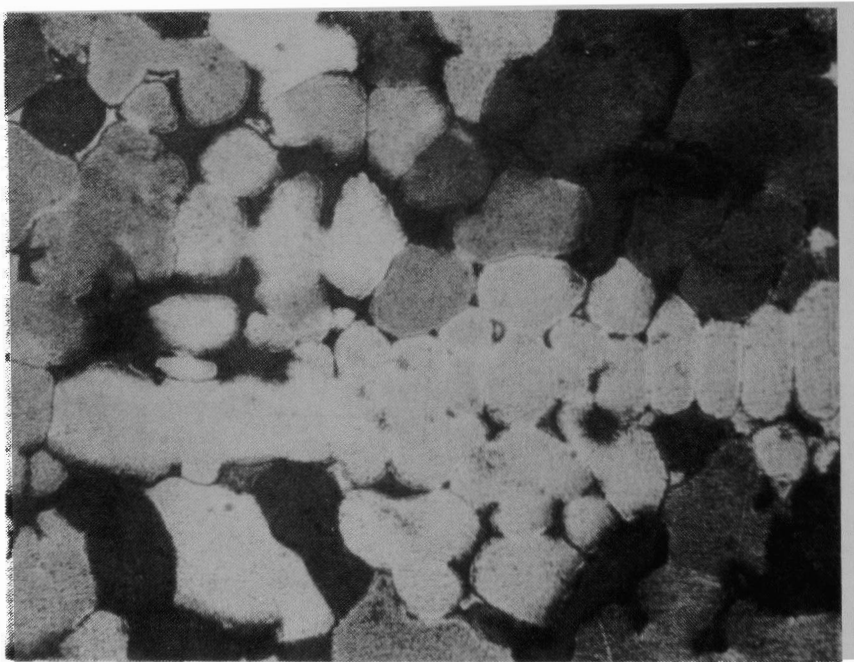
Figure 30. Previously melted Ag-Cd-In control material in plenum spring region of sample M-15.



86M-937, etched

a) Control material in plenum spring region
(Sample M-15)

100 μm



86M-1026, etched

b) Control material \sim 13 cm lower than (a)

100 μm

Figure 31. Previously melted control material in rod 3-14C/G.

hydriding in the sample from the upper plenum region varied significantly around the circumference of the guide tube as shown in Figure 32. The degree of hydriding at the 270-degree orientation in the upper plenum was comparable to that observed approximately 13 cm lower on the longitudinal metallographic sample M-13, also shown in Figure 32 as view c. It is apparent that significant variations in hydriding behavior occurred over very short distances, which indicates that very localized steam and high temperature conditions existed in the core.

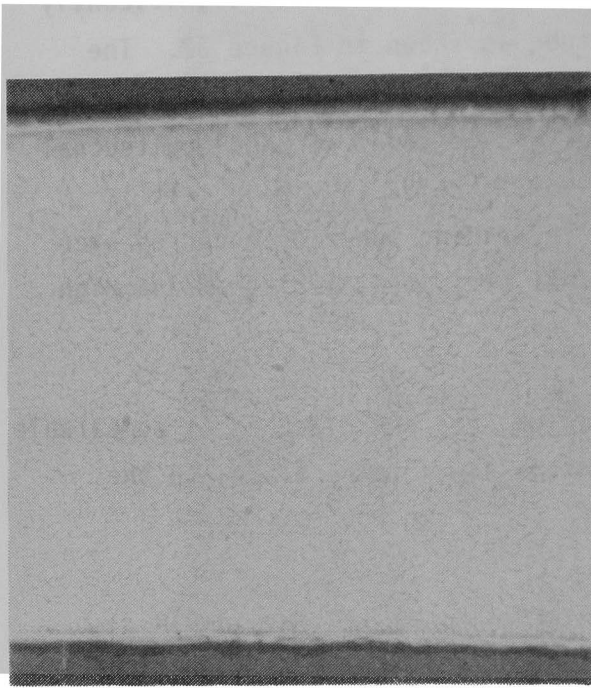
Zircaloy hydriding was not observed on fuel rod cladding at comparable axial locations. This is attributed to the lower temperatures in the control rod/guide tubes.

Measurements of the oxide layer thicknesses at the two sample locations on this guide tube are presented in Table 5. Small continuous ZrO_2 and alpha-Zr(O) layers were present on the outer surface at both axial locations. On the inner surfaces, a small continuous alpha-Zr(O) was present at both elevations, but a ZrO_2 layer was only observed over a small region at the higher elevation. None of the unoxidized zircaloy had transformed to the prior-beta structure, which indicates that peak temperatures in this unoxidized region were less than 1133 K.

6.2 Fuel Rod Metallurgical Examinations

The neutron radiographs of the two fuel rods that were destructively examined (3-30 and 3-42) are shown on Figure 33. Fuel rod 3-30 was located adjacent to control rod 3-1C near the outer edge of the assembly as shown on the core map in Figure 15. Fuel rod 3-42 was centrally located and was not adjacent to a control rod.

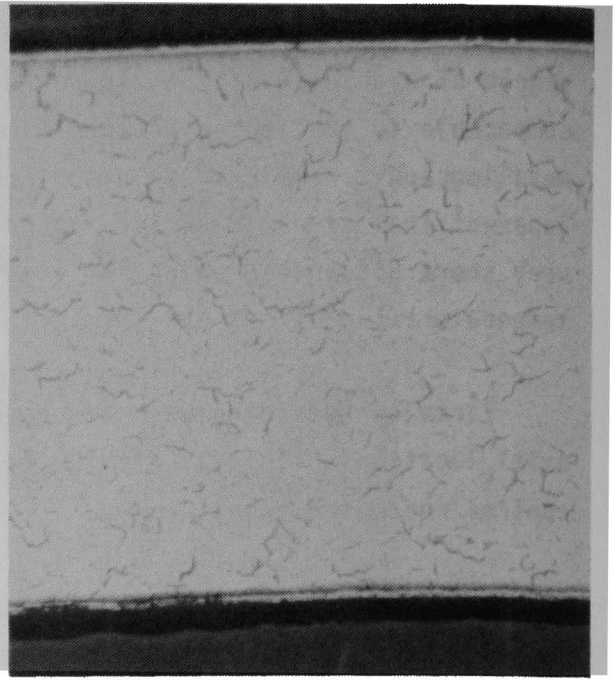
The neutron radiographs show a darkened region in the top portion of the fuel rods. This is due to highly borated water that was entrapped in these fuel rods while they were lying in the flooded reactor core. These fuel rods were neutron-radiographed in the vertical position with the top end down. Close examination reveals a meniscus on the end of the darkened region, and water droplets were observed during sectioning of these rods.



86M-933, etched

50 μm

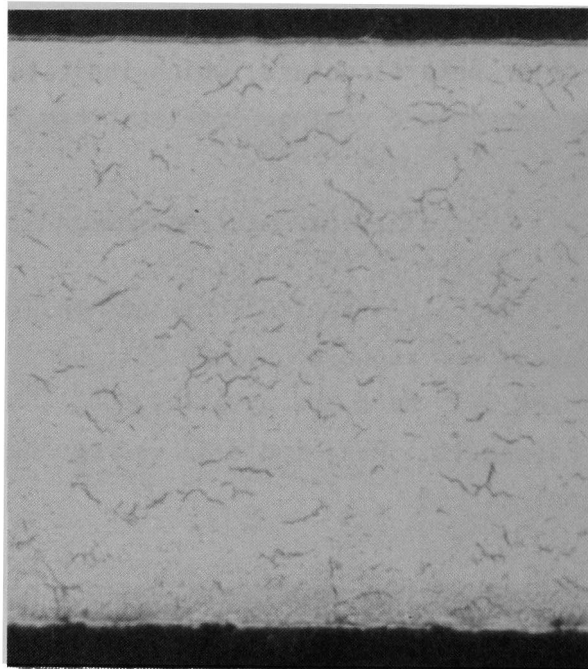
(a) Hydriding in plenum region at 90°



86M-934, etched

50 μm

(b) Hydriding in plenum region at 270°



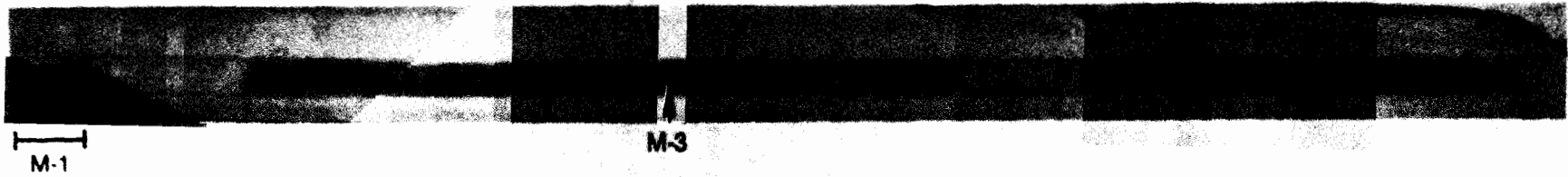
86M-1023, etched

50 μm

(c) Hydrides ~ 13 cm lower than (a) and (b)

Figure 32. Zircaloy hydrides in the guide tube of control rod 3-14C/G.

TMI-2 fuel rod 3-30



TMI-2 fuel rod 3-42

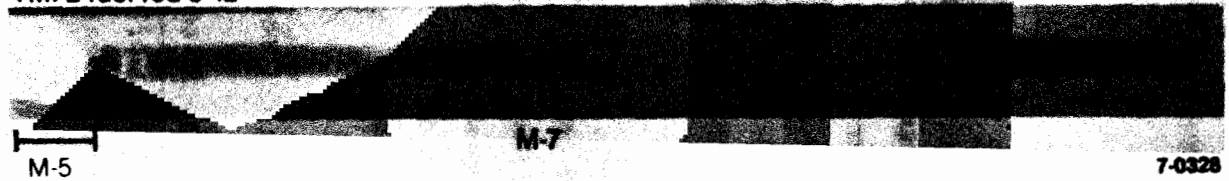


Figure 33. Neutron radiographs of fuel rods 3-30 and 3-42 (top of the rods is to the right in this figure).

TABLE 5. OXIDE LAYER MEASUREMENTS ON ZIRCALOY GUIDE TUBE 3-14C/G

<u>Microstructure</u>	<u>Layer Thickness</u> (μm)			
	<u>Longitudinal</u> <u>Sample M-13^a</u>		<u>Transverse</u> <u>Sample M-15^b</u>	
	<u>Average</u>	<u>Range</u>	<u>Average</u>	<u>Range</u>
ZrO ₂	6	6	3	0 to 5
Alpha-Zr(O)	4	3 to 4	5	5
ZrO ₂ (inner surface)	0	0	1	0 to 4
Alpha-Zr(O) (inner surface)	3	3	5	4 to 5

a. 15.9 to 17.8 cm below the cut end.

b. 3.2 cm below the cut end.

In addition, a visual examination section (sample V-4A), which was cut through a portion of the darkened region on fuel rod 3-30, revealed only the plenum spacer and spring.

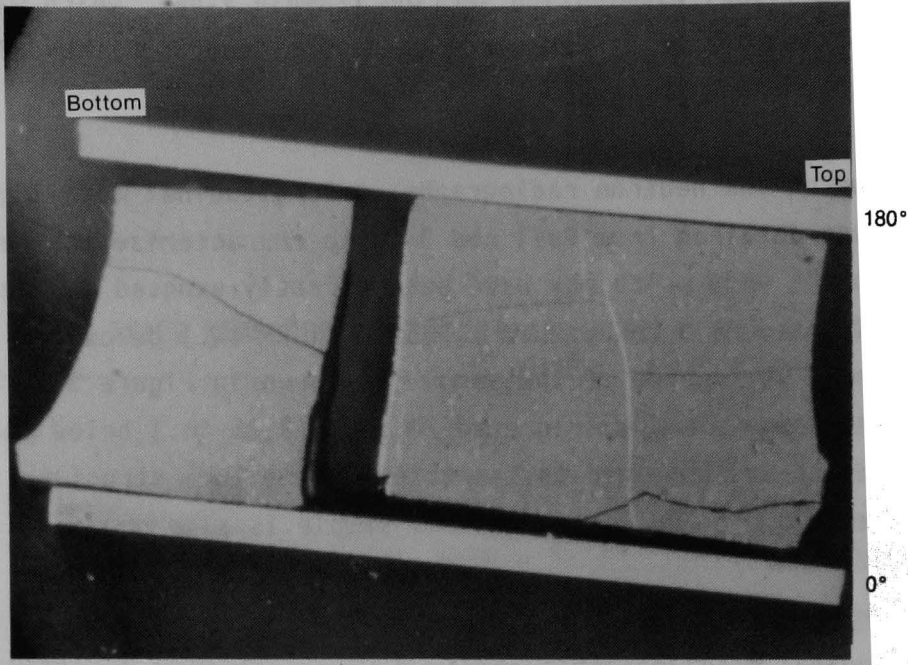
As shown on the neutron radiographs, a longitudinal metallographic sample M-1 was obtained from fuel rod 3-30 to characterize the fuel structure on the end, which may have been directly exposed to steam. This sample was located 34.3 to 36.2 cm (13.5 to 14.25 in.) below the top of the fuel rod, and a photograph of the sample is shown in Figure 34. Transverse metallographic sample M-3 was located 23.5 cm (9.25 in.) below the top of the fuel rod and was obtained to characterize the fuel structure away from the broken endtip. A photograph of this sample is also provided in Figure 34.

Longitudinal metallographic sample M-5 was obtained from fuel rod 3-42 to characterize the fuel structure near the endtip. This sample was located 26.0 to 27.9 cm (10.25 to 11.0 in.) below the top of the fuel rod, and photographs are provided in Figure 35. Transverse metallographic sample M-7 was sectioned to provide fuel structure information away from the broken endtip. It was located 16.5 cm (6.5 in.) below the top of the rod. A photograph is provided in Figure 35.

Characterization of the fuel morphology and the zircaloy cladding behavior was obtained from the examinations of these metallographic samples. Each of these topics is discussed in the following sections.

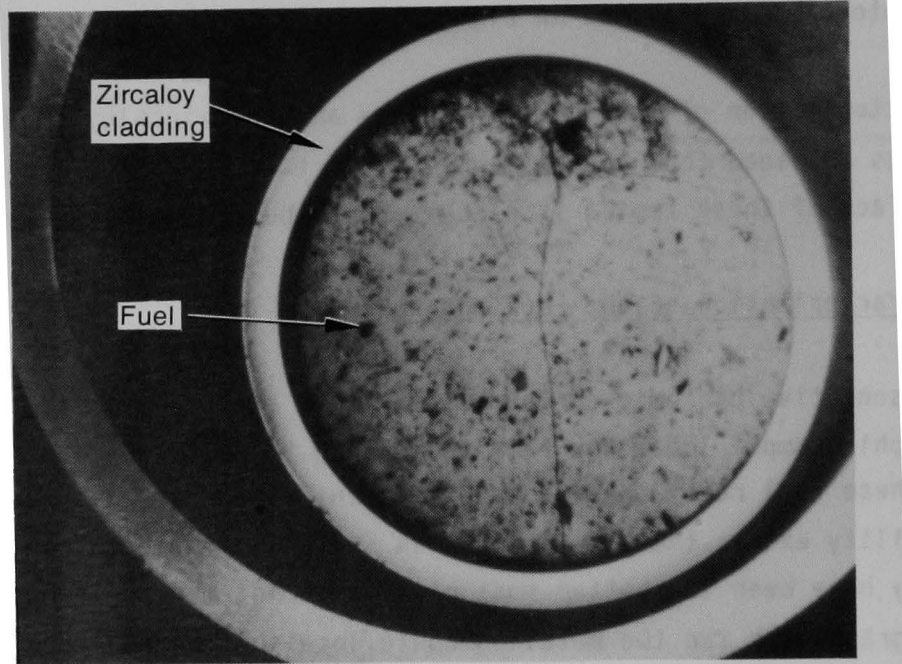
6.2.1 Characterization of the Fuel Morphology

Representative photomicrographs of the fuel structure at the two metallographic sample locations from fuel rod 3-30 are shown in Figures 36 and 37. These fuel rods appeared to have been broken off at some time, and the possibility exists that the pellets in the bottom of each rod may not necessarily have been the bottom-most pellets during the accident. Similar photomicrographs for the two metallographic locations on fuel rod 3-42 are shown in Figures 38 and 39. None of the fuel structures exhibited any



86M-913, as polished

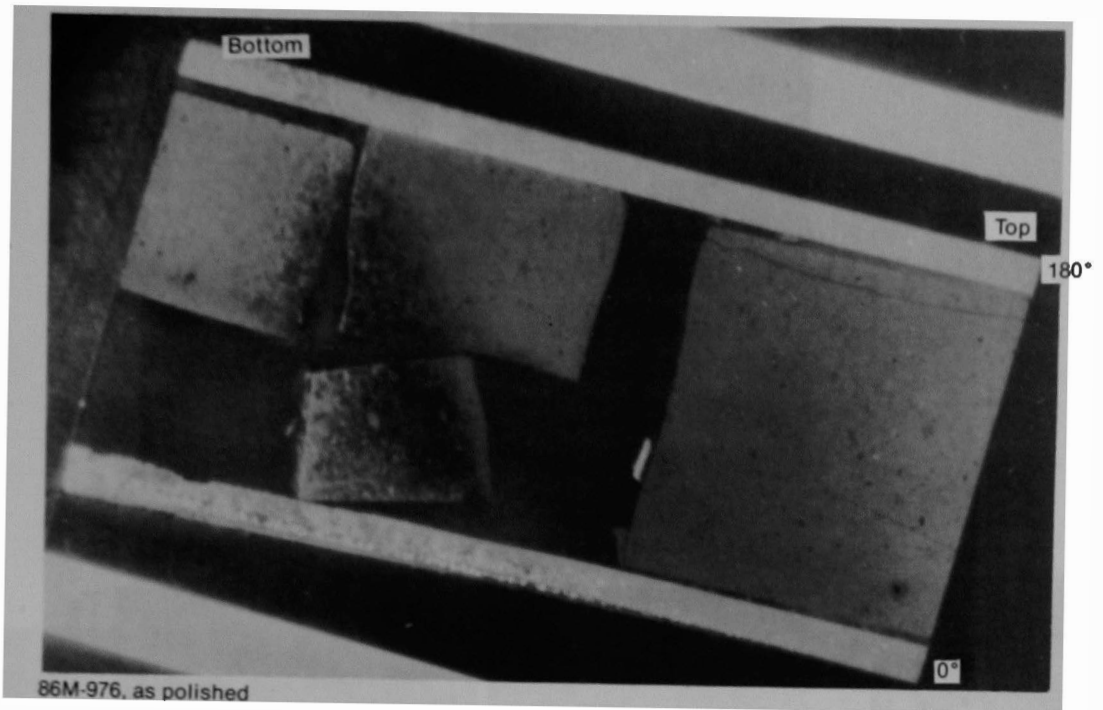
a) Sample M-1



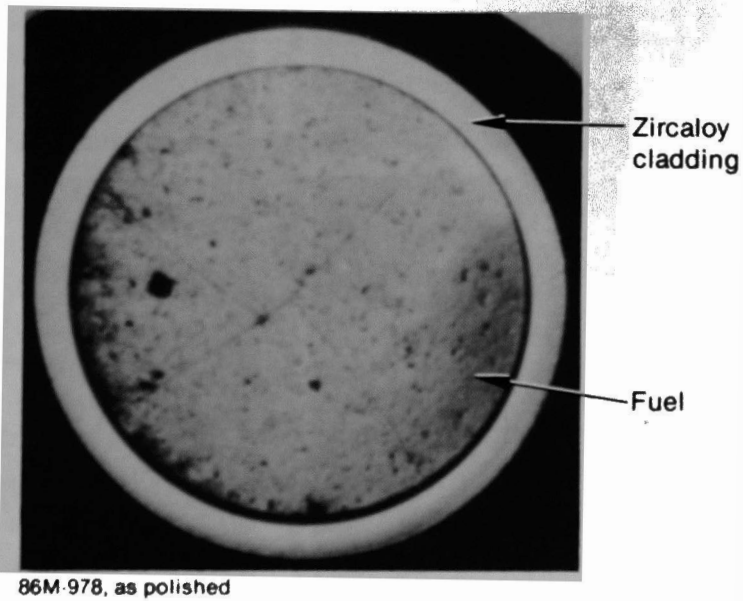
86M-977, as polished

b) Sample M-3

Figure 34. Metallographic samples from fuel rod 3-30.



a) Sample M-5



b) Sample M-7

Figure 35. Metallographic samples from fuel rod 3-42.

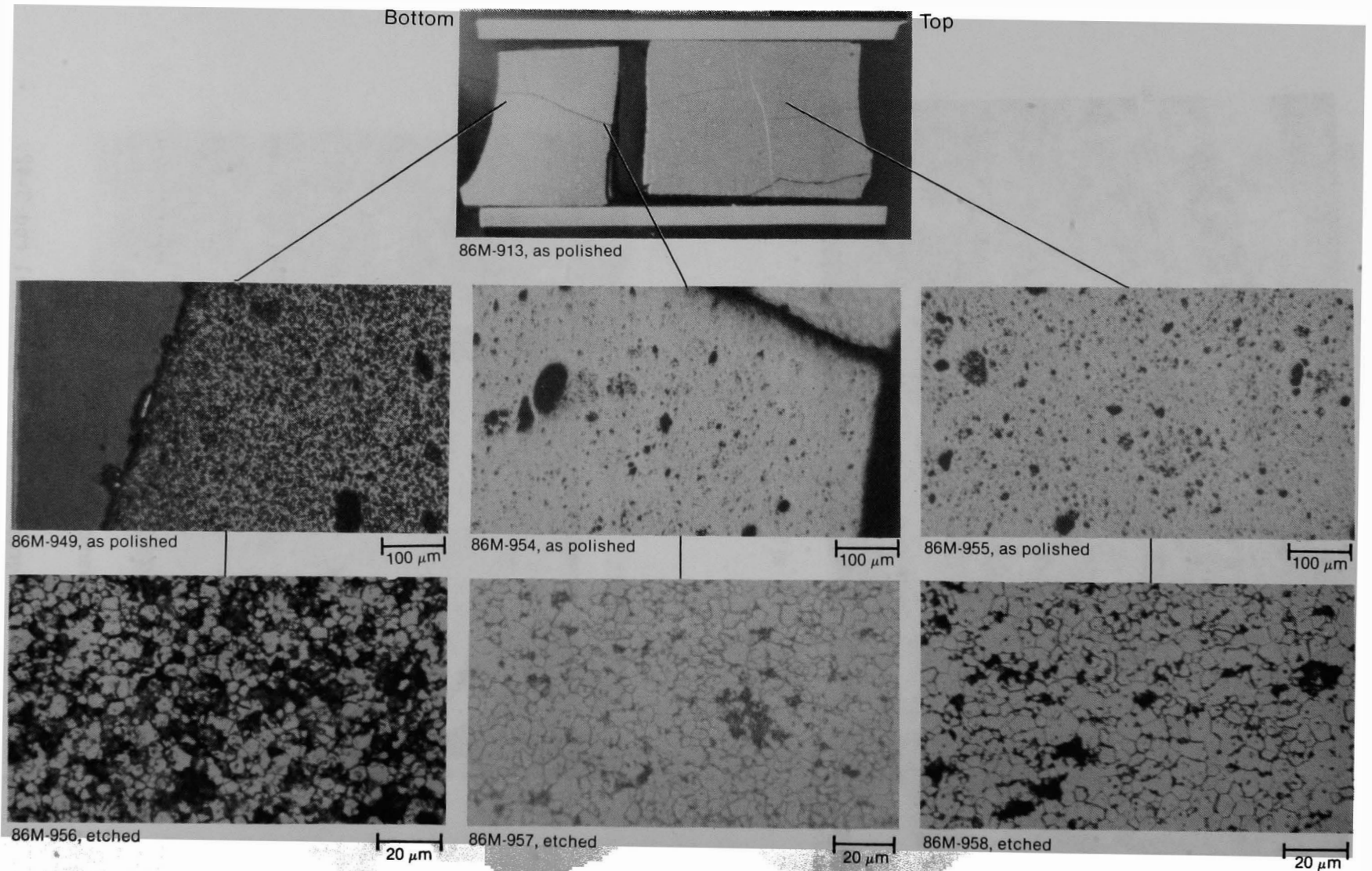


Figure 36. Fuel morphology in sample M-1 near broken end of fuel rod 3-30.

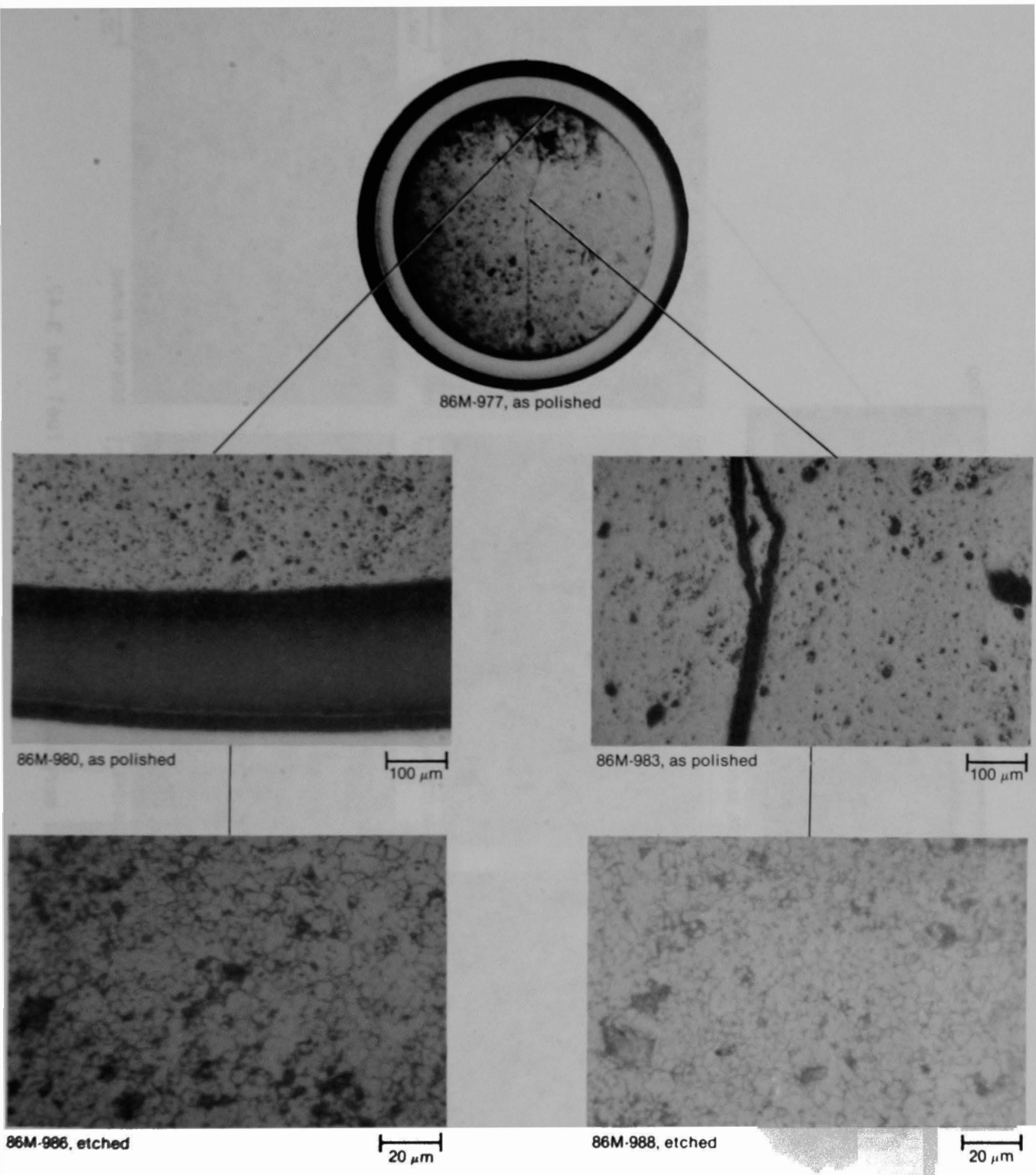


Figure 37. Fuel morphology in sample M-3 from fuel rod 3-30.

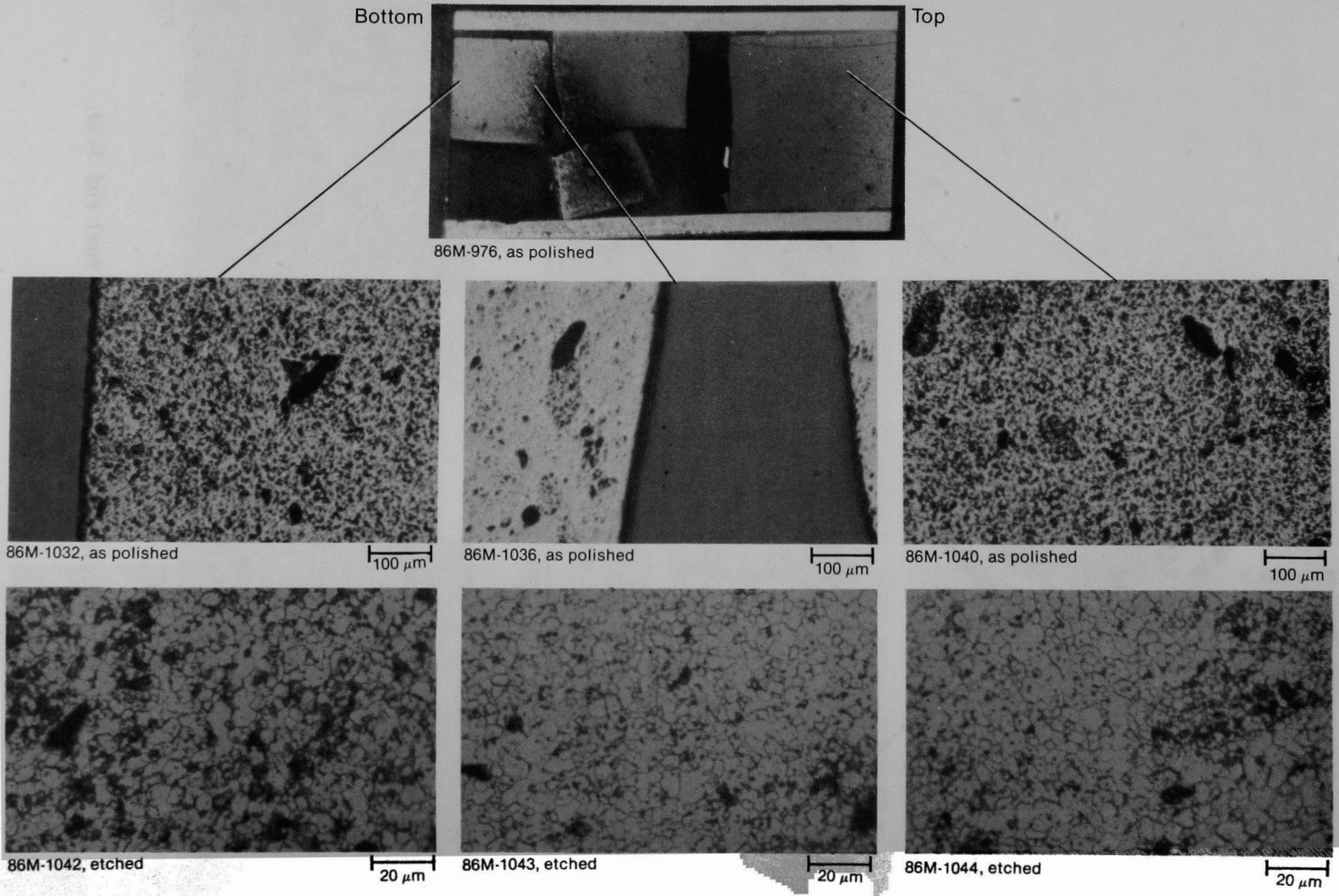


Figure 38. Fuel morphology in sample M-5 from fuel rod 3-42.

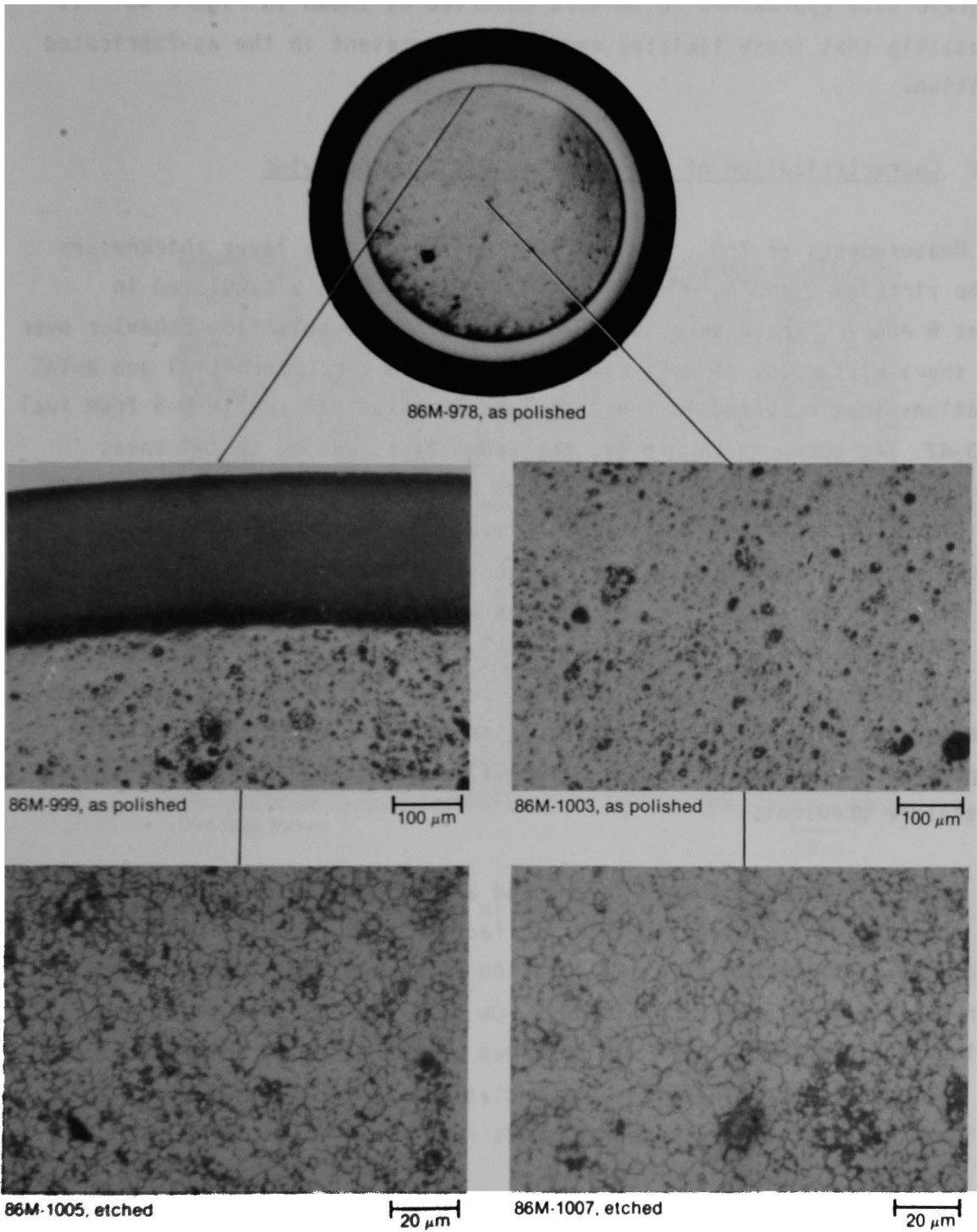


Figure 39. Fuel morphology in sample M-7 from fuel rod 3-42.

unusual characteristics or any definite evidence of fuel oxidation. The typical grain size of the fuel was 5-7 μm , however isolated regions where the grain size approached 10 μm were observed as shown in Figure 40. It is possible that these isolated regions were present in the as-fabricated condition.

6.2.2 Characterization of the Zircaloy Cladding Behavior

Measurements of ZrO_2 , $\alpha\text{-Zr(O)}$, and prior-beta layer thicknesses on the zircaloy cladding of fuel rods 3-30 and 3-42 are tabulated in Tables 6 and 7. There were large variations in the oxidation behavior over very short distances, as best exemplified by the circumferential and axial variations that occurred in the 2-cm-long longitudinal sample M-5 from fuel rod 3-42. As shown in Figure 41, the ZrO_2 layers varied in thickness from the arbitrarily referenced 0 degree orientation to the opposite side (180 degree orientation) at the same elevation. On the other hand, at only a short distance (approximately 2 cm) above this elevation (not shown on this figure), the ZrO_2 layer thicknesses were approximately 40 μm on both sides of the sample. Much less oxidation was observed on fuel rod 3-30 at comparable axial locations, and even at much lower elevations. These results illustrate the steep gradients in material behavior that occurred as a result of localized steam flow conditions and/or steep temperature gradients.

Small, intermittent ZrO_2 layers and a continuous $\alpha\text{-Zr(O)}$ layer were observed on the cladding inner surface of fuel rod 3-42 near the bottom end. At the higher axial location of sample M-7, both of these inner surface layers were continuous. On fuel rod 3-30, only a small continuous $\alpha\text{-Zr(O)}$ layer was observed on the cladding inner surface near the bottom end. These results indicate that zircaloy oxidation continued to occur after these fuel rods ruptured.

All of the unoxidized zircaloy cladding in sample M-5 from the bottommost end of fuel rod 3-42 had transformed to the prior-beta structure. Approximately 10 cm above this elevation, at the M-7 location, temperatures were not hot enough to cause this transformation. The minimum temperature for this phase change is 1133 K. Sample M-1 from the bottom

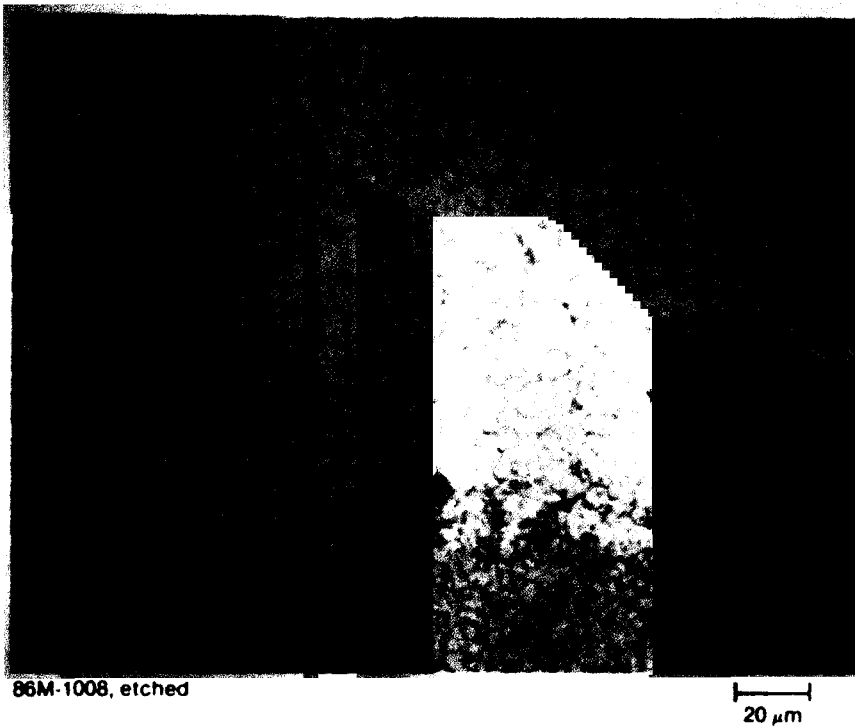


Figure 40. Isolated region of enlarged grain size in sample M-7.

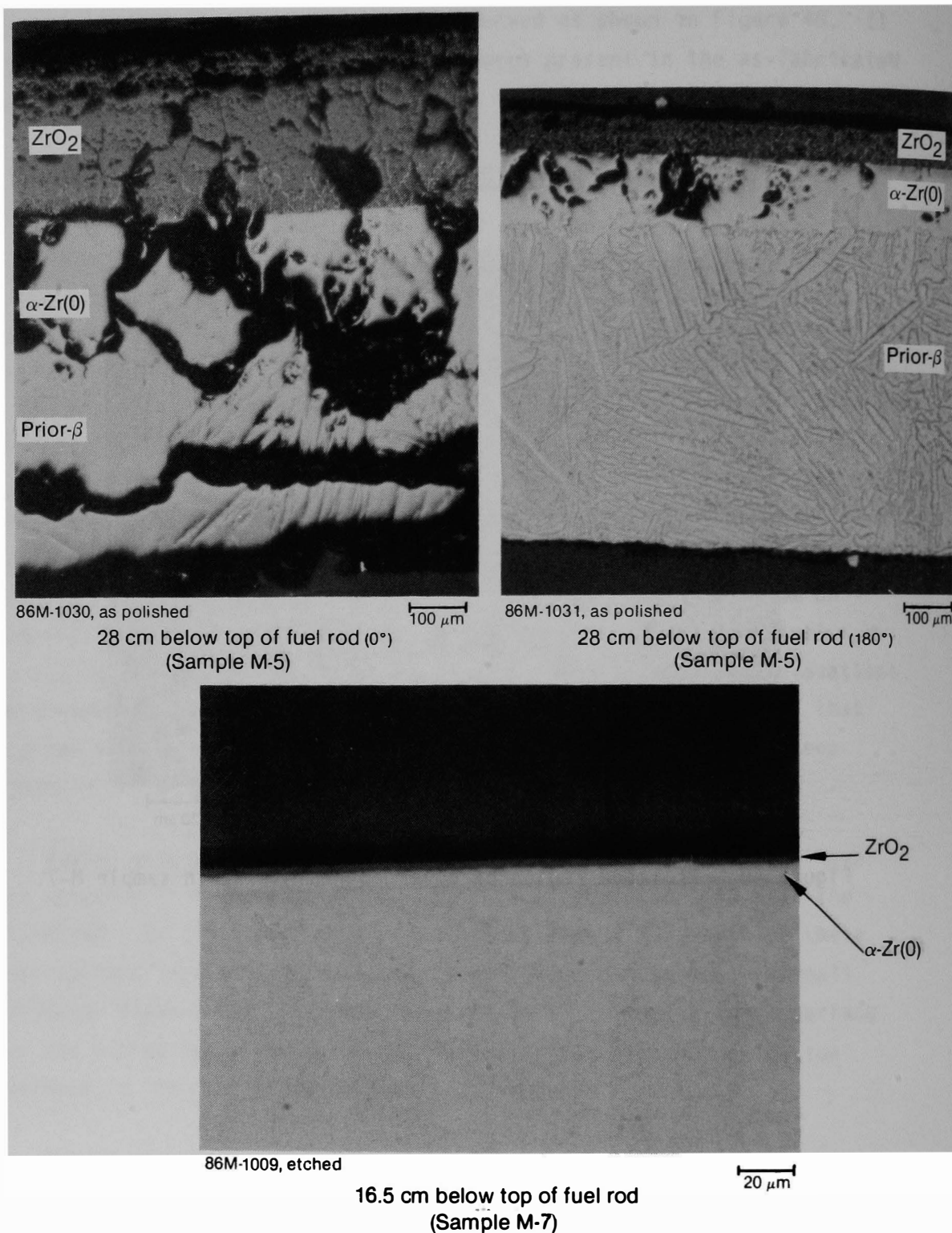


Figure 41. Variations in zircaloy oxidation on fuel rod 3-42.

TABLE 6. ZIRCALOY CLADDING MEASUREMENTS FROM FUEL ROD 3-30

Microstructure	Layer Thickness (μm)			
	Longitudinal Sample M-1 ^a		Transverse Sample M-3 ^b	
	Average	Range	Average	Range
ZrO ₂	11	10 to 12	5	3 to 6
Alpha-Zr(O)	16	10 to 20	5	5
Prior-beta	592	0 to 790	0	0
ZrO ₂ (inner surface)	0	0	0	0
Alpha-Zr(O) (inner surface)	4	4	--	--

a. 34.3 to 36.2 cm below top of rod.

b. 23.5 cm below top of rod.

TABLE 7. ZIRCALOY CLADDING MEASUREMENTS FROM FUEL ROD 3-42

Microstructure	Layer Thickness (μm)			
	Longitudinal Sample M-5 ^a		Transverse, Sample M-7 ^b	
	Average	Range	Average	Range
ZrO ₂	114	38 to 305	3	3 to 4
Alpha-Zr(O)	118	38 to 254	5	4 to 6
Prior-beta	656	580 to 730	0	0
ZrO ₂ (inner surface)	-- ^c	-- ^c	4	2 to 5
Alpha-Zr(O) (inner surface)	5	4 to 5	2	2

a. 26.0 to 27.9 cm below top of rod.

b. 16.5 cm below top of rod.

c. Intermittent thin layer.

most endtip of fuel rod 3-30 was in a transition region for this phase transformation. On one side of this longitudinal sample, all of the unoxidized zircaloy was transformed to prior-beta structure, but on the opposite side, the prior-beta structure was only present on the lower half of the sample. This indicates that at comparable axial locations, fuel rod 3-30 was not as hot as fuel rod 3-42. Rod 3-42 was located near the center of the assembly, whereas rod 3-30 was located nearer the edge of the assembly.

6.3 Radionuclide and Elemental Analyses

The objectives of performing radionuclide and elemental analyses on the TMI-2 distinct components were to characterize the distribution of fission products and core structural materials on surfaces in the upper core region (i.e., part of the intact upper fuel assemblies), to measure the retention of fission products in intact fuel material, and to determine if the control rod material had decomposed in intact rods. To characterize the distribution of radionuclides and/or structural components on surfaces in the upper core region, two methods were used: (a) the intact fuel rods, control rods, and guide tubes were analyzed using gamma spectroscopy to evaluate the distribution of the deposited fission products, and (b) thirteen samples were obtained from the intact rods for quantitative radiochemical and elemental analyses.

To evaluate fission product retention in the intact fuel, gamma spectroscopy measurements were made on some fuel rods to evaluate the variation in fission product generation in the fueled portions of the rods. Also, samples of the rods were obtained for a quantitative measurement of fission product retention in the intact fuel.

The results of the gross and isotopic gamma spectroscopy analyses performed on the twenty selected fuel rods, control rods, and guide tubes are discussed in Section 6.3.1. From the twenty rods and guide tubes, five were chosen for destructive analysis. From these rods, thirteen samples were analyzed. Table 8 lists the analyses performed and the locations

TABLE 8. SELECTED COMPONENTS FOR RADIOCHEMICAL ANALYSIS

Rod Identification	Rod Type	Sample ^a Location	Sample Identification	Material	Leached Surface		Radiochemical Analysis			
					Inner	Outer	Gamma Spectroscopy	I-129	Sr-90	Elemental
3-30	Fuel Rod	34 20	SE-2	Cladding	X	X	X	X	X	X
			SE-4	Fuel Pellet			X	X	X	
				Cladding	X	X	X	X	X	X
3-42	Fuel Rod	23 13 21	SE-6	Cladding	X	X	X	X	X	X
			SE-8	Cladding	X	X	X	X	X	X
			SE-21	Fuel Pellet			X	X	X	
3-1C	Control Rod	33 18 18	SE-9	Cladding	X	X	X	X	X	X
			SE-11	Cladding	b	X	X	X	X	X
			SE-11	Pellet						X
3-1G	Guide Tube	3 18 29 31	SE-17	Cladding	X	X	X	X	X	X
			SE-18	Cladding	X	X	X	X	X	X
			SE-19	Cladding	X	X	X	X	X	X
			SE-20	Cladding	c	c	X	X	X	X
3-14C/G	Control Rod and Guide Tube	20 2 2	SE-14	Cladding	c	c	X	X	X	X
			SE-16	Cladding	X	X	X	X	X	X
			SE-16	Pellet						X

a. Distance from the top of rod or tube where sample was removed (cm) except for control rods and guide tubes which were cut approximately 5 cm below the top of the rod. For comparison purposes, 6.5 cm should be added to the listed length of control rod and guide tube 3-1C/G and 9 cm to the listed length of control rod and guide tube 3-14C/G.

b. Sample was not leached on the inside because it had a stuck control rod in it.

c. Sample leached on both surfaces simultaneously.

where the thirteen samples were obtained. The elemental and radionuclide analysis results are discussed in Sections 6.3.2.1 and 6.3.2.2, respectively.

6.3.1 Gamma Spectroscopy of Intact Rods

Figures 42 through 46 show the gross gamma spectroscopy results for the five components chosen for radiochemical analysis, and Table 9 lists the isotopic analysis results for these samples. The locations where isotopic analyses were performed are noted on the gross scans. It should be noted that all discussions reference the intact rod end containing the spring as the top end of the rod (0 cm in the gross scan plots). Also, the isotopic data are semi-quantitative and cannot be treated as quantitative results as discussed in the footnote to Table 9. The gross gamma scan and isotopic data for the remaining components on which analyses were performed are shown or tabulated in Appendix B. The gross and isotopic data for each of the five rod sections chosen for radiochemical analysis are discussed below.

Rod 3-30. Rod 3-30 was obtained from rod position N11 in assembly C7. This location is next to a control rod and is approximately 2.9 cm from the edge of the assembly. From the neutron radiograph in Appendix Figure A-6, the total rod length is 40.4 cm of which the first 11.5 cm is the 304 SS spring region followed by a spacer and gap (3.5 cm), a fueled region of 19.4 cm, and 6 cm of empty cladding. This is the same total length of rod indicated in Figure 42, the gross gamma scan of this rod.

In Figure 42, a relatively small activity peak is present between 0 and 14 cm. The neutron radiograph of this sample indicates that the only rod components in this region are cladding, the 304 SS spring, and the zircaloy spacer. The isotopic analyses listed in Table 9 indicate that at 2.5 cm most measurable fission products (including Ce-144) were detected; however, the predominant radionuclides are Cs-137 and Co-60. The presence of Ce-144, a nonvolatile fission product, on a portion of the rod which does not contain fuel suggests the presence of particulate fuel material

TABLE 9. RADIOISOTOPIC SURFACE ACTIVITIES

Rod Identification	Rod ^b Type	Distance from the Top End of the Rod (cm)	Radionuclide Activity ($\mu\text{Ci/cm length}$) ^a						
			Cs-137 $\mu\text{Ci/cm}$	Cs-134 $\mu\text{Ci/cm}$	Co-60 $\mu\text{Ci/cm}$	Sb-125 $\mu\text{Ci/cm}$	Ce-144 $\mu\text{Ci/cm}$	Ru-106 $\mu\text{Ci/cm}$	Eu-154 $\mu\text{Ci/cm}$
3-30	FR	2.5	3.20 ± 0.01 E03	3.05 ± 0.05 E01	2.33 ± 0.01 E02	1.13 ± 0.02 E02	1.82 ± 0.26 E02	7.52 ± 0.56 E02	c
		10	2.33 ± 0.01 E02	c	5.75 ± 0.01 E03	5.61 ± 0.29 E01	c	c	c
		15	5.74 ± 0.01 E02	1.04 ± 0.04 E01	8.98 ± 0.06 E01	1.37 ± 0.01 E02	1.97 ± 0.41 E02	c	c
		24	2.61 ± 0.01 E04	2.25 ± 0.01 E02	1.02 ± 0.05 E01	3.08 ± 0.02 E02	1.70 ± 0.05 E03	9.14 ± 0.05 E02	5.28 ± 0.14 E01
		26	2.46 ± 0.01 E04	2.44 ± 0.01 E02	7.68 ± 0.32 E00	6.07 ± 0.07 E02	1.64 ± 0.05 E03	7.87 ± 0.04 E02	6.31 ± 0.13 E01
		34	3.03 ± 0.01 E04	3.89 ± 0.01 E02	8.36 ± 0.21 E00	3.72 ± 0.04 E02	1.92 ± 0.03 E03	1.13 ± 0.01 E03	9.39 ± 0.10 E01
		38	1.39 ± 0.01 E03	3.04 ± 0.04 E01	2.02 ± 0.03 E01	2.69 ± 0.03 E02	3.04 ± 0.34 E02	c	9.74 ± 0.71 E00
		51	c	c	c	c	c	c	c
3-42	FR	2.5	2.99 ± 0.02 E02	1.03 ± 0.05 E01	3.50 ± 0.01 E02	1.38 ± 0.01 E02	c	c	c
		11	1.01 ± 0.01 E02	c	7.20 ± 0.01 E03	3.71 ± 0.27 E01	c	c	c
		15	2.49 ± 0.01 E03	1.51 ± 0.05 E01	2.10 ± 0.01 E02	1.31 ± 0.01 E02	3.49 ± 0.31 E02	c	c
		25	2.64 ± 0.01 E04	2.35 ± 0.01 E02	6.24 ± 0.16 E00	9.90 ± 0.06 E02	1.98 ± 0.03 E03	8.22 ± 0.06 E02	6.69 ± 0.07 E01
		30	1.03 ± 0.01 E03	1.16 ± 0.03 E01	3.76 ± 0.15 E00	6.43 ± 0.01 E01	c	c	5.49 ± 0.56 E00
3-1C ^d	CR	0	2.97 ± 0.25 E00	c	c	c	c	c	c
		2.5	2.35 ± 0.01 E02	6.27 ± 0.17 E00	c	c	c	c	c
		5	5.19 ± 0.02 E02	1.34 ± 0.03 E01	c	c	c	c	c
		10	8.86 ± 0.01 E02	2.31 ± 0.02 E01	2.16 ± 0.09 E00	c	c	c	c
		13	1.78 ± 0.01 E02	4.61 ± 0.14 E00	c	c	c	c	c
		23	4.30 ± 0.01 E02	1.05 ± 0.02 E01	c	c	c	c	c
		33	3.98 ± 0.01 E02	1.06 ± 0.01 E01	3.50 ± 0.08 E00	3.04 ± 0.02 E01	c	c	c
		38	c	c	c	c	c	c	c
3-1G ^d	GT	0	4.15 ± 0.16 E00	c	c	c	c	c	c
		5	2.15 ± 0.01 E02	6.64 ± 0.16 E00	4.01 ± 0.13 E00	4.93 ± 0.04 E01	c	c	c
		10	2.37 ± 0.01 E02	7.20 ± 0.17 E00	6.44 ± 0.17 E00	8.27 ± 0.08 E01	c	c	c
		15	2.02 ± 0.01 E02	7.27 ± 0.19 E00	7.88 ± 0.18 E00	1.22 ± 0.01 E02	c	c	c
		20	2.00 ± 0.01 E02	8.33 ± 0.21 E00	1.03 ± 0.02 E01	1.66 ± 0.02 E02	c	c	c
		23	2.01 ± 0.01 E02	1.02 ± 0.01 E01	1.13 ± 0.01 E01	1.88 ± 0.03 E02	c	c	c
		30.5	2.20 ± 0.01 E02	1.27 ± 0.02 E01	1.41 ± 0.02 E01	2.30 ± 0.03 E02	c	c	c
		38	7.91 ± 0.98 E-01	c	3.16 ± 1.26 E-01	c	c	c	c
3-14C/G ^e	CR/GT	2.5	5.21 ± 0.02 E02	1.29 ± 0.02 E01	3.48 ± 0.18 E00	3.40 ± 0.01 E01	c	c	c
		7.5	6.87 ± 0.01 E02	1.82 ± 0.03 E01	6.56 ± 0.22 E00	5.43 ± 0.03 E01	c	c	c
		13	7.92 ± 0.01 E02	2.10 ± 0.02 E01	6.52 ± 0.11 E00	8.52 ± 0.07 E01	c	c	c
		18	7.54 ± 0.02 E02	2.06 ± 0.03 E01	1.14 ± 0.03 E01	1.17 ± 0.01 E02	c	c	c
		28	c	c	c	c	c	c	c

a. Calibration of these spectra was by normalization to one of the spectra from a fuel rod. The data are semiquantitative and are affected by changes in the composition of the rod. Therefore quantitative comparisons of the data cannot be made. The data are reported in $\mu\text{Ci/cm}$ of rod length as much of the data are not from surface deposited species. Quantitative data is obtained from the sample analysis results.

b. FR = Fuel Rod, CR = Control Rod, and GT = Guide Tube.

c. Not detected.

d. Add 6.5 cm for comparison to fuel rod locations.

e. Add 9.0 cm for comparison to fuel rod locations.

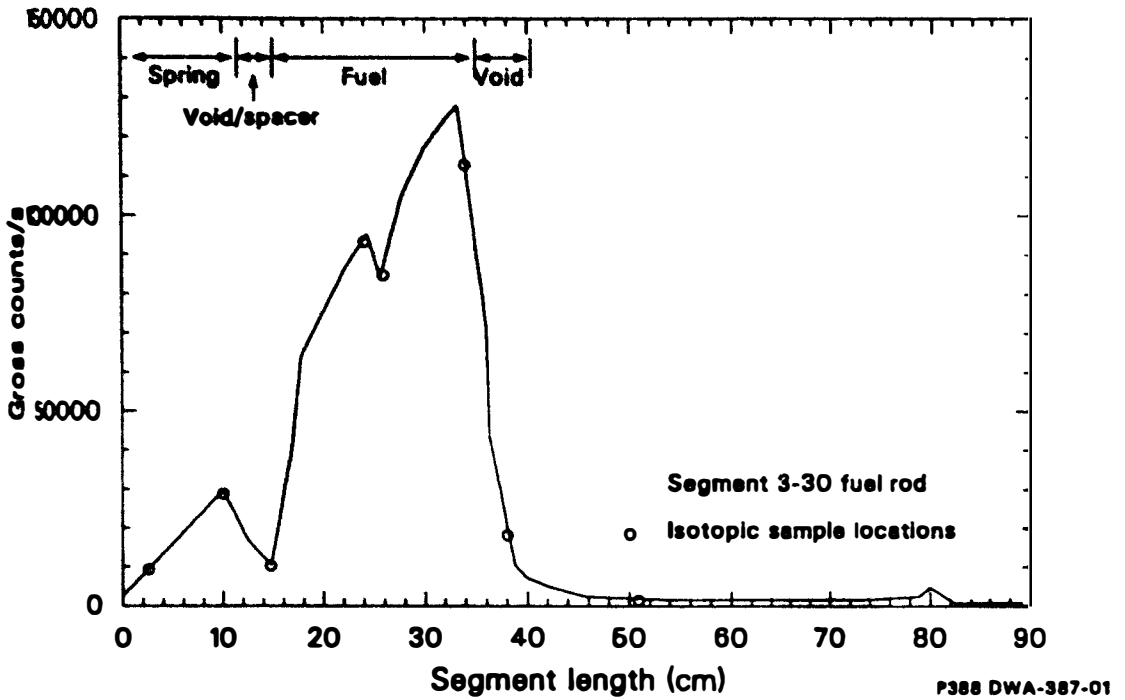


Figure 42. Gross gamma scan of segment 3-30 fuel rod.

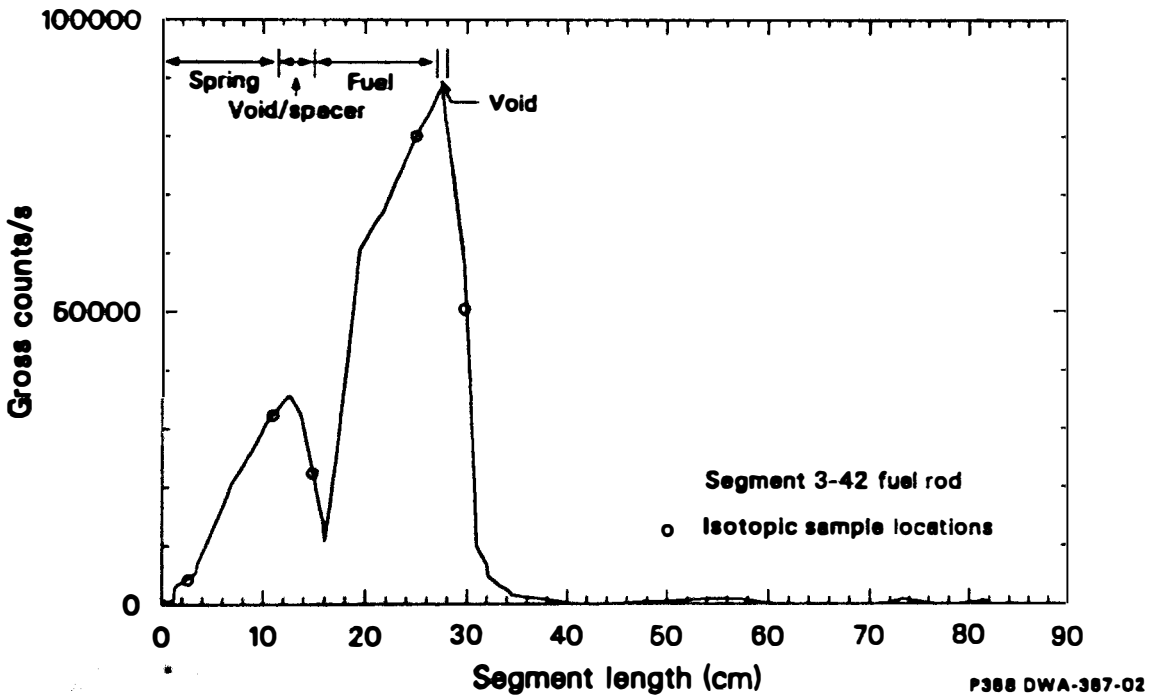


Figure 43. Gross gamma scan of segment 3-42 fuel rod.

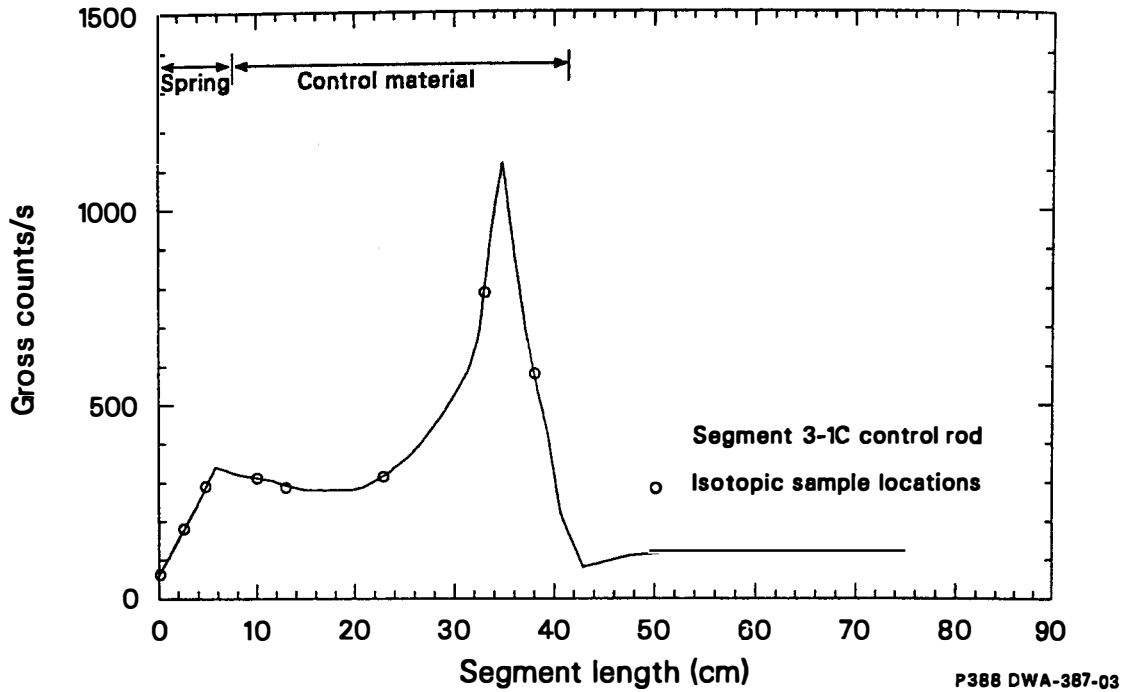


Figure 44. Gross gamma scan of segment 3-1C control rod.

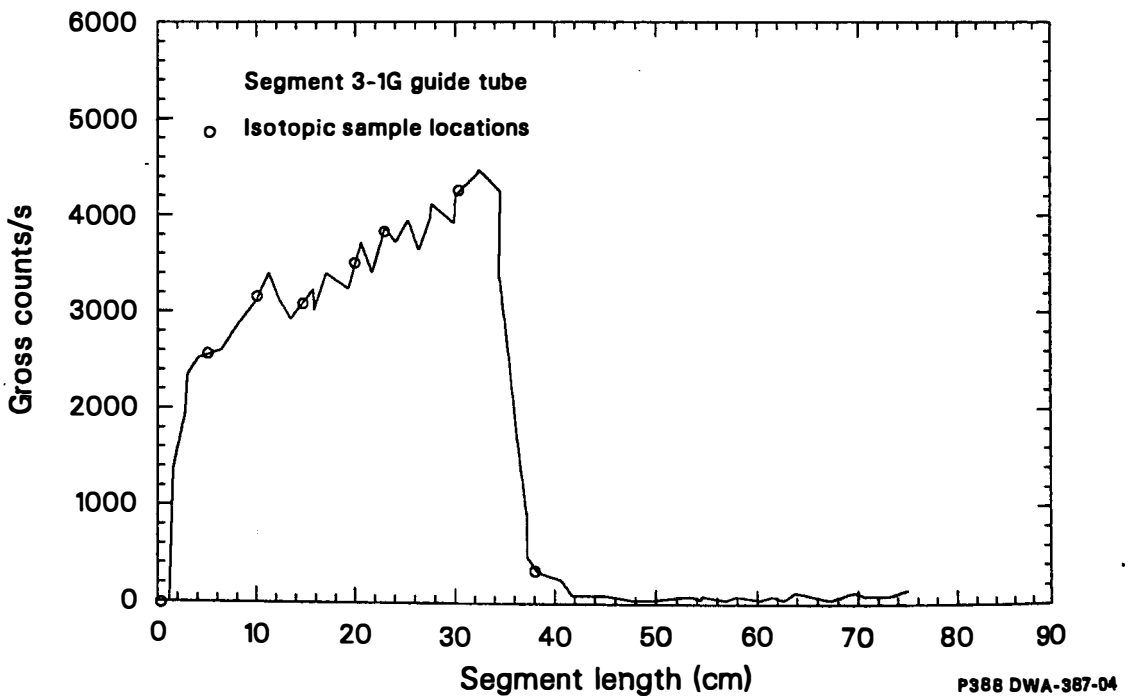


Figure 45. Gross gamma scan of segment 3-1G guide tube.

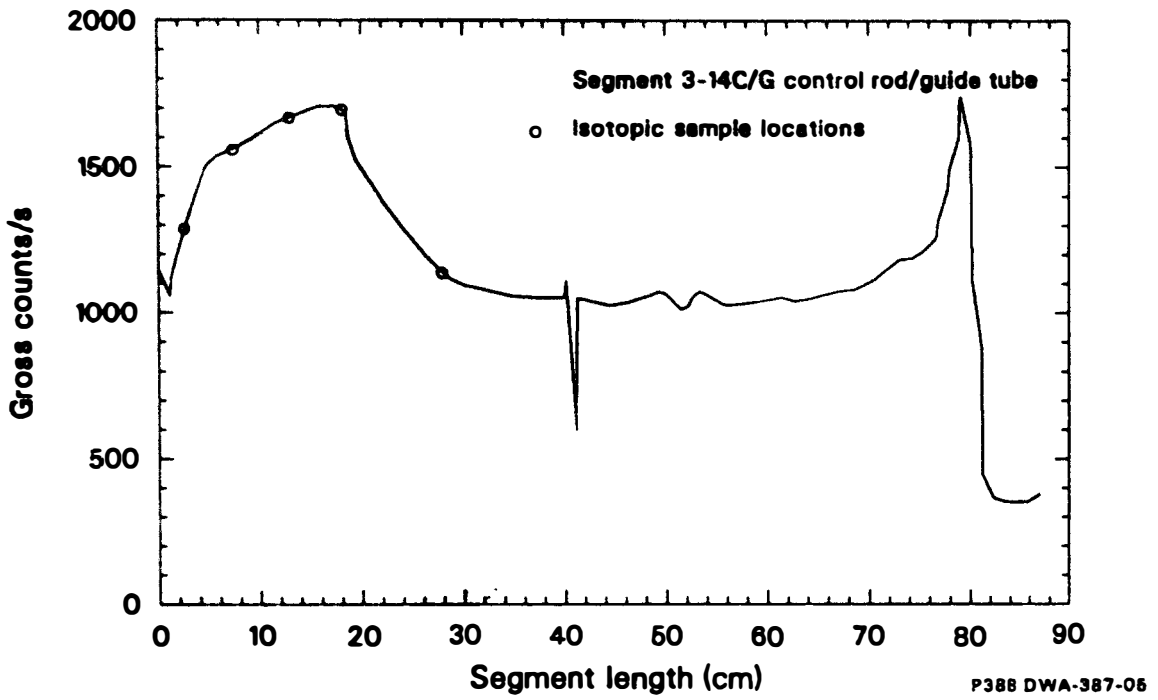


Figure 46. Gross gamma scan of segment 3-14C/G control rod/guide tube.

deposited on the surface of the rod and also explains the measurable quantities of other fission products present on the rod.

At 10 cm, Ce-144 is not measurable, indicating that no particulate fuel material is present on this part of the fuel rod; however, Co-60, Cs-137, and Sb-125 are still measurable. The Co-60 relative activity at 10 cm is 10^2 greater than the activity anywhere else on the rod. The source of this higher Co-60 activity is the greater neutron activation of the 304 SS spring at locations closer to the fueled region of the core. The presence of Cs-137 without Ce-144 on this nonfueled portion of the rod suggests that this radionuclide was probably separated from the fuel and surface-deposited on the fuel rod. Sb-125 is an activation product of tin and may be present in the nonfueled region as either the surface-deposited fission product or via activation of the cladding.

The reduction in activity from 12 to 15 cm (see Figure 42) is due to the void and zircaloy spacer as shown in the neutron radiograph of this portion of the rod. Below 15 cm is the fueled portion of the fuel rod. The visible increase in activity in Figure 42 from 15 to 35 cm is due to the increased neutron flux causing more fissions at lower locations in the assembly. The isotopic data indicate corresponding increases in activity from 15-34 cm for the measurable fission products. Also, Co-60 is measurable at most locations due to the activation of a component of the fuel rod cladding. The measured activities in the clad fuel region are 10^1 - 10^2 less than those measured in the spring region, which is to be expected because of the substantially smaller amount of Co-59 present in the cladding than in the 304 SS spring.

As shown in the neutron radiographs, between 35 and 40 cm (the open end of the rod) is a void region. The gross gamma scan indicates a significant reduction in activity through this region, and the isotopic gamma scan point (38 cm) also indicates a factor of 10 reduction for most fission products. These fission products are still measurable in an empty portion of the rod due to probable surface deposition of particulate fuel on the interior surface of the rod. It is interesting to note, however, that the Co-60 activity increased, and the Sb-125 activity decreased by

only 30%. The increase in Co-60 activity is explainable by the greater exposure of the cladding to the detector (i.e., there is no fuel in the rod to act as a shield for the Co-60 in the bottom half of the rod). The small reduction of the Sb-125 activity suggests that activation of the tin in the cladding is responsible for the approximately 2.7×10^2 $\mu\text{Ci}/\text{cm}$ of length measurable at 38 cm from the end of the rod.

A comparison of the surface deposition on the rod can only be made at locations where Ce-144 was not detectable and the only location on this fuel rod where Ce-144 was not detectable was at the 10 cm location. The only fission product that is identifiable as a surface-deposited species is Cs-137. Data on surface deposition are discussed below for rods which do not contain fuel material.

Rod 3-42. Rod 3-42 was obtained from position F8 in fuel assembly C7, which is near the center of the assembly and is surrounded by other fuel rods. It is located about 8.6 cm from the periphery of the assembly. Similar to rod 3-30, the neutron radiograph of this rod (Appendix Figure A-8) indicates that the top 11.5 cm of the rod is the 304 SS spring region followed by a spacer/void region of 3.5 cm. This rod segment had a total fueled region of about 12.1 cm followed by a 1 cm void for a total length of 28.1 cm.

Inspection of Figure 43 indicates a very similar gross gamma scan to that observed for fuel rod 3-30 (Figure 42) except that the rod (3-42) is located at about 2 cm from the bottom of the tube, thereby offsetting the rod components. As shown in Figure 43, a high activity peak is associated with the spring region (0-11.5 cm) of the rod. This peak is similar in shape to that observed for rod 3-30; however, higher count rates (15 to 20%) were measurable for this rod than were observed on rod 3-30. This would be expected as there is no adjoining control rod to reduce the available neutron flux at the location of rod 3-42. The isotopic data for the spring/spacer region of rod 3-42 (Table 9) indicates lower activities than those observed on rod 3-30 for all fission products; however, the Co-60 activities are substantially higher and would account for the increase in gross activity (Figure 43) over rod 3-30. Neither Ce-144 nor

Ru-106 were detected at either the 2.5 or 11 cm isotopic analysis locations. This suggests that fuel particles were not present near the upper end of this fuel rod when the measurements were made.

The fueled region for rod 3-42 is from 15-25 cm from the top of the rod as determined from the neutron radiographs. The gross scan data in Figure 43 show expected increases in radionuclide activity due to increases in the neutron flux at lower locations in the core and consequential increases in fissioning of the fuel material.

The isotopic data at 30 cm from the top end of the rod are from the end of the fuel column (as indicated in the neutron radiograph) and show the presence of significant amounts of Cs-137, Sb-125 and Co-60. This activity may be due to the presence of loose fuel material in the end of the rod.

Control Rod 3-1C and Guide Tube 3-1G. Control rod 3-1C and guide tube 3-1G were obtained from the N10 position next to fuel rod 3-30. This control rod/guide tube combination was located 2.9 cm from the edge of the assembly. Control rod 3-1C is 37 cm in length of which 31 cm contains control material, and the associated guide tube (3-1G) is about 36 cm in length. The control rod was separated from the guide tube, and each section was analyzed separately. The gross gamma scan results for the 3-1C control rod are shown in Figure 44 and indicate a relatively low concentration of fission products on the rod, with the greatest activity located approximately 35 cm from the end of the rod, which corresponds to the end of the guide tube. Isotopic data for the control rod 3-1C indicate a relatively similar concentration of Cs-137 along the length of the rod. The Cs-137 could have been deposited by coolant which flowed into the guide tubes through holes in the cladding after the accident. Sb-125 was only measurable on the control rod at the bottom end of the section. These data suggest possible surface deposition of Sb-125 at this location as there is no indication of particulate fuel (i.e., Ce-144), and the control rod cladding is 304 SS.

Guide tube 3-1G has a substantially different gross activity profile (shown in Figure 45) than that observed on the associated control rod. These data indicate a general increase in total activity from the top end of the guide tube to lower locations in the core. Based upon the isotopic data, the principal radionuclides present are Cs-137, Co-60, and Sb-125. The Cs-137 appears to be evenly deposited over the surface of the tube at concentrations approximately similar to those observed on the control rod. The Co-60 and Sb-125 concentrations increase from the top end of the tube to the broken end at about 35 cm. This increase is probably due to neutron activation of the iron (Fe) and tin (Sn) constituents of the zircaloy guide tube.

Control rod and guide tube 3-14C/G. The 3-14C/G was obtained from position C6, approximately 2.9 cm from the edge of the assembly. The control rod and guide tube were not separated for this analysis. The guide tube section is approximately 24 cm long and the control rod is about 17.8 cm long, as shown in the neutron radiograph in Appendix Figure A-30. The gross gamma scan (Figure 46) indicates a relatively constant distribution of activity along the length of the rod. This activity ends at the approximate end of the guide tube (about 25 cm). Beyond 25 cm, the activity measured is due to background in the tube from loose debris and surface contamination of the tube interior during handling. The isotopic data in Table 9 indicate similar activities for all radionuclides to those observed for guide tube 3-1G.

Summary. Listed below are summary observations obtained from the gamma spectroscopy analyses of the distinct components (intact fuel and control rods) described above.

- Particulate fuel deposition appears to have occurred near the top of some of the fuel rods; however, for most of the rods, including the control rods and guide tubes, there is little or no particulate fuel deposited anywhere on the rods. This would suggest that little particulate fuel deposition remains on the upper core region surfaces; however, as previously stated, current deposition data may provide little or no data on the

deposition of fuel material on incore surfaces that occurred during or shortly after the accident as the fuel assemblies sampled have been subjected to the action of reactor coolant for five years and to severe handling during their removal from the core.

- Cs-137 appears to be deposited on most surfaces of the rods that were analyzed. The data, however, indicate that the relative activities range from $2.3 \text{ E}+2$ to $8.6 \text{ E}+2 \text{ } \mu\text{Ci/cm}$ length on surfaces exposed to the coolant and suggest a relatively uneven distribution of this fission product on surfaces of the C7 assembly. This makes estimation of the deposition of Cs-137 on upper core surfaces relatively uncertain. The uneven distribution may be due to the handling the assembly received during loading and unloading.
- Sb-125 was found on the end of the 3-1C control rod without evidence of fuel material deposition (i.e., Ce-144), which suggests that Sb-125 may separate from the fuel material matrix or from the activated zircaloy and deposit on incore surfaces.

6.3.2 Radiochemical and Chemical Analysis Results

In a hot cell, cladding segments approximately 1.3 cm long were cut from selected fuel rod pieces and the pellets removed from the cladding. Specific sample locations are listed in Appendix B. Leaching of the samples was performed in 20 ml of 6M HCL at room temperature for times ranging from 2 to 4 hr. I-131 and Sr-85 were introduced into the leach solution to obtain radiometric yields for I-129 content by neutron activation and Sr-90 by beta analysis.

The outer surface of nine of twelve cladding segments was leached separately from the inner surface. Each cladding segment was closed at each end with a glass plug epoxied in place to seal it. Leaching of the outer surface was then done, and the leachate solution kept. The plugs were then removed with an epoxy dissolver and the leaching process repeated

with fresh acid to release radionuclides from the inner surface. Based on the appearance of the outer surface and some experiments, it was determined that the first leaching removed any significant amounts of fission products from the outer surface. The second leach would then have significant contributions only from the inner surface. Three pieces were not leached on both outer and inner surfaces; one (SE-11) was leached only on the outer surface because the contents (control rod material) were crimped into the cladding from the cutting process and would not come out, and the others (SE-14 and SE-20) were perforated so that leaching involved both the inner and outer surfaces. These segments were therefore leached without the use of glass plugs. After completion of leaching, the cladding was removed and the leachate was heated to boiling for 15 min and the iodine (i.e., I-131 tracer and I-129) driven off and trapped. The leachate was then brought up to 60 ml volume by addition of 6M HCL and analyzed by gamma spectroscopy for nuclide content. Aliquots of the solution were also analyzed for Sr-90, fissile material content, and elemental composition.

6.3.2.1 Chemical Analysis Results. The elements for which analyses were performed were selected to characterize the five groups of materials (see Table 1) present in the core: uranium fuel and zircaloy cladding, Ag-In-Cd control rod materials, burnable poison rod materials (A, Gd, and B), structural materials (stainless steel and Inconel), and Te. The objectives of the elemental analysis include determination of the retention or release of volatile core materials (e.g., Ag-In-Cd).

Elemental analyses were performed on the twenty-one leachate samples obtained from the exterior and interior surfaces of the fuel rod cladding, two samples of control material guide tubes, and control rod cladding to evaluate surface deposition and retention of core materials. Elemental analyses were not performed on the fuel material samples as they were obtained from undamaged fuel pellets from relatively intact fuel rods.

Results of the ICP elemental analysis for the fuel and control rod cladding and guide tube surface deposits are presented in Tables 10, 11, and 12. Results are listed in $\mu\text{g}/\text{cm}^2$ of the element removed. The total uncertainty associated with each result is 10 to 15%. Table 13 lists

TABLE 10. FUEL ROD SEGMENT SURFACE DEPOSIT ELEMENTAL ANALYSIS RESULTS
($\mu\text{g}/\text{cm}^2$)

Element	SE-2 Fuel Rod 3-30 (34 cm)		SE-4 Fuel Rod 3-30 (20 cm)		SE-6 Fuel Rod 3-42 (23 cm)		SE-8 Fuel Rod 3-42 (13 cm)	
	Exterior	Interior	Exterior	Interior	Exterior	Interior	Exterior	Interior
<u>Fuel</u>								
U	5.86 E02	2.88 E01	4.82	<5.14	1.92 E02	7.41	1.05 E02	1.59 E01
Zr ^a	1.50 E02	1.39 E02	1.54 E01	9.51 E01	8.71 E01	5.53 E01	3.59 E02	1.46 E02
Sn ^a	2.82 E01	<2.06 E01	<1.93 E01	7.71	3.21 E01	8.55	3.45 E02	<2.12 E01
<u>Control Rod</u>								
Ag	4.67 E01	1.18 E01	4.80 E-01	<0.51	9.39 E01	<5.70 E-01	6.33 E01	<5.29 E-01
In	5.68 E-1	<1.03 E-1	<9.64	<1.03 E01	6.76 E01	<1.14 E01	6.56 E01	<1.06 E01
Cd	5.73	<1.03	<9.64 E-01	<1.03	4.38	<1.14	5.88	<1.06
<u>Burnable Poison</u>								
Al	8.37	<2.06	5.78	<2.06	1.22 E01	<5.13	1.45 E01	<2.12
B	1.63 E01	<4.11	<3.86	<4.11	3.41 E01	<4.56	1.29 E02	<3.70
Gd	<1.32	<1.54	<1.45	<1.54	<1.46	<1.71	<1.36	<1.59
<u>Structural</u>								
Fe ^a	1.59 E01	2.06	4.80 E-01	<1.03	4.62 E01	1.71	1.09 E03	6.35
Ni ^a	7.93	<1.03 E01	<9.64	<1.03 E01	3.55 E01	<1.14 E01	1.56 E02	<1.06 E01
Cr	3.08	<3.60	<3.37	<3.60	<3.41	<3.99	3.45 E02	<3.70
Mn	8.80 E-01	5.10 E-01	4.80 E-01	5.10 E-01	1.46	5.70 E-01	1.40 E01	1.06
Mo	<3.52	4.11	<3.86	<4.11	<3.89	<4.56	4.52	<4.23
Co	3.52	1.03	1.45	1.03	3.41	1.14	3.17 E01	2.12
Si ^b	2.64	<2.06	<1.93	<2.06	7.30	<2.28	1.18 E01	<2.12
Nb	1.76	2.57	2.41	2.06	2.43	2.85	2.26	2.565

a. Component of structural material (zircaloy).

b. May be present as a contaminant from the dissolution.

TABLE 11. CONTROL ROD AND CONTROL ROD/GUIDE TUBE SURFACE DEPOSIT ELEMENTAL ANALYSIS RESULTS
($\mu\text{g}/\text{cm}^2$)

Element	SE-9 Control Rod 3-1C (33 cm)		Control Rod 3-1C Outer Only ^{d,b} (18 cm)	SE-11 Control Rod Guide Tube 3-14 (20 cm) ^c	SE-16 Control Rod Guide Tube 3-14 (2 cm) ^{b,c}	
	Outer	Inner			Inner	Outer
<u>Fuel</u>						
U	1.01 E02	2.16 E01	8.42 E01	3.37 E01	3.16 E01	<4.13
Zr	2.58 E03	6.12 E02	2.54 E01	7.37 E02 ^d	1.42 E01 ^d	1.11 E01 ^d
Sn	9.40 E03	3.49 E03	1.62 E04	3.37 E01 ^d	3.24 E01 ^d	6.88 ^d
<u>Control Rod</u>						
Ag	1.48 E02	1.84 E02	7.85 E01	3.60 E01	5.98 E01	<4.13
In	1.62 E02	2.37 E01	2.94 E02	3.86 E01	4.88 E-01	<8.26
Cd	5.13 E01	6.33	2.20 E01	5.71	1.09 E01	<9.17 E-01
<u>Burnable Poison</u>						
Al	1.62 E01	2.11	7.66	1.14 E01	1.52 E01	<1.83
B	1.39 E02	1.43 E01	2.06 E01	4.26 E01	2.99 E-1	<3.68
Gd	3.33	<1.58	6.70	<8.57 E-01	<1.26	<1.38
<u>Structural</u>						
Fe	2.22 E04 ^e	1.02 E04 ^e	6.04 E04 ^e	5.51 E01 ^d	9.43 E01 ^d	3.53 E01 ^d
Ni	3.95 E03 ^e	1.56 E03 ^e	7.38 E01 ^e	2.17 E01	3.03 E01	<9.17
Cr	5.32 E03 ^e	3.11 E03 ^e	1.23 E04 ^e	6.29 ^d	1.01 E01 ^d	1.28 E-1 ^d
Mn	7.22 E02 ^e	2.56 E02 ^e	1.34 E03 ^e	8.57 E-01	1.68	4.59 E-01
Mo	6.41 E01	4.33 E01	1.43 E02	<2.29	<3.37	<3.68

TABLE 11. (continued)

Element	SE-9 Control Rod 3-1C (33 cm) ^a		Control Rod 3-1C Outer Only, ^{a,b} (18 cm)	SE-11 Control Rod Guide Tube 3-14 (20 cm) ^c	SE-16 Control Rod Guide Tube 3-14 (2 cm) ^{b,c}	
	Outer	Inner			Inner	Outer
Co	4.85 E01	2.16 E01	9.09 E01	2.00	8.42 E-01	4.59 E-01
Si ^f	2.09 E02 ^e	8.97 E01 ^e	3.13 E02 ^e	4.29	5.47	<1.83
Nb	3.80 E01	1.85 E01	1.72 E01	8.57 E-01	8.42 E-01	<9.17 E-01

a. Add 6.5 cm for comparison to fuel rod locations.

b. Elemental analysis of the control rod material was also performed to determine the distribution of the materials in prior molten control rods. Listed below are the relative distributions for the samples in percent:

	SE-11 (%)	SE-16 (%)
Ag	80.0	76.4
In	15.1	18.6
Cd	5.0	5.0

c. Add 9.0 cm for comparison to fuel rod locations.

d. Component of structural material (zircaloy).

e. Component of structural material (stainless steel).

f. May be present as a contaminant from the dissolution.

TABLE 12. GUIDE TUBE SURFACE DEPOSIT ELEMENTAL ANALYSIS RESULTS
($\mu\text{g}/\text{cm}^2$)

Element	SE-17	SE-18		SE-19		SE-20
	Guide Tube 3-1GT Outer (3 cm) ^a	Guide Tube 3-1G (18 cm) ^a		Guide Tube 3-1G (29 cm) ^a		Guide Tube 3-1G (31 cm) ^a
		Inner	Outer	Inner	Outer	
<u>Fuel</u>						
U	2.83 E01	1.31 E01	5.25	1.08 E01	1.11 E01	2.37 E01
Zr ^b	2.20 E02	1.97 E02	1.71 E02	2.00 E02	9.57 E01	1.68 E02
Sn ^b	2.87 E01	4.76 E01	6.06	2.37 E01	<1.59 E01	3.23 E01
<u>Control Rod</u>						
Ag	8.64 E01	7.64 E01	2.42	4.09 E01	1.40 E01	5.15 E01
In	4.16 E01	6.63 E01	8.48	2.40 E01	7.95	3.47 E01
Cd	3.14	3.00	1.62	8.77 E-01	4.45	6.09
<u>Burnable Poison</u>						
Al	9.43	8.24	4.04	9.06	7.95	1.18 E01
B	2.28 E01	1.42 E01	4.85	9.36	1.49 E01	9.55 E-01
Gd	<1.18	<1.12	<1.21	<8.77 E-01	<9.54 E-01	<3.97 E-01
<u>Structural</u>						
Fe ^b	4.79 E01	6.40 E01	2.18 E01	1.75 E01	4.23 E01	5.34 E01
NI	1.96 E01	4.12 E01	1.17 E01	1.70 E01	2.07 E01	2.78 E01
Cr ^b	7.07	5.99	6.46	4.68	5.09	3.71
Mn	1.18	1.12	8.08 E-01	8.77 E-01	6.36 E-01	7.95 E-01
Mo	<3.14	<3.00	<3.23	<2.34	<2.54	<1.06

TABLE 12. (continued)

Element	SE-17	SE-18		SE-19		SE-20
	Guide Tube 3-1GT Outer (3 cm) ^a	Guide Tube 3-1G (18 cm) ^a		Guide Tube 3-1G (29 cm) ^a		Guide Tube 3-1G (31 cm) ^a
		Inner	Outer	Inner	Outer	
Co	1.18	1.50	1.21	1.17	1.25	1.06
Si ^c	6.29	2.25	2.02	6.43	3.82	3.97
Nb	1.18	1.12	8.08 E-01	8.77 E-01	6.36 E-01	3.97 E-01

- a. Add 6.5 cm for comparison to fuel rod locations.
- b. Component of structural material (zircaloy).
- c. May be present due to contamination from the dissolution.

TABLE 13. AVERAGE AND RANGE OF ELEMENTAL SURFACE CONCENTRATIONS FOR CORE CONSTITUENTS

Element	Fuel Rod Average Concentration ^a (μg/cm ²)	Extrapolated ^b Material Core Surface (kg)	Control Rod Average Concentration ^a (μg/cm ²)	Extrapolated ^b Material on Core Surface (kg)	Guide Tube Average Concentration ^a	Extrapolated ^b Material of Core Surface (kg)	Content Average (kg)	Range
<u>Fuel</u>								
U	2.21 E+2	2.0	9.3 E+1	0.8	1.1 E+1	0.1	1.0	11-586
Zr	1.53 E+2 ^c	--	1.30 E+3	12.0	9.3 E+1 ^c	--	12.0	15-737
Sn	1.0 E+2 ^c	--	1.28 E+4	115.0	4.3 E0 ^c	--	115.0	24-345
<u>Control Rods</u>								
Ag	5.1 E+1	0.5	1.1 E+1	0.10	5.5 E0	0.05	0.2	36-94
In	3.3 E+1	0.3	2.3 E+2	2.1	5.5 E0	0.05	0.8	24-68
Cd	4.0 E0	0.04	3.6 E+1	0.3	2.0 E0	0.02	0.1	0.9-11
<u>Burnable Poison Rods</u>								
Al	1.0 E+1	0.09	1.2 E+1	0.1	4.0 E0	0.04	0.08	5.8-16
B	4.5 E+1	0.40	8.0 E+1	0.7	6.6 E0	0.06	0.4	9.4-129
Gd	ND	--	5.0 E0	0.04	ND	--	0.04	3.3-6.7
<u>Structural Material</u>								
Fe	2.88 E+2 ^c	--	4.13 E+4 ^c	--	3.3 E+1 ^c	--	--	0.48-1.1 E+3
Cr	8.7 E+1	0.78	8.81 E+3 ^c	--	3.9 E0	0.04	0.4	3.0-345
Mn	4.2 E0	0.04	1.03 E+3 ^c	--	6.3 E-1	0.01	0.04	0.48-14
Mo	1.1 E0	0.01	1.03 E+2	0.9	ND	--	0.3	--
Co	1.0 E+1	0.09	6.9 E+1	0.6	9.7 E-1	0.01	0.35	0.8-31.7
Ni	5.0 E+1 ^c	--	2.01 E+3 ^c	--	1.3 E+1 ^c	--	0.09	7.9-156
Nb	2.2 E0	0.02	2.8 E+1	0.25	6.6 E-10.01	0.01	0.8	0.88-2.4
Si	5.4 E0	0.05	2.61 E+2	2.3	3.0 E0	0.03	--	--

a. Average includes zero values to provide more accurate indication of the average concentration.

b. Total material on incore surfaces is calculated by multiplying the surface concentration by the surface area (NSAC 25) of the top 33% of all fuel assemblies in the core. This provides a conservative estimate of availability surface area.

c. Component of the base material.

the average and range of concentrations for the surfaces exposed to the reactor vessel. Also shown is an extrapolation of these concentrations to the total surface area of intact fuel assemblies in the upper one-third of the core region. This analysis is imprecise and is expected to provide only an indication of the quantity of material that may have been deposited in the upper region of the core. More recent evaluations based on the ultrasonic topography of the upper core (Reference 4) suggest that the actual surface area available for surface deposition is approximately 20% of the surface area used for these evaluations. The results of the elemental analyses for the four groups of materials in the reactor core are discussed below.

Uranium Fuel and Zircaloy Cladding. Uranium and zirconium, the principal components of the fuel and cladding, were measurable on both interior and exterior surfaces of the cladding, control rod, and guide tube samples. Tin, a minor component of the zircaloy cladding, was also measurable on most outer surfaces and at high concentrations with respect to zirconium. The high concentrations of uranium on the exterior surfaces (up to $586 \mu\text{g}/\text{cm}^2$) were substantially greater than those measured on the interior surfaces (up to $40 \mu\text{g}/\text{cm}^2$). The higher concentrations of uranium on the exterior surfaces were confined principally to the fuel rods, with the surface concentrations on the guide tubes lower than the fuel rods by a factor of 4 to 5. The reason for the higher concentrations on the fuel rods is not known, but at the low concentrations measured, surface contamination during the cutting of the fuel samples is suspected.

The average and range data listed in Table 13 for uranium indicate a fairly wide range of concentrations, but the extrapolated deposition in the upper region of the core (i.e., fuel assembly surfaces) is quite limited at ~1 kg. Some surface deposition is to be expected because these surfaces were exposed for approximately six years to the deposition of small particles of fuel material suspended in the reactor coolant.

The variation in uranium concentrations on the exterior surfaces (Table 10) is probably due to removal of the surface deposition by the handling and cutting operations. This is particularly apparent for

Sample SE-4 where there are no measurable concentrations of uranium on either the interior or exterior surface of the fuel rod cladding. (Initial gross radiation readings also indicated that this sample had little associated radioactive surface deposition.) The interior surfaces of the guide tubes and both surfaces of the control rods have a relatively consistent concentration of uranium ranging from $7 \mu\text{g}/\text{cm}^2$ to 34 cm^2 , which would indicate a relatively even deposit at these locations. The presence of uranium on these surfaces, which were not exposed to the reactor coolant, would indicate probable contamination during the cutting operations.

Zirconium (Zr) is the principal constituent of the fuel rod cladding and guide tubes. As would be expected, Zr is measurable in all of the zircaloy fuel cladding and guide tube samples at varying concentrations (variations in content are due to differences in leaching periods and solubility). However, the highest concentrations of Zr ($6.1 \text{ E}+2$ to $2.6 \text{ E}+3$) are measurable on the stainless steel control rod [sample 3-1C (SE-9)]. This would indicate that for some currently unknown reason, substantial amounts of Zr have become associated with the stainless steel cladding.

The Tin (Sn) concentrations are substantially higher than expected for all samples. Table 13 indicates that the average concentration of Sn is approximately 34% of that measured for Zr; however, it would be expected that the amount of Sn in the dissolved sample would be proportional to the ratio of Zr present in Zircaloy (Zr/Sn = 61.2).

Table 14 lists the Zr/Sn ratios for all samples. These data indicate substantial amounts of excess Sn for the amount of Zr present. The Zr/Sn ratios range from 1 to 8 for the Zircaloy components and from 10^{-2} to 10^{-3} for the stainless steel control rods. The source of the substantial amounts of Sn is not known, but the large quantities present on the 3-1C control rod ($3.4 \text{ E}+3$ to $9.4 \text{ E}+3 \mu\text{g}/\text{cm}^2$) suggest that the quantity of Sn has been enhanced in the upper portion of the core possibly due to oxidation of the zircaloy and release of the tin as Sn metal or SnO_2 .

TABLE 14. ZIRCONIUM/TIN RATIO^a

Sample	Surface Ratio	
	Inner	Outer
Fuel Rod 3-30 (SE-2) (34 cm)	5.3	--b
Fuel Rod 3-30 (SE-4) (20 cm)	--b	12
Fuel Rod 3-42 (SE-6) (23 cm)	2.7	65
Fuel Rod 3-42 (SE-8) (13 cm)	1.0	--b
Control Rod 3-1C (SE-9) (33 cm) ^c	0.27	0.18
Control Rod 3-1C (SE-11) (18 cm) ^c	1.6 E-3	--b
Control Rod/Guide Tube 3-14C/G (SE-14) (20 cm) ^d	2.2	--b
Control Rod/Guide Tube 3-14C/G (SE-16) (2 cm) ^d	4.4	16
Guide Tube 3-1G (SE-17) (3 cm) ^c	7.7	--b
Guide Tube 3-1G (SE-18) (18 cm) ^c	4.1	28
Guide Tube 3-1G (SE-19) (29 cm) ^c	8.4	--b
Guide Tube 3-1G (SE-20) (31 cm) ^c	5.2	--b

- a. The zirconium to tin ratio in zircaloy is 61.2.
- b. No sample or a detection limit analysis.
- c. Add 6.5 cm for comparison to fuel rod locations.
- d. Add 9.0 cm for comparison to fuel rod locations.

which would be expected to deposit on colder surfaces in the core. Further analyses are needed to provide a better explanation of the high Sn concentrations.

Ag-In-Cd Control Rod Materials. The materials present in the core were originally present in the control rods in an alloy of 80% Ag, 15% In, and 5% Cd. Two samples of control rods (SE-11 and SE-16) were analyzed for control material content. The control rods from which these samples were taken had been molten as evidenced by the presence of control material in the plenum region of the rods. The Ag-In-Cd data for samples SE-11 and SE-16 listed in Table 13 indicate that although the material had been molten, the composition of the rods remained in the as-manufactured condition. These data suggest that the highly volatile Cd is not released or segregated in the intact control rods when the control material is liquified.

Table 13 indicates that the control rod materials (Ag-In-Cd) were found on all exposed surfaces except on the inner surface of the fuel rod cladding. The concentrations listed in Tables 10 through 12 indicate a relatively narrow range of concentrations: a factor of 3 for Ag and In and a factor of 12 for Cd. The data indicate that the external surface deposition is similar for the control rod/guide tubes and the fuel rod surfaces. This would suggest that no thermophoretic aerosol deposition occurred (i.e., the irreversible surface deposition may have occurred after the fuel rods had cooled to ambient temperature).

Table 13 lists the average concentrations and the ranges for the Ag, In, and Cd concentrations. Also listed is the total content of the upper core fuel assemblies if the concentration of each element were extrapolated to the surface area of the upper core region. The data suggest that very little of the core inventories of the Ag, In, and Cd are deposited on exterior surfaces in the upper core region.

The average concentrations listed in Table 13 suggest that some proportions of the constituents in the control rod material deposited on surfaces were not the same as the proportions in the as-manufactured

control rods. Table 15 lists the Ag/In, Ag/Cd, and In/Cd ratios for the external surface samples. The data indicate that there are substantial differences between the as-built control rod alloy ratios and those measured on the exterior core surfaces. The lower than expected Ag/In ratios indicate that proportionally there is substantially more In (by a factor of 4) than Ag in the surface deposits. This suggests that these elements were not deposited on the surface as the alloyed control rod material, but that they had been segregated probably by accident-related effects (either the high temperatures during the early portion of the accident or longterm leaching). The magnitude of the disproportion and the fact that neither element is soluble to any significant extent in the slightly basic reactor coolant at TMI-2 would suggest that the elements were separated due to their relatively high vapor pressures during the high temperature portion of the accident.

The Ag/Cd ratios are lower than the alloy ratio for the majority of the fuel and control rod surfaces and higher than expected for the guide tube surfaces. Also, the Ag/Cd ratios range over approximately a factor of 6, whereas the Ag/In ratios are similar to a factor of 2. The diversity in the Cd data suggests very uneven deposition of this element on the incore surfaces as compared to Ag and In. The reason for these substantial differences is not known but may be related to the relatively low boiling point of metallic Cd (1040 K).

The In/Cd ratios are significantly higher than the alloy ratio and are probably due to the higher than expected amounts of In as indicated by the Ag/In ratio. In summary, these data indicate significant accumulation of the In with relative depletion of both the Ag and Cd.

Burnable Poison Materials. The burnable poison materials measurable were Al, B, and Gd. Al and B are elements used in the burnable poison rod assemblies and Gd was used in the fuel pellets of four experimental fuel assemblies located at core positions 88, H4, H12, and N8. Al and B were measurable principally on surfaces exposed to the coolant in the reactor vessel. Gd was measurable only on the outer surface of the 3-1C control rod (SE-9 and SE-11).

TABLE 15. ELEMENTAL RATIOS FOR Ag, In, AND Cd^a

Sample	Outer Surfaces		
	Ag/In	Ag/Cd	In/Cd
Fuel Rod 3-30 (SE-2) (34 cm)	0.8	8.2	9.9
Fuel Rod 3-30 (SE-4) (20 cm)	--b	--b	--b
Fuel Rod 3-42 (SE-6) (23 cm)	1.4	21	15
Fuel Rod 3-42 (SE-8) (13 cm)	1.0	10.8	11
Control Rod/Guide Tube 3-14C/G (SE-14) (20 cm) ^c	0.9	6.3	6.8
Control Rod/Guide Tube 3-14C/G (SE-16) (2 cm) ^c	1.2	5.5	4.5
Guide Tube 3-1G (SE-17) (3 cm) ^d	1.9	28	15
Guide Tube 3-1G (SE-18) (18 cm) ^d	1.1	25	22
Guide Tube 3-1G (SE-14) (29 cm) ^d	1.7	46	27
Guide Tube 3-1G (SE-20) (31 cm) ^d	1.5	8.5	5.7

a. Expected ratios for an intact control rod are: Ag/In = 5.33, In/Cd = 3, Ag/Cd = 16.0.

b. Not detected.

c. Add 9.0 cm for comparison to fuel rod locations.

d. Add 6.5 cm for comparison to fuel rod locations.

The average Al and B concentrations were 11 and 31 $\mu\text{g}/\text{cm}^2$, respectively. The range of concentrations for Al was only a factor of 3, whereas the range for B was a factor of 14. The fact that Al was measurable is significant, as the major source of this element is the burnable poison rods. This suggests that the measurable Al might be due to the reduction of the Al_2O_3 in the poison rods and the subsequent volatilization of the metallic aluminum (B.p. = 2330 K).⁴

The presence of B on the surfaces in the core is expected because of the high concentrations in the reactor coolant (up to 5000 pm).

Gd was measurable only on the outer surfaces of control rod 3-1C (Samples SE-9 and SE-11). The data suggest that some interaction has occurred between the stainless steel clad on the control rods and Gd. The nearest source of Gd is fuel assembly D8, which is adjacent to the C7 assembly and is the only probable source of the Gd. The remaining 3 assemblies containing Gd are located in the remaining three quadrants of the core. Finding measurable Gd in the upper reactor core is unexpected as the entire core inventory of this element is 13 kg; however, the extrapolation data in Table 13 indicate that total deposition in the upper core region would be only 0.04 kg. There is no reason known for the selective presence of Gd on the surface of the 3-1C control rod.

Structural Material. The 8 structural materials in the reactor core for which analyses were performed are listed in Table 13. As noted, a number of elements are constituents of the sample matrix (e.g., iron) and are not indicative of surface deposition. The data in Table 13 indicate a very small amount of structural material deposition on the upper core region assemblies (~1.2 kg total) with the principal contributions from Cr and Ni. Deposition of Fe cannot be evaluated as it is a component of all base materials that were leached. An inspection of the composition data for stainless steel indicates that all elements are in approximately the correct ratios (i.e., none of the elements are either enhanced or depleted relative to the others).

Summary. Listed below is the summary of the observations and conclusions of the elemental analyses performed on the surface deposits from the distinct components obtained from the upper portion of the reactor core. The listed observations and conclusions are based only on the samples analyzed. These samples may not be representative of the upper core region as they make up only a small fraction of the total material in this part of the reactor core. The observations and conclusions are:

- The total quantity of all fuel rod, control rod, and structural materials, excluding Zr and Sn, is calculated to be about 4.6 kg.
- Surface deposition of the principal constituent of the fuel material U ranges over a factor of 20 depending upon the material type. The total quantity estimated to be deposited on the incore surfaces (1 to 2 kg) may have been affected by contamination during cutting of the material.
- As Zr and Sn are components of the base material for the fuel rod cladding and guide tubes, surface deposition cannot be estimated from these surfaces. However, estimated retention from the SS control rod cladding, 12 kg for Zr and 115 kg for Sn, is much higher than any other deposited material. These data indicate significant interaction between these elements and stainless steel or significant contamination of the stainless steel surface. Currently, no explanation for these high concentrations is known.
- Ag-In-Cd present in intact control rods that have been molten remains in the as-manufactured composition without depletion of Cd.
- Ag-In-Cd from the control rods is relatively evenly distributed on all surfaces exposed to the reactor coolant; however, the total weight of the deposited Ag-In-Cd is about 1.1 kg.

- There appears to be a disproportionately high concentration of In deposited on the surfaces exposed to the reactor coolant as compared to Ag and Cd.
- Aluminum, a constituent of the burnable poison rods, has a relatively constant concentration (4 to 12 $\mu\text{g}/\text{cm}^2$) on the incore surfaces. The probable source of this material is metallic aluminum produced from the reduction of Al_2O_3 and deposited on the core surfaces.
- Gd, a minor constituent of the burnable poison rods (a core inventory of 13 kg) appears to have become associated with the stainless steel control rod cladding.
- The total amount of structural material deposited on upper core surfaces is <1.2 kg, and the elemental distribution is similar to that found in stainless steel. This indicates that no constituent of the stainless steel has been depleted or enhanced in the surface deposition.

6.3.2.2 Radiochemical Analysis Results. Radiochemical analyses were performed on fuel pellets and on samples of fuel rod cladding, guide tubes, and control rod cladding as listed in Table 2. The radiochemical analyses were performed to evaluate the radionuclide content of selected fuel pellets and of the surface deposition on the cladding and guide tubes. Tables 16 through 19 list the radionuclide content of the fuel pellet samples and of the surface deposition samples, respectively.

The radionuclide content of the fuel samples is compared to the ORIGEN2 predicted concentrations for intact fuel from the upper portion of the core,¹¹ and the radionuclide content of the surface deposition samples is discussed in groups from the lowest to the highest volatility.¹² The low volatility materials include elements from the noble metals, some rare earths and actinides, tetravalents, and early transition elements. Generally, the oxides of these elements have low

TABLE 16. FUEL PELLET RADIONUCLIDE CONCENTRATIONS^a
($\mu\text{Ci/gm}$)

<u>Radionuclide</u>	<u>SE-4 Fuel Rod 3-30^b (20 cm)</u>	<u>SE-21 Fuel Rod 3-42^b (21 cm)</u>
<u>Low Volatility</u>		
Ce-144	6.09 \pm 0.22 E+1	6.40 \pm 0.15 E+1
U-235	1.88 \pm 0.19 E+4 ^c	1.92 \pm 0.19 E+4 ^c
<u>Medium Volatility</u>		
Sr-90	1.43 \pm 0.14 E+3	1.77 \pm 0.18 E+3
Eu-154	2.34 \pm 0.28 E0	3.44 \pm 0.35 E0
Eu-155	2.44 \pm 0.08 E+1	2.24 \pm 0.09 E+1
Ru-106	3.35 \pm 0.13 E+1	3.41 \pm 0.15 E+1
Sb-125	2.09 \pm 0.01 E+1	2.40 \pm 0.15 E+1
<u>High Volatility</u>		
Cs-137	2.16 \pm 0.01 E+3	2.22 \pm 0.01 E+3
Cs-134	1.12 \pm 0.03 E+1	1.27 \pm 0.03 E+1
I-129	5.5 \pm 0.6 E-4	5.7 \pm 0.6 E-4

a. Data decay corrected to April 1, 1987.

b. The results represent the average of two analyses performed on each sample to ensure that accurate and precise results were obtained.

c. U-235 concentrations are listed in $\mu\text{g/gm}$ of fuel material (PPM).

TABLE 17. FUEL ROD SEGMENT SURFACE DEPOSIT RADIOCHEMICAL ANALYSIS RESULTS
($\mu\text{Ci}/\text{cm}^2$)^a

Element	SE-2 Fuel Rod 3-30 (34 cm)		SE-4 Fuel Rod 3-30 (20 cm)		SE-6 Fuel Rod 3-42 (23 cm)		SE-8 Fuel Rod 3-42 (13 cm)		
	Outer (4.54 cm ²)	Inner ₂ (3.89 cm ²)	Outer ^b (4.15 cm ²)	Inner ₂ (3.89 cm ²)	Outer ₂ (4.11 cm ²)	Inner ₂ (3.51 cm ²)	First Outer (4.42 cm ²)	Second Outer (4.42 cm ²)	Inner ₂ (3.78 cm ²)
Low Volatility									
Ce-144	1.85 ± 0.09 E-01	--C	--C	--C	2.75 ± 0.28 E-02	--C	--C	--C	--C
Medium Volatility									
Sr-90	7.53 ± 1.13 E00	7.15 ± 1.07 E-01	1.55 ± 0.23 E-01	6.84 ± 1.03 E-02	1.57 ± 0.24 E00	1.69 ± 0.25 E-01	2.22 ± 0.33 E00	--C	1.49 ± 0.22 E-01
Eu-154	1.91 ± 0.15 E-02	--C	--C	--C	--C	--C	--C	--C	--C
Eu-155	7.44 ± 0.30 E-02	--C	--C	--C	1.13 ± 0.10 E-02	--C	--C	--C	--C
Ru-106	1.54 ± 0.12 E-01	6.80 ± 2.00 E-03	3.30 ± 0.12 E-02	3.82 ± 0.69 E-03	3.53 ± 0.43 E-02	--C	--C	--C	--C
Sb-125	1.56 ± 0.01 E00	6.37 ± 0.12 E-02	3.30 ± 0.57 E-01	7.50 ± 0.08 E-02	3.11 ± 0.03 E-01	2.17 ± 0.12 E-02	3.31 ± 0.07 E-01	3.19 ± 0.08 E-01	<1.00 E-02
High Volatility									
Co-60	7.86 ± 0.14 E-02	3.12 ± 0.18 E-03	1.05 ± 0.07 E-03	4.30 ± 0.45 E-04	7.59 ± 0.11 E-02	7.52 ± 0.33 E01	5.65 ± 0.04 E00	5.21 ± 0.02 E00	7.10 ± 0.07 E-02
Cs-134	1.29 ± 0.02 E-01	7.48 ± 0.23 E-03	2.27 ± 0.11 E-03	1.49 ± 0.10 E-03	5.52 ± 0.06 E-02	2.68 ± 0.13 E-03	6.29 ± 0.26 E-02	6.49 ± 0.32 E-02	<2.02 E-03
Cs-137	9.05 ± 0.12 E00	4.72 ± 0.02 E-02	1.07 ± 0.03 E-01	6.89 ± 0.06 E-02	2.01 ± 0.01 E00	1.44 ± 0.01 E-01	3.00 ± 0.02 E00	2.84 ± 0.02 E00	<1.09 E-01
I-129	5.80 ± 0.08 E-06	<5.57 E-07	<1.50 E-07	<2.40 E-07	4.14 ± 0.07 E-06	<3.36 E-07	1.61 ± 0.06 E-06	--C	<2.82 E-07
U-235	2.17 ± 4.34 E01	6.07 ± 1.21 E-01	3.45 ± 0.69 E-02	4.88 ± 0.93 E-02	3.89 ± 0.78 E00	1.45 ± 0.29 E-01	2.24 ± 0.45 E00	--C	3.07 ± 0.61 E-01

a. Decay corrected to April 1, 1987.

b. This sample may have had substantial amounts of surface deposition removed during handling.

c. Not detected.

TABLE 18. CONTROL ROD AND CONTROL ROD/GUIDE TUBE SURFACE DEPOSIT RADIOCHEMICAL ANALYSIS RESULTS
($\mu\text{Ci}/\text{cm}^2$)^a

Element	SE-9 Control Rod 3-1C (33 cm) ^b		SE-11 Control Rod 3-1C (18 cm) ^b	SE-14 Control Rod Guide Tube 3-14CG ^c (20 cm) ^c	SE-16 Control Rod Guide Tube 3-14CG (2 cm) ^c	
	Outer (4.21 cm ²)	Inner (3.79 cm ²)	Outer Only Solid Piece (4.18 cm ²)	Outer and Inner Torn Piece (~7.00 cm ²)	Outer (4.75 cm ²)	Inner (4.36 cm ²)
<u>Low Volatility</u>						
Ce-144	--d	--d	--d	1.17 ± 0.16 E-02	--d	--d
<u>Medium Volatility</u>						
Ru-106	--d	--d	--d	1.52 ± 0.38 E-02	--d	--d
Sb-125	1.30 ± 0.06 E-01	9.70 ± 0.2 E-02	--d	1.90 ± 0.02 E-01	1.52 ± 0.03 E-01	9.19 ± 0.57 E-03
Eu-155	--d	--d	--d	--d	--d	--d
Eu-154	--d	--d	--d	--d	--d	--d
Sr-90	7.44 ± 0.11 E-01	2.02 ± 0.30 E-02	3.61 ± 0.54 E-01	1.18 ± 0.18 E00	2.27 ± 0.34 E00	9.79 ± 1.47 E-02
<u>High Volatility</u>						
Co-60	4.79 ± 0.12 E-02	8.85 ± 0.32 E-03	4.36 ± 0.13 E-02	9.86 ± 0.10 E-02	8.12 ± 0.11 E-02	4.50 ± 0.45 E-04
Cs-134	2.25 ± 0.02 E-01	2.07 ± 0.07 E-02	3.61 ± 0.03 E-01	3.19 ± 0.05 E-02	9.31 ± 0.11 E-02	1.44 ± 0.07 E-03
Cs-137	1.07 ± 0.01 E-01	9.82 ± 0.03 E-01	1.51 ± 0.01 E00	1.48 ± 0.01 E00	4.19 ± 0.01 E00	7.25 ± 0.06 E-02
I-129	9.68 ± 0.08 E-06	<1.85 E-07	<3.10 E-07	6.33 ± 0.07 E-6	5.53 ± 0.77 E-07	<1.84 E-07
U-235	1.21 ± 0.24 E00	9.50 ± 1.90 E-02	6.27 ± 1.25 E-02	8.63 ± 1.73 E-01	8.83 ± 0.16 E-01	2.48 ± 0.50 E-02

a. Decay corrected to April 1, 1987.

b. Add 6.5 cm for comparison to fuel rod locations.

c. Add 9.0 cm for comparison to fuel rod locations.

d. Not detected.

TABLE 19. GUIDE TUBE SURFACE DEPOSIT RADIOCHEMICAL ANALYSIS RESULTS
($\mu\text{Ci}/\text{cm}^2$)^a

Element	SE-17 Guide Tube 3-1G (3 cm) ^b		SE-18 Guide Tube 3-1G (18 cm) ^b		SE-19 Guide Tube 3-1G (29 cm) ^b		SE-20 Guide Tube 3-1G (31 cm) ^b
	Outer (5.09 cm ²)	Inner (4.75 cm ²)	Outer (5.34 cm ²)	Inner (4.95 cm ²)	Outer (6.84 cm ²)	Inner (6.29 cm ²)	Outer and Inner Torn Piece (~15.00 cm ²)
<u>Low Volatility</u>							
Ce-144	--	5.91 ± 0.77 E-03	--	--	--	3.92 ± 1.94 E-03	8.39 ± 1.8 E-03
<u>Medium Volatility</u>							
Ru-106	--	--	--	--	--	5.1 ± 1.6 E-03	--
Sb-125	2.52 ± 0.02 E-01	5.15 ± 0.08 E-02	4.44 ± 0.03 E-01	5.13 ± 0.08 E-02	--	7.14 ± 0.07 E-02	3.72 ± 0.02 E-01
Eu-155	--	--	--	--	--	1.76 ± 0.27 E-03	4.80 ± 1.2 E-03
Eu-154	--	--	--	--	--	4.44 ± 0.22 E-04	1.04 ± 0.23 E-01
Sr-90	9.63 ± 0.14 E-01	1.52 ± 0.23 E00	1.34 ± 0.20 E00	5.39 ± 0.81 E-01	4.09 ± 0.61 E-01	2.81 ± 0.42 E-01	1.15 ± 0.17 E00
<u>High Volatility</u>							
Co-60	5.26 ± 0.09 E-02	4.08 ± 0.05 E-02	9.80 ± 0.08 E-02	2.70 ± 0.03 E-02	4.20 ± 0.05 E-02	9.49 ± 0.07 E-02	1.41 ± 0.01 E-01
Cs-134	3.02 ± 0.05 E-02	7.45 ± 0.22 E-03	4.22 ± 0.08 E-02	7.09 ± 0.15 E-03	1.31 ± 0.02 E-02	8.59 ± 0.21 E-03	3.57 ± 0.05 E-02
Cs-137	1.40 ± 0.01 E00	3.52 ± 0.03 E-01	1.94 ± 0.01 E00	3.31 ± 0.01 E-1	6.12 ± 0.02 E-01	3.92 ± 0.02 E-01	1.64 ± 0.01 E00
I-129	6.14 ± 0.07 E-06	1.59 ± 0.73 E-07	4.55 ± 0.05 E-06	<1.68 E-07	2.08 ± 0.03 E-06	2.86 ± 0.57 E-07	2.78 ± 0.03 E-06
U-235	6.68 ± 1.34 E-01	7.28 ± 1.46 E-01	3.24 ± 0.65 E-01	1.42 ± 0.28 E-01	2.59 ± 0.52 E-01	2.67 ± 0.53 E-01	5.45 ± 1.09 E-01

a. Decay corrected to April 1, 1987.

b. Add 6.5 cm for comparison to fuel rod locations.

volatilities; however, LaO and possibly CeO are more volatile than the element. The only radionuclide from this group that is now measurable is Ce-144.

The medium volatility fission products are characterized by boiling points of less than 3100 K (UO_2 melting). These materials include elements from the Group VA metals, alkaline earths, some of the rare earths, and actinides. The volatility of this group of elements is strongly dependent on the chemical form of the material. Fission products in this group that are measurable are Sr-90, Eu-154, Eu-155, Ru-106, and Sb-125.

The high volatility elements are the noble gases, halogens, alkali metals, and heavy chalcogens. These elements and their chemical forms are characterized by boiling points of less than 1600 K. Fission products in this group that are measurable are Cs-134, Cs-137, and I-129. A discussion of the fission product content of the fuel pellets is below, followed by a discussion of the surface deposition analyses.

6.3.2.3 Fuel Pellet Analyses. Fuel pellets from rods 3-30 (SE-2) and 3-42 (SE-21) were dissolved and analyzed for radionuclide content. The results, which were decay-corrected to April 1, 1987, are listed in Table 16. Both pellets were obtained from the C-7 assembly (an assembly with an enrichment of 1.98%) at 20 cm (SE-4) and 21 cm (SE-21) from the top end of the rod. Duplicate analyses were performed on each pellet to ensure accurate results. The radionuclide concentrations for both analyses were comparable within 20%. The core location where the samples were obtained are 4 and 6 cm into the fueled region of the rods, respectively. This corresponds to a burnup of about 1870 MWd/MTU as listed in the ORIGEN2 analysis performed for the TMI-2 reactor.¹¹

Table 20 lists the calculated radionuclide retention for the two fuel samples as compared to the corresponding data from the ORIGEN2 analysis for an average burnup of 1863 MWd/MTU. These retentions were calculated using the following equation:

TABLE 20. CALCULATED RADIONUCLIDE RETENTION FOR THE INTACT PELLETS

<u>Radionuclide</u>	<u>ORIGEN2 Predicted Concentration^a ($\mu\text{Ci/gm}$)</u>	<u>SE-2 Rod 3-30^b (34 cm)</u>	<u>SE-21 Rod 3-42^b (22 cm)</u>
<u>Low Volatility</u>			
Ce-144	1.25 E+2	55	58
<u>Medium Volatility</u>			
Sr-90	4.34 E+3	37	46
Eu-154	2.17 E+1	12	18
Eu-155	7.95 E+1	35	32
Ru-106	9.3 E+1	41	42
Sb-125	1.28 E+2	18	21
<u>High Volatility</u>			
Cs-137	4.96 E+3	49	51
Cs-134	5.86 E+1	21	25
I-129	1.62 E-3	38	39

a. ORIGEN2 predicted concentration are for the 1.98% fuel, group 1 (average burnup 1863 MWD/MTU). Data decay corrected to April 1, 1987.

b. The concentrations listed in Table 15 were increased by 13% to account for the oxygen content of the UO_2 . The ORIGEN2 data are listed as $\mu\text{Ci/gm U}$.

$$\text{Radionuclide Concentration (mCi/g U)} \times \frac{100}{\text{ORIGEN2 predicted radionuclide concentration (mCi/g uranium)}} = \text{Fission Product Retention (\% Retention)}$$

This comparison suggests low retentions of between 30 and 60% of the expected content of the pellets; however, these data cannot be used to conclude that these radionuclides were released from the fuel pellets to the listed extent because the samples were from intact pellets that had not been exposed to high temperatures and would not be expected to exhibit substantial release for any radionuclides. The low measured retentions, are, however, indicative of the limited accuracy of the ORIGEN2 code at this location in the core (i.e., the periphery). The pellets were obtained from near the top of the core, which is a region where the ORIGEN2 code has a high degree of uncertainty because the slope of the increase in the neutron flux profile is very steep and cannot be modeled with accuracy. Also, the production of fission products is not a linear process, and, consequently, the variation in retention cannot be treated as releases of these fission products.

A preliminary analysis of these data can be performed based on the relative retention of the radionuclides. The radionuclide with the highest retention, Ce-144, also has the lowest expected volatility (see Table 20). These data should be treated as inconclusive results. An assessment of the ORIGEN2 code calculations for TMI-2 is now being performed.¹³ The results of these measurements will be compared with the distinct components results in the final examination report to be published in FY-1988. This radionuclide has a calculated retention of ~50% with all others at lower concentrations. Table 21 lists the relative retention for all radionuclides normalized to the Ce-144 retention. Cs-137 has the highest normalized radionuclide retention, indicating that the measured concentrations most closely approximate those calculated by ORIGEN2 for an appropriate burnup. The normalized retentions for Sr-90, Ru-106, and I-129 range from 66-82% and indicate lesser agreement than that shown by the Cs-137. Sb-125, Cs-134, Eu-154, and Eu-155 indicate the worst agreement. For Cs-134, Eu-154, and Eu-155, this result is understandable as these radionuclides are not directly produced by fission, but are produced by the

TABLE 21. AVERAGE RADIONUCLIDE RETENTION NORMALIZED TO Ce-144

<u>Radionuclide</u>	<u>Normalized Retention^a (%)</u>
<u>Medium Volatility</u>	
Sr-90	66-82
Eu-154	22-32
Eu-155	56-62
Ru-106	72-74
Sb-125	32-38
<u>High Volatility</u>	
Cs-137	86-90
Cs-134	38-44
I-129	68-70

a. It should be noted that the radionuclide concentrations and consequently the normalized retentions are affected by the neutron flux spectrum as well as by the total flux and that the flux spectrum near the top of the core can be significantly different than the core average.

neutron activation of fission products (i.e., Cs-133, Eu-153, and Eu-154). This mode of production substantially increases the uncertainty associated with the ORIGEN2 calculations because the quantity of radionuclide produced is affected by the quantity and neutron cross section of the nuclide to be activated, which is produced at differing rates depending on the neutron flux in that area of the reactor core. The reason for the low retention for Sb-125 is not known because the production of this radionuclide should be predicted relatively accurately by ORIGEN2.

Surface Deposition Analysis Results. Tables 17 through 19 list the results of the radionuclide analyses performed on the 22 surface deposition samples. Table 22 presents the averages and the range of concentrations for the surface samples exposed directly to the reactor coolant. These analysis results and the results for the unexposed surfaces are discussed below, in order of relative volatility.

Low Volatility. The only low volatility fission product that is measurable is Ce-144; however, for comparison purposes, the content of U-235, another low volatile isotope, was also measured to assess the fuel content of the surface debris. Inspection of Table 17, the fuel rod cladding analysis results, indicates that Ce-144 was measurable only on the exterior surfaces at SE-2 and SE-6. As indicated by the U-235 analysis results, these locations correspond to the largest accumulations of fuel material. The presence of U-235 is indicated on all surfaces, but at substantially greater concentrations at the noted locations.

The control rod and control rod/guide tube data listed in Table 18 again indicate the presence of Ce-144 only at a sample location containing significant amounts of fuel. Higher U-235 concentrations are present at other locations, but the Ce-144 was not detectable, probably due to variations in the count times of the samples for the gamma ray spectroscopy analyses.

Table 19 indicates the presence of Ce-144 at concentrations substantially lower than the average on two inner guide tube surfaces and on SE-20.

TABLE 22. AVERAGE RADIONUCLIDE CONCENTRATION ON EXTERIOR SURFACES
($\mu\text{Ci}/\text{cm}^2$)

<u>Radionuclide</u>	<u>Exterior Surfaces^a</u>	
	<u>Average</u>	<u>Range</u>
<u>Low Volatility</u>		
Ce-144	7.4 E-2 ^b	0 - 1.8 E-1
<u>Medium Volatility</u>		
Sr-90	7.0 E-2 ^c	1.0 E-3 - 0.14
Eu-154	5.9 E-2 ^d	0 - 1.0 E-1
Eu-155	3.0 E-2 ^d	0 - 7.4 E-2
Ru-106	2.0 E0	0.41 - 7.5
Sb-125	5.7 E-2 ^e	0 - 1.5 E-1
<u>High Volatility</u>		
Cs-137	3.0 E0	0.61 - 9.0
Cs-134	4.1 E-6	1.6 E-7 - 9.7 E-6
I-129	4.7 E-1	0 - 1.6 E0

a. Exterior surface samples are Fuel Rods 3-30 (SE-2 and SE-4), 3-42 (SE-6 and SE-8), Control Rod Guide Tubes 3-14C/G (SE-16) and Guide Tubes 3-1G (SE-17, SE-18, SE-19, and SE-20). All data is decay corrected to April 1, 1987.

b. Only three analyses showed Ce-144 on exterior surfaces.

c. Excludes the outer surface of SE-8, which has a very high surface concentration of Co-60.

d. Both radionuclides were measurable in only 2-3 analyses.

e. Only detectable some in analyses.

The Ce-144 and U-235 data indicate isolated, relatively low concentrations of fuel material with no consistent pattern of deposition on the surfaces. This is consistent with the conclusion arrived at from the elemental data.

Medium Volatiles. The medium volatile radionuclides are Eu-154, Eu-155, Sr-90, Ru-106 and Sb-125. The average concentration data in Table 22 indicate relatively low concentrations for Eu-154 and Eu-155. The data in Tables 17 through 19 indicate that Eu-154 and Eu-155 are found only where Ce-144 is present. Based on the previous discussion, this would suggest that the Eu-154 and Eu-155 are found only in association with the fuel material.

The average Sr-90 data in Table 22 indicate a range of external surface concentrations of about a factor of 18 with an average of $2.0 \mu\text{Ci}/\text{cm}^2$. Inspection of the data indicates relatively high concentrations ($1-6 \mu\text{Ci}/\text{cm}^2$) on most external surfaces. The inner surfaces, including the inner surface of the guide tubes, which were exposed to reactor coolant, have surface concentrations that are lower by factors of 2 to 10 than the outer surfaces. The data indicate no apparent correlation with fuel material, and the data suggest that the Sr-90 was most probably deposited on the surfaces by the reactor coolant by surface adsorption. The inner surfaces of both cladding and guide tubes were not exposed to the coolant to as great an extent as the exterior surfaces or else they were exposed to relatively stagnant coolant; this accounts for the lower concentrations observed. This explanation is consistent with the known behavior of Sr-90. The majority of the Sr-90 available for surface deposition was most likely released during the accident and was subsequently adsorbed on the surfaces in the reactor vessel. This conclusion is based on reactor coolant system analyses that indicate the principal source of Sr-90 available for surface deposition was released during the early stages of the accident (although a fraction of the total was leached from the fuel into the reactor coolant during the 5 yr that the assembly was immersed in the reactor coolant).

The Ru-106 is found principally only on the surfaces of the fuel rod cladding and is found only where there is a significant amount of U-235. These data indicate that the measurable Ru-106 is associated with the fuel material and was deposited as a constituent of the particulate fuel on the upper core surfaces.

Analysis of the surface deposition of Sb-125 is difficult because this radionuclide is produced both as a fission product and as an activation product of the tin in the zircaloy. Therefore, the quantity of Sb-125 measured is affected by the total amount of structural zircaloy dissolved in the samples. The data indicate possible surface deposition of this radionuclide because the exterior surface concentrations are significantly higher ($10^1 - 10^2$ at some locations) than the interior surfaces. However, these concentrations may be affected by the Sb-125 content of the fuel material deposited on the surface. Therefore, the Sb-125 data are generally inconclusive and surface deposition of this radionuclide cannot be evaluated.

High Volatiles. The two high volatile radionuclides measurable are Cs-137 and I-129. The average concentrations listed in Table 22 indicate a substantial range of concentrations for these radionuclides. Cs-137 has a range of concentrations of approximately 15, and I-129 has a range of 60. Cs-137 was measurable on all surfaces. For the fuel rod data in Table 17, the exterior surface concentrations are 10^1 to 10^2 higher than those measured for the interior surfaces of the fuel rod cladding. These data indicate significant exterior surface deposition of this radionuclide. There is no correlation between the fuel (U-235) content and the Cs-137 content of the surface deposition. These data would suggest that the Cs-137 was not deposited with the fuel material, but was separately adsorbed on the surface. This is consistent with the known solubility of cesium.

The Cs-137 and I-129 concentration data in Tables 18 and 19 for the control rods and guide tubes are generally similar to the fuel rod data and indicate higher concentrations on exterior exposed surfaces.

The I-129 data for the fuel rod surfaces indicate similar surface deposition on the exterior surfaces of the rods with concentrations ranging from 1 to 6 E-6 $\mu\text{Ci}/\text{cm}^2$. There is no measurable I-129 on the interior surfaces of the fuel rod cladding. This would indicate that, for an intact rod in the TMI-2 core, no I-129 would be expected to be irreversibly deposited on the interior surface of the zircaloy cladding.

The data in Tables 18 and 19 indicate that I-129 is deposited on exterior surfaces, including the control rods at very similar concentrations. It is not measurable on any interior, unexposed surfaces. These data would indicate that I-129 is a surface-deposited species that may have been deposited by either volatilization and surface deposition (this is consistent with the very narrow range of concentrations) or plateout from the reactor coolant and normal surface adsorption.

Summary. Listed below are the observations and conclusions obtained from the radiochemical analyses performed on the distinct components. As previously stated, the number of samples are limited and may not be representative of the upper core region in general. Also, the data indicate that handling and cutting operations may have affected the surface deposition. The principal observations and conclusions obtained are:

- The calculated fission product retentions for the two fuel pellets are substantially lower than expected (40 to 70%). These pellets were obtained from within 10 cm of the top of the fuel in an area where there are large uncertainties both in the neutron flux and in the ORIGEN2 predicted production of radionuclides. The comparison data are to be further evaluated in subsequent examination reports.
- Table 23 lists the total inventory of fission products present on upper core surfaces exposed to the reactor coolant, if the average concentrations are extrapolated to the surface of the upper one-third of the assemblies in the core. The data indicate

TABLE 23. RADIONUCLIDE CONTENT OF UPPER CORE SURFACES

<u>Radionuclide</u>	<u>Total Inventory^a</u> <u>(μCi)</u>
<u>Medium Volatility</u>	
Sr-90	0.63
Eu-154	0.66
Eu-155	0.27
Ru-106	18.00
Sb-125	0.50
<u>High Volatility</u>	
Cs-137	27.0
Cs-134	3.7 E-5
I-129	4.2

a. This is the total quantity of fission products deposited on upper core surfaces, if the average concentration data is the extrapolated surface area of $8.98 \text{ E}+6 \text{ cm}^2$ (i.e., the surface area for one-third of all upper assemblies).

that an insignificant fraction (substantially less than 0.1%) of the core inventory of any radionuclide is deposited on the upper core surfaces.

- Ce-144, Ru-106, Eu-154, and Eu-155 deposition on the incore surfaces appear to be present as the constituents of particulate fuel material, with no evidence of release and deposition of these radionuclides individually.
- The Sr-90 data indicate similar surface deposition on surfaces exposed to the reactor coolant and no apparent association with the fuel content of the surface. These data suggest that Sr-90 was deposited on the surfaces by the reactor coolant.
- Sb-125 may be surface-deposited on the core independent of the fuel material; however, the data is inconclusive because Sb-125 is also produced as an activation product of the Sn in Zircaloy.
- Cs-137 is deposited in widely varying concentrations on most surfaces.
- I-129 is deposited on most surfaces exposed to the reactor coolant at relatively similar concentrations (within a factor of 6).

7. SUMMARY AND CONCLUSIONS

The results of the examinations of the partial fuel assemblies from the TMI-2 core are as follows:

The distinct components from the south and west sides of the reactor core were at least partially intact to the upper spacer grid elevation and were the only assemblies with partially intact fuel rods. In contrast, all the other retrieved components were intact only to just above the tie plate elevation. This suggests slightly less damage occurred on the south and west sides of the reactor, which is consistent with results from the video surveys and ultrasonic topographic mappings of the ceiling of the core.¹⁴ The overall vertical extent of the damage to these distinct components was fairly uniform.

Steep temperature gradients were present throughout the components, as evidenced by the melting behavior of different materials that were near each other and by differences in the prior molten state of a single material across an assembly. These temperature differences and/or localized steam flow conditions also resulted in significant differences in zircaloy oxidation, hydriding, and phase changes.

In general, the peak temperatures of the components examined from the south and west sides of the reactor core were near 1500 to 1600 K at the upper spacer grid elevation, and the peak temperatures of the components examined from other areas of the reactor core were generally around 1650 to 1750 K near the tie plate elevation. However, the steep temperature gradients and individual behavior of each assembly should be considered before applying this statement to a particular case.

Prior-molten Ag-Cd-In control rod material relocated into the upper plenum spring region of the control rods that were examined. Variations in the dendritic structure indicate that differences in cooling behavior existed over very short distances.

Zircaloy hydriding was observed only on the one control rod/guide tube examined. Significant variations in the amount of hydriding were observed circumferentially and axially. Zircaloy hydriding was not observed on fuel rods from the same assembly at comparable axial locations. This is attributed to the lower temperatures in the guide tubes.

Zircaloy oxidation was observed on all the fuel rod and guide tube samples examined from the C7 core position component D-141-3. Significant variations in the degree of oxidation were present circumferentially, axially, and between fuel rods. This oxidation extended to the top of the rods in this assembly.

The total quantity of all fuel rod, control rod, and structural materials that has been calculated to be deposited on upper core surfaces (i.e., fuel assembly surfaces) is <2.0 kg. (Note: This estimate is relatively conservative because calculations, based on the core topography studies, indicate that only about 20% of the original upper core region assemblies remained intact after the accident. Therefore, the actual extrapolated total surface deposition is probably closer to 0.4 kg.) Surface deposition of the principal constituents of the fuel material and cladding (U and Zr) is relatively inconsistent for all surfaces and suggests that the U and Zr have been deposited as particulate material on the surfaces. The total quantity of both elements present on upper core surfaces is very small (<3.0 kg) with more Zr (2.0 kg) than U.

There is substantially more Sn (a minor component of zircaloy) present on the upper core surfaces than would be expected from the amount of Zr present. The data suggest that this element may be concentrated on upper core surfaces; however, no data were obtained that provide information on the structural form (i.e., aerosol, hydrosol, or volatile deposition) nor the mechanism which caused the increase. This data is important as it may impact the understanding of some radionuclide behavior.

Ag-In-Cd from the control rods is relatively evenly distributed on all surfaces exposed to the reactor coolant. However, the extrapolated Ag-In-Cd surface deposition is small (<1 kg). These data indicate that

chemisorption on these surfaces was relatively minor; however, no information concerning aerosol surface deposition can be obtained from these data as aerosols would have been preferentially washed from the surfaces during the reflood portion of the accident. There appears to be significant depletion of the Cd present in the material as compared to Ag and In. This disproportionation and the relatively even distribution of the elements may result from the relatively high volatility of these elements.

The total amount of structural material deposited on upper core surfaces is <2.0 kg, and the elemental distribution is similar to that found in stainless steel. This indicates that no constituent of the stainless steel has been depleted or enhanced in the surface deposition.

The calculated fission product retentions for the two fuel pellets are substantially lower than expected (40-70%), probably because these pellets were obtained from within 10 cm of the top of the fuel column in any area where there are uncertainties both in the neutron flux and in the ORIGEN2 predicted production of radionuclides.

The fission product retentions for the two fuel pellets were also normalized to the Ce-144 content of the samples to remove some burnup-related effects from the comparisons. These data indicate lower than expected retentions for Sb-125 and the radionuclides produced by neutron activation of other fission products (i.e., Cs-134, Eu-154, and Eu-155). These results will be further reviewed as part of the TMI-2 ORIGEN2 validation study to be completed in FY-1988 (Reference 13).

An extrapolation of the surface deposition data to the surface area of the upper core region indicates that an insignificant fraction (substantially less than 0.1%) of the core inventory of any radionuclide is deposited on the upper core (fuel assembly) surfaces.

Measurements were performed to evaluate the difference in radionuclide concentrations between the inner and outer surfaces of the fuel rods, control rods, and guide tubes. Typically, most radionuclides were found at

higher concentrations on exterior rather than interior cladding surfaces. This was particularly apparent for the more volatile radionuclides (i.e., Cs-137 and I-129).

Ce-144, Ru-106, Eu-154, and Eu-155 deposition on the incore surfaces appear to be present as the constituents of particulate fuel material with no evidence of release and deposition of these radionuclides individually.

The Sr-90 data indicate similar surface deposition on surfaces exposed to the reactor coolant and no apparent association with the fuel content of the surface debris. These data suggest that Sr-90 was deposited by the reactor coolant at fairly consistent concentrations on exposed surfaces.

Cs-137 is deposited in widely varying concentrations on most surfaces. The data suggest that the Cs-137 was surface-deposited by a different mechanism than the Sr-90.

I-129 is deposited on most surfaces exposed to the reactor coolant at similar concentrations (a factor of 6), which indicates possible surface deposition by a number of mechanisms.

8. REFERENCES

1. M. L. Russell et al., TMI-2 Accident Evaluation Program Sample Acquisition and Examination Plan, EGG-TMI-7132, January 1986.
2. E. L. Tolman et al., TMI-2 Accident Evaluation Program, EGG-TMI-7048, February 1986.
3. M. L. Russell, TMI-2 Core Cavity Sides and Floor Examinations, December 1985 and January 1986, GEND-INF-074, EG&G Idaho Inc., February 1987.
4. TMI-2 Accident Core Heat-Up Analysis, NSAC-25, Nuclear Associates International and Energy Incorporated, June 1981.
5. R. W. Garner et al., An Assessment of the TMI-2 Axial Power Shaping Rod Dynamic Test Results, GEND-INF-038, EG&G Idaho Inc., April 1983.
6. L. S. Beller and H. L. Brown, Design and Operation of the Core Topography Data Acquisition System for TMI-2, GEND-INF-012, EG&G Idaho Inc., May 1984.
7. P. R. Bengel, TMI-2 Reactor Vessel Head Removal, GEND-044, GPU Nuclear Corp., September 1985.
8. V. R. Fricke, Results of End Fitting Separation in Preparation for Plenum Jacking, TPB-84-2, GPU Nuclear Corp., November 1984.
9. D. C. Wilson, TMI-2 Reactor Vessel Plenum Final Lift, GEND-054, GPU Nuclear Corporation, January 1986.
10. P. Hofmann, Reaction Kinetics Between Absorber Material (Ag, In, Cd Alloy) and Zircaloy-4 or Inconel 718 and Between Zircaloy-4 and Inconel 718 Spacer Grid Material, PNS-Annual Report 1985, KfK Report 4000, 1986.
11. B. G. Schmitzler and J. B. Briggs, TMI-2 Isotopic Inventory Calculations, EGG-PBS-6798, August 1985.
12. D. W. Akers et al., TMI-2 Core Debris Grab Samples--Examination and Analysis, Part I, GEND-INF-075, September 1986.
13. D. W. Akers et al., Fission Product Inventories for the TMI-2 Reactor, to be published.
14. E. L. Tolman et al., TMI-2 Accident Scenario Update, EGG-TMI-7489, December 1986.

APPENDIX A
RESULTS OF NEUTRON RADIOGRAPHY EXAMINATIONS

This section shows the neutron radiographies of the fuel rods, control rods, and control rodguide tubes. The assembly is divided into the following: (a) fuel rods, (b) control rods, (c) guide tubes, and (d) control rodguide tubes.

There are 52 radiographies: Figures 5-7 through 5-57.

The following is an index of Appendix A:

**APPENDIX A
RESULTS OF NEUTRON RADIOGRAPHY EXAMINATIONS**

Figure	Item	View	Remarks
5-7	Fuel Rod	Top	
5-8	Fuel Rod	Side	
5-9	Fuel Rod	Bottom	
5-10	Fuel Rod	Top	
5-11	Fuel Rod	Side	
5-12	Fuel Rod	Bottom	
5-13	Fuel Rod	Top	
5-14	Fuel Rod	Side	
5-15	Fuel Rod	Bottom	
5-16	Fuel Rod	Top	
5-17	Fuel Rod	Side	
5-18	Fuel Rod	Bottom	
5-19	Fuel Rod	Top	
5-20	Fuel Rod	Side	
5-21	Fuel Rod	Bottom	
5-22	Fuel Rod	Top	
5-23	Fuel Rod	Side	
5-24	Fuel Rod	Bottom	
5-25	Fuel Rod	Top	
5-26	Fuel Rod	Side	
5-27	Fuel Rod	Bottom	
5-28	Fuel Rod	Top	
5-29	Fuel Rod	Side	
5-30	Fuel Rod	Bottom	
5-31	Fuel Rod	Top	
5-32	Fuel Rod	Side	
5-33	Fuel Rod	Bottom	
5-34	Fuel Rod	Top	
5-35	Fuel Rod	Side	
5-36	Fuel Rod	Bottom	
5-37	Fuel Rod	Top	
5-38	Fuel Rod	Side	
5-39	Fuel Rod	Bottom	
5-40	Fuel Rod	Top	
5-41	Fuel Rod	Side	
5-42	Fuel Rod	Bottom	
5-43	Fuel Rod	Top	
5-44	Fuel Rod	Side	
5-45	Fuel Rod	Bottom	
5-46	Fuel Rod	Top	
5-47	Fuel Rod	Side	
5-48	Fuel Rod	Bottom	
5-49	Fuel Rod	Top	
5-50	Fuel Rod	Side	
5-51	Fuel Rod	Bottom	
5-52	Fuel Rod	Top	
5-53	Fuel Rod	Side	
5-54	Fuel Rod	Bottom	
5-55	Fuel Rod	Top	
5-56	Fuel Rod	Side	
5-57	Fuel Rod	Bottom	

APPENDIX A
RESULTS OF NEUTRON RADIOGRAPHY EXAMINATIONS

This section shows the neutron radiographs of the fuel rods, control rods, and control rod/guide tube sections. The appendix is divided into four sections: (a) fuel rods, (b) control rods, (c) guide tubes, and (d) control rod/guide tubes.

There are 31 radiographs (Figures A-1 through A-31).

The following is an index to Appendix A.

<u>Rod/Tube Type</u>	<u>Number</u>	<u>Figure Number</u>	<u>Page Number</u>
Fuel rod	3-6	A-1	A-5
Fuel rod	3-14	A-2	A-5
Fuel rod	3-18	A-3	A-5
Fuel rod	3-20	A-4	A-6
Fuel rod	3-28	A-5	A-6
Fuel rod	3-30	A-6	A-6
Fuel rod	3-35	A-7	A-7
Fuel rod	3-42	A-8	A-7
Fuel rod	3-61	A-9	A-7
Fuel rod	3-70	A-10	A-8
Fuel rod	3-88	A-11	A-8
Fuel rod	3-89	A-12	A-8
Fuel rod	3-94	A-13	A-9
Fuel rod	3-98	A-14	A-9
Fuel rod	3-102	A-15	A-9
Fuel rod	11-1	A-16	A-10
Fuel rod	11-2	A-17	A-10
Fuel rod	11-3	A-18	A-10
Fuel rod	11-4	A-19	A-11
Fuel rod	11-5	A-20	A-11
Fuel rod	11-7	A-21	A-11
Fuel rod	11-9	A-22	A-12
Control rod	3-1C	A-23	A-12
Guide tube	3-1G	A-24	A-12
Control rod	3-3C	A-25	A-13
Guide tube	3-3G	A-26	A-13
Guide tube	3-7G	A-27	A-13
Control rod/guide tube	3-9C/G	A-28	A-14
Control rod/guide tube	3-13C/G	A-29	A-14
Control rod/guide tube	3-14C/G	A-30	A-14
Control rod/guide tube	3-16C/G	A-31	A-15

APPENDIX A
RESULTS OF NEUTRON RADIOGRAPHY EXAMINATIONS

This section shows the neutron radiograph of the fuel rods, control rods, and control rodguide tube sections. The appendix is divided into four sections: (a) fuel rods; (b) control rods; (c) guide tubes; and (d) control rodguide tubes.

There are 31 radiograph stations A-1 through A-31.

The following is an index to Appendix A.

Station	Component	Material	Tube Type
A-1	Fuel rod	UO ₂	Fuel rod
A-2	Fuel rod	UO ₂	Fuel rod
A-3	Fuel rod	UO ₂	Fuel rod
A-4	Fuel rod	UO ₂	Fuel rod
A-5	Fuel rod	UO ₂	Fuel rod
A-6	Fuel rod	UO ₂	Fuel rod
A-7	Fuel rod	UO ₂	Fuel rod
A-8	Fuel rod	UO ₂	Fuel rod
A-9	Fuel rod	UO ₂	Fuel rod
A-10	Fuel rod	UO ₂	Fuel rod
A-11	Fuel rod	UO ₂	Fuel rod
A-12	Fuel rod	UO ₂	Fuel rod
A-13	Fuel rod	UO ₂	Fuel rod
A-14	Fuel rod	UO ₂	Fuel rod
A-15	Fuel rod	UO ₂	Fuel rod
A-16	Fuel rod	UO ₂	Fuel rod
A-17	Fuel rod	UO ₂	Fuel rod
A-18	Fuel rod	UO ₂	Fuel rod
A-19	Fuel rod	UO ₂	Fuel rod
A-20	Fuel rod	UO ₂	Fuel rod
A-21	Fuel rod	UO ₂	Fuel rod
A-22	Fuel rod	UO ₂	Fuel rod
A-23	Fuel rod	UO ₂	Fuel rod
A-24	Control rod	Ag-In-Cd	Control rod
A-25	Control rod	Ag-In-Cd	Control rod
A-26	Control rod	Ag-In-Cd	Control rod
A-27	Control rod	Ag-In-Cd	Control rod
A-28	Control rod	Ag-In-Cd	Control rod
A-29	Control rod	Ag-In-Cd	Control rod
A-30	Control rod	Ag-In-Cd	Control rod
A-31	Control rod	Ag-In-Cd	Control rod



Figure A-1. Neutron radiograph of fuel rod segment 3-6.



Figure A-2. Neutron radiograph of fuel rod segment 3-14.



Figure A-3. Neutron radiograph of fuel rod segment 3-18.

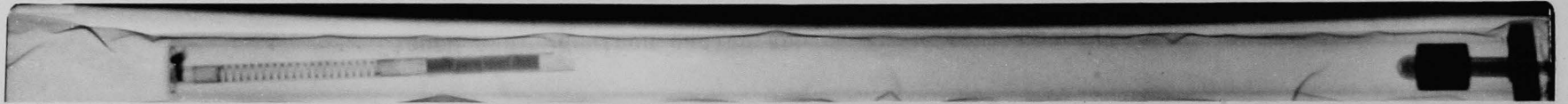


Figure A-4. Neutron radiograph of fuel rod segment 3-20.

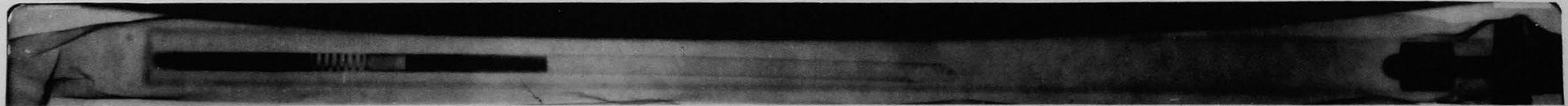


Figure A-5. Neutron radiograph of fuel rod segment 3-28.



Figure A-6. Neutron radiograph of fuel rod segment 3-30.



Figure A-7. Neutron radiograph of fuel rod segment 3-35.



Figure A-8. Neutron radiograph of fuel rod segment 3-42.



Figure A-9. Neutron radiograph of fuel rod segment 3-61.

A-7

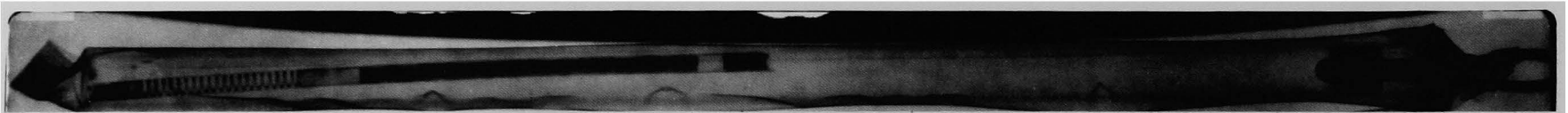


Figure A-10. Neutron radiograph of fuel rod segment 3-70.

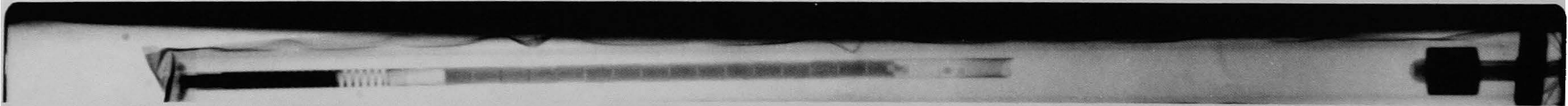


Figure A-11. Neutron radiograph of fuel rod segment 3-88.



Figure A-12. Neutron radiograph of fuel rod segment 3-89.



Figure A-13. Neutron radiograph of fuel rod segment 3-94.



Figure A-14. Neutron radiograph of fuel rod segment 3-98.

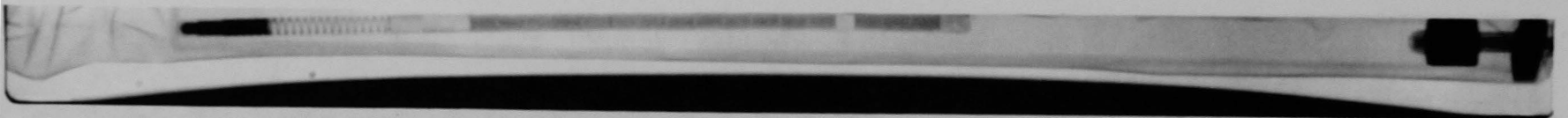


Figure A-15. Neutron radiograph of fuel rod segment 3-102.



Figure A-16. Neutron radiograph of fuel rod segment 11-1.



Figure A-17. Neutron radiograph of fuel rod segment 11-2.



Figure A-18. Neutron radiograph of fuel rod segment 11-3.



Figure A-19. Neutron radiograph of fuel rod segment 11-4.

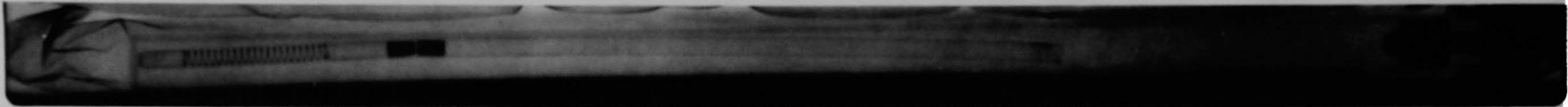


Figure A-20. Neutron radiograph of fuel rod segment 11-5.



Figure A-21. Neutron radiograph of fuel rod segment 11-7.



Figure A-22. Neutron radiograph of fuel rod segment 11-9.



Figure A-23. Neutron radiograph of control rod segment 3-1C.



Figure A-24. Neutron radiograph of guide tube segment 3-1G.

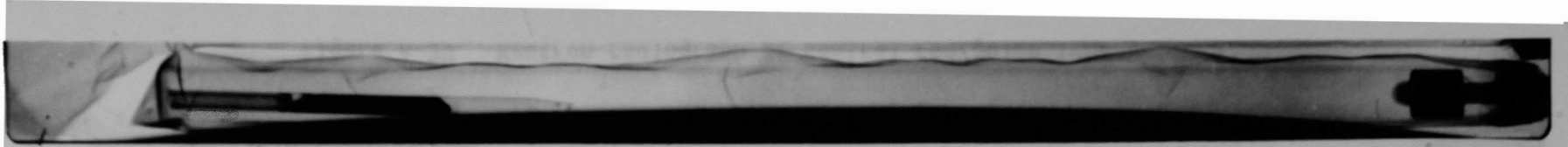


Figure A-25. Neutron radiograph of control rod segment 3-3C.

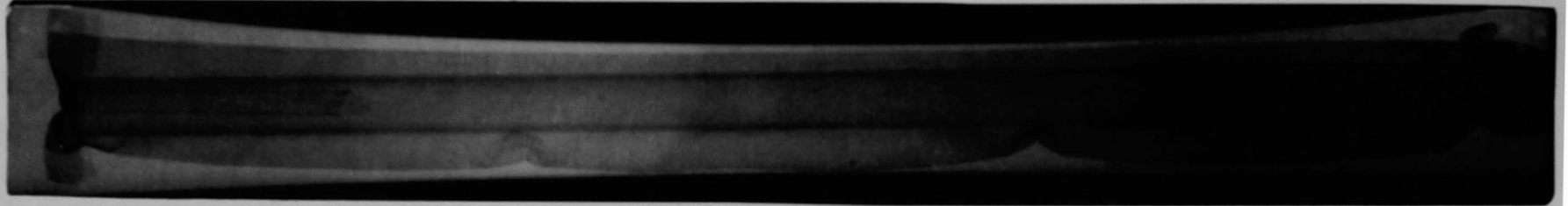


Figure A-26. Neutron radiograph of guide tube segment 3-3G.

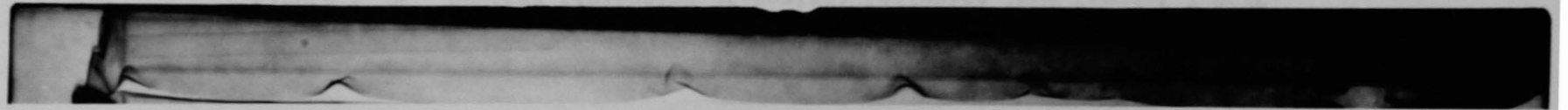


Figure A-27. Neutron radiograph of guide tube segment 3-7G.



Figure A-28. Neutron radiograph of control rod/guide tube segment 3-9C/G.



Figure A-29. Neutron radiograph of control rod/guide tube segment 3-13C/G.



Figure A-30. Neutron radiograph of control rod/guide tube 3-14C/G.

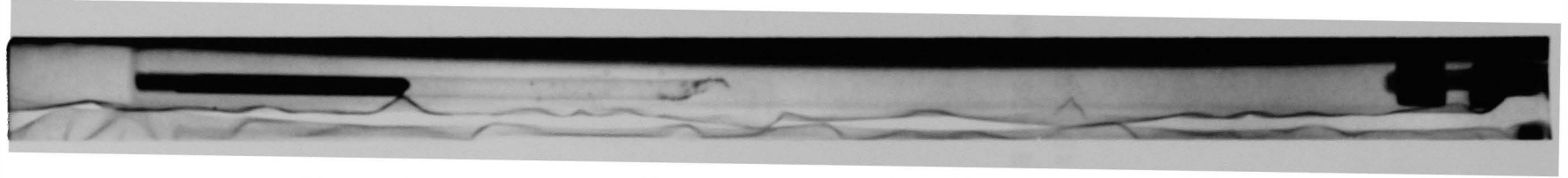
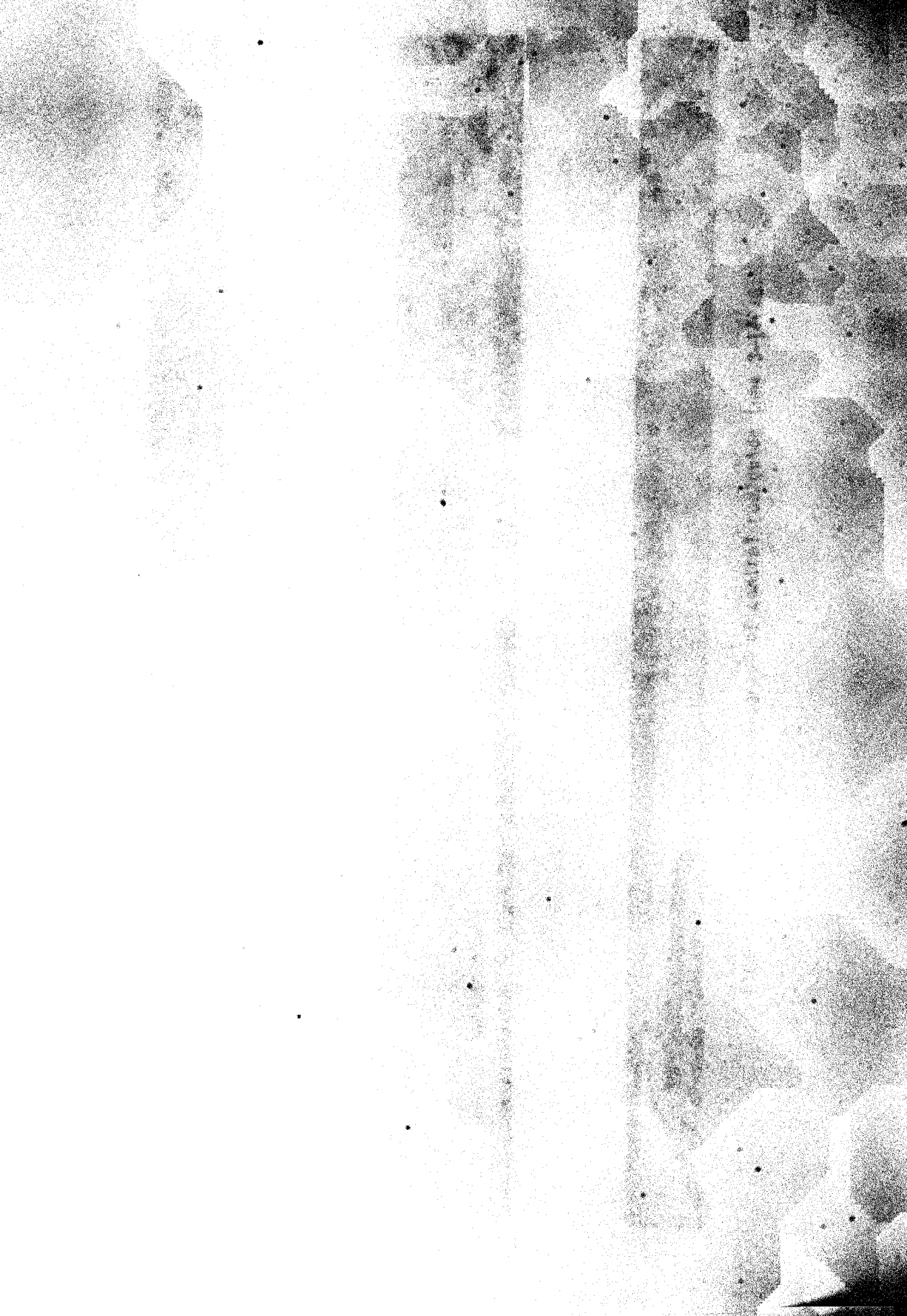


Figure A-31. Neutron radiograph of control rod/guide tube 3-16C/G.



SECRET

APPENDIX B
GAMMA SCAN RESULTS

This section presents the gross gamma scan data and the isotopic analyses results of representative distinct component samples. Additional measurements were obtained, but the results were not analyzed because the neutron radiographs indicate similar compositions and material distributions to the samples analyzed. The gross gamma scans along with the isotopic results were taken in early September 1986. The gross gamma scans (Figures B-1 through B-20) are for designated fuel rods, control rods, guide tubes and control rod/guide tube combinations. The locations where isotopic analyses were performed are shown on each gross scan. The results of the isotopic analyses are listed in Table B-1. These results are relative and are not quantitative. They have been decay-corrected to April 1, 1987.

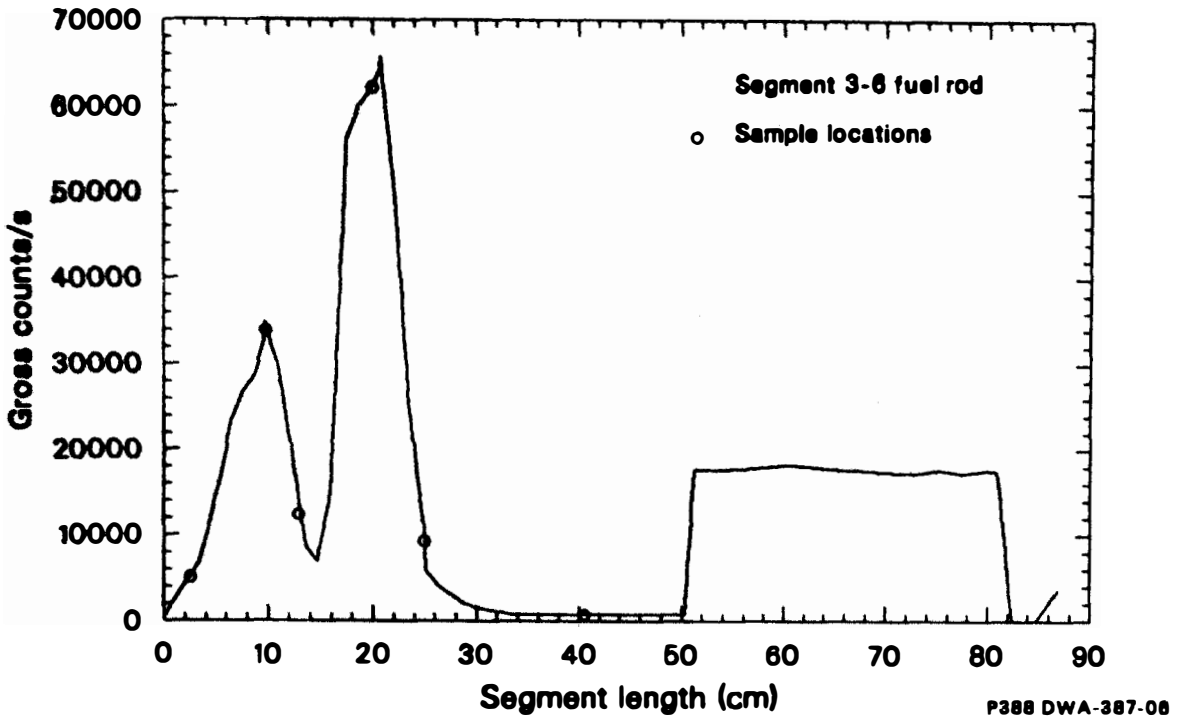


Figure 8-1. Gross gamma scan of fuel rod segment 3-6.

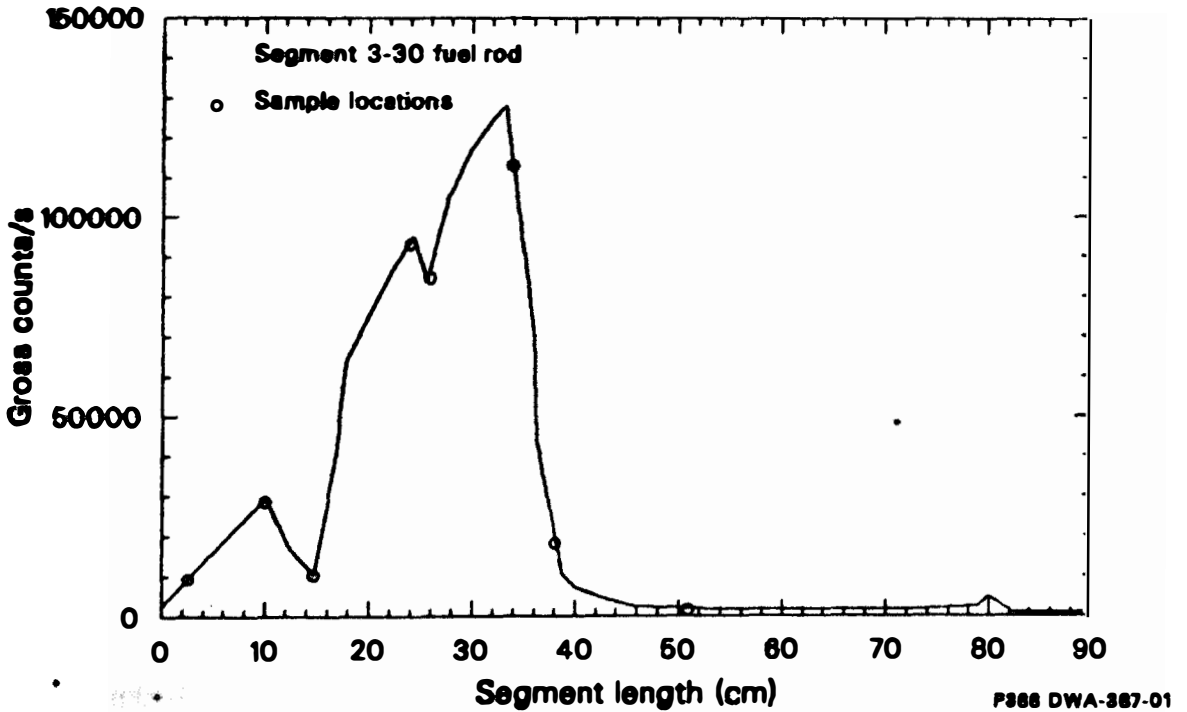


Figure 8-2. Gross gamma scan of fuel rod segment 3-30.

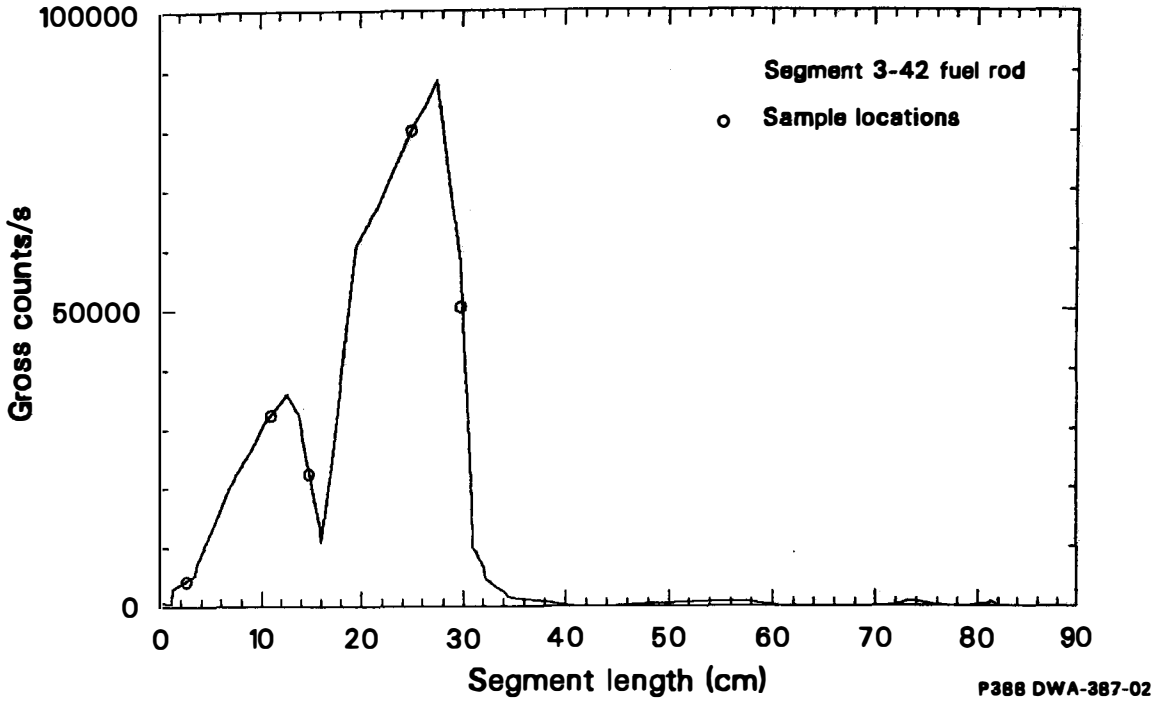


Figure B-3. Gross gamma scan of fuel rod segment 3-42.

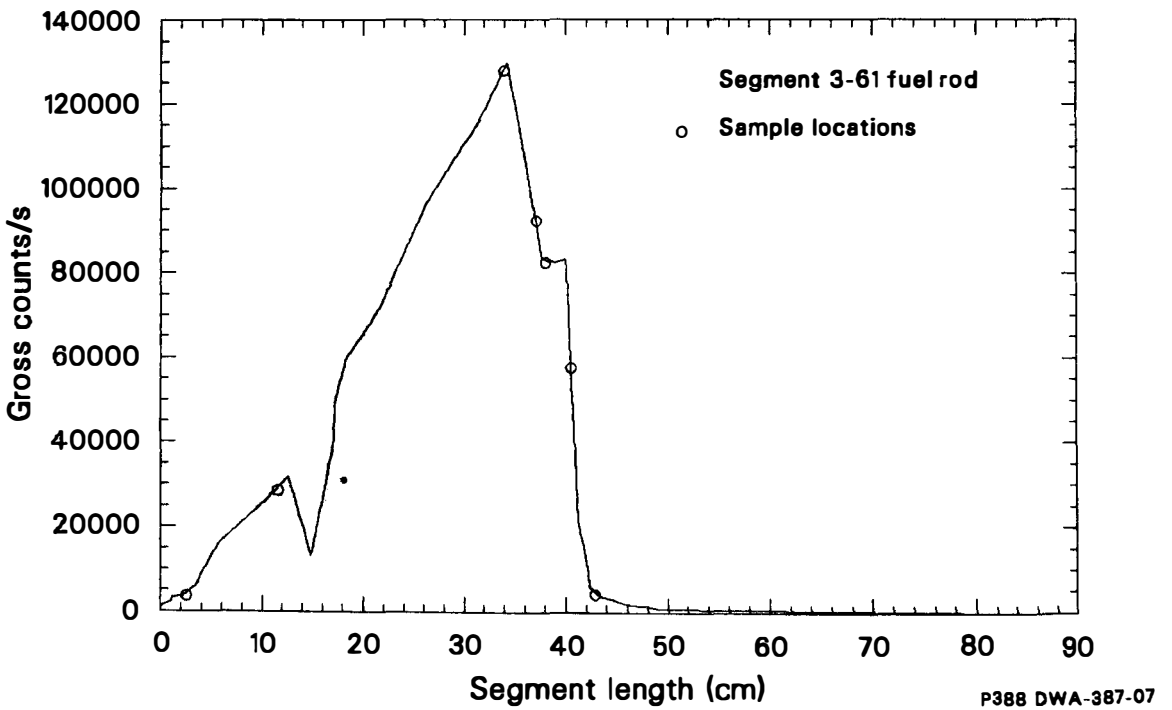


Figure B-4. Gross gamma scan of fuel rod segment 3-61.

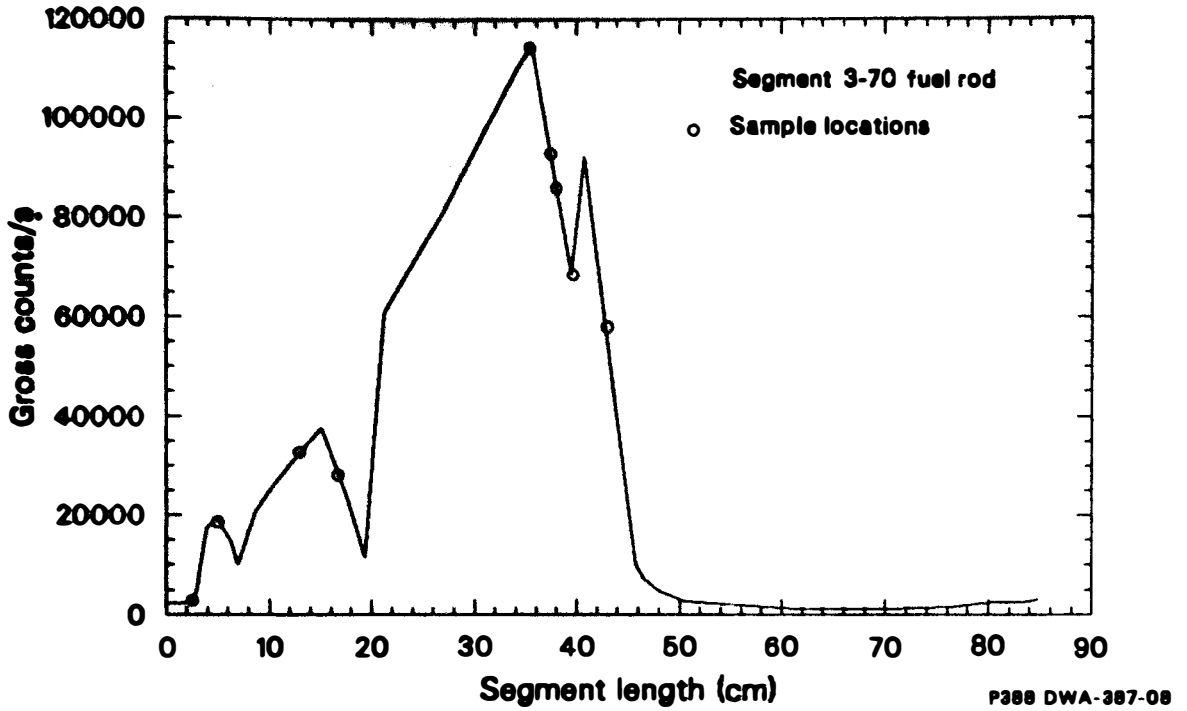


Figure B-5. Gross gamma scan of fuel rod segment 3-70.

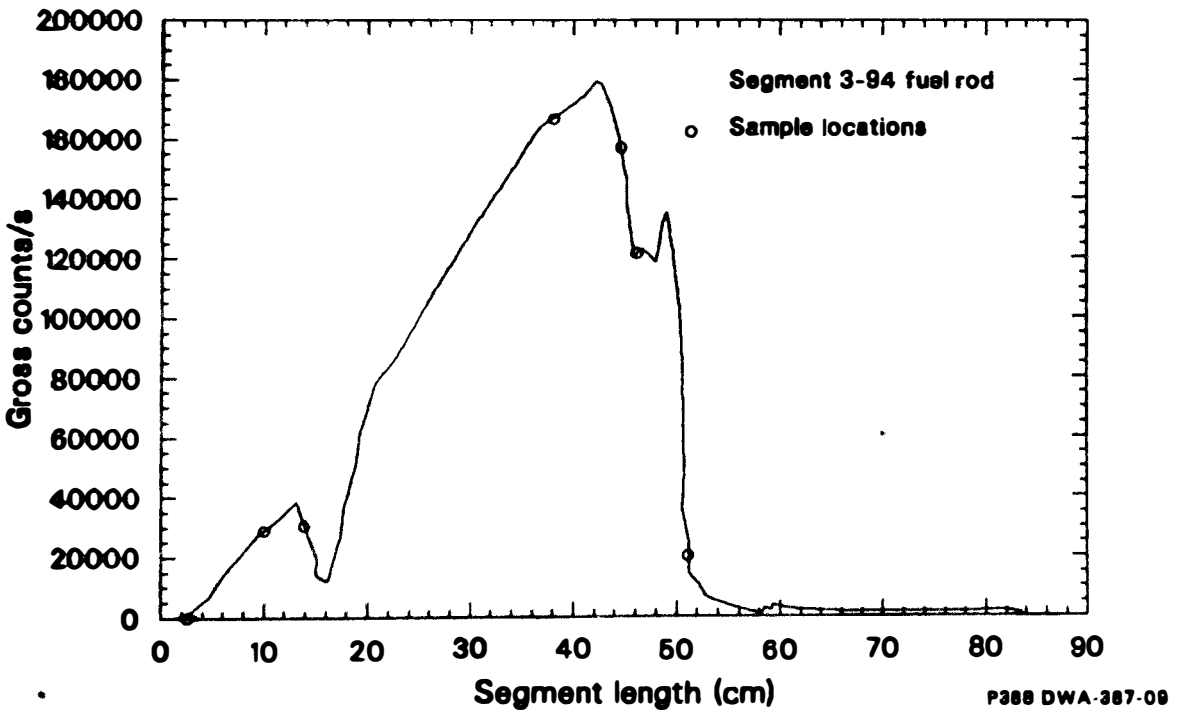


Figure B-6. Gross gamma scan of fuel rod segment 3-94.

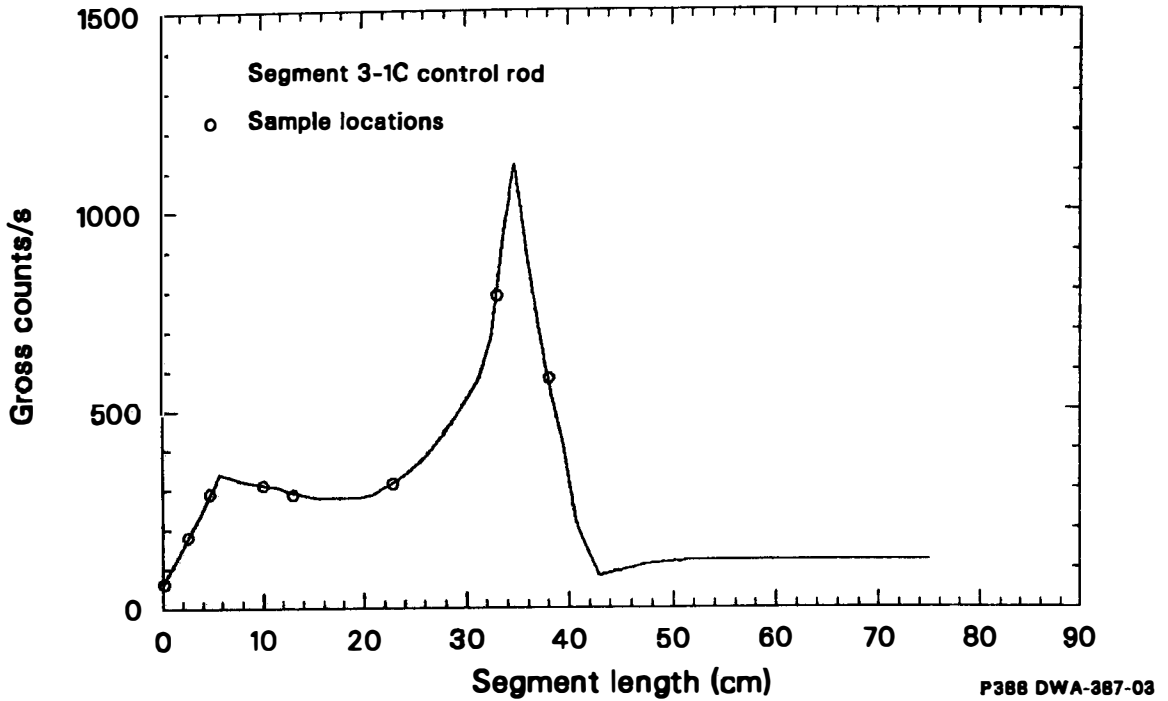


Figure B-7. Gross gamma scan of control rod segment 3-1C.

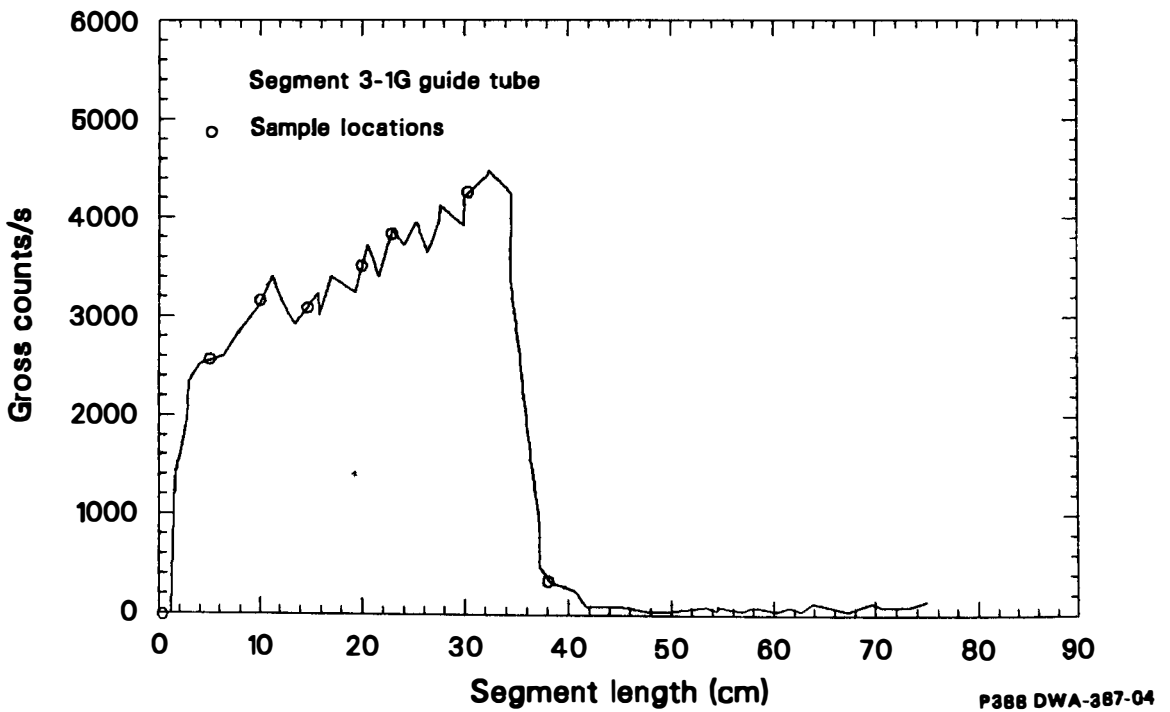


Figure B-8. Gross gamma scan of control rod/guide tube segment 3-1G.

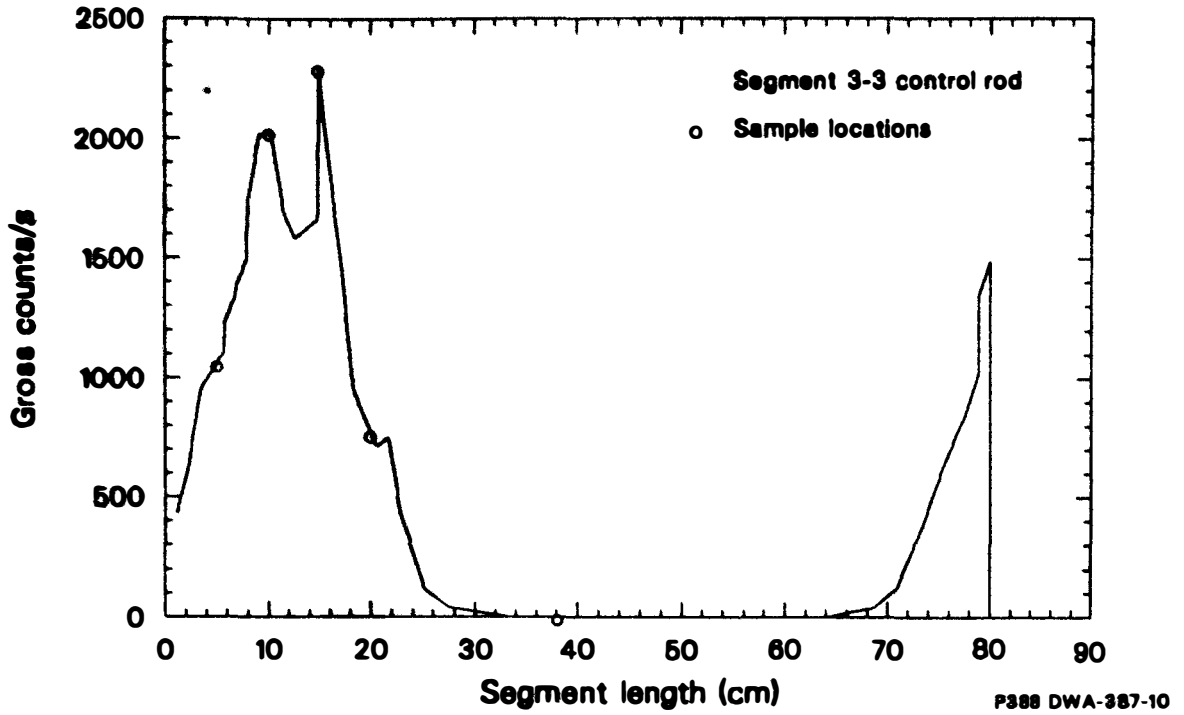


Figure B-9. Gross gamma scan of control rod segment 3-3.

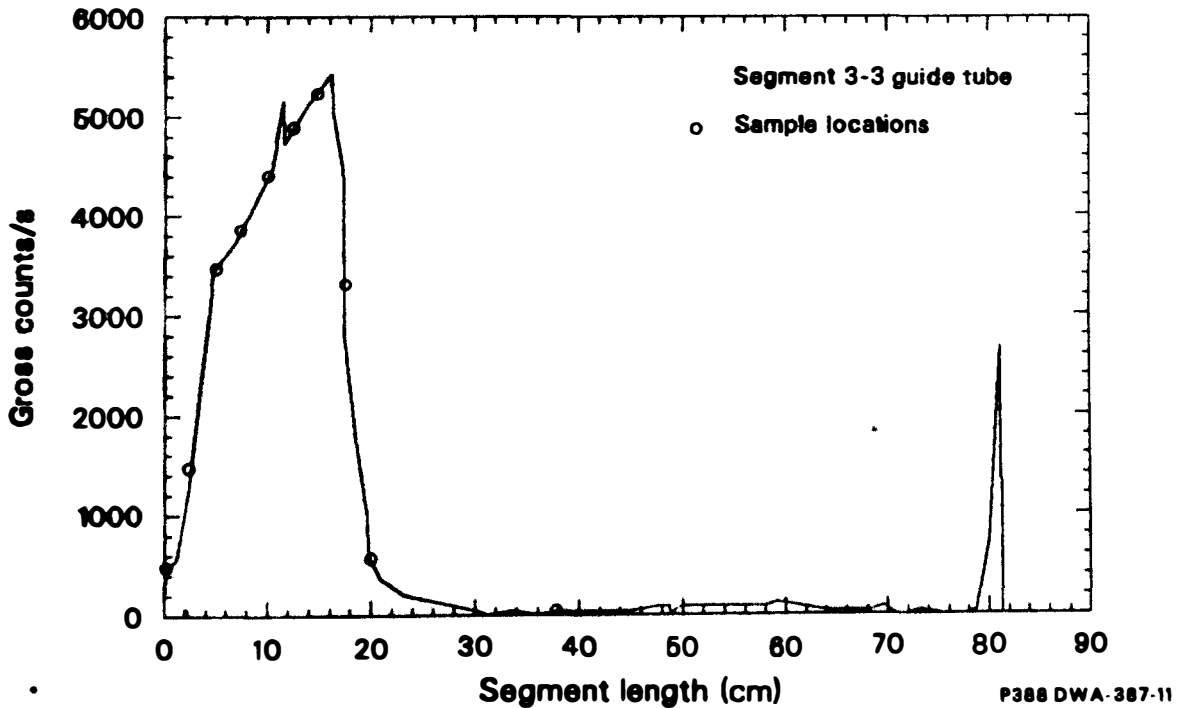


Figure B-10. Gross gamma scan of guide tube segment 3-3.

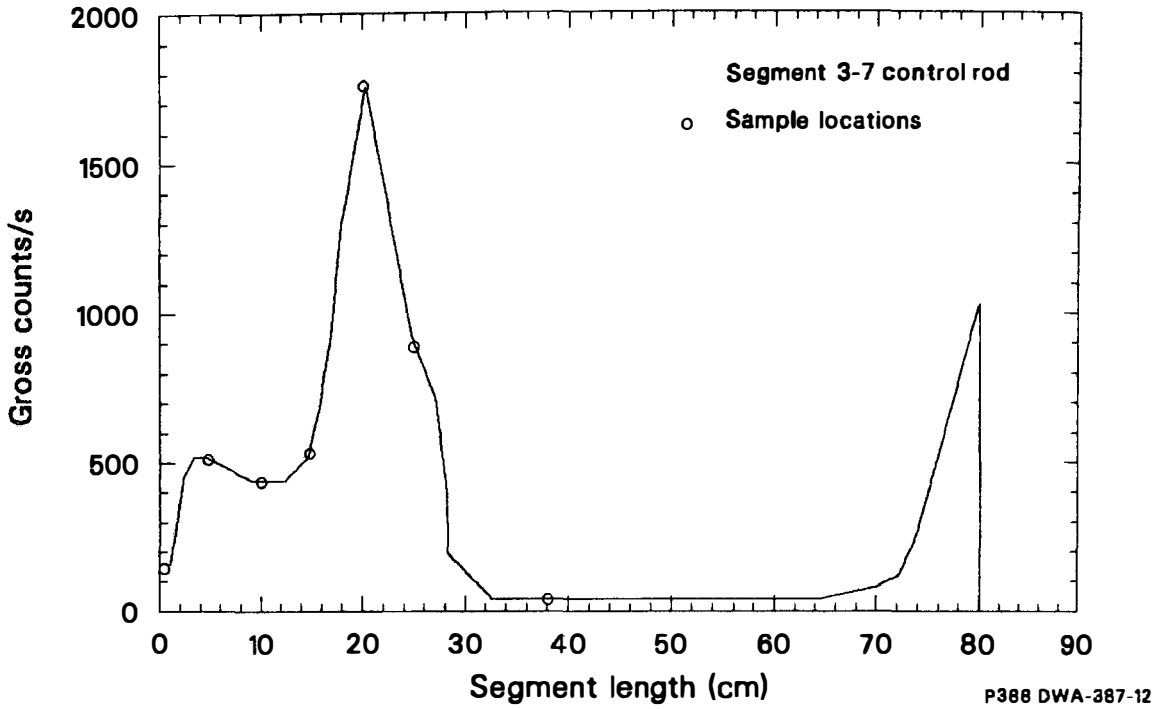


Figure B-11. Gross gamma scan of control rod segment 3-7.

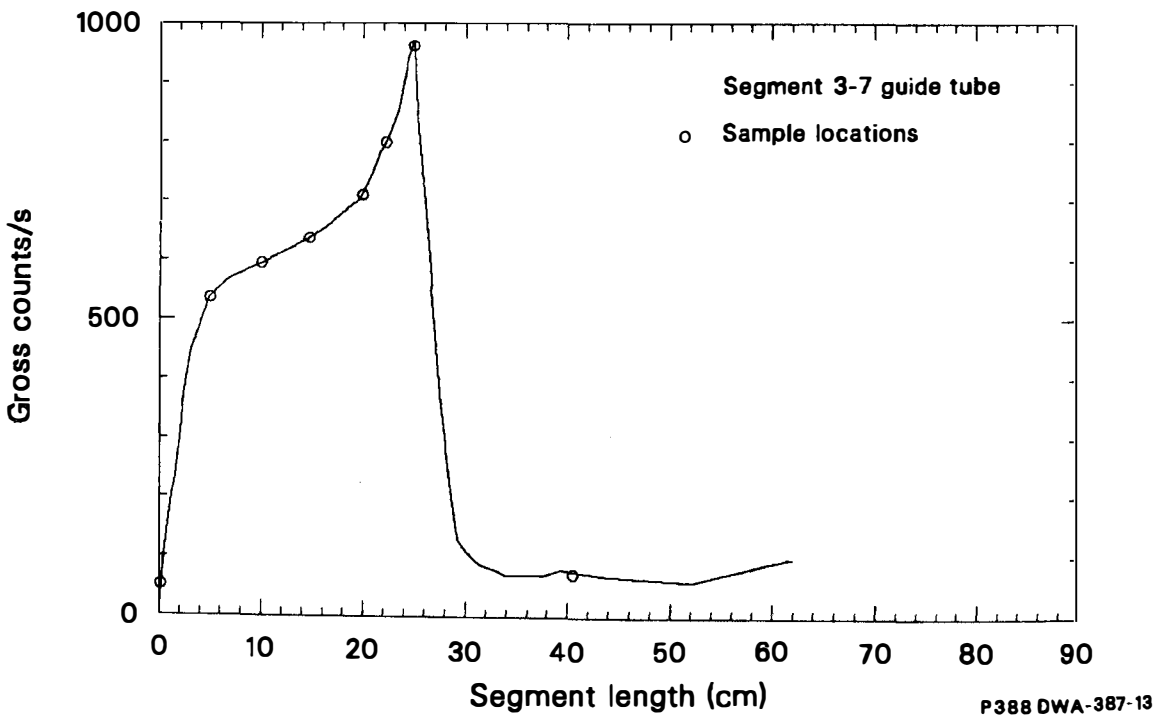


Figure B-12. Gross gamma scan of guide tube segment 3-7.

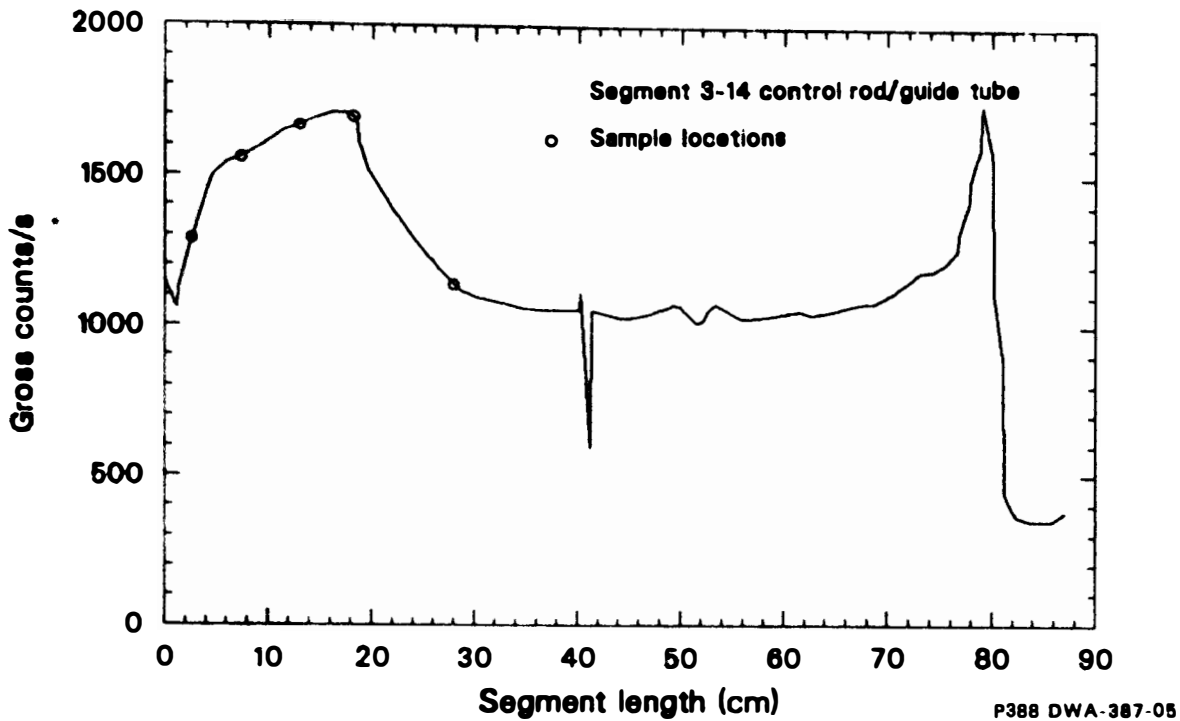


Figure B-13. Gross gamma scan of control rod/guide tube segment 3-14.

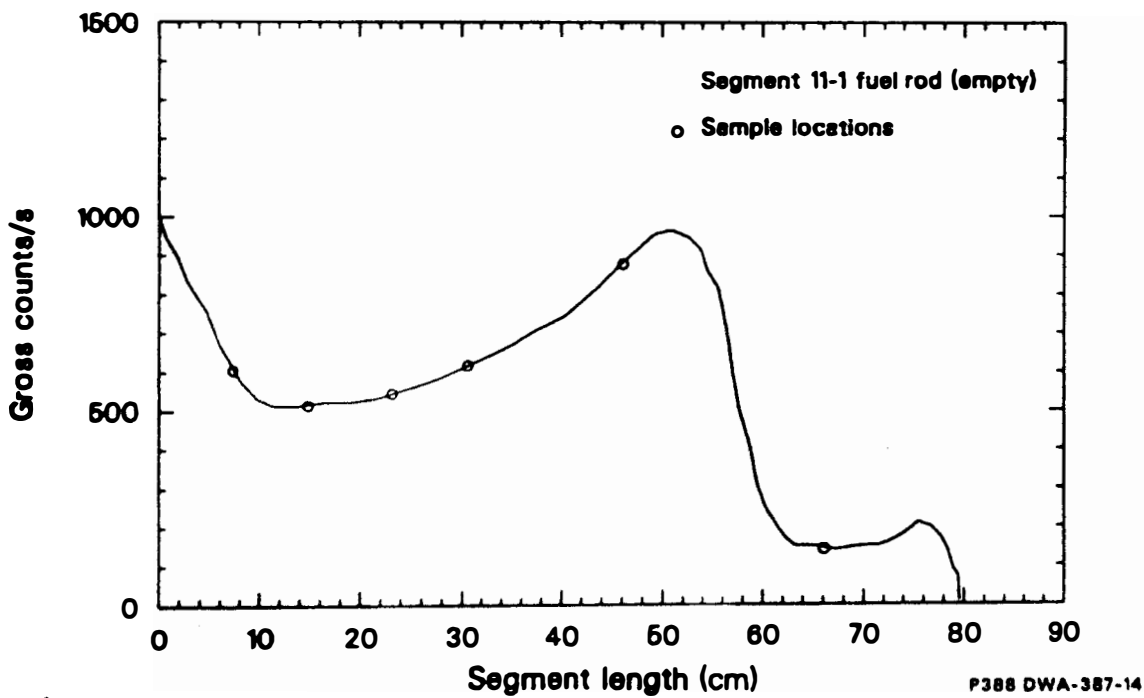


Figure B-14. Gross gamma scan of fuel rod segment 11-1.

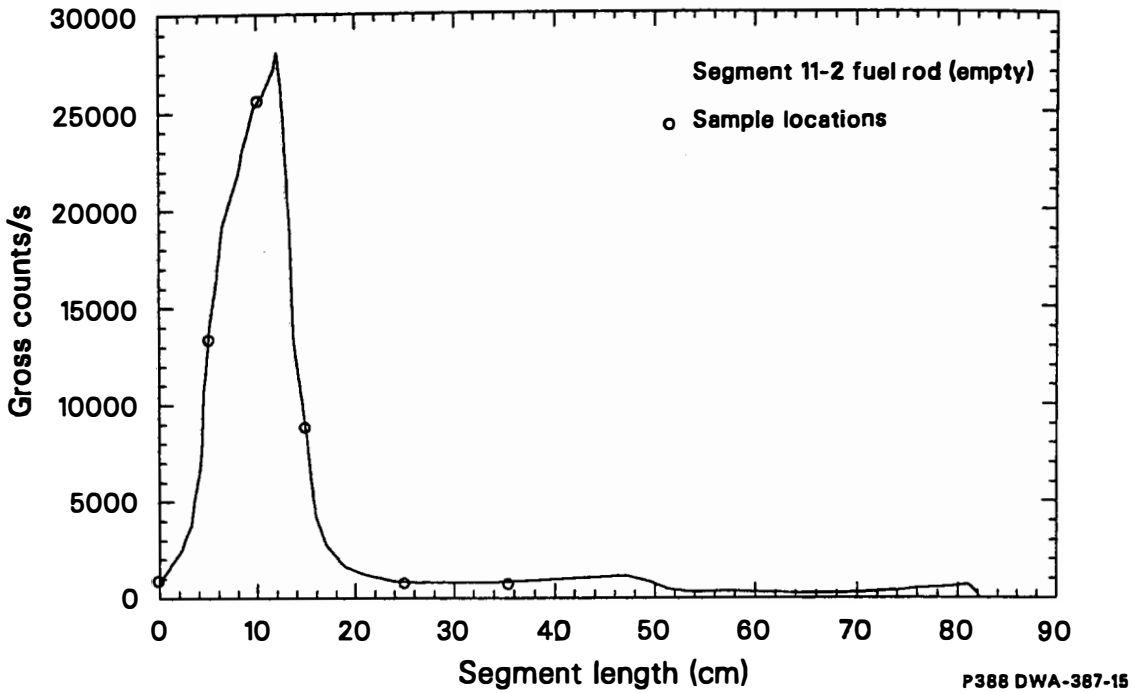


Figure B-15. Gross gamma scan of fuel rod segment 11-2.

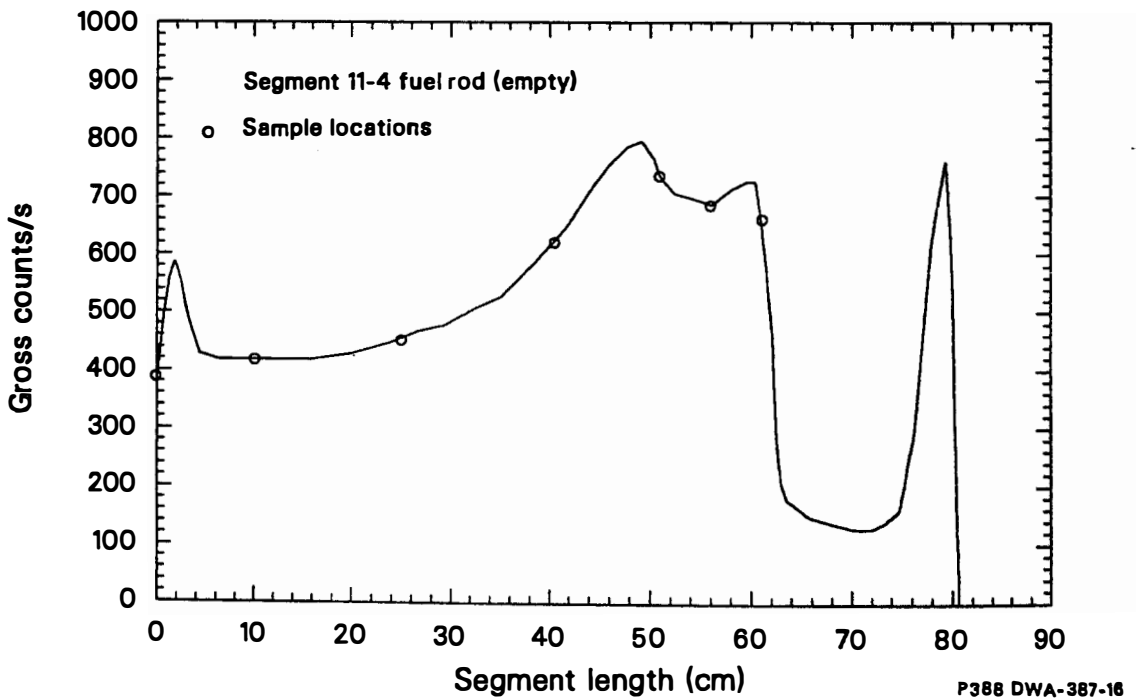


Figure B-16. Gross gamma scan of fuel rod segment 11-4.

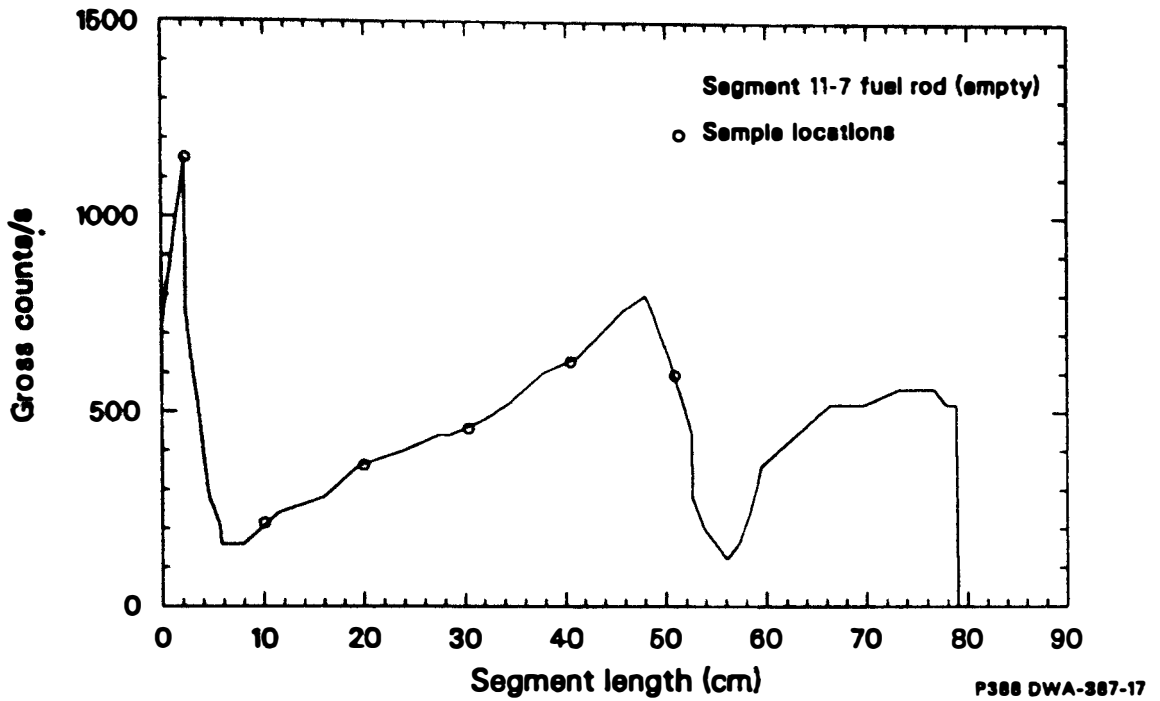


Figure B-17. Gross gamma scan of fuel rod segment 11-7.

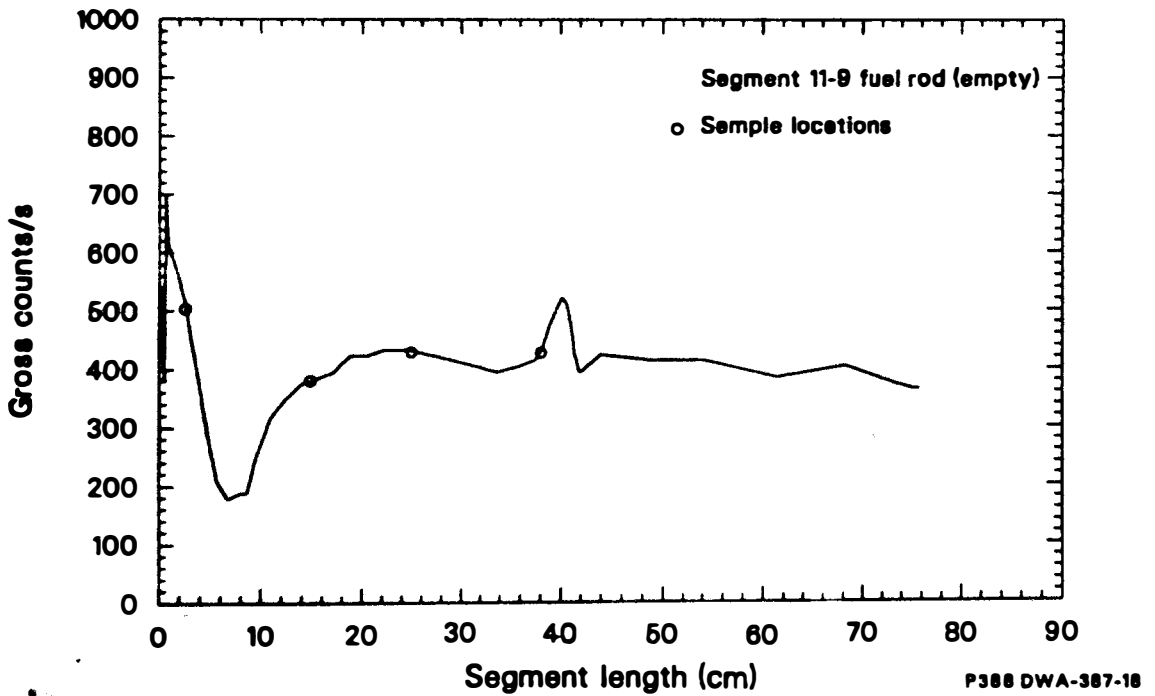


Figure B-18. Gross gamma scan of fuel rod segment 11-9.

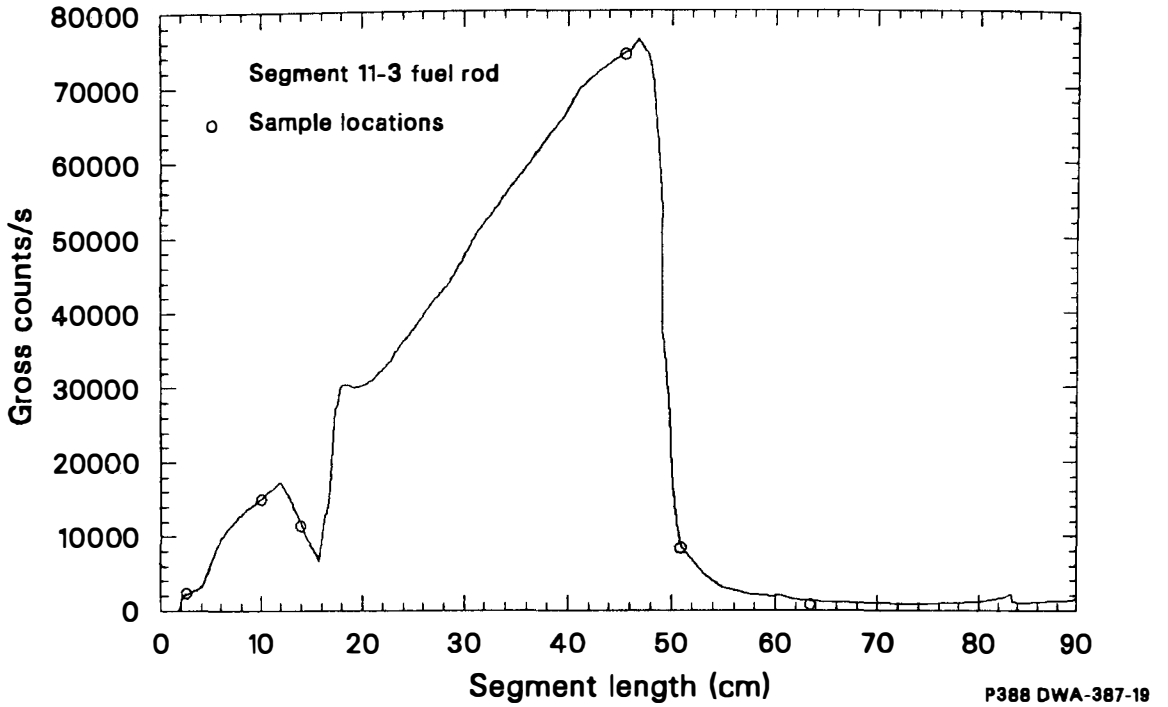


Figure B-19. Gross gamma scan of fuel rod segment 11-3.

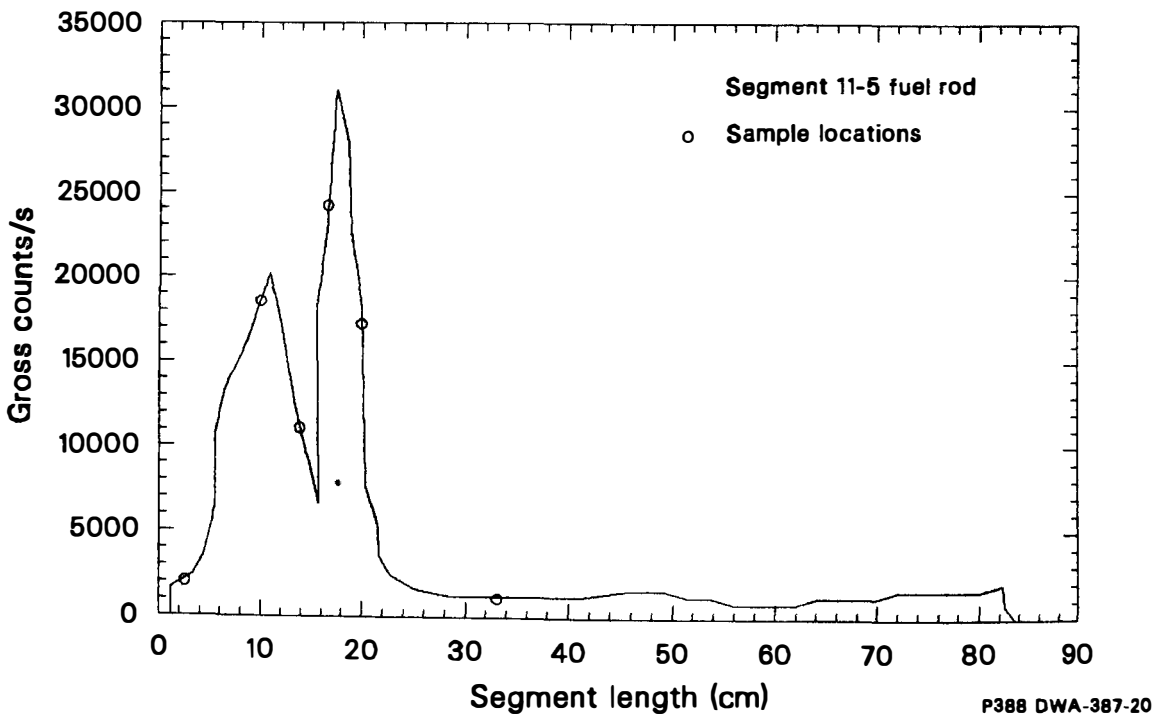


Figure B-20. Gross gamma scan of fuel rod segment 11-5.

TABLE B-1. RADIOISOTOPIC SURFACE ACTIVITY RESULTS

Rod ^a Identification	Rod ^b Type	Distance from the Top End of the Rod (cm)	Cs-137 μCi/cm	Cs-134 μCi/cm	Co-60 μCi/cm	Sb-125 μCi/cm	Co-144 μCi/cm	Ru-106 μCi/cm	Eu-154 μCi/cm
3-6	FR	2.5	8.11 ± 0.02 E02	1.43 ± 0.05 E01	2.68 ± 0.01 E02	1.26 ± 0.01 E02	c	c	c
		10	1.94 ± 0.02 E02	c	7.02 ± 0.01 E03	3.58 ± 0.25 E01	c	c	c
		13	1.94 ± 0.01 E02	c	6.07 ± 0.02 E02	1.09 ± 0.01 E02	c	c	c
		20	2.28 ± 0.01 E04	1.55 ± 0.01 E02	7.40 ± 0.15 E00	2.60 ± 0.03 E02	1.72 ± 0.03 E03	6.65 ± 0.05 E02	c
		25	2.50 ± 0.01 E02	9.08 ± 0.24 E00	1.23 ± 0.02 E01	1.56 ± 0.02 E02	c	c	c
		40.5	c	c	c	c	c	c	c
3-30	FR	2.5	3.20 ± 0.01 E03	3.05 ± 0.05 E01	2.33 ± 0.01 E02	1.13 ± 0.02 E02	1.82 ± 0.26 E02	7.52 ± 0.56 E01	c
		10	2.33 ± 0.01 E02	c	5.75 ± 0.01 E03	5.61 ± 0.29 E01	c	c	c
		15	5.74 ± 0.01 E02	1.04 ± 0.04 E01	8.98 ± 0.06 E01	1.37 ± 0.01 E02	1.97 ± 0.41 E02	c	c
		24	2.61 ± 0.01 E04	2.25 ± 0.01 E02	1.02 ± 0.05 E01	3.08 ± 0.02 E02	1.70 ± 0.05 E03	9.14 ± 0.05 E02	5.28 ± 0.14 E01
		26	2.46 ± 0.01 E04	2.44 ± 0.01 E02	7.68 ± 0.32 E00	6.07 ± 0.07 E02	1.64 ± 0.05 E03	7.87 ± 0.04 E02	6.31 ± 0.13 E01
		34	3.03 ± 0.01 E04	3.89 ± 0.01 E02	8.36 ± 0.21 E00	3.72 ± 0.04 E02	1.92 ± 0.03 E03	1.13 ± 0.01 E03	9.39 ± 0.10 E01
		38	1.39 ± 0.01 E03	3.04 ± 0.04 E01	2.02 ± 0.03 E01	2.69 ± 0.03 E02	3.04 ± 0.34 E02	c	9.74 ± 0.71 E00
		51	c	c	c	c	c	c	c
3-42	FR	2.5	2.99 ± 0.02 E02	1.03 ± 0.05 E01	3.50 ± 0.01 E02	1.38 ± 0.01 E02	c	c	c
		11	1.01 ± 0.01 E02	c	7.20 ± 0.01 E03	3.71 ± 0.27 E01	c	c	c
		15	2.49 ± 0.01 E03	1.51 ± 0.05 E01	2.10 ± 0.01 E02	1.31 ± 0.01 E02	3.49 ± 0.31 E02	c	c
		25	2.64 ± 0.01 E04	2.35 ± 0.01 E02	6.24 ± 0.16 E00	9.90 ± 0.06 E02	1.98 ± 0.03 E03	8.22 ± 0.06 E02	6.69 ± 0.07 E01
30	1.03 ± 0.01 E03	1.16 ± 0.03 E01	3.76 ± 0.15 E00	6.43 ± 0.01 E01	c	c	5.49 ± 0.56 E00		
3-61	FR	2.5	1.74 ± 0.01 E02	c	2.55 ± 0.01 E02	1.00 ± 0.01 E02	c	c	c
		11.5	9.21 ± 0.14 E01	c	6.52 ± 0.01 E03	4.49 ± 0.26 E01	c	c	c
		34	2.96 ± 0.01 E04	3.68 ± 0.01 E02	7.53 ± 0.18 E00	3.40 ± 0.03 E02	1.93 ± 0.03 E03	1.02 ± 0.01 E03	9.91 ± 0.09 E01
		37	2.26 ± 0.01 E04	3.04 ± 0.01 E02	1.19 ± 0.03 E01	5.34 ± 0.06 E02	1.47 ± 0.04 E03	6.51 ± 0.04 E02	7.15 ± 0.13 E01
		38	2.61 ± 0.01 E04	3.46 ± 0.01 E02	1.44 ± 0.04 E01	3.75 ± 0.03 E02	1.90 ± 0.05 E03	9.67 ± 0.06 E02	8.40 ± 0.13 E01
		40.5	2.39 ± 0.01 E03	3.73 ± 0.05 E01	4.06 ± 0.19 E00	8.91 ± 0.21 E01	4.85 ± 0.31 E02	8.73 ± 0.03 E01	1.24 ± 0.06 E01
43	9.68 ± 0.24 E00	c	c	c	c	c	c		
3-70	FR	2.5	8.03 ± 0.01 E03	1.03 ± 0.01 E02	4.28 ± 0.05 E01	1.56 ± 0.02 E02	4.25 ± 0.27 E02	2.55 ± 0.01 E02	2.25 ± 0.08 E01
		5	4.32 ± 0.02 E02	c	1.57 ± 0.01 E03	4.46 ± 0.18 E01	c	c	c
		13	9.51 ± 0.14 E01	c	7.12 ± 0.01 E03	7.58 ± 0.55 E01	c	c	c
		16.5	4.98 ± 0.02 E02	7.48 ± 0.52 E00	5.68 ± 0.02 E02	1.51 ± 0.01 E02	c	c	c
		35.5	2.92 ± 0.01 E04	3.38 ± 0.01 E02	7.26 ± 0.18 E00	3.37 ± 0.03 E02	1.76 ± 0.03 E03	1.03 ± 0.01 E03	8.16 ± 0.08 E01
		37.5	2.13 ± 0.01 E04	2.67 ± 0.01 E02	9.39 ± 0.27 E00	3.20 ± 0.03 E02	1.68 ± 0.05 E03	6.02 ± 0.04 E02	7.35 ± 0.13 E01
		38	2.15 ± 0.01 E04	2.69 ± 0.01 E02	1.02 ± 0.03 E01	3.03 ± 0.02 E02	1.44 ± 0.05 E03	6.59 ± 0.03 E02	6.31 ± 0.13 E01
		39.5	2.80 ± 0.01 E04	3.58 ± 0.01 E02	1.01 ± 0.03 E01	3.85 ± 0.03 E02	1.16 ± 0.05 E03	1.02 ± 0.01 E03	9.13 ± 0.16 E01
		43	9.07 ± 0.06 E01	2.04 ± 0.19 E00	c	c	c	c	3.74 ± 0.92 E00
		c	c	c	c	c	c	c	c
3-94	FR	2.5	1.77 ± 0.01 E02	c	1.25 ± 0.01 E03	4.07 ± 0.12 E01	c	c	c
		10	1.26 ± 0.02 E02	c	7.47 ± 0.01 E03	5.82 ± 0.29 E01	c	c	c
		14	2.80 ± 0.01 E03	2.11 ± 0.05 E01	1.67 ± 0.01 E02	1.56 ± 0.01 E02	3.64 ± 0.39 E02	c	c
		38	2.95 ± 0.01 E04	4.33 ± 0.01 E02	7.74 ± 0.19 E00	3.71 ± 0.04 E02	1.93 ± 0.04 E03	1.09 ± 0.01 E03	1.20 ± 0.01 E02
		44.5	2.35 ± 0.01 E04	3.85 ± 0.01 E02	1.19 ± 0.03 E01	4.36 ± 0.04 E02	1.82 ± 0.06 E03	8.34 ± 0.05 E02	9.93 ± 0.15 E01
		46	3.05 ± 0.01 E04	5.03 ± 0.02 E02	1.34 ± 0.04 E01	4.38 ± 0.04 E02	1.57 ± 0.06 E03	1.01 ± 0.01 E03	1.20 ± 0.02 E02
		51	1.65 ± 0.04 E01	c	c	c	c	c	c

B-15

TABLE B-1. (continued)

Rod ^a Identification	Rod ^b Type	Distance from the Top End of the Rod (cm)	Cs-137 μCi/cm	Cs-134 μCi/cm	Co-60 μCi/cm	Sb-125 μCi/cm	Ce-144 μCi/cm	Ru-106 μCi/cm	Eu-154 μCi/cm
3-1	CR	0	2.97 ± 0.25 E00	c	c	c	c	c	c
		2.5	2.35 ± 0.01 E02	6.27 ± 0.17 E00	c	c	c	c	c
		5	5.19 ± 0.02 E02	1.34 ± 0.03 E01	c	c	c	c	c
		10	8.86 ± 0.01 E02	2.31 ± 0.02 E01	2.16 ± 0.09 E00	c	c	c	c
		13	1.78 ± 0.01 E02	4.61 ± 0.14 E00	c	c	c	c	c
		23	4.30 ± 0.01 E02	1.05 ± 0.02 E01	c	c	c	c	c
		33	3.98 ± 0.01 E02	1.06 ± 0.01 E01	3.50 ± 0.08 E00	3.04 ± 0.02 E01	c	c	c
		38	c	c	c	c	c	c	c
		3-1	GT	0	4.15 ± 0.16 E00	c	c	4.93 ± 0.04 E01	c
5	2.15 ± 0.01 E02			6.64 ± 0.16 E00	4.01 ± 0.13 E00	8.27 ± 0.08 E01	c	c	c
10	2.37 ± 0.01 E02			7.20 ± 0.17 E00	6.44 ± 0.17 E00	1.22 ± 0.01 E02	c	c	c
15	2.02 ± 0.01 E02			7.27 ± 0.19 E00	7.88 ± 0.18 E00	1.66 ± 0.02 E02	c	c	c
20	2.00 ± 0.01 E02			8.33 ± 0.21 E00	1.03 ± 0.02 E01	1.88 ± 0.03 E02	c	c	c
23	2.01 ± 0.01 E02			1.02 ± 0.01 E01	1.13 ± 0.01 E01	2.30 ± 0.03 E02	c	c	c
30.5	2.20 ± 0.01 E02			1.27 ± 0.02 E01	1.41 ± 0.02 E01	c	c	c	
38	7.91 ± 0.98 E-01			c	3.16 ± 1.26 E-01	c	c	c	
3-3	CR			5	5.19 ± 0.02 E02	1.31 ± 0.02 E01	1.61 ± 0.29 E00	7.42 ± 0.95 E00	c
		10	8.86 ± 0.01 E02	2.31 ± 0.02 E01	2.16 ± 0.01 E00	c	c	c	
		15	7.70 ± 0.02 E02	1.87 ± 0.03 E01	2.02 ± 0.16 E00	c	c	c	
		20	3.07 ± 0.02 E02	7.46 ± 0.25 E00	3.23 ± 0.21 E00	3.14 ± 0.02 E01	c	c	
		38	c	c	c	c	c		
3-3	GT	0	1.62 ± 0.10 E00	c	c	c	c	c	c
		2.5	1.56 ± 0.01 E02	4.36 ± 0.18 E00	1.74 ± 0.14 E00	2.80 ± 0.02 E01	c	c	c
		5	3.03 ± 0.02 E02	9.03 ± 0.24 E00	4.30 ± 0.18 E00	5.98 ± 0.04 E01	c	c	c
		7.5	3.32 ± 0.02 E02	9.52 ± 0.25 E00	6.24 ± 0.22 E00	7.60 ± 0.06 E01	c	c	c
		10	3.65 ± 0.01 E02	1.10 ± 0.03 E01	8.18 ± 0.26 E00	97.2 ± 0.09 E01	c	c	c
		12.5	3.94 ± 0.02 E02	1.26 ± 0.03 E01	9.51 ± 0.25 E00	1.29 ± 0.01 E02	c	c	c
		15	4.41 ± 0.02 E02	1.41 ± 0.03 E01	1.00 ± 0.03 E01	1.87 ± 0.02 E02	c	c	c
		17.5	d	d	d	d	d	d	d
		20	1.31 ± 0.13 E00	c	c	c	c	c	c
		38	1.06 ± 0.20 E01	c	c	c	c	c	
3-7	CR	0	3.66 ± 0.04 E01	1.10 ± 0.07 E00	c	c	c	c	c
		5	2.17 ± 0.01 E02	5.41 ± 0.14 E00	9.87 ± 1.04 E-01	c	c	c	
		10	1.80 ± 0.01 E02	4.13 ± 0.15 E00	1.07 ± 0.09 E00	c	c	c	
		15	2.51 ± 0.01 E02	6.24 ± 0.14 E00	1.15 ± 0.09 E00	c	c	c	
		20	8.04 ± 0.01 E02	1.46 ± 0.20 E01	3.49 ± 0.08 E00	2.52 ± 0.08 E01	c	c	
		25	4.93 ± 0.02 E02	1.16 ± 0.02 E01	3.79 ± 0.13 E00	2.61 ± 0.02 E01	c	c	
		38	c	c	c	c	c		

TABLE B-1. (continued)

Rod ^a Identification	Rod ^b Type	Distance from the Top End of the Rod (cm)	Cs-137 μCi/cm	Cs-134 μCi/cm	Co-60 μCi/cm	Sb-125 μCi/cm	Cs-144 μCi/cm	Ru-106 μCi/cm	Eu-154 μCi/cm
3-7	GT	0	7.00 ± 0.17 E00	c	c	c	c	c	c
		5		d	d	6.35 ± 0.06 E01	c	c	c
		10	1.90 ± 0.01 E02	7.24 ± 0.25 E00	7.69 ± 0.23 E00	8.74 ± 0.09 E01	c	c	c
		15	1.81 ± 0.01 E02	7.11 ± 0.21 E00	9.40 ± 0.23 E00	1.23 ± 0.01 E02	c	c	c
		20	1.87 ± 0.01 E02	9.13 ± 0.26 E00	1.23 ± 0.03 E01	1.62 ± 0.02 E02	c	c	c
		22.5	2.38 ± 0.01 E02	8.38 ± 0.07 E00	1.23 ± 0.01 E01	1.71 ± 0.03 E02	c	c	c
		25	2.40 ± 0.01 E02	9.28 ± 0.20 E00	8.17 ± 0.22 E00	1.47 ± 0.02 E02	c	c	c
		40.5	c	c	c	c	c	c	c
3-14	CR/GT	2.5	5.21 ± 0.02 E02	1.29 ± 0.02 E01	3.48 ± 0.18 E00	3.40 ± 0.01 E01	c	c	c
		7.5	6.87 ± 0.01 E02	1.82 ± 0.03 E01	6.56 ± 0.22 E00	5.43 ± 0.03 E01	c	c	c
		13	7.92 ± 0.01 E02	2.10 ± 0.02 E01	6.52 ± 0.11 E00	8.52 ± 0.07 E01	c	c	c
		18	7.54 ± 0.02 E02	2.06 ± 0.03 E01	1.14 ± 0.03 E01	1.17 ± 0.01 E02	c	c	c
		28	c	c	c	c	c	c	c
11-1	FR	7.5	1.44 ± 0.01 E02	4.37 ± 0.16 E00	2.82 ± 0.15 E00	3.57 ± 0.03 E01	c	c	c
		15	1.49 ± 0.01 E02	5.39 ± 0.23 E00	4.39 ± 0.21 E00	4.83 ± 0.03 E01	c	c	c
		23	1.40 ± 0.01 E02	4.66 ± 0.24 E00	3.69 ± 0.19 E00	5.79 ± 0.05 E01	c	c	c
		30.5	1.44 ± 0.01 E02	6.75 ± 0.28 E00	4.56 ± 0.20 E00	8.42 ± 0.08 E01	c	c	c
		46	2.29 ± 0.01 E02	7.75 ± 0.12 E00	7.23 ± 0.12 E00	1.30 ± 0.02 E02	c	c	c
		66	c	c	c	c	c	c	c
11-2	FR	0	1.18 ± 0.04 E01	c	5.76 ± 0.17 E00	2.40 ± 1.44 E00	c	c	c
		5	9.46 ± 0.09 E01	c	2.82 ± 0.01 E03	4.16 ± 0.14 E01	c	c	c
		10	4.93 ± 0.09 E01	c	5.73 ± 0.01 E03	2.28 ± 0.17 E01	c	c	c
		15		d			d	d	d
		35.5	1.31 ± 0.01 E02	3.21 ± 0.21 E00	5.06 ± 0.17 E00	7.61 ± 0.08 E01	c	c	c
11-4	FR	0	1.31 ± 0.03 E01	8.74 ± 2.04 E-01	c	7.61 ± 0.53 E00	c	c	c
		10	1.28 ± 0.01 E02	4.50 ± 0.24 E00	3.56 ± 0.17 E00	3.95 ± 0.32 E01	c	c	c
		25	1.24 ± 0.01 E02	4.72 ± 0.20 E00	3.92 ± 0.19 E00	5.74 ± 0.52 E01	c	c	c
		40.5	1.61 ± 0.01 E02	3.56 ± 0.24 E00	6.45 ± 0.22 E00	9.80 ± 0.11 E01	c	c	c
		51	2.26 ± 0.01 E02	6.18 ± 0.15 E00	7.13 ± 0.11 E00	1.21 ± 0.01 E02	c	c	c
		56	1.69 ± 0.01 E02	4.11 ± 0.29 E00	7.93 ± 0.21 E00	1.32 ± 0.01 E02	c	c	c
		61	1.17 ± 0.01 E02	2.74 ± 0.92 E00	9.56 ± 0.06 E01	1.10 ± 0.01 E02	c	c	c
11-7	FR	2.5	2.96 ± 0.04 E01	2.04 ± 0.16 E00	1.04 ± 0.08 E00	2.35 ± 0.02 E01	c	c	c
		10	1.20 ± 0.01 E02	3.65 ± 0.15 E00	3.87 ± 0.15 E00	3.28 ± 0.02 E01	c	c	c
		20	1.58 ± 0.01 E02	4.51 ± 0.17 E00	3.42 ± 0.16 E00	4.43 ± 0.04 E01	c	c	c
		30.5	1.63 ± 0.01 E02	5.40 ± 0.17 E00	4.77 ± 0.15 E00	7.45 ± 0.07 E01	c	c	c
		40.5	1.95 ± 0.01 E02	6.21 ± 0.22 E00	6.46 ± 0.19 E00	1.08 ± 0.01 E02	c	c	c
		51	2.91 ± 0.01 E02	9.22 ± 0.13 E00	8.52 ± 0.11 E00	1.37 ± 0.02 E02	c	c	c
11-9	FR	2.5	6.23 ± 0.22 E00	c	1.03 ± 0.11 E00	c	c	c	
		15	9.33 ± 0.29 E00	c	1.39 ± 0.20 E00	c	c	c	
		25	9.50 ± 0.12 E00	4.15 ± 0.61 E-01	1.09 ± 0.05 E00	c	c	c	
		38	1.32 ± 0.03 E01	c	1.76 ± 0.12 E00	c	c	c	

TABLE B-1. (continued)

Rod ^a Identification	Rod ^b Type	Distance from the Top End of the Rod (cm)	Cs-137 μCi/cm	Cs-134 μCi/cm	Co-60 μCi/cm	Sb-125 μCi/cm	Ce-144 μCi/cm	Ru-106 μCi/cm	Eu-154 μCi/cm
11-3	FR	2.5	2.34 ± 0.01 E02	c	5.03 ± 0.02 E02	7.73 ± 0.06 E01	c	c	c
		10	1.39 ± 0.02 E02	c	3.57 ± 0.01 E03	5.42 ± 0.43 E01	c	c	c
		14	1.51 ± 0.01 E03	5.29 ± 0.56 E00	1.37 ± 0.01 E02	5.61 ± 0.17 E01	2.13 ± 0.31 E02	c	c
		45.5	2.48 ± 0.01 E04	1.56 ± 0.01 E02	6.25 ± 0.16 E00	2.92 ± 0.03 E02	1.74 ± 0.03 E03	6.84 ± 0.05 E02	3.17 ± 0.02 E01
		51	2.19 ± 0.01 E02	6.66 ± 0.24 E00	8.09 ± 0.22 E00	1.20 ± 0.01 E02	c	c	c
		63.5	c	c	c	c	c	c	c
11-5	FR	2.5	1.30 ± 0.01 E02	c	3.95 ± 0.02 E02	4.42 ± 0.11 E01	c	c	c
		10	1.44 ± 0.01 E02	c	4.39 ± 0.01 E03	4.15 ± 0.31 E01	c	c	c
		14	2.82 ± 0.01 E03	8.83 ± 0.38 E00	1.25 ± 0.01 E02	8.61 ± 0.05 E01	3.59 ± 0.62 E02	c	c
		16.5	1.39 ± 0.01 E04	3.35 ± 0.03 E01	7.34 ± 0.14 E00	1.48 ± 0.01 E02	7.66 ± 0.15 E02	3.64 ± 0.02 E02	7.43 ± 0.41 E00
		20	1.96 ± 0.01 E02	4.30 ± 0.30 E00	3.26 ± 0.15 E00	5.11 ± 0.03 E01	c	c	c
		33	1.24 ± 0.01 E02	2.47 ± 0.16 E00	5.52 ± 0.19 E00	8.61 ± 0.08 E01	c	c	c

a. Rods with identifications 3-X were taken from fuel bundle C7. Rods with identifications 11-X were taken from fuel bundle H1.

b. FR = Fuel Rod, CR = Control Rod, and GT = Guide Tube.

c. Not detected.

d. Results lost due to analysis problems.

APPENDIX C
DISTINCT COMPONENT ACQUISITION

APPENDIX C
DISTINCT COMPONENT ACQUISITION

EXHIBIT C
DISTRICT COURT AND COUNTY

APPENDIX C
DISTINCT COMPONENT ACQUISITION

C.1 Loading of Canisters at TMI-2

Removal of distinct components from the damaged TMI-2 core was initiated in November 1985. The procedure involved reaching into the core cavity with a long-handled grappling tool, picking up loose debris, usually in the form of upper end fittings from which all the fuel and/or control rods had fallen out (or were otherwise removed), and putting the debris into specially designed "fuel canisters" that had been placed in the reactor vessel, as shown in Figure C-1. Figure C-2 shows a longitudinal cross-section of a fuel canister, which is cylindrical in shape but has a rectangular 8.5 in. x 8.5 in. cavity that is approximately 137 in. long.

Loading the debris into the fuel canister under several feet of, in many cases, turbid water, with only an underwater camera for visual assistance, was difficult. Subsequent viewing of the video tapes obtained during canister loadings also showed that in several cases some of the components had to be inverted and/or forcefully hammered into the canisters because of misshapen spider assemblies, distorted fuel and control rods, and missing pieces of end boxes. This forced loading further damaged the end pieces and made it difficult in some cases to retrieve the components from the canisters. In addition, at the time the components were loaded into the canisters, it was difficult in many cases to identify the specific components because fuel assembly identification numbers could not be easily read by the underwater camera. During FY-1986 a total of 49 fuel canisters had been loaded and transferred to the TMI Fuel Handling Buildings and 21 of these had been shipped to the Idaho National Engineering Laboratory (INEL) for unloading and/or interim storage.

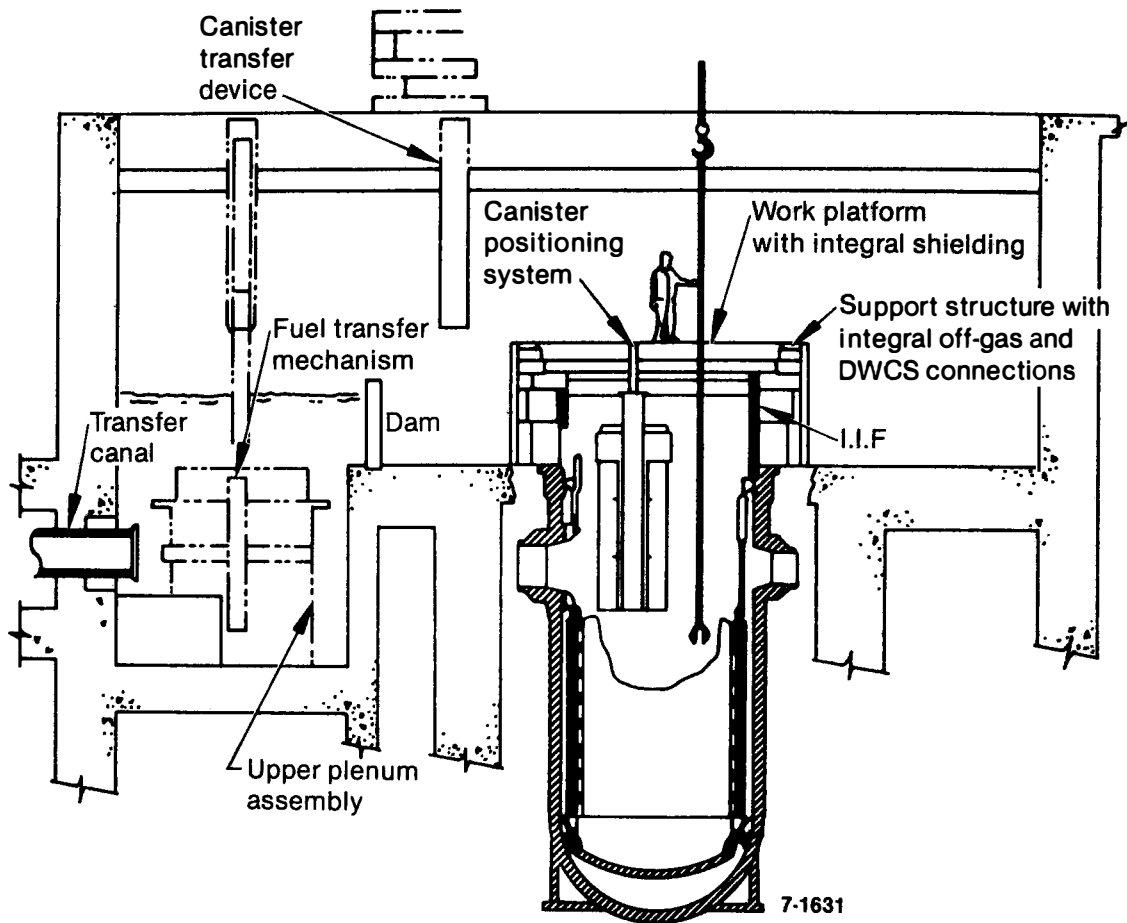


Figure C-1. Diagram showing positioning of fuel canister in TMI-2 reactor vessel during loading of distinct components.

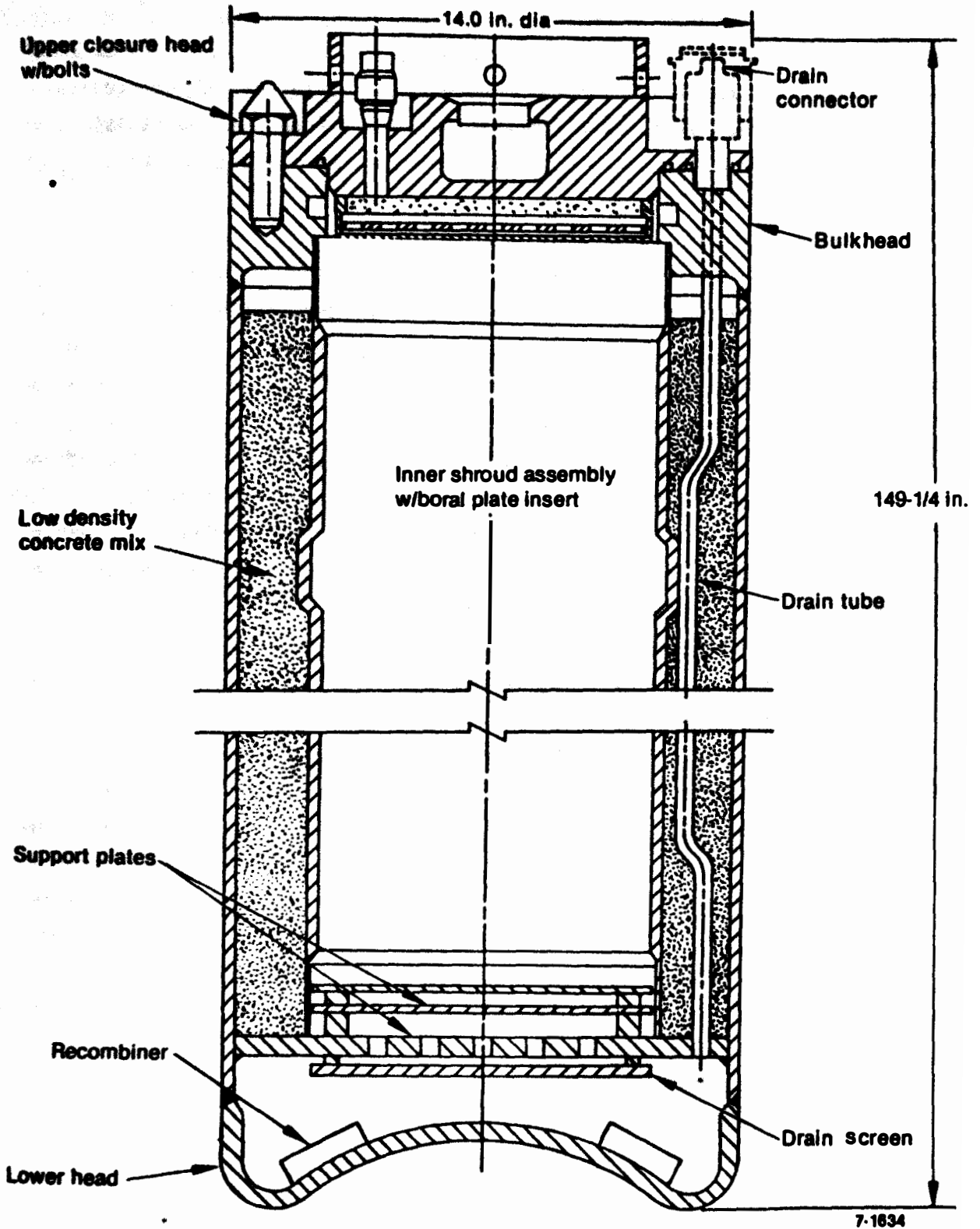


Figure C-2. Cross section of fuel canister.

C.2 Unloading of Canisters at the INEL

Fuel canisters D-141 and D-153 were unloaded in the TAN Hot Cell at the INEL in August 1986. The components removed from the two canisters are listed in Tables C-1 and C-2. Table C-3 shows the contents of all 21 canisters at the INEL as of October 1, 1986.

Figures C-3 through C-8 show photographs of the canister handling and unloading equipment and tools that had been designed and built especially for these purposes.^a A fuel canister weighs approximately 3000 lb and must be set on the rotating table prior to removal of the canister head by the automated head-removal machine. The rotating table is shown in Figure C-3 empty, and in Figure C-4 with a canister in place. In addition to providing a platform from which to remove the contents from the canisters, the rotating table is capable of rotating a canister to permit more flexibility in inserting various unloading tools into a canister and in loosening components that may become stuck.

In addition to the rotating table, the other major components of the canister unloading equipment included the head removal machine, shown in Figures C-5 and C-6, and the carriage table shown in Figure C-7. The purpose of the head removal was to loosen the eight bolts in the head of each canister, attach to the head with a grapple, and remove the head from in front of the canister by rotating away from the canister, taking the head with it. With the canister head removed, one or more of the component removal hooks or other tools shown in Figure C-8 could be used to attach to the TMI-2 core component and the carriage table could be used to pull the component out of the canister.

Many difficulties were encountered in attempting to remove the 11 components from canister D-141 and the 13 components from canister D-153. For example, since the inside dimensions of the canisters

a. A more complete description of the design and use of fuel canister and sample handling equipment was presented at the Waste Management '87 meeting at Tuscon, Arizona on March 1-5, 1987 and is published in the meeting proceedings.

TABLE C-1. FUEL CANISTER D-141 CONTENTS

Canister Item Number	Core Position	Description	Identification Marking
1	E13	Fuel assembly partial upper end fitting and control rod spider.	C-157
2 ^a	C11	Partially melted control rod spider.	C-156
3 ^a	C7	Fuel assembly upper section with 119 fuel rod and 16 control rod/guide tube upper segments.	NJ 00Q8
4 ^a	N9	Fuel assembly partial upper end fitting (burnable poison rod assembly site).	NJ 00RZ
5 ^a	N9	Burnable poison rod assembly partial upper end fitting.	B-181
6 ^a	L3	Burnable poison rod assembly retainer.	L-051
7 ^a	K15	Peripheral fuel assembly partial upper end fitting.	NJ 00UV
8 ^a	M9	Fuel assembly partial upper end fitting Control rod assembly partial upper end fitting.	NJ 00RI C-167
9	L8	Fuel assembly partial upper end fitting Control rod assembly partial upper end fitting.	NJ 00RO C-142
10 ^a	H8	Fuel assembly partial upper end fitting Control rod assembly partial upper end fitting.	NJ 00RR C-123
11 ^a	H1	Peripheral fuel assembly upper section with 7 fuel rod and some guide tube upper segments (core instrument string is missing).	NJ 00UU

a. Stored in drums for possible future examinations.

TABLE C-2. FUEL CANISTER D-153 CONTENTS

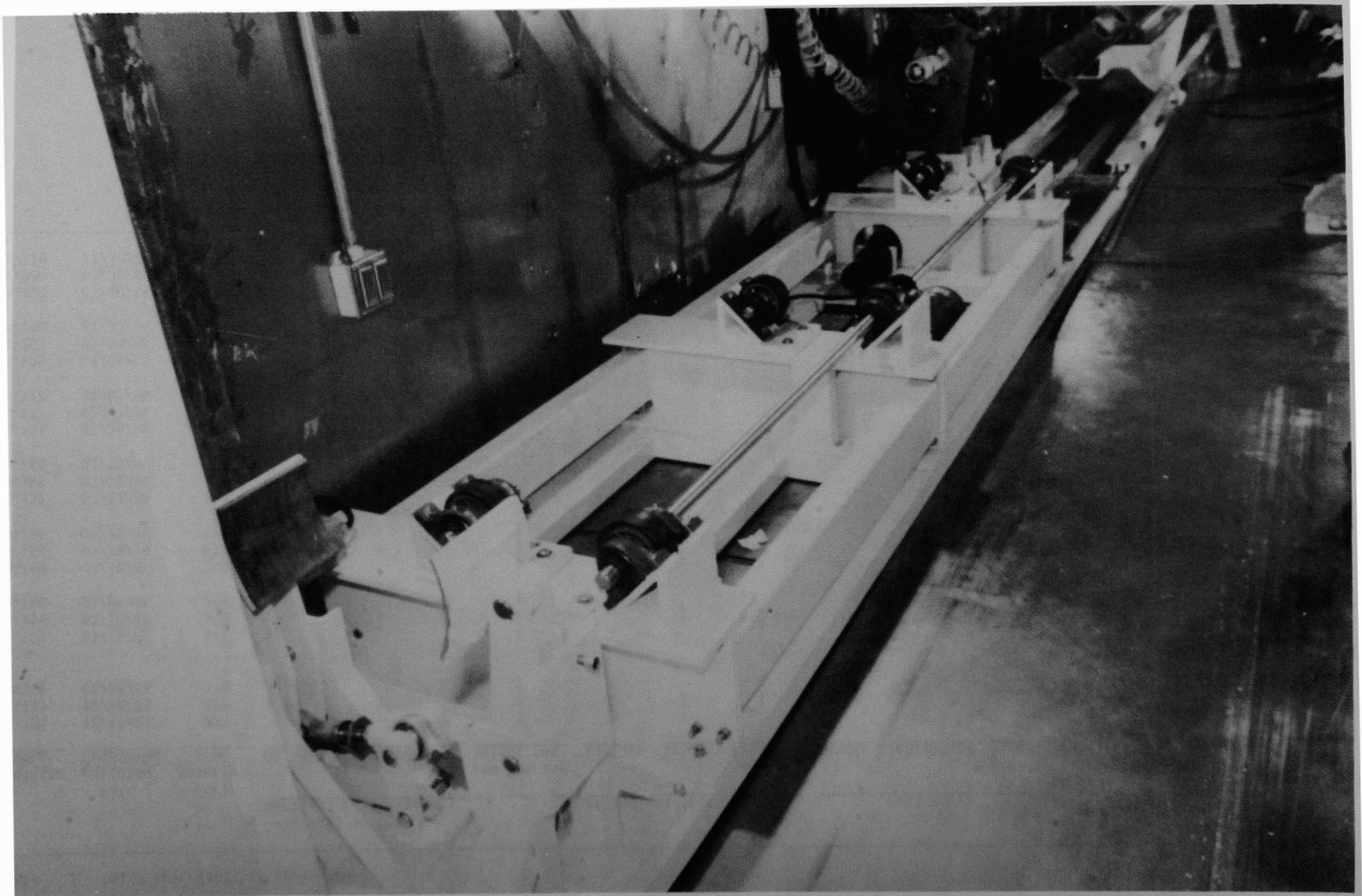
Canister Item Number	Core Position	Description	Identification Marking
1 ^a	K4	Burnable poison rod assembly retainer	L045
2	G14	Burnable poison rod assembly retainer	L037
3 ^a	D8	Fuel assembly partial upper end fitting Control rod assembly upper end fitting	Missing C-144
4 ^a	G3	Fuel assembly partial upper end fitting Control rod assembly upper end fitting	Missing C-178
5	E2	Peripheral fuel assembly upper end (without fuel rods)	NJ 00UZ
6 ^a	010	Burnable poison rod assembly partial upper end fitting	NJ 00SU
7	R7	Peripheral fuel assembly upper end fitting corner	NJ 00TL
8 ^a	P6	Fuel assembly partial upper end fitting Control rod assembly upper end fitting	NJ 00UP
9 ^a	B8	Fuel assembly partial upper end fitting Control rod assembly upper end fitting	NJ 00UB C-124
10	D4	Fuel assembly partial upper end fitting Control rod assembly upper end fitting	NJ 00PV C-155
11	F14	Control rod fuel assembly upper end fitting corner	NJ 00UQ
12	06	APSR fuel assembly partial upper end fitting	NJ 00UA
13 ^a	B10	Fuel assembly partial upper end fitting Control rod assembly upper end fitting	NJ 00UA C-132

a. Stored in drums for possible future examinations.

TABLE C-3. TRI-2 FUEL CANISTER CONTENTS

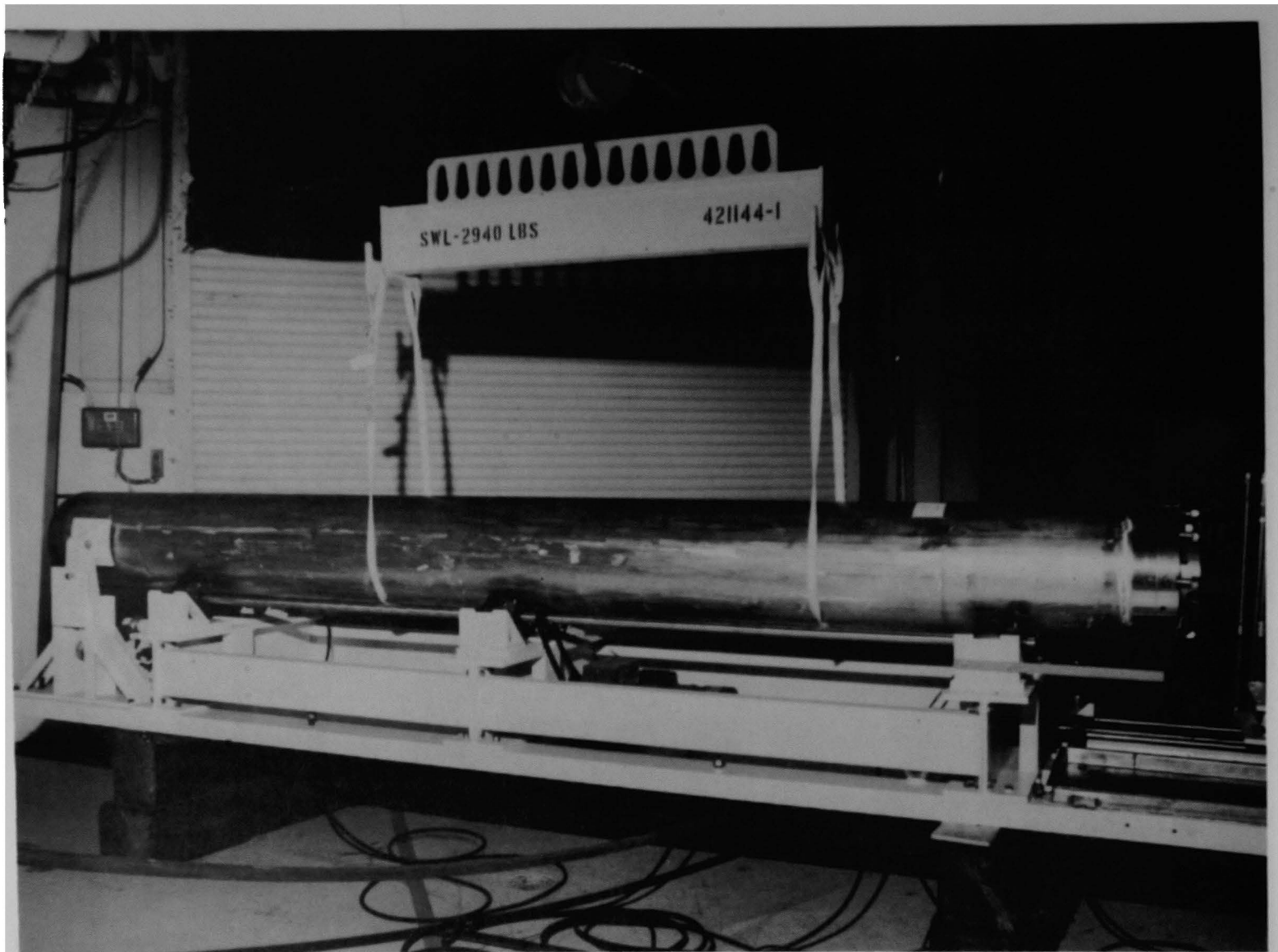
Canister Number	Date Loading Completed	Core Material (lb)	Partial (Upper Section) Fuel Assembly			Upper End Fittings				Fuel Beds			Unseq. Loose Debris	Comments	
			CR	BPR	Perimeter	No ID	End Box and Spider Set	End Box	Spider	BPR Retainer	Bundle	Individual			Debris Bucket
0-136	12/11/85	277				2	3	6	1			2			
0-141	12/14/85	320	1		1		4	2	2	1					
0-139	01/08/86	310					3	9		2					One BPR Upper End Fitting Set
0-153	01/16/86	345	2				4	5		2					
0-155	01/18/86	350	1		1		5	4	3	3					
0-140	01/09/86	260					4	4					1		
0-160	01/20/86	245					4	5	5	2	1				
0-154	01/23/86	652			1		2	3							
0-138	01/29/86	233					3	3	2				2		
0-137	02/03/86	710													
0-163	03/08/86	1422													X
0-144	03/16/86	1355													X
0-131	03/25/86	1293													X
0-117	02/27/86	1343													X
0-128	04/02/86	1358													X
0-125	04/06/86	1332													X
0-201	07/30/86	68													
0-198	07/30/86	63													Core bores N5 and N12 Core bores G8 and G12
0-159	07/30/86	64													Core bores B8 and K9
0-200	07/30/86	42													Core bores K6 and B4
0-118	07/30/86	51													Core bores O7 and O9

C-9



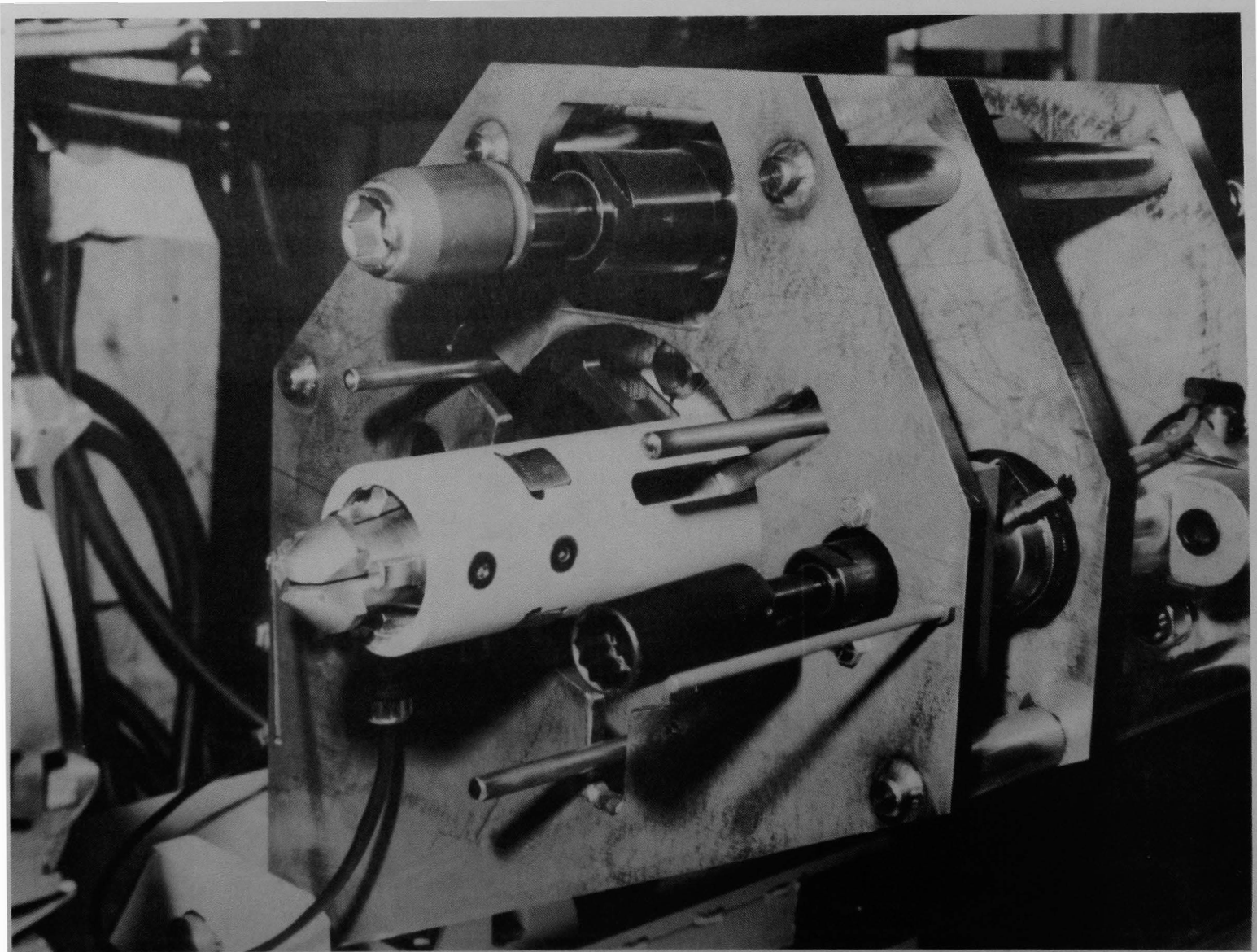
86-374-1-7

Figure C-3. TMI-2 fuel canister rotating table used during unloading.



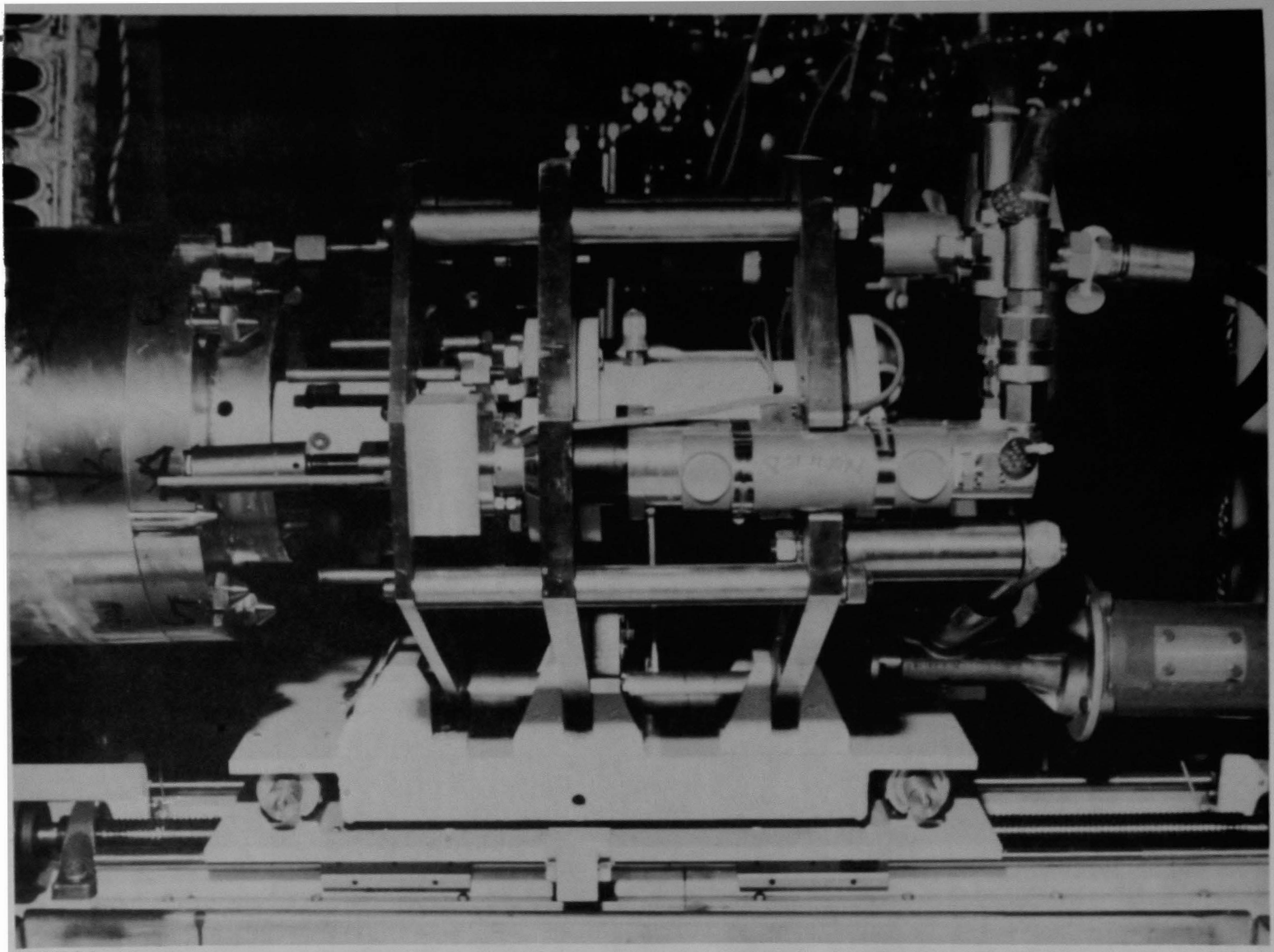
86-275-3-12

Figure C-4. TMI-2 fuel canister in-place on rotating table.



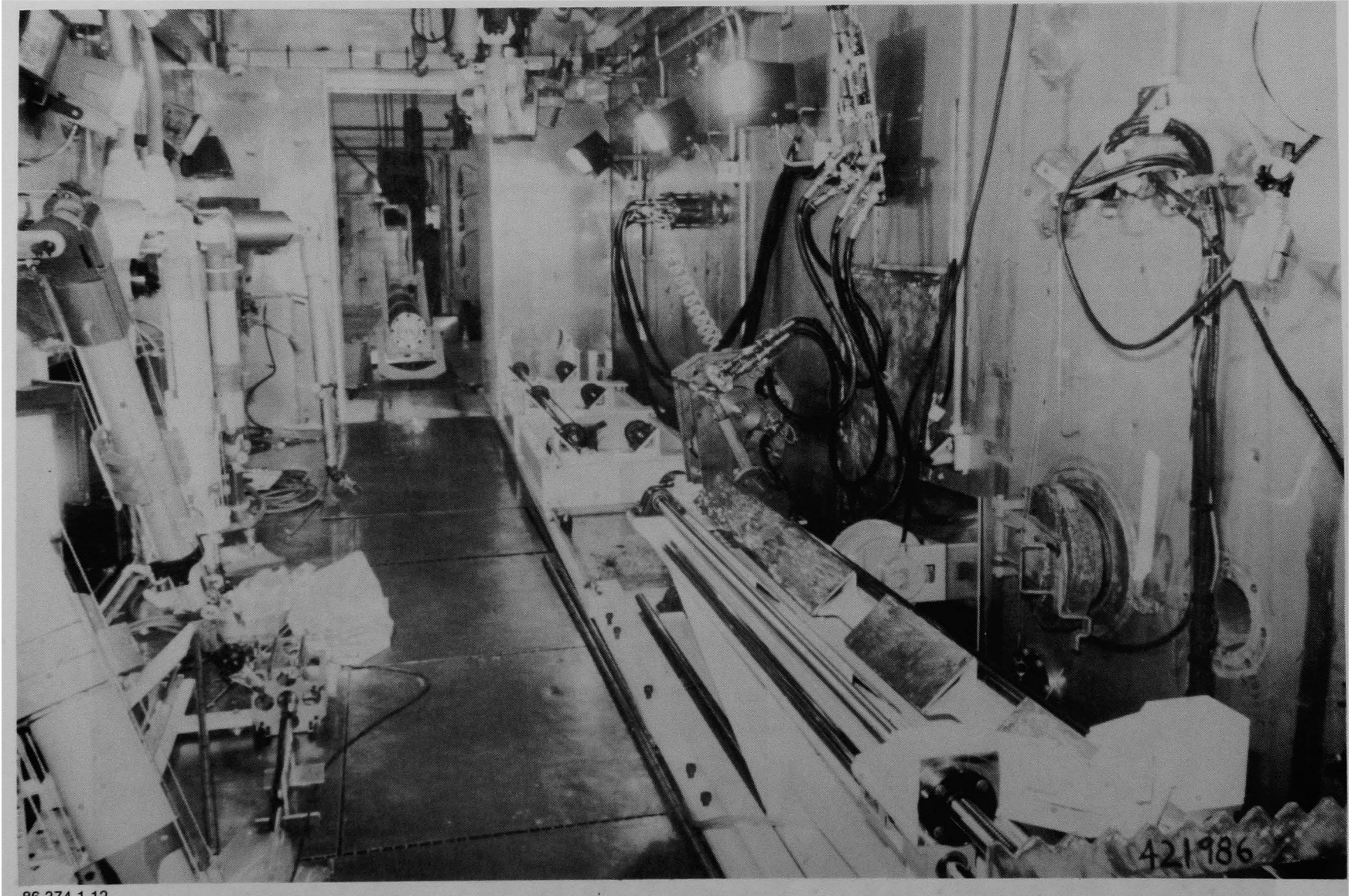
86-275-3-6

Figure C-5. TMI-2 fuel canister head removal machine--end view.



86-275-3-1

Figure C-6. TMI-2 fuel canister head removal machine--side view.



86-374-1-12

Figure C-7. TMI-2 fuel canister unloading carriage table.

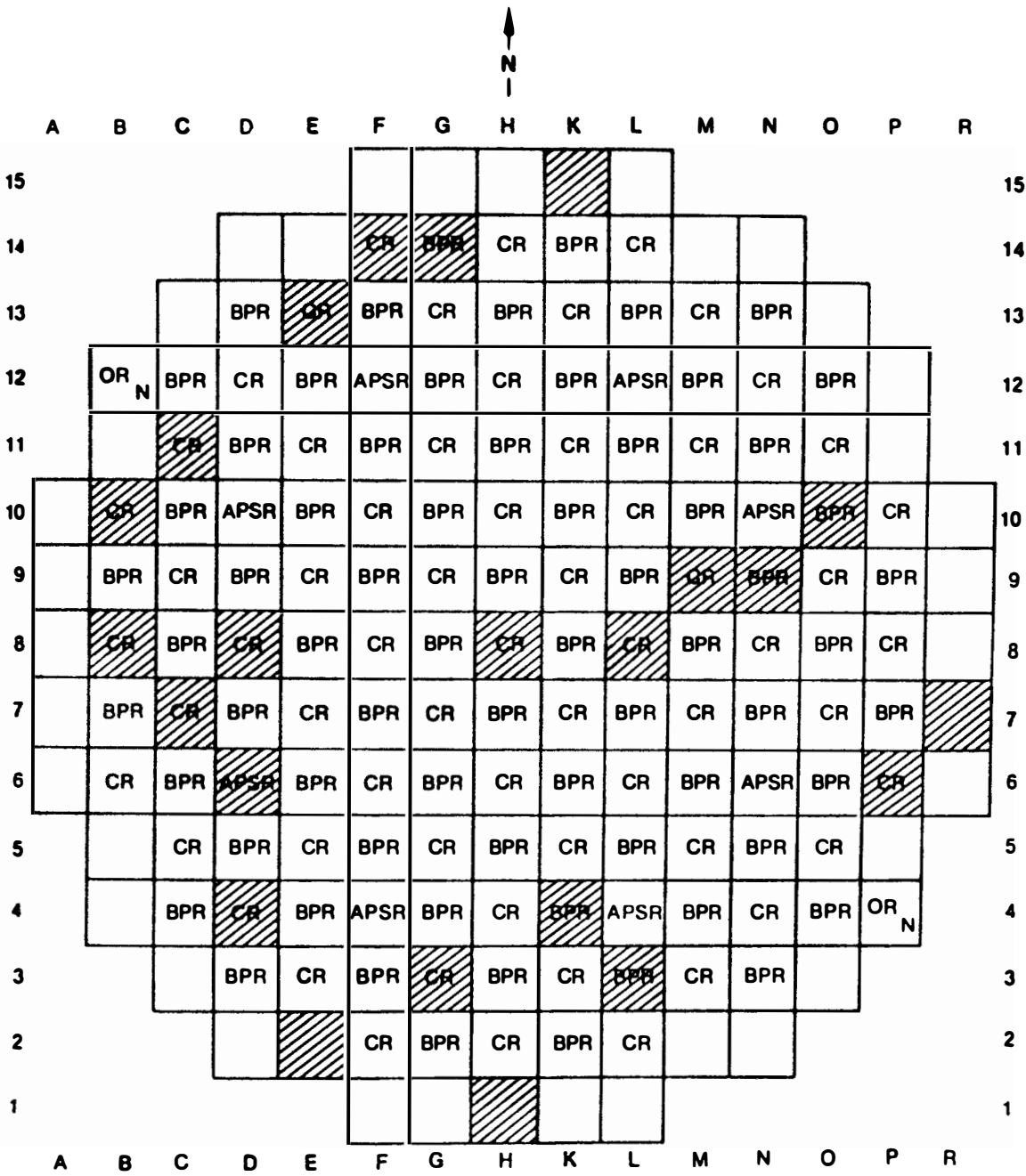


86-275-4-4

Figure C-8. Assortment of TMI-2 fuel canister unloading tools.

are only slightly larger than the as-built dimensions of the upper end boxes and partial fuel assemblies, the components, when pulled on, could become wedged by small loose debris. Dislodging the components usually required pushing back and pulling forward. In many cases, this push-pull operation was necessary many times to move a component a short distance. As components were removed, it was necessary to work farther down inside the canister, which required a video camera with a light source so that the technicians could see how to attach the tools to the different components. Figure C-9 shows the TMI-2 core loading diagram with the specific locations from which the identified components removed from both canisters D-141 and D-153 originally came.

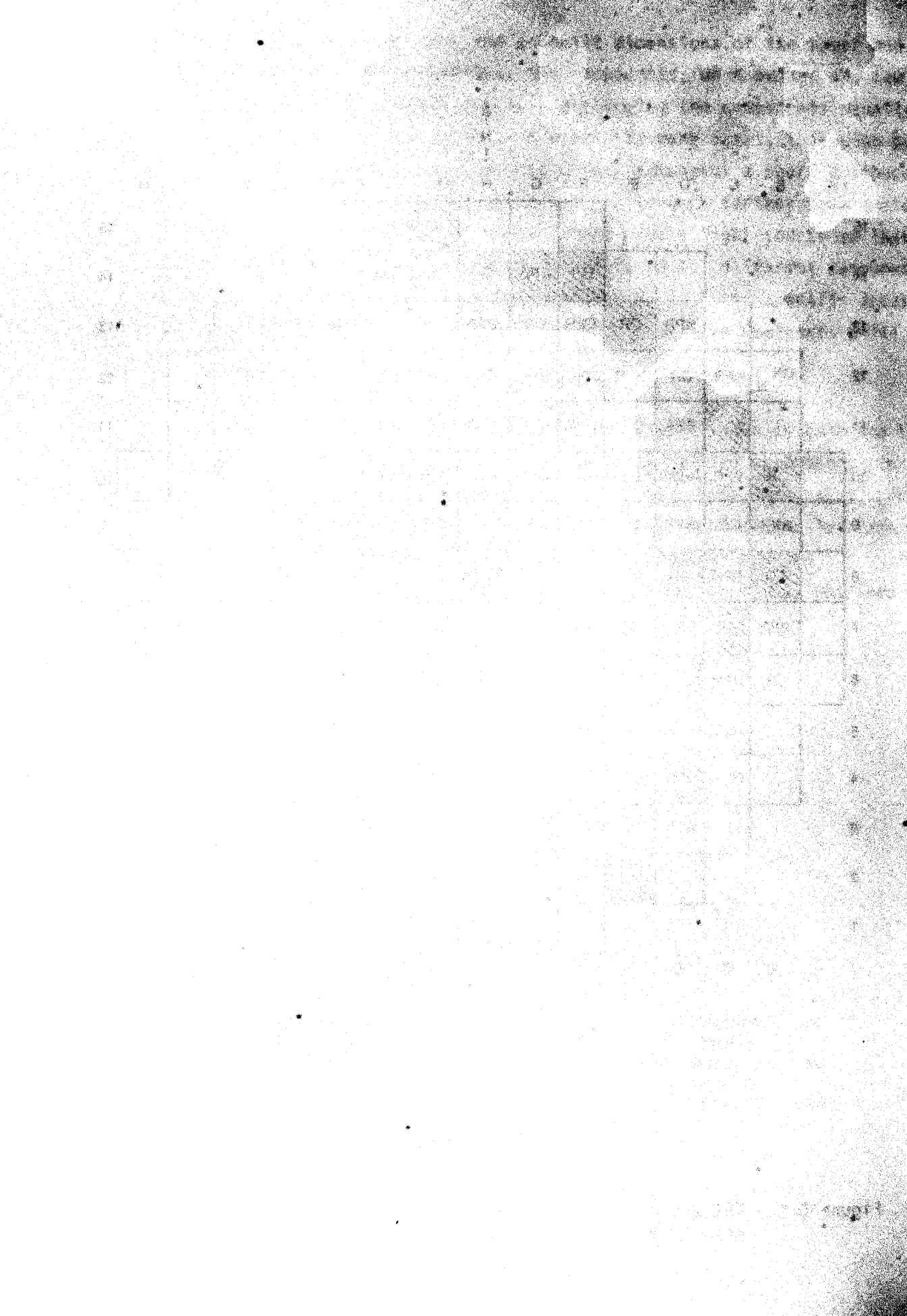
All components removed from the canisters were visually examined to identify areas of melting and other temperature-related phenomena. In addition to the visual examinations, specific fuel rods and control rods inside guide tubes were selected from the partial fuel assemblies from core positions C7 and H1 for full-length gamma scanning and neutron radiography. Selected fuel and control rod samples were then obtained for metallographic and radiochemical examinations.



- | | |
|---|---|
| <p>OR Orifice Rod Assembly</p> <p>CR Control Rod Assembly</p> <p>BPR Burnable Poison Rod Assembly</p> | <p>APSR Axial-Power-Shaping Rod Assembly</p> <p>N Primary Neutron Source</p> <p style="text-align: center;"> Components removed</p> |
|---|---|

7-1633

Figure C-9. TMI-2 core loading diagram showing locations of components removed from canisters D-141 and D-153.



VISUAL EXAMINATION DATA AND TEMPERATURE ESTIMATION

This section presents the results of the visual examination of the subject components from the upper region of the 300 degree. These observations are provided to assist in the determination of the condition of the components during the accident. These observations are being provided to assist in the determination of the condition of the components during the accident. The results of the visual examination, the estimated temperature, and the estimated melting points are listed in Table D-1. In addition, the estimated melting points are listed in Table D-2. In addition, the estimated melting points are listed in Table D-2. In addition, the estimated melting points are listed in Table D-2.

APPENDIX D

VISUAL EXAMINATION DATA AND TEMPERATURE ESTIMATION

In the following paragraphs an attempt is made to describe the physical appearance of the components and reference is made to the top of the assembly and to the bottom of the assembly. The estimated melting points are listed in Table D-1. In addition, the estimated melting points are listed in Table D-2. In addition, the estimated melting points are listed in Table D-2.

D.1. Visual Examination

These observations were recorded from October 2-11. These observations were recorded from October 2-11. These observations were recorded from October 2-11.

Estimated Melting Points are listed in Table D-1 and D-2.

- Estimated Melting Points are listed in Table D-1 and D-2.
- Estimated Melting Points are listed in Table D-1 and D-2.
- Estimated Melting Points are listed in Table D-1 and D-2.
- Estimated Melting Points are listed in Table D-1 and D-2.

APPENDIX D

VISUAL EXAMINATION DATA AND TEMPERATURE ESTIMATION

This section presents the results from visual examinations of the distinct components from the upper regions of the TMI-2 core. These examinations provided information on the peak temperature distribution in these regions during the accident. These temperature estimates were based upon the observance of the melted/unmelted boundary on various components. The pertinent assembly components, their material types, and their minimum melting points are listed in Table D-1. In addition, the possibility exists of a Fe-Zr eutectic interaction between the zircaloy guide tubes and the 304 SS tie plate and control rod cladding at a minimum temperature of approximately 1220 K, and similarly a Ni-Zr eutectic interaction between the zircaloy guide tubes and the Inconel spacer grids at a minimum temperature of approximately 1220 K.

In the following discussions of information obtained from the individual components, all orientations are referenced looking down on the top of the assembly and it is assumed that all assemblies had been loaded into the TMI-2 core with the end fitting identification markings facing the south side of the core. Consequently, in views looking at the bottom side of a component, east and west appear switched from their normal compass positions.

D.1 D-141 Canister Components

Eleven components were removed from canister D-141. Each component is described here three ways: in tabular form, verbally, and through the use of photographs.

Component D-141-1: Partially melted end fitting and control rod spider

Core Position: E13

Upper End Fitting Identification: Unavailable

Spider Hub Identification: C157

Illustrated in: Figures D-1 and D-2

TABLE D-1. MELTING POINTS OF SIGNIFICANT COMPONENTS

<u>Material</u>	<u>Melting Point</u>
304 SS End fitting Grill Mixing cup Apron Spring retainer	1673 K
Inconel 718 Spacer grids	1533 K
Inconel X-750 Holddown spring	1666 K
Ag-In-Cd control material	1073 K
Zircaloy Fuel rod cladding	2030 K
UO ₂ Fuel	~3120 K
Al ₂ O ₃ -B ₄ C Burnable poison rod	~2300 K



Figure D-1. Southwest corner of component D-141-1. Partially melted end fitting and control rod spider.



86-384-1-5

Figure D-2. Bottom view of component D-141-1.

The apron and all material below the tie plate are missing from component D-141-1 except for a few small stubs of control rod material. The heaviest damage occurred in the southwest corner where the tie plate, mixing cup, upper regions of the end fitting, the spring retainer, and the control rod spider have melted away. Drips of previously melted material are present on portions of the end fitting and spider. The holddown spring is completely missing. The tie plate is generally intact on the eastern half of the assembly, while the upper end fitting (above the tie plate elevation) is, with the exception of the southwest corner, generally intact.

The presence of previously melted regions on the tie plate, end box, mixing cup, and control rod cladding in the southwest corner indicates that temperatures were in excess of 1673 K in this region from the tie plate to the upper portions of the end fitting. Temperatures were generally less than 1673 K at the tie plate elevation on the eastern half of the assembly.

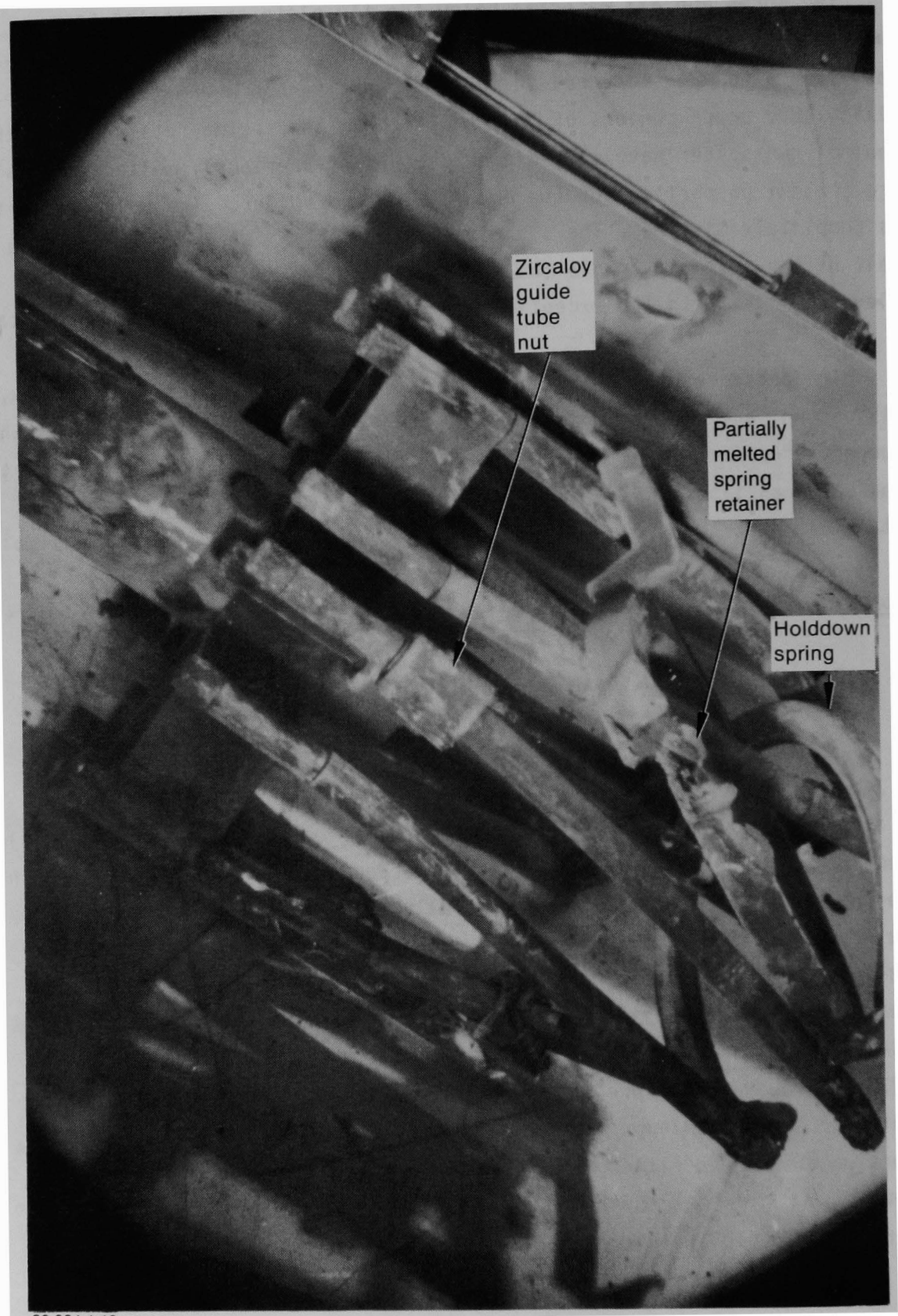
Component D-141-2: Partially melted control rod spider

Core Position: C11

Spider Hub Identification: C156

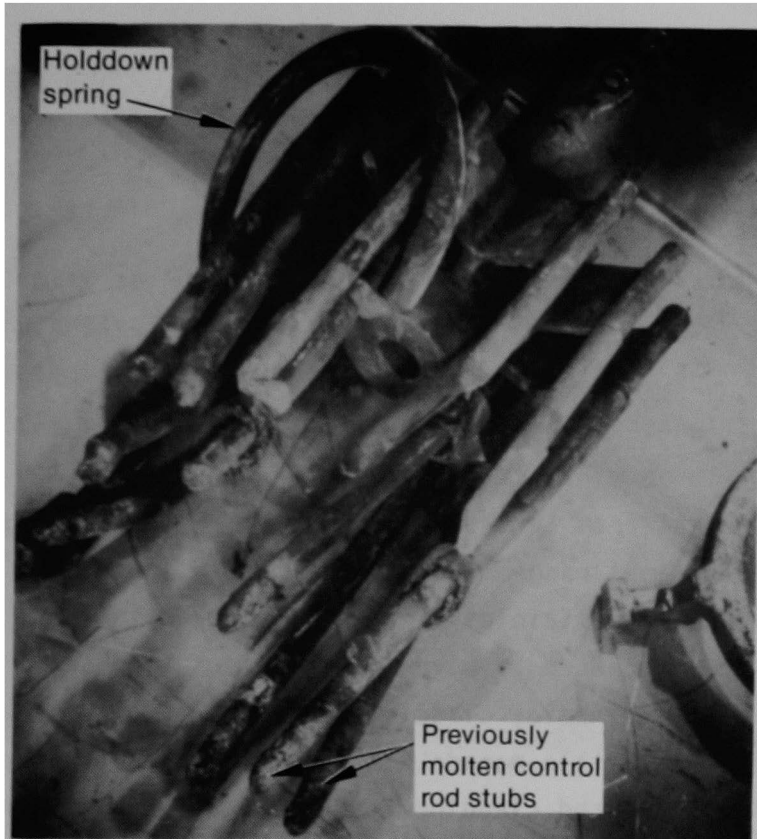
Illustrated in: Figures D-3 and D-4

Approximately 15 to 20 cm (6 to 8 in.) of control rod cladding still remains on component D-141-2. This corresponds to the approximate length to the tie plate when the spider is fully inserted. Some of the zircaloy guide tube nuts have slipped upward and most, if not all, were partially melted. The melting could have occurred as a result of a Fe-Zr eutectic reaction between the zircaloy guide tube nuts and either the 304 SS tie plate or the control rod cladding at a minimum temperature of approximately 1220 K. However, the presence of prior-molten regions on the spring retainer indicates temperatures were in excess of 1673 K near the upper portion of the end fitting. The presence of prior-molten endpoints on the remaining portion of the holddown spring further supports temperatures in excess of 1666 K in this region.



86-384-1-13

Figure D-3. Component D-141-2. Partially melted control rod spider.



86T-6

Figure D-4. Bottom view of component D-141-2. Control rod spider.

It should be noted that this component was located in a core position that was symmetrically similar to that of component D-141-1, centered about core position D12. Both control rod spider assemblies exhibited similar damage.

Component D-141-3: Partial fuel assembly and control rod spider

Core Position: C7

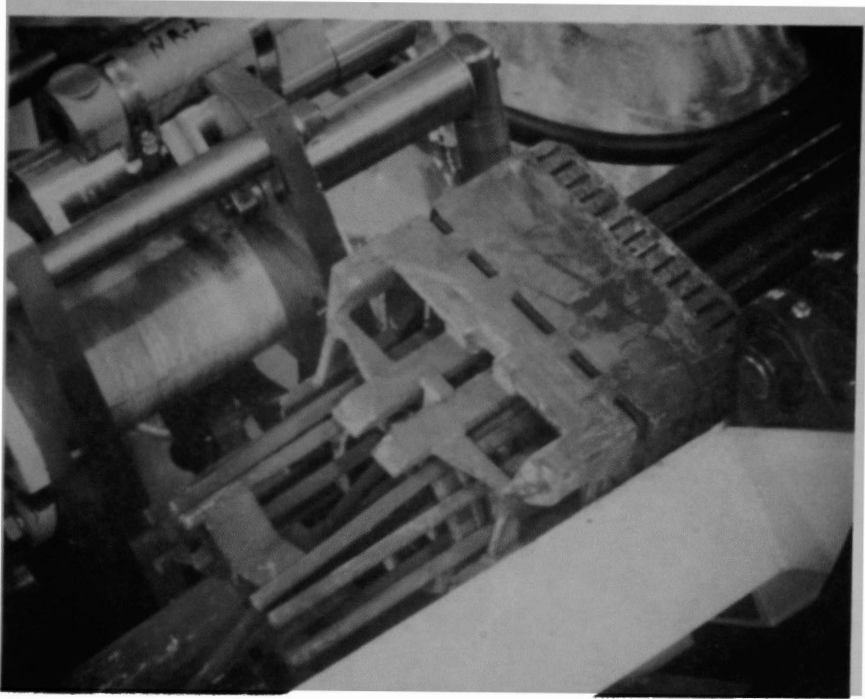
Upper End Fitting Identification: NJ 00Q8

Spider Hub Identification: C179

Illustrated in: Figures D-5 through D-8

Component D-141-3 was intact from the upper spacer grid to the top of the control rod spider and had fuel and control rods extending well below the upper spacer grid. Most of the fuel rods were later removed from the assembly and had lengths ranging from approximately 47 cm (19 in.) in the southwest corner to about 20 cm (8 in.) in the northeast corner. The control rods were cut from the assembly just below the upper spacer grid, and the removed sections ranged from approximately 15 to 38 cm (6 to 15 in.) in length. The stainless steel cladding on the lower ends of some of the control rods appeared to have been previously melted; however, all the lower ends of the zircaloy cladding on the fuel rods appeared to have been broken off in a brittle manner. Typical examples are shown in Figure D-6. These fuel rod cladding fractures, along with some bent endtips on control rods (Figure D-7), probably occurred when this component fell to the debris floor in the reactor or during loading into the canister. The small region of damage to the apron and spacer grid on the northwest corner (Figure D-8), and similar damage on the southeast corner, may have occurred in getting the component in and out of the shipping canister.

The presence of intact stainless steel cladding on the control rods, which in some cases was melted near the endtips, indicates temperatures were near 1673 K, approximately 20 to 25 cm (8 to 10 in.) below the upper spacer grid in the southeast corner, and approximately 35 cm (14 in.) below



86T-49

Figure D-5. Component D-141-3. Partial fuel assembly in disassembly trough.

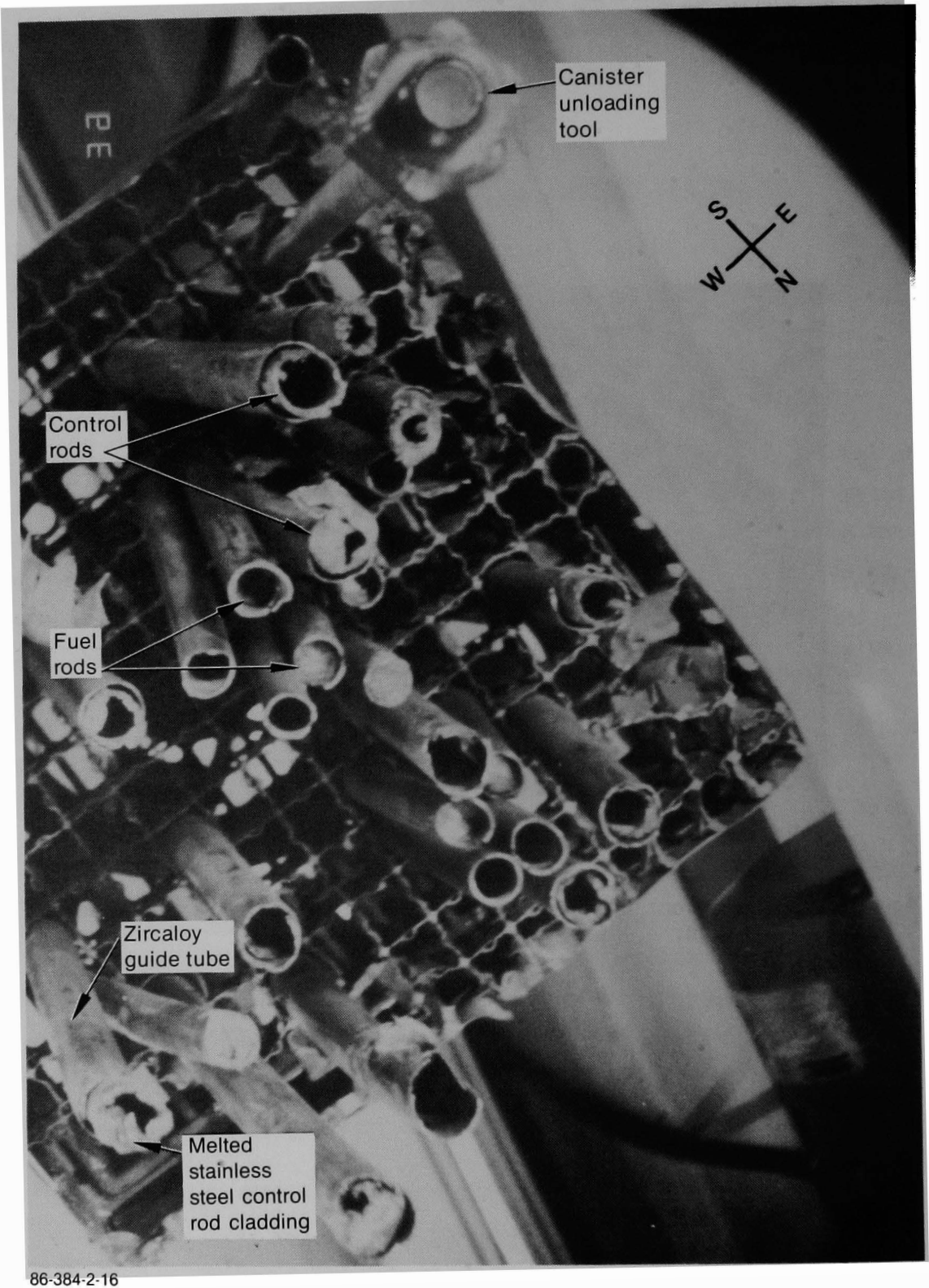
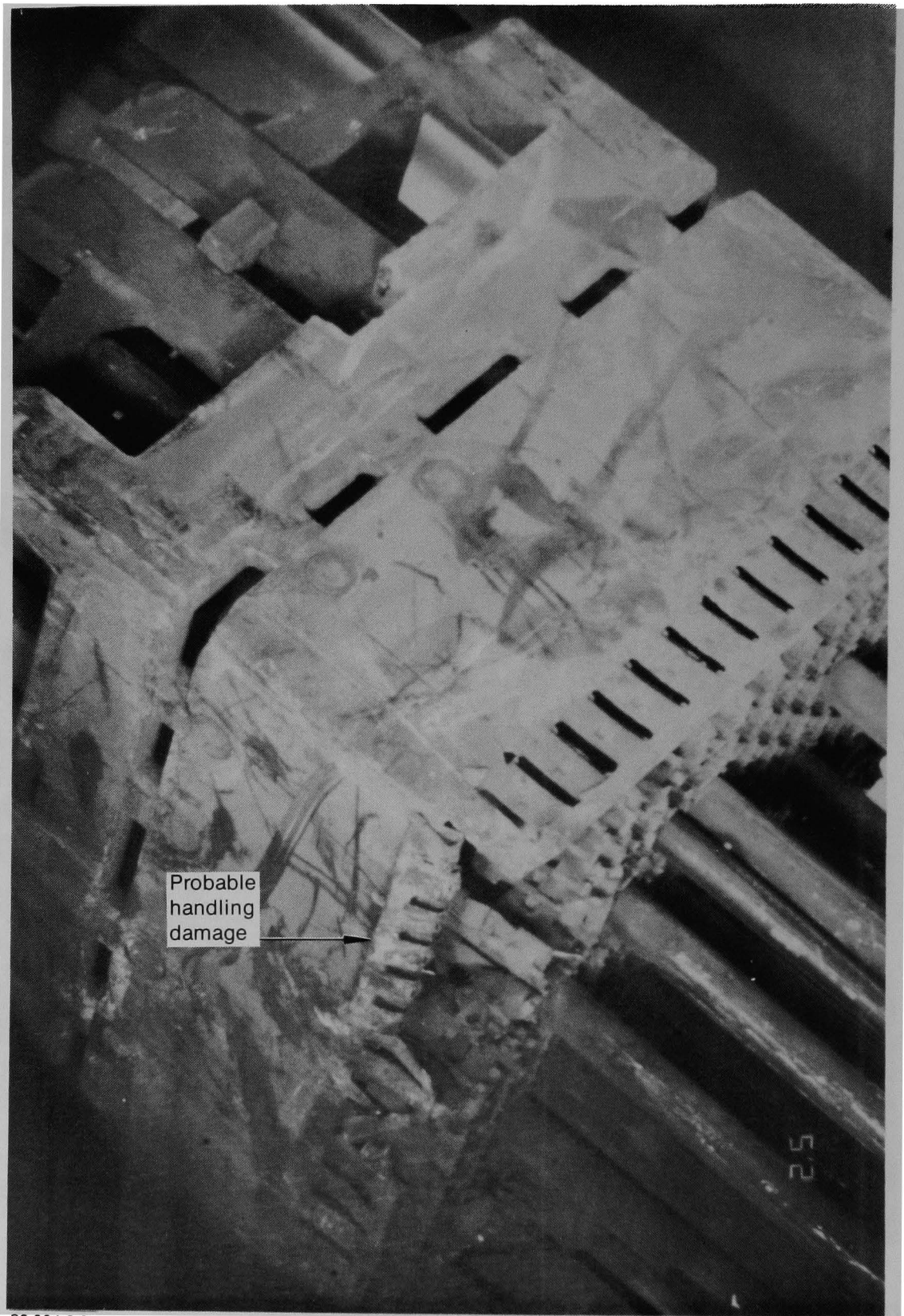


Figure D-6. Bottom view of component D-141-3 after removal of most fuel rods.



Figure D-7. Control rod stubs of component D-141-3 after removal of most fuel rods.



86-384-2-2

Figure D-8. Northwest corner of component D-141-3 showing damaged apron.

the upper spacer grid on the west side of the assembly. The presence of the intact spacer grid indicates temperatures were less than 1533 K at this elevation.

Some of the fuel and control rod/guide tubes removed from this assembly were examined by neutron radiography and gamma scanning and were then sectioned to obtain samples for metallography and radiochemical analyses of surface deposits. The results of those examinations are presented in Section 5 in the main body of this report.

Component D-141-4: Partially melted burnable poison rod fuel assembly upper end fitting

Core Position: N9

Upper End Fitting Identification: NJ OORZ

Illustrated in: Figures D-9 through D-11

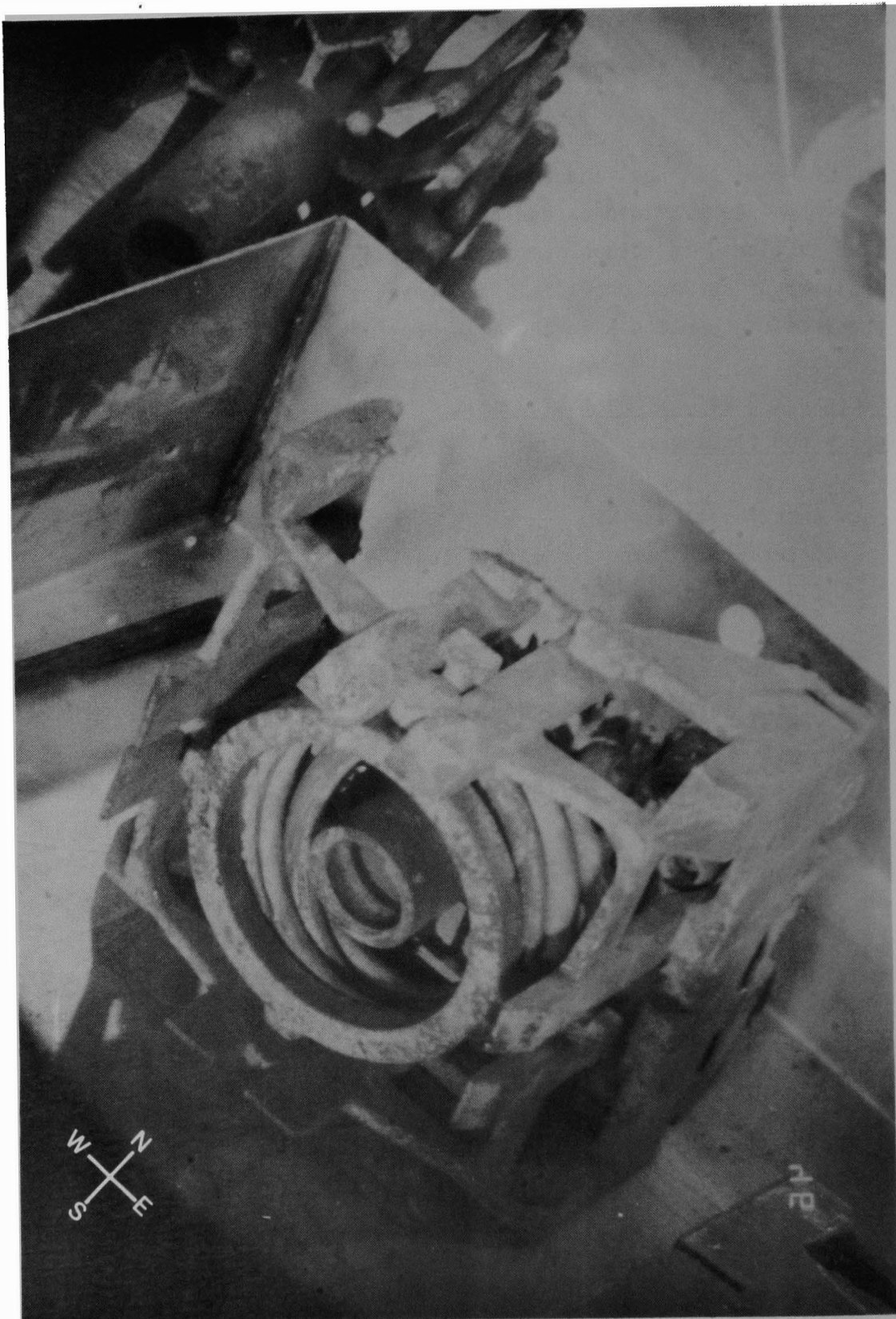
The greatest damage to component D-141-4 occurred on the north side where the prior-molten region included the tie plate and the upper sides of the end fitting. On the west side, the tie plate had partially melted away and some minor melting of the sides of the end fitting above this elevation also occurred. Figure D-11 shows details of the melted/unmelted transition zone around the burnable poison rod/guide tube positions in the tie plate. The damage immediately surrounding the guide tube positions may be due to a Fe-Zr eutectic reaction, however this is uncertain unless detailed examinations are performed. In the regions on the north and west side where the tie plate and end fitting sides were melted, peak temperatures were greater than 1673 K.

Component D-141-5: Burnable poison rod spider

Core Position: N9

Spider Hub Identification: B181

Illustrated in: Figure D-12



86-384-3-7

Figure D-9. Component D-141-4. Partially melted burnable poison rod fuel assembly upper end fitting.



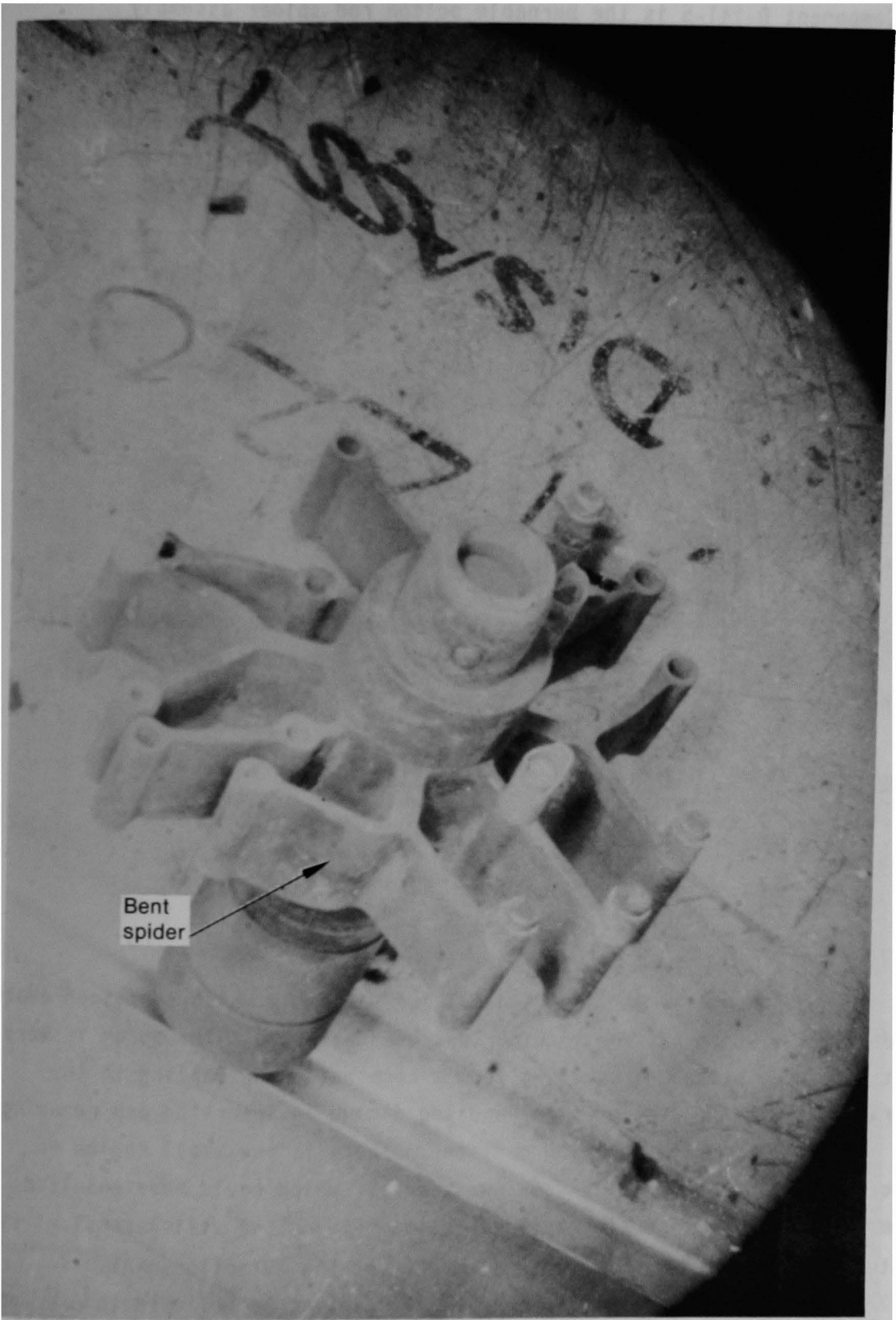
86-384-3-6

Figure D-10. Bottom view of component D-141-4.



86T-103

Figure D-11. Details of melted transition region around burnable poison rod positions in component D-141-4.



86-384-3-3

Figure D-12. Component D-141-5. Burnable poison rod spider from end fitting component D-141-4.

Component D-141-5 is the burnable poison rod spider assembly corresponding to the upper end fitting identified as component D-141-4. The arms on the spider are bent and only 8 of the 16 burnable poison rod stubs are present. No melted regions are apparent and the rod stubs appear to have been broken off. The bending of the spider arms may have occurred during loading into the fuel canister. The condition of this component further indicates that temperatures were lower than 1673 K in the upper regions of core position N9 where this and component D-141-4 were originally located.

Component D-141-6: Burnable poison rod assembly retainer

Core Position: L3
Identification: L051
Identified in: Figure D-13

No prior-molten regions or damage were observed on component D-141-6. This component fits over the top of the spider and presses down on the spring retainer.

Component D-141-7: Partial upper end fitting

Core Position: K15
Upper End Fitting Identification: NJ 00UV
Identified in: Figures D-14 and D-15

Component D-141-7 was a peripheral fuel assembly which contained empty guide tubes. No rod assembly spider was ever attached. The apron is very bent and torn, probably resulting from a combination of falling to the debris floor in the reactor, and handling damage in inserting and removing the component from the shipping canister. There is one small region of prior-molten tie plate in the southwest corner which could have resulted from a localized Fe-Zr eutectic interaction between the stainless steel tie plate and the zircaloy guide tube sleeves. At the eutectic point (~1220 K), the stainless steel-zircaloy interaction is believed to proceed very slowly; however, at temperatures above 1470 K the reaction approaches

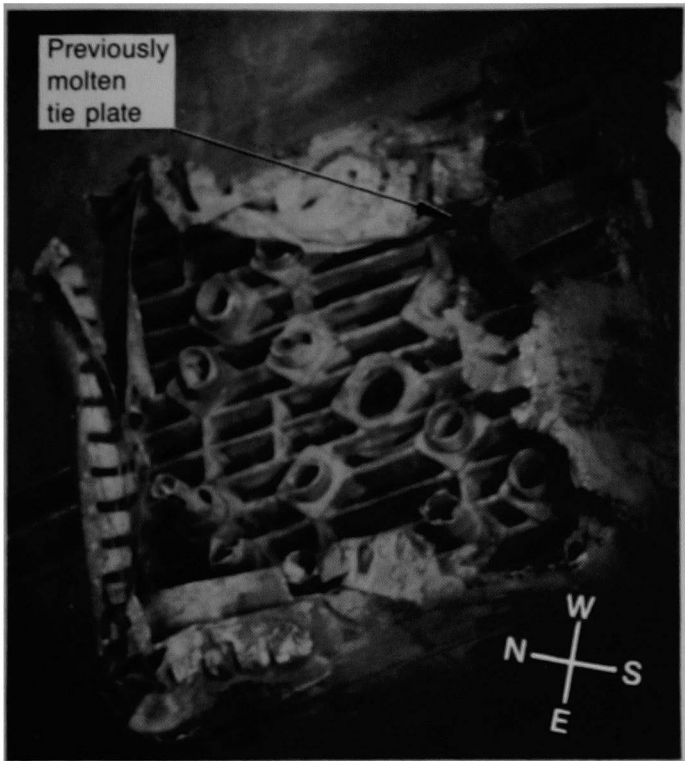


86-384-3-4

Figure D-13. Component D-141-6. Burnable poison rod assembly retainer.



Figure D-14. Component D-141-7. Partial upper end fitting from peripheral fuel assembly.



86T-112

Figure D-15. Bottom view of component D-141-7.

equilibrium in a matter of minutes.^{D1} Considering the limited extent of melted material in this instance, the best estimate of peak temperatures in this localized region is between 1470 K and 1673 K. Over the rest of the assembly, peak temperatures were less than 1673 K at the tie plate elevation.

Component D-141-8: Control rod spider and partially melted upper end fitting

Core Position: M9

Upper End Fitting Identification: NJ 00RI

Spider Hub Identification: C167

Identified in: Figures D-16 and D-17

The greatest damage to component D-141-8 occurred on the north side where the upper end fitting is completely gone. There is also a small region of incipient melting on the spring retainer on this side of the assembly. The control rods on the north side were melted above the tie plate elevation and the guide tube nuts are gone. In contrast, the control rods are intact down to the guide tube nuts on the south side of the assembly. The tie plate and apron are completely gone over the entire assembly, and the one remaining spring coil was melted on at least one end. The bottom portion of the mixing cup was also partially melted (this fell out of the end fitting after it was removed from the canister).

Peak temperatures were generally in excess of 1673 K across the entire assembly at the tie plate elevation, and to the top of the end fitting on the north side. Temperatures were also in excess of 1673 K where the spring retainer and mixing cup were melted, and the melted holddown spring indicates temperatures were greater than 1666 K in this region. The distribution of control rod lengths is further evidence that peak temperatures were above 1673 K above the tie plate on the north side, but were slightly cooler on the south side of the assembly.



86-384-4-11

Figure D-16. Component D-141-8. Control rod spider and partially melted upper end fitting.

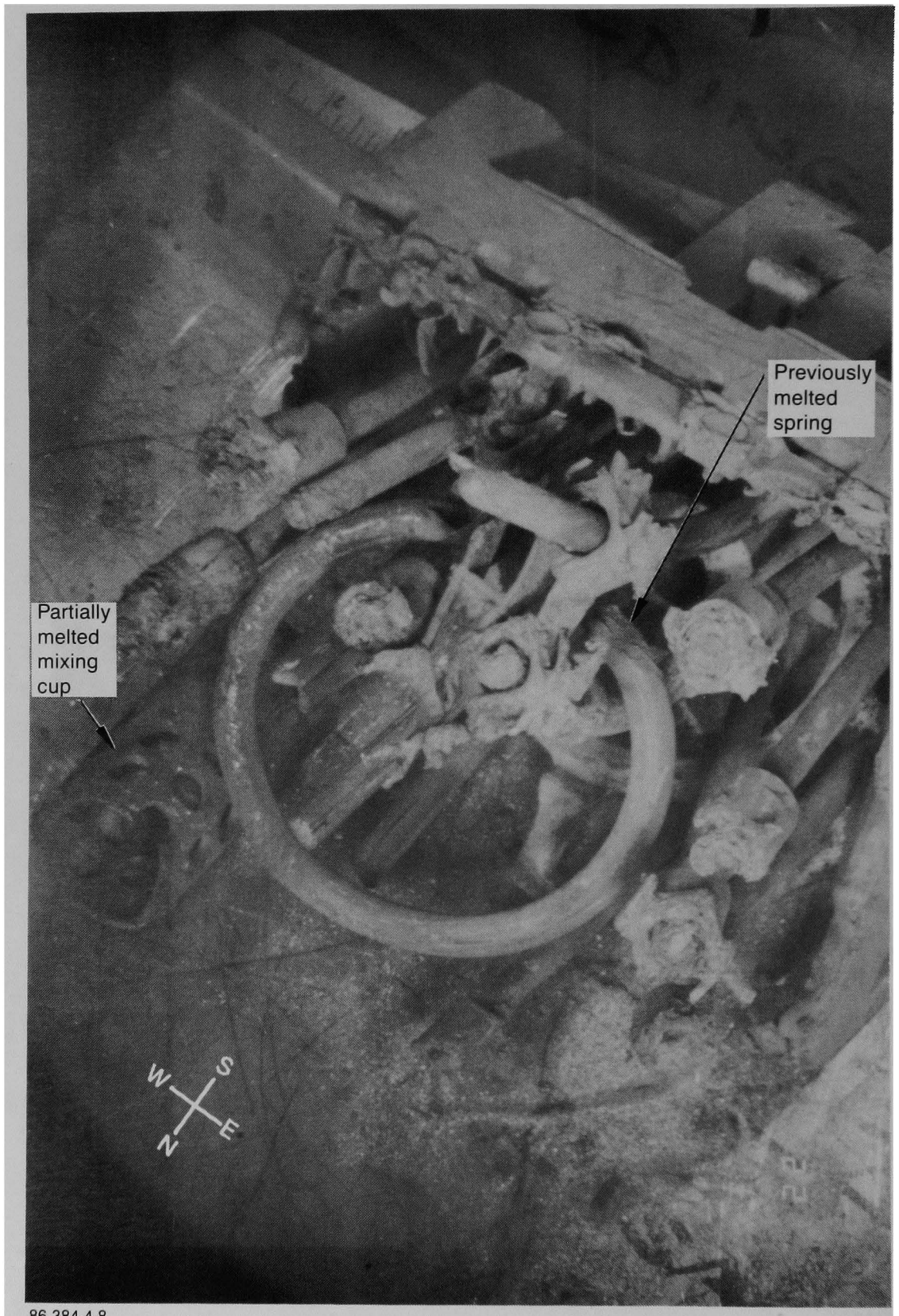


Figure D-17. Bottom view of component D-141-8.

Component D-141-9: Control rod spider and partially melted upper end fitting

Core Position: L8

Upper End Fitting Identification: NJ 00R0

Spider Hub Identification: C142

Illustrated in: Figures D-18 and D-19

The outer edges of component D-141-9's upper end fitting show drips of partially melted stainless steel on the south and west sides above the tie plate elevation. Bent identification markings and slumping in the upper portions of the end fitting near the southwest corner are further evidence of near melting temperatures in this region. The tie plate is completely gone except in the northeast corner. There is some indication of a possible eutectic interaction between the zircaloy guide tube and stainless steel grill in one area (Figure D-19). Peak temperatures were generally greater than 1673 K near the grill elevation except in the northeast corner.

Component D-141-10: Control rod spider and partially melted upper end fitting

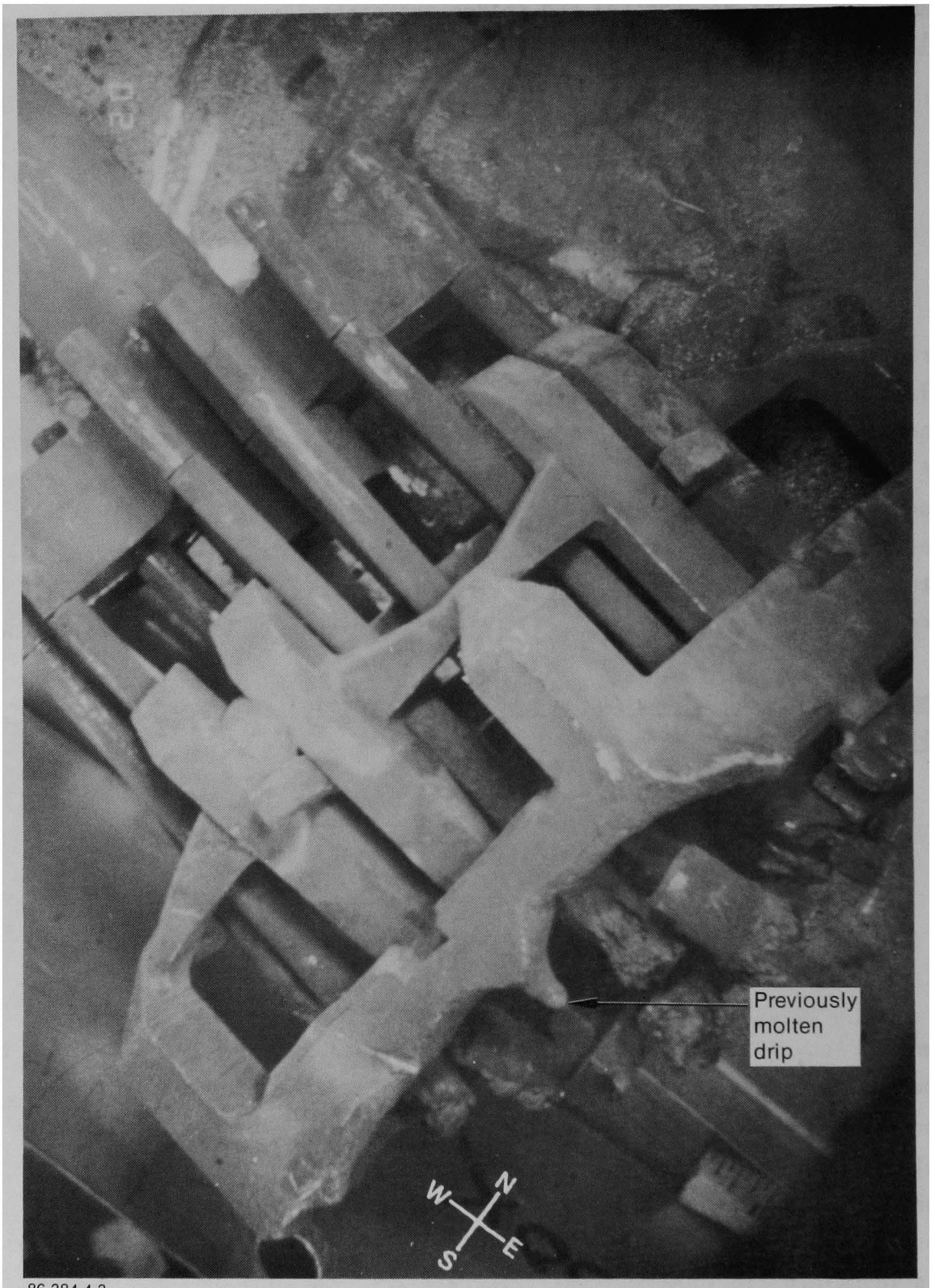
Core position: H8 (core centerline)

Upper End Fitting Identification: NJ 00RR

Spider Hub Identification: C123

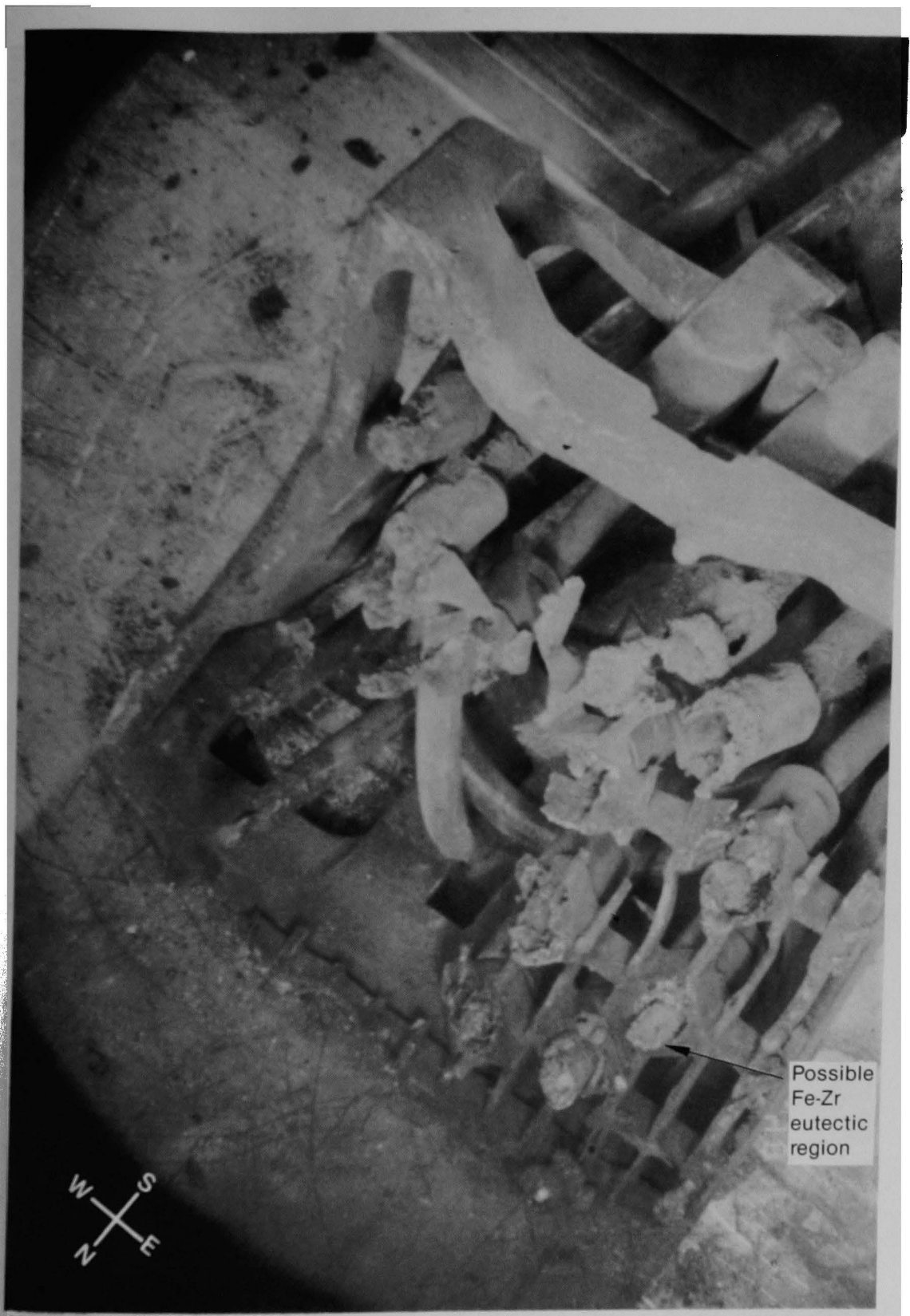
Illustrated in: Figures D-20 through D-22

In component D-141-10, the tie plate has melted away on the outer peripheries of the north and west sides and has partially melted on the south side. The upper end fitting is completely gone in the southwest corner, and it has slumped in the northwest corner. The arm of the spring retainer has also slumped on the west side, and there is a melted spring endtip just below the slumped spring retainer. There are indications of a possible eutectic interaction zone between the zircaloy guide tube sleeve and the tie plate in some areas (Figure D-22), and many of the zircaloy guide tube nuts were partially melted. Peak temperatures were generally below 1673 K at the tie plate elevation; however, temperatures did exceed



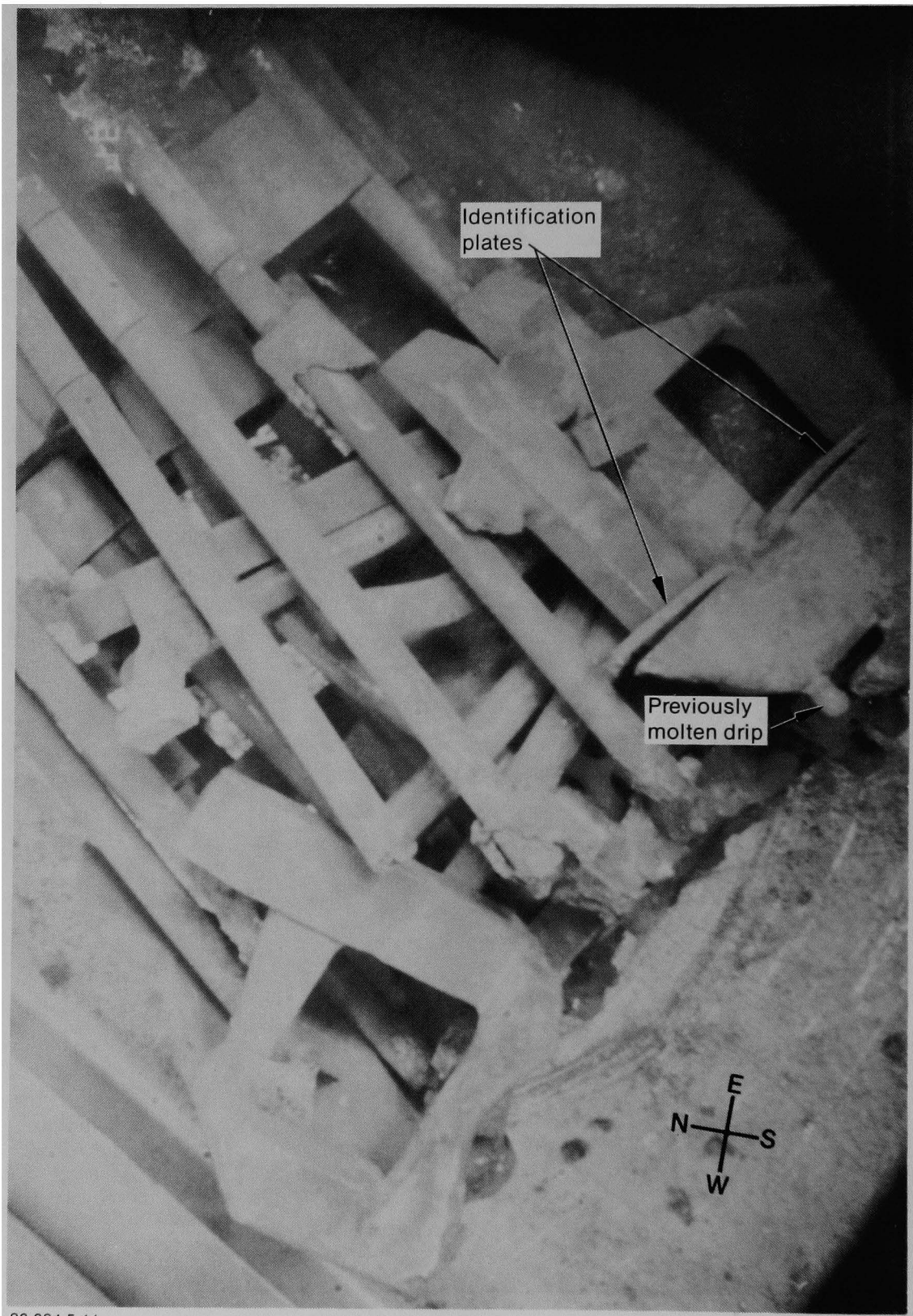
86-384-4-3

Figure D-18. Component D-141-9. Control rod spider and partially melted upper end fitting.



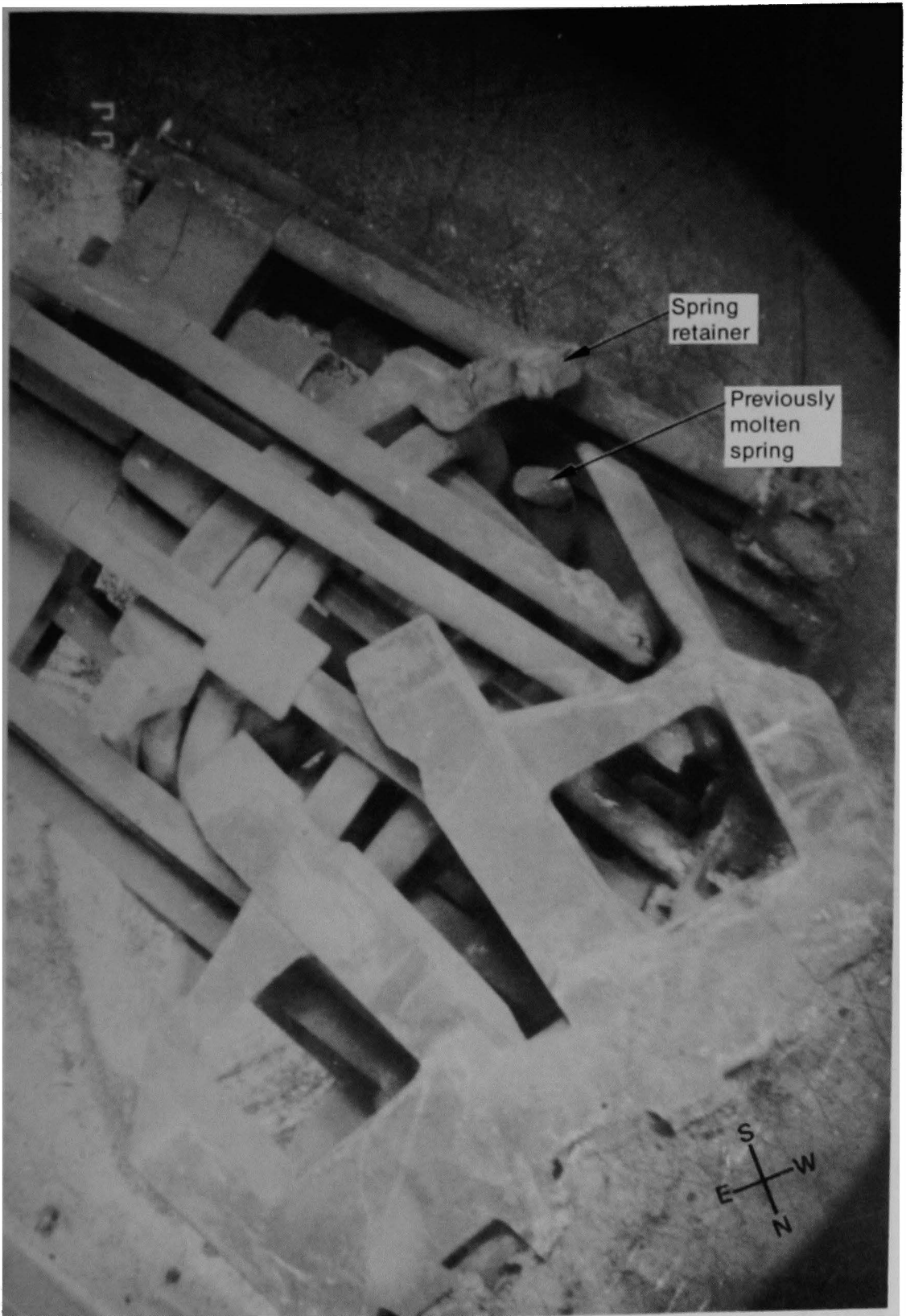
86-384-4-1

Figure D-19. Bottom view of component D-141-9.



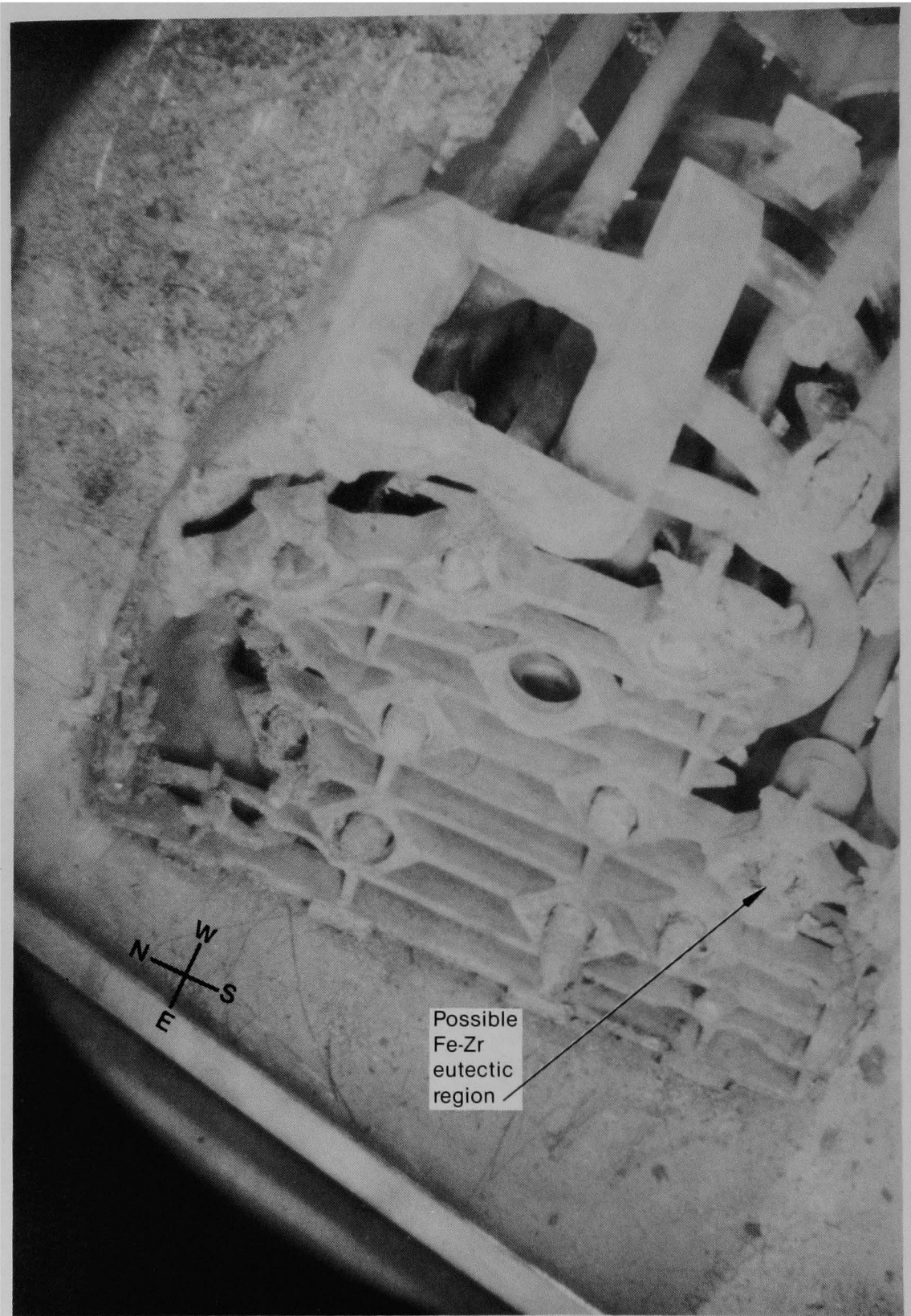
86-384-5-11

Figure D-20. Component D-141-10. Control rod spider and partially melted upper end fitting.



86 384 5 12

Figure D-21. Northwest corner of component D-141-10.



86-384-5-10

Figure D-22. Bottom view of component D-141-10.

1673 K around the southwest corner to the top of the end fitting. Local temperatures exceeded 1666 K on the west side where the holddown spring melted (Figure D-21).

Leadscrews from the H8 (central) and B8 (mid-radius on the east side) core location were examined and peak temperatures for the leadscrews were evaluated. These data indicate that at the core center (H8), temperatures ranged from 1255 K at the bottom of the plenum assembly to 700 K, approximately 3 m up into the assembly. At B8, the temperatures were slightly lower, ranging from 1116 K to 755 K. These temperatures, as expected, are substantially lower than those observed for the distinct components.

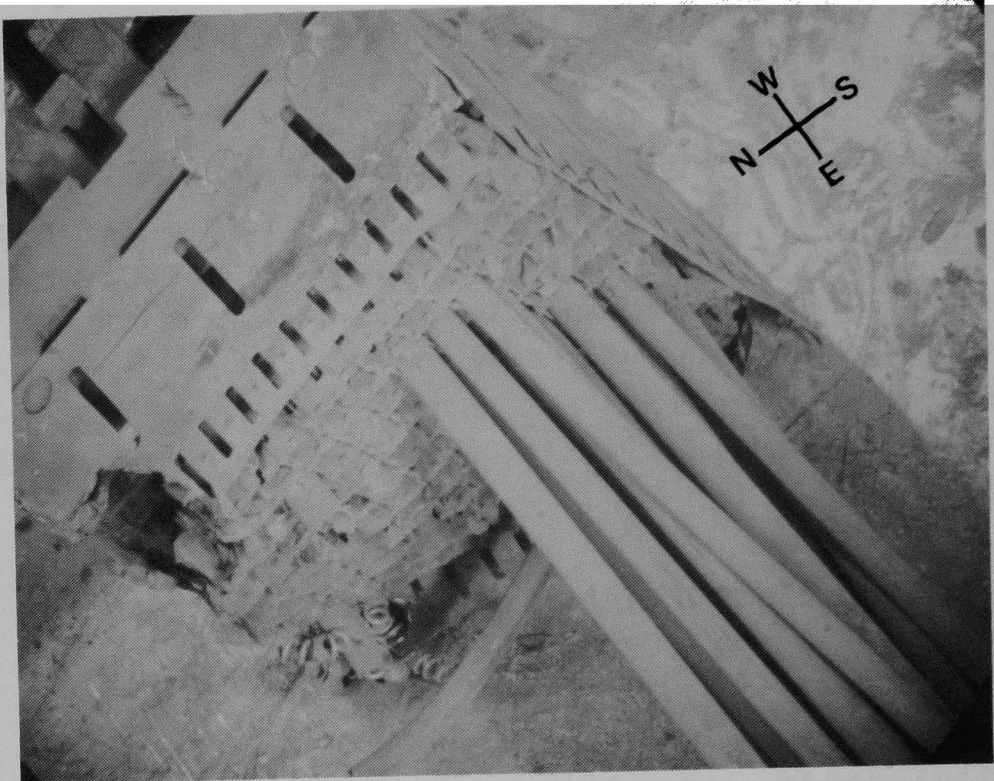
Component D-141-11: Peripheral partial fuel assembly

Core Position: H1

Upper End Fitting Identification: NJ 00UU

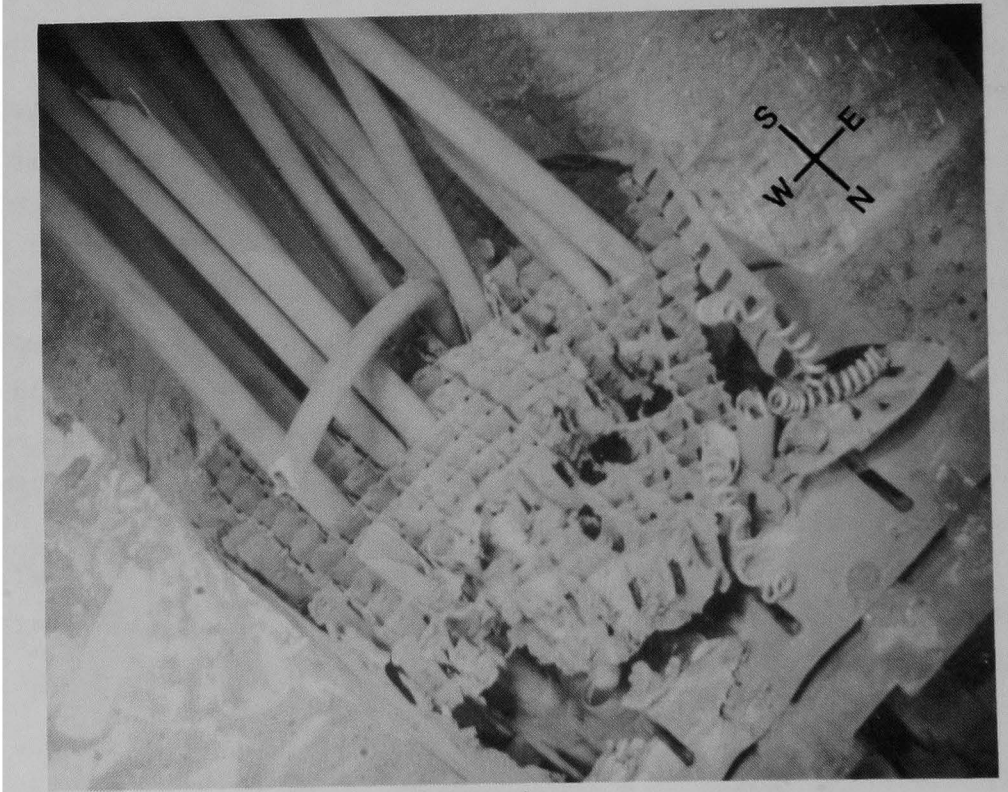
Illustrated in: Figure D-23

Fuel rods extended well below the upper spacer grid in component D-141-11. Eleven fuel rods, which were subsequently removed, ranged from 40 to 60 cm (16 to 24 in.) in length and appeared to have been broken off when the fuel assembly toppled over after removal of the plenum assembly. This fuel assembly, still standing, is shown in the still-image video survey described in Reference D2. Neutron radiographs of some of these fuel rods are presented in Appendix A of this report. Some empty guide tubes were also still present. The apron and upper spacer grid were badly deformed in some areas, some of which probably occurred when the component was loaded into the shipping canister. There may possibly be some previously melted apron and upper spacer grid material in the northwest corner, but most of these materials remained intact. Peak temperatures can generally be considered to have been lower than 1533 K at the upper spacer grid location.



86T-137

a) Southwest corner



86T-138

b) Bottom view

Figure D-23. Component D-141-11. Peripheral partial fuel assembly.

D.2 D-153 Canister Components

Twelve individual components were removed from canister D-153. Each component is described here three ways: in tabular form, verbally, and with photographs.

Component D-153-1: Burnable poison rod assembly retainer

Core Position: K4

Identification: L045

Illustrated in: Figure D-24

As shown in Figure 11, in the main body of this report, core position K4 was in a highly damaged region. However, no melted or damaged regions were present on component D-153-1. This indicates that damage did not penetrate into the plenum assembly.

Component D-153-2: Burnable poison rod assembly retainer

Core Position: G14

Identification: L037

Illustrated in: Figure D-25

No melted or damaged regions were present on component D-153-2.

Component D-153-3: Partial gadolinium fuel assembly and control rod spider

Core Position: D8

Upper End Fitting Identification: NJ OORC

Spider Hub Identification: C144

Illustrated in: Figure D-26

The most damage to component D-153-3 occurred on the east side where the apron has melted away, and this prior-molten region extends around to the midpoint of the north side. The least damage occurred in the southwest corner where the apron, fuel rods and springs, and deformed pieces of the



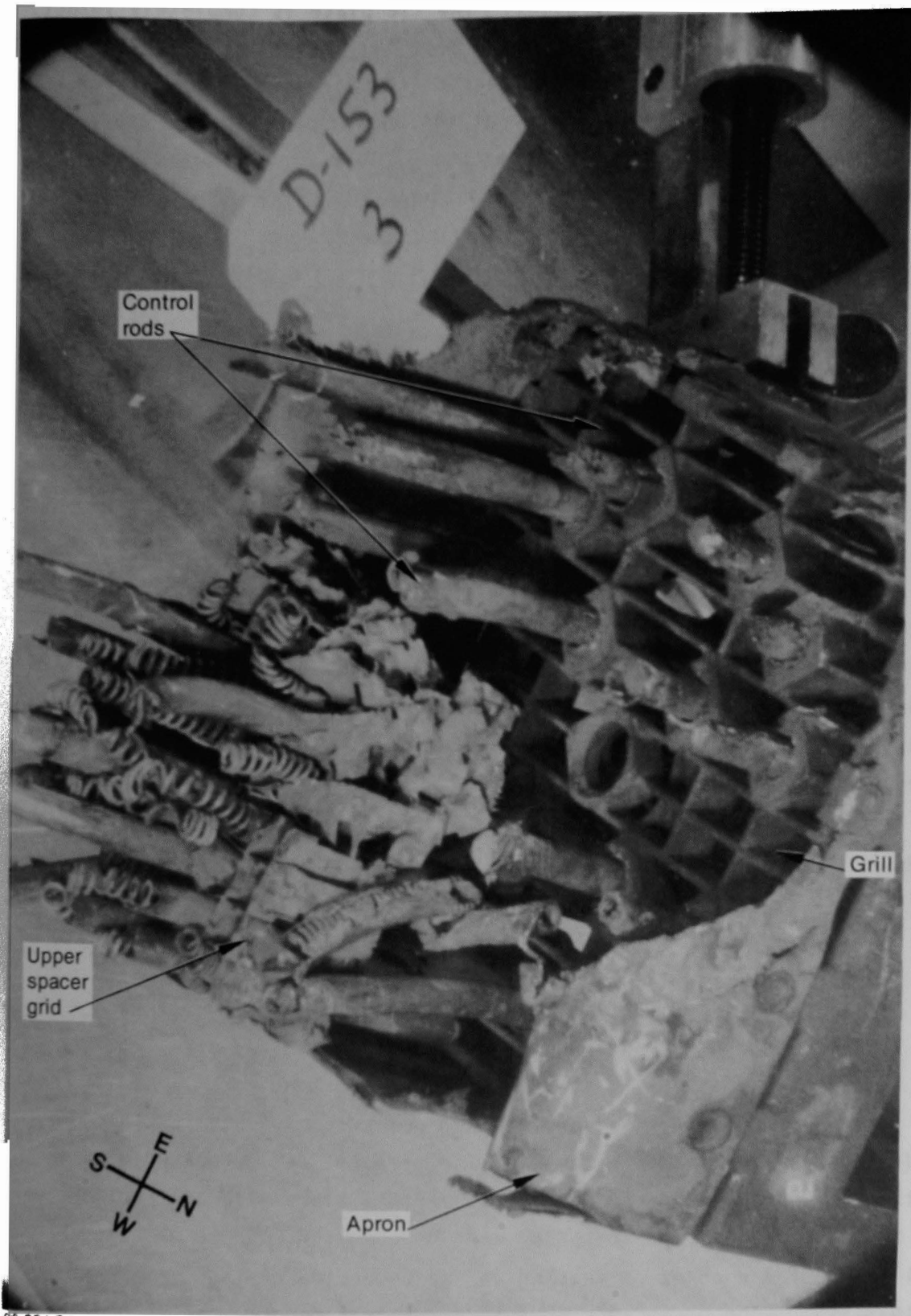
86T-164

Figure D-24. Component D-153-1. Burnable poison rod assembly retainer.



86T-166

Figure D-25. Component D-153-2. Burnable poison rod assembly retainer.



86-384-7-5

Figure D-26. Component D-153-3. Partial gadolinium poison rod fuel assembly.

upper spacer grid are still present. The tie plate is completely intact, and there is no apparent damage to any material above this elevation. Peak temperatures were lower than 1673 K across the tie plate and were lower than 1533 K in the southwest corner at the upper spacer grid elevation. However, peak temperatures were in excess of 1533 K over most of the assembly at the upper spacer grid elevation.

Component D-153-4: Partially melted end fitting and control rod spider

Core Position: G3

Upper End Fitting Identification: NJ 00QV

Spider Hub Identification: C178

Illustrated in: Figures D-27 and D-28

The most damage to component D-153-4 occurred on the east side where the tie plate, sides of the end fitting, control rod cladding, and portions of the holddown spring, spring retainer, and mixing cup were once melted. On the west side, the tie plate and even portions of the apron were still intact. Peak temperatures were generally higher than 1673 K on the east side of this assembly. On the western half of the assembly temperatures were lower than 1673 K at the tie plate elevation.

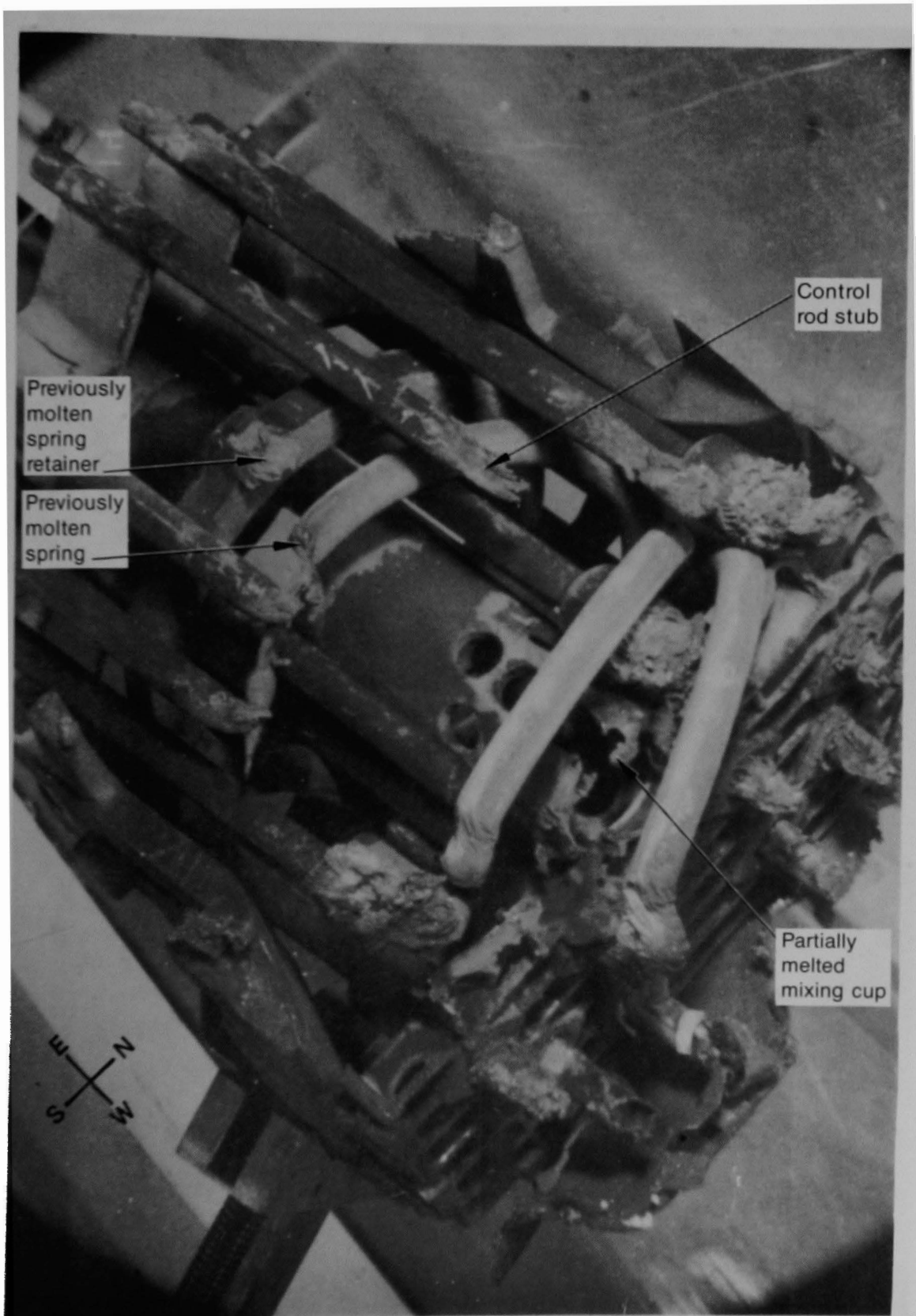
Component D-153-5: Fuel assembly upper end fitting and partial upper spacer grid

Core Position: E2

Upper End Fitting Identification: NJ 00UZ

Illustrated in: Figures D-29 and D-30

Component D-153-5 was a peripheral fuel assembly which contained empty guide tubes and no spider assembly. The greatest damage occurred on the north side where the upper spacer grid, apron, tie plate, and portions of the mixing cup and holddown spring were once melted. There was also an indication of the onset of melting on the underside of the spring retainer on this side. The north side of this assembly faced towards core center, and the postaccident condition indicates steep temperature gradients



86-384.7.10

Figure D-27. Component D-153-4. End fitting and control rod spider.



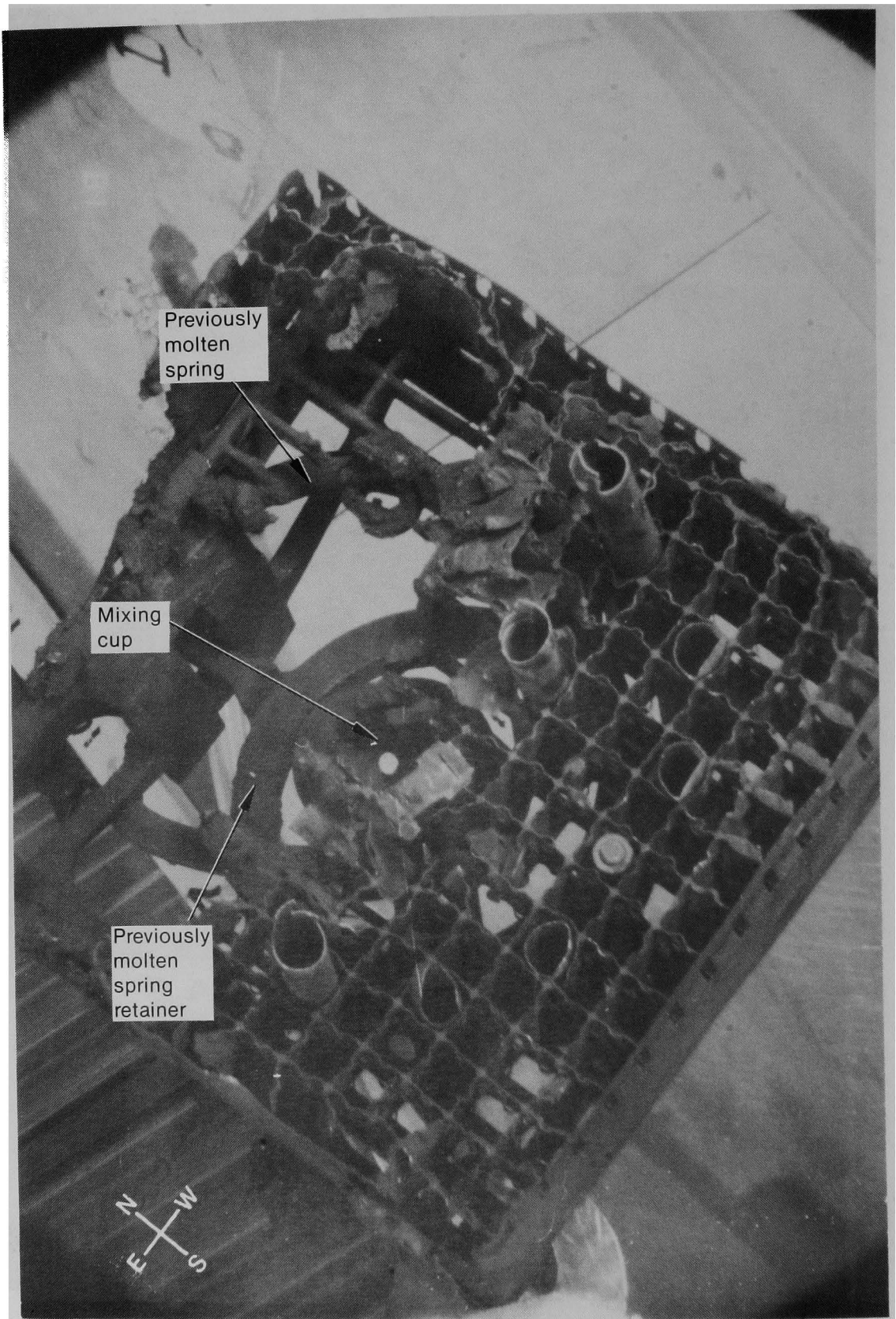
86-384-7-8

Figure D-28. Bottom view of component D-153-4.



86-384-7-16

Figure D-29. North side of component D-153-5. Peripheral fuel assembly upper end fitting.



86-384-7-14

Figure D-30. Bottom view of component D-153-5.

existed in this peripheral fuel assembly. On the north side, peak temperatures were in excess of 1673 K up to the lower surface of the spring retainer in the interior of the assembly; however, portions of the apron and outer surfaces of the end fitting are still intact, as are portions of the mixing cup and hold-down springs. In contrast, on the south side temperatures were lower than 1533 K at the upper spacer grid location. This end-fitting is shown still attached to the fuel bundle in the still-image video survey described in Reference D2.

Component D-153-6: Partial burnable poison rod fuel assembly upper end fitting

Core Location: 010

Upper End Fitting Identification: NJ 00SU

Illustrated in: Figure D-31

On component D-153-6, almost all of the tie plate has melted away, and the greatest damage is in the southeast corner where the entire end fitting has melted away. Some slumping of the upper regions of the end fitting occurred on the west side. The spring retainer is intact and undamaged. Peak temperatures generally exceeded 1673 K at the grill elevation, but were lower than 1673 K at the spring retainer elevation. As shown in Figure 11, in the main body of this report, the fuel assembly upper grid plate was essentially undamaged at the 010 location.

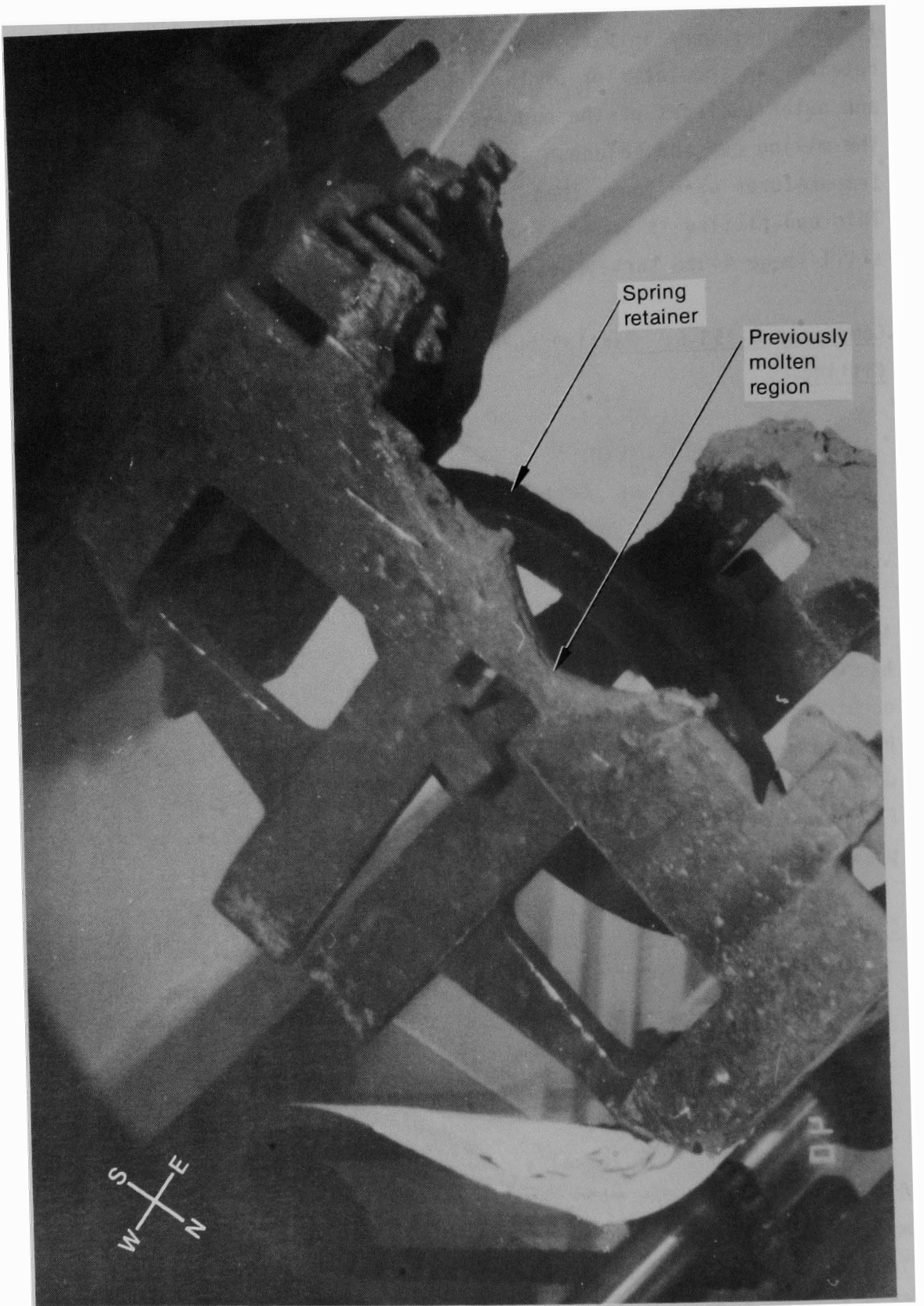
Component D-153-7: Corner of a peripheral fuel assembly upper end fitting

Core Position: R7

Upper End Fitting Identification: NJ 00TL

Illustrated in: Figures D-32 and D-33

Component D-153-7 actually consisted of two pieces that had broken apart while in the shipping canister. The larger piece was a partially melted corner of an upper end fitting with the partial identification letters of NJ stamped on it (Figure D-32). The melted regions extended from the tie plate elevation in the corner to the upper regions of the end



86-384-9-18

Figure D-31. Component D-153-6. Partial burnable poison rod assembly upper end fitting.



86-384-8-8

Figure D-32. Portion of component D-153-7. Corner of peripheral fuel assembly upper end fitting.



86T-238

Figure D-33. Portion of component D-153-7. Upper end fitting.

fitting on the east side. The other piece appeared to fit together with the first piece and had the identification letters OOTL stamped on it (Figure D-33). These core fragments indicate that peak temperatures were generally higher than 1673 K near the tie plate elevation and slightly above. As shown in Figure 11, in the main body of this report, the fuel assembly upper grid plate was essentially undamaged at the R7 location.

Component D-153-8: Control rod spider and partial upper end fitting

Core Position: P6

Upper End Fitting Identification: NJ 00UP

Spider Hub Identification: C136

Illustrated in: Figures D-34 and D-35

The greatest damage to component D-153-8 occurred in the northwest corner, and to a lesser extent in the southeast corner. The tie plate was generally intact except in these corners. The mixing cup, holddown springs, and spring retainer were partially melted in the northwest corner. Control rod stubs extended below the tie plate where it was intact, but were melted above the tie plate in the heavily damaged corners. Peak temperatures were generally either near or above 1673 K at the tie plate elevation, but reached 1673 K in the northwest corner at the location of the spring retainer.

Component D-153-9: Control rod spider and partial fuel assembly

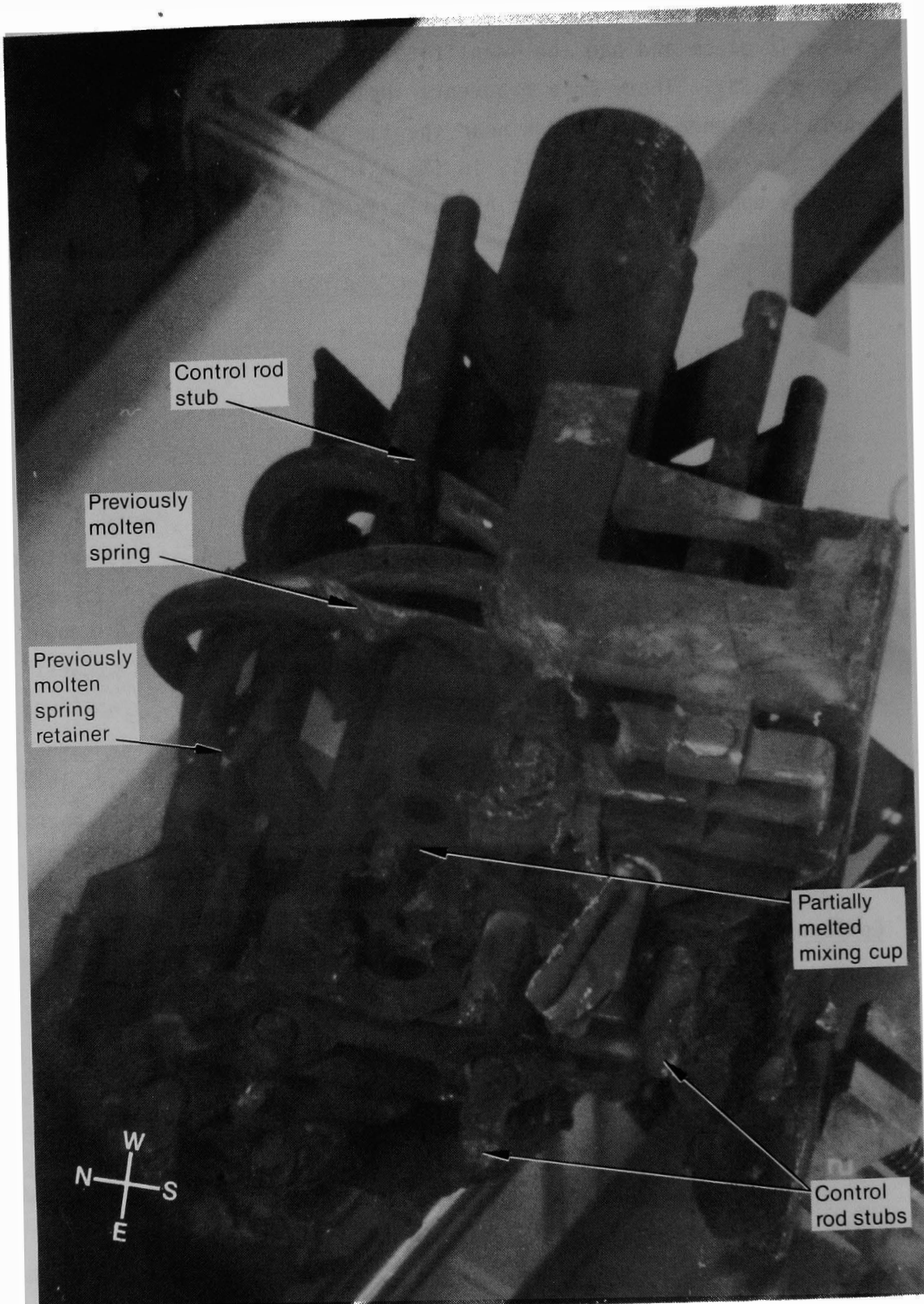
Core Position: 88

Upper End Fitting Identification: NJ 00UB

Spider Hub Identification: C124

Illustrated in: Figures D-36 and D-37

The greatest damage to component D-153-9 occurred in the northwest corner of the assembly, and particularly along the north side. The upper spacer grid and tie plate were intact except in this region, with the damage to the tie plate limited to the extreme northwest corner. Portions of the apron were also melted on the north and west sides. Most of the



86-384-10-36

Figure D-34. West side of component D-153-8. Control rod spider and partial upper end fitting.

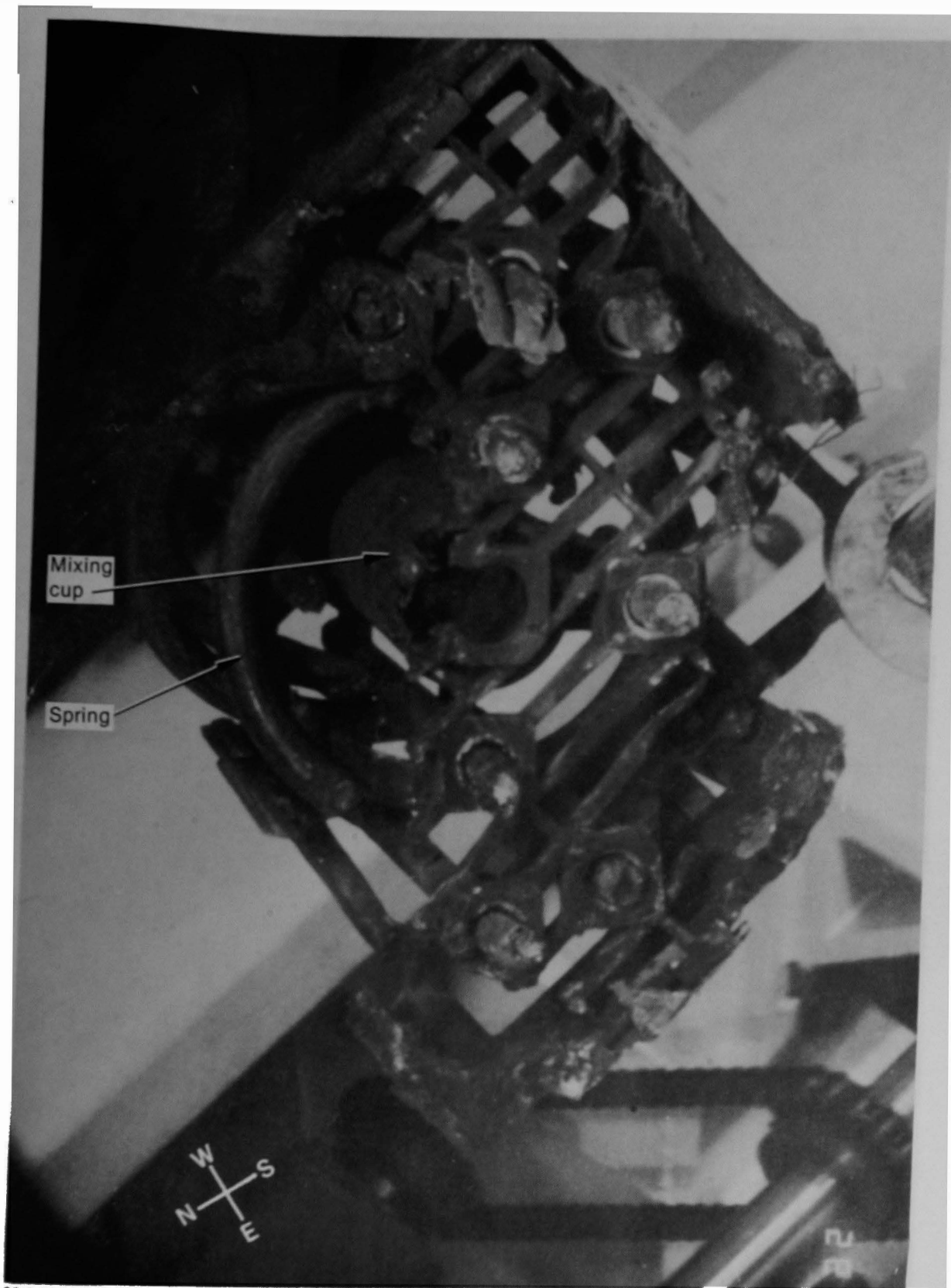
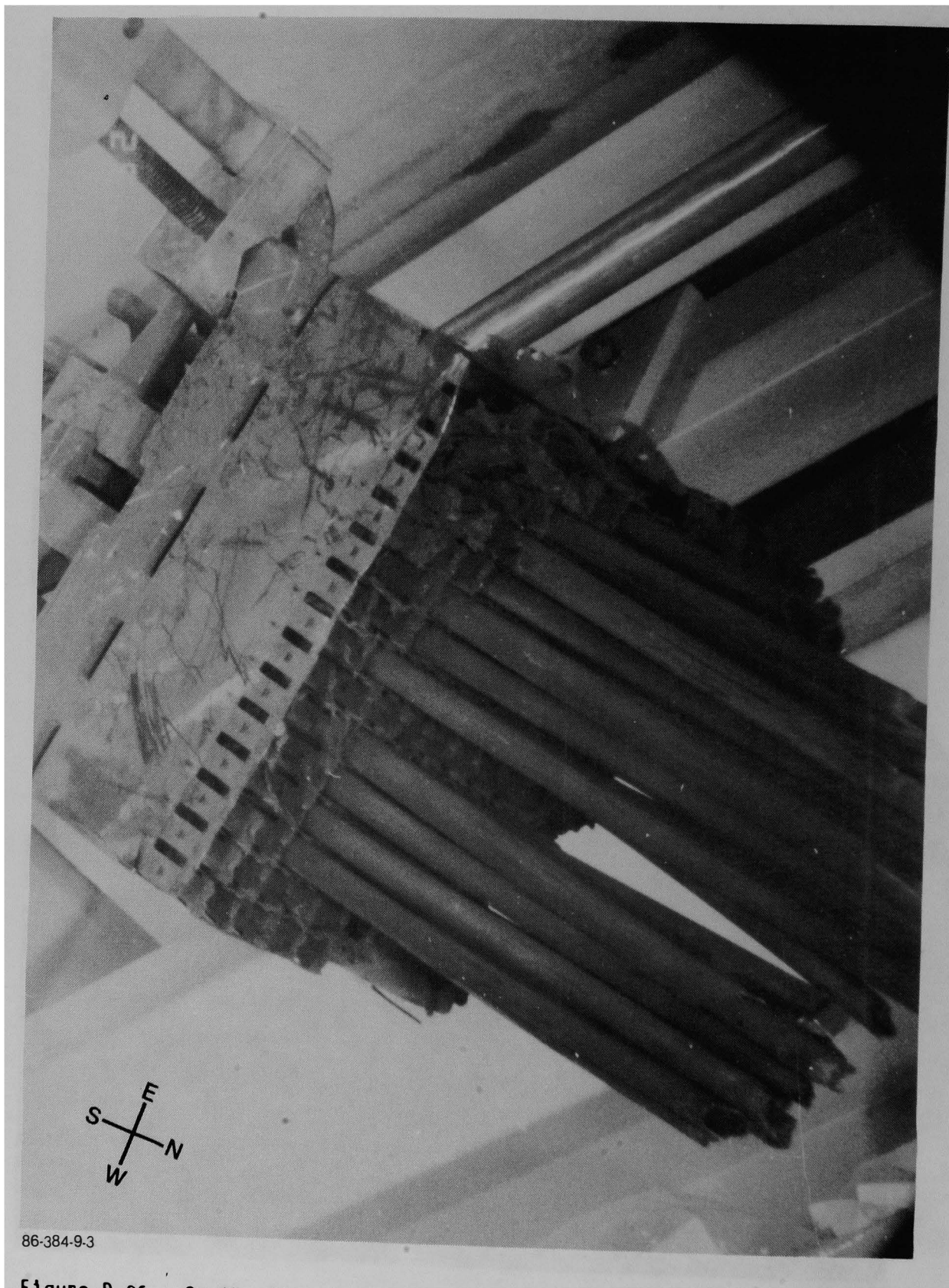


Figure D-35. Bottom view of component D-153-8.



86-384-9.3

Figure D-36. South side view of component D-153-9. Control rod spider and partial fuel assembly.



06-154-92

Figure D-37. Bottom view of component D-153-9.

fuel and control rods were intact 20 to 25 cm below the upper spacer grid on the southeastern half of the assembly. Peak temperatures exceeded 1673 K in the extreme northwest corner of the assembly at the tie plate elevation, but were generally lower than this across the entire tie plate. Temperatures were higher than 1533 K on the northwestern half of the assembly at the upper spacer grid elevation, but were lower than this on the southeastern side. In the extreme southeastern corner, approximately 25 cm below the upper spacer grid, the peak temperatures were near 1673 K. These peak temperatures were evidenced by partially melted control rod cladding (see Figure D-37).

As previously noted, the leadscrew temperatures ranged from 1255 K at the core center (H8) to 1116 K at the mid-radius (88) location. These temperatures are substantially lower than the estimated distinct component temperatures.

Component D-153-10: Control rod spider and upper end fitting

Core Position: D4

Upper End Fitting Identification: NJ 00PV

Spider Hub Identification: C155

Illustrated in: Figures D-38 and D-39

In component D-153-10, the tie plate is intact except for a small portion in the northwest corner. The apron is gone except on the south side and in a partially melted area on the west side. The upper spacer grid is gone except for a badly mangled portion on the south side. Control rod stubs extend from just below the tie plate on the north side to well below the crumpled upper spacer grid on the south side. The mixing cup and holddown springs are undamaged. Peak temperatures ranged from lower than 1533 K on the south side at the upper spacer grid elevation to higher than 1673 K in the extreme northwest corner at the tie plate elevation.



86-384-9-30

Figure D-38. West side view of component D-153-10. Control rod spider and upper end fitting.



86-384-9-28

Figure D-39. Bottom view of component D-153-10.

Component D-153-11: Partial control rod upper end fitting

Core Position: F10

Upper End Fitting Identification: NJ 0009

Illustrated in: Figures D-40 and D-41

Component D-153-11 is from a peripheral control rod fuel assembly. The section is from the southeast corner, which in this instance faces toward the core center. The remaining tie plate, mixing cup, spring retainer, and portions of the sides of the upper end fitting that faced the northwest corner were all previously melted. A previously melted mass is present at the mixing cup location. Control rod springs are still present in the guide tube positions. Peak temperatures were higher than 1673 K in the northwest corner (which was on the outer edge of the core) up to the spring retainer location. However, temperatures were lower than 1673 K in the southeast corner at the tie plate elevation. As shown in Figure 11, in the main body of this report, the fuel assembly upper grid plate was essentially undamaged at the F14 location.

Component D-153-12: Axial power shaping rod fuel assembly partial end fitting

Core Position: D6

Upper End Fitting Identification: NJ 0004

Illustrated in: Figures D-42 and D-43

Component D-153-12 was most heavily damaged in the southeast corner where the tie plate and portions of the sides of the end fitting above the tie plate elevation were melted. A small portion of the lower part of the holddown spring in the southeast corner was also melted. Portions of the remaining apron on the north and west sides were also melted. Peak temperatures were in excess of 1673 K in the southeast corner at the tie plate elevation and were higher than 1666 K where the holddown spring melted just above the tie plate. Temperatures were lower than 1673 K across the remainder of the assembly at the tie plate elevation.

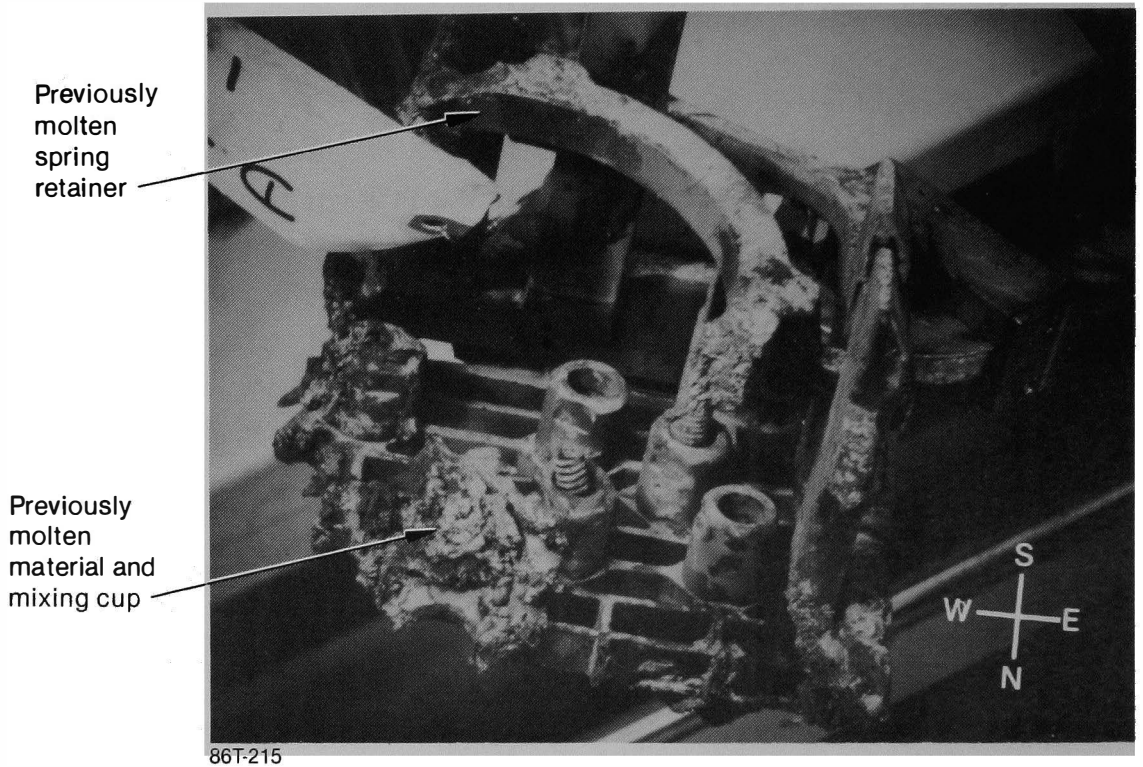


Figure D-40. Component D-153-11. Partial control rod upper end fitting.



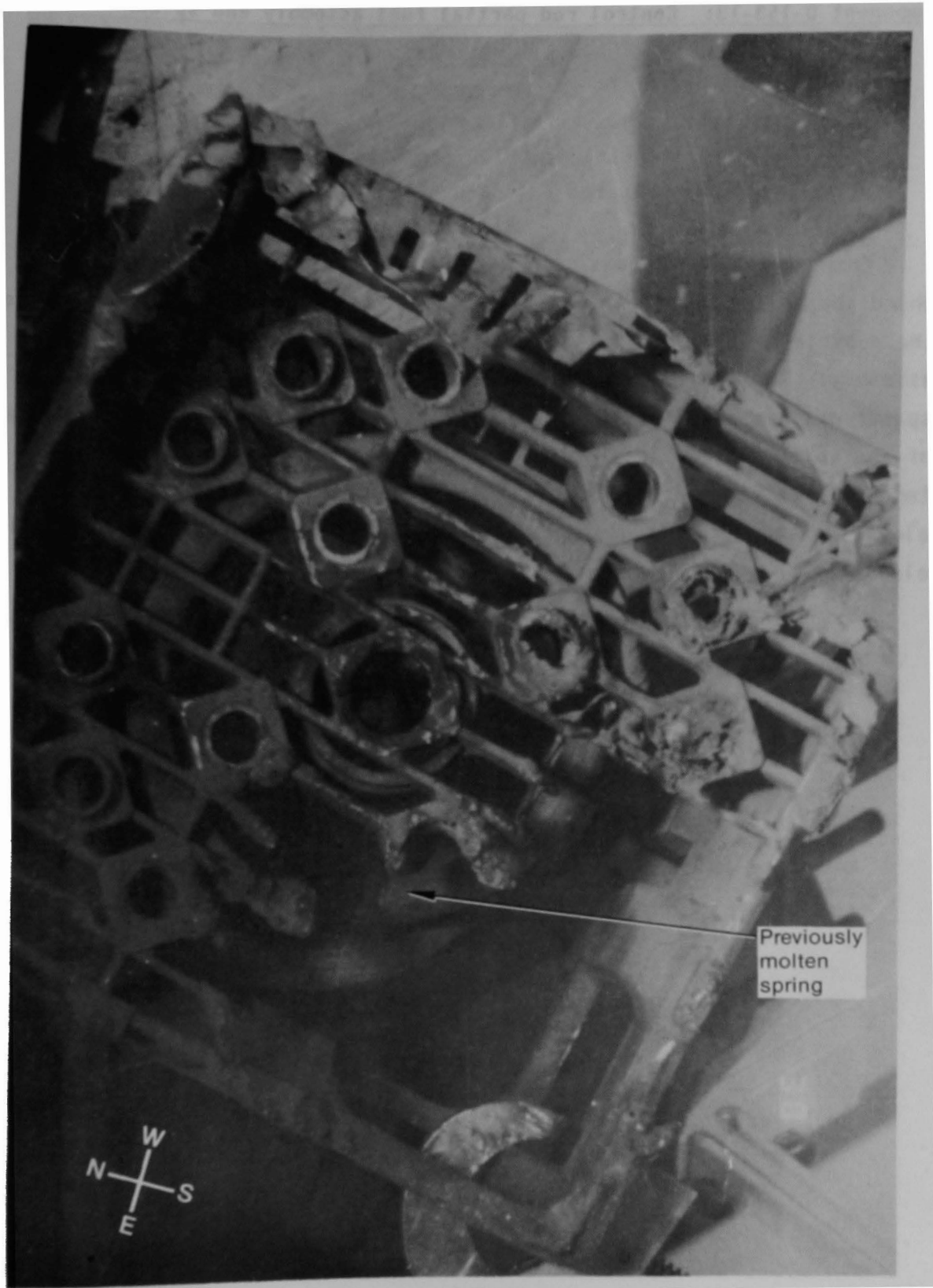
66-384 9-25

Figure D-41. Melted material near mixing cup on component D-153-11.



86-384-9-10

Figure D-42. Component D-153-12. Axial power shaping rod fuel assembly end fitting.



88-384-9-8

Figure D-43. Bottom view of component D-153-12.

Component D-153-13: Control rod partial fuel assembly and spider

Core Position: B10

Upper End Fitting Identification: NJ 00UA

Spider Hub Identification: C132

Illustrated in: Figures D-44 and D-45

Component D-153-13 was most heavily damaged in the southeast corner where the melted region included the tie plate and portions of the sides of the upper end fitting. This corner faced core center in this peripheral assembly. The least damage occurred on the west side where the upper spacer grid is still present. This side faced a fuel assembly on the edge of the core. The mixing cup and holddown spring were undamaged. Peak temperatures ranged from 1673 K in the southeast corner at the tie plate elevation and slightly above to less than 1533 K at the upper spacer grid elevation on the west side.

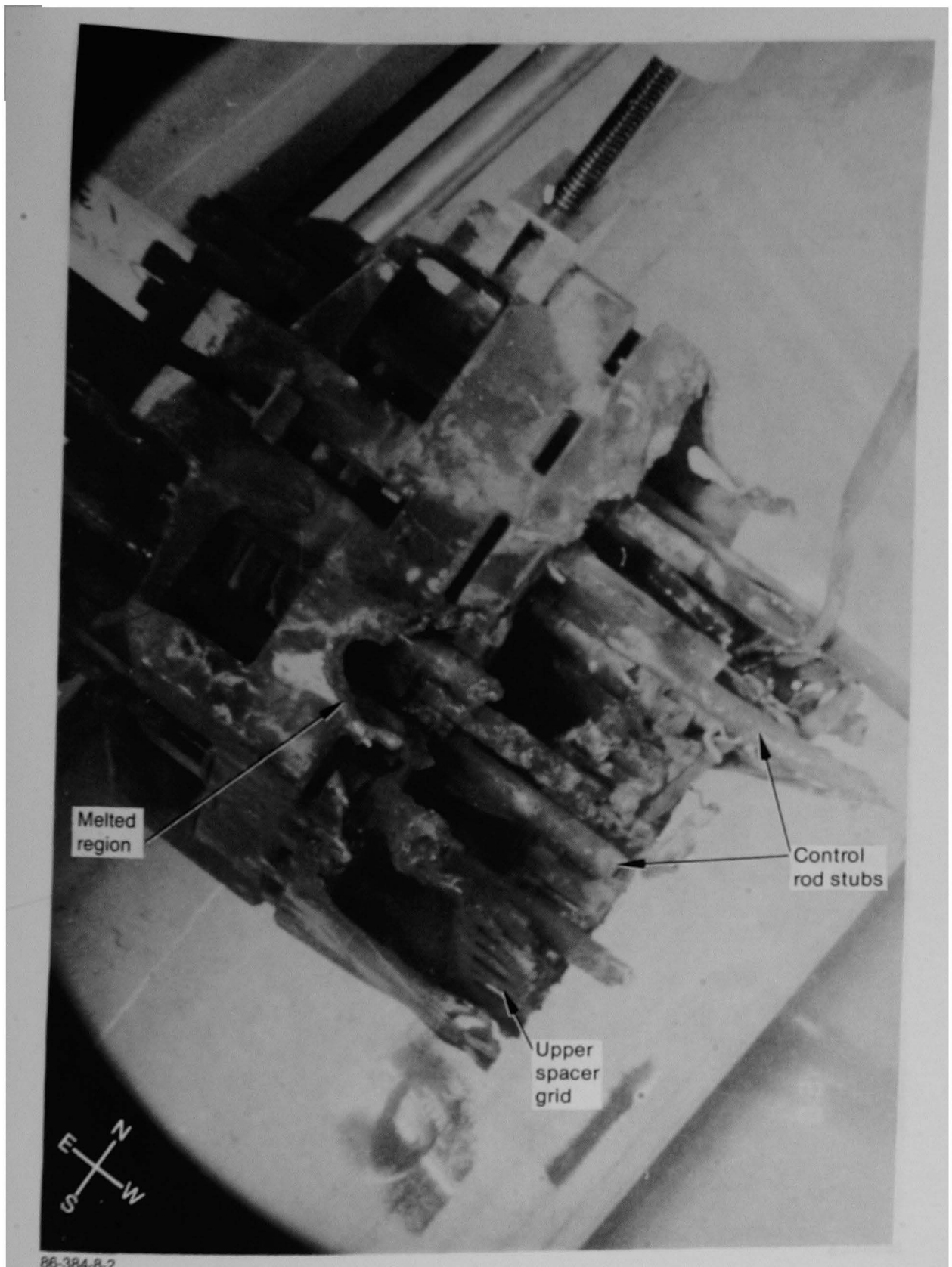
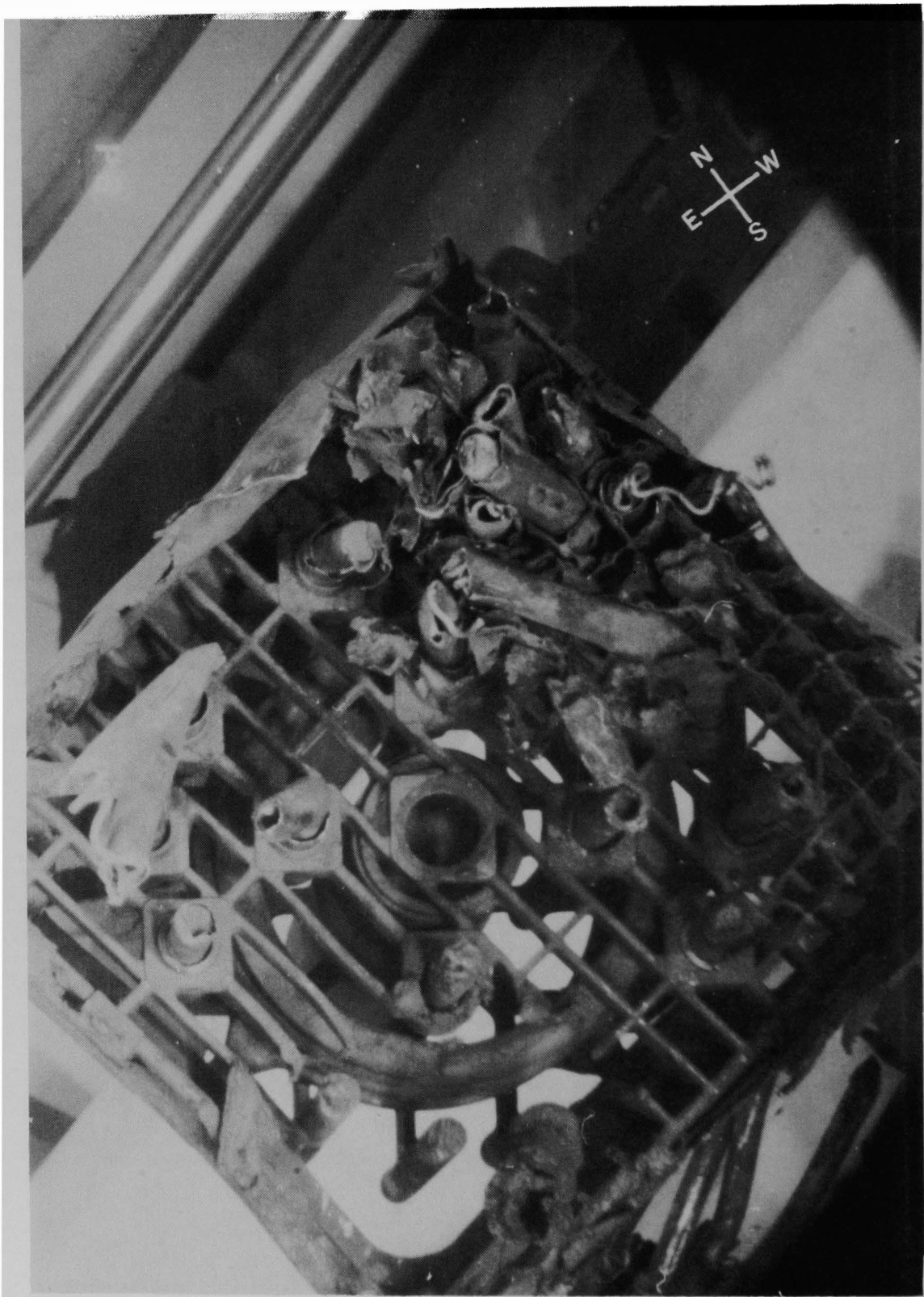


Figure D-44. East side view of component D-153-13. Control rod partial fuel assembly and spider.



86-384-8-6

Figure D-45. Bottom view of component D-153-13.

References

01. P. Hofmann, Reaction Kinetics Between Absorber Material (Ag, In, Cd Alloy) and Zircaloy-4 or Inconel 718 and Between Zircaloy-4 and Inconel 718 Spacer Grid Material, PNS-Annual Report 1985, KfK Report 4000, 1986.
02. M. L. Russell, TMI-2 Core Cavity Sides and Floor Examinations, December 1985 and January 1986, GEND-INF-074, EG&G Idaho Inc., February 1987.



